THE ELECTROCHEMISTRY OF METAL IONS IN INDUSTRIAL STREAMS

Anton van Aswegen

A dissertation submitted to the Faculty of Science, University of the Witwatersrand, in fulfilment of the requirements for the degree of Master of Science.

Johannesburg, 2005

DECLARATION

I declare that this dissertation is my own work. It is being submitted for the Degree of Master of Science in the University of the Witwatersrand, Johannesburg. It has not been submitted before for any degree or examination in any other University.

I obtained the information used in this dissertation whilst employed at the the Anglo Platinum Research Centre.

_____

A van Aswegen

____ day of _____ _____

ABSTRACT

The electrochemical recovery of low concentrations (< 200 mg l^{-1}) of palladium and platinum from a selected refinery effluent was investigated.

Cyclic Voltammetry (CV) provided qualitative evidence that palladium and platinum contained in an effluent with an acid chloride matrix could be deposited on a graphite cathode. Experimental techniques related to *(i)* the use of synthetic solutions *(ii)* the variation of potential scan ranges, *(iii)* the use of a witness ion (Fe^{3+}), and *(iv)* the use of glassy carbon or platinum disc working electrodes were used to assist with the interpretation of voltammograms.

Exhaustive electrolysis experiments via a graphite working electrode demonstrated the recovery of palladium and platinum in the refinery effluent to concentrations of < 1 mg l^{-1}. Copper present in the effluent was co-deposited with the precious metals.

Exchange current densities (j_o), electron transfer coefficients (α), standard rate constants (k_s) and mass transfer coefficients (k_m) were determined for selected reduction-oxidation (redox) couples via a custom made Rotating Disc Electrode (RDE).

In memory of my grandfather

Albert Binoir

ACKNOWLEDGEMENTS

I would like to acknowledge and thank the following parties:

- Prof Ignacy Cukrowski for his guidance and supervision of the project.
- Ms Bronwynne Ferreira, for the provision of relevant information and data related to the research project.
- Management of Anglo Platinum (in particular Mr Peter Charlesworth, Mr Harald Müller, Dr Stephen Woollam and Ms Marie Humphries) for funding the project, the provision of PGM solutions, and the opportunity to complete this dissertation.
- My wife Tercia, and children André, Alissa and Tiaan for their support and patience.

CONTENTS

LIST OF FIGURES

LIST OF TABLES

LIST OF SYMBOLS

The normal units of expression associated with each of the symbols listed are shown. If different units were used, it was noted in the text.

A	area of electrode (m^2)
c	concentration in bulk solution (mol dm^{-3})
c_O	concentration of species O in bulk solution (mol dm^{-3})
$(c_O)_{x=0}$	concentration of species O at the electrode surface (mol dm^{-3})
c_R	concentration of species R in bulk solution (mol dm^{-3})
$(c_R)_{x=0}$	concentration of species R at the electrode surface (mol dm^{-3})
D	diffusion coefficient (m^2 s^{-1})
E	potential versus a reference electrode (V)
E_e	equilibrium potential (V)
E°	standard electrode potential (V)
$E^{\circ\prime}$	formal electrode potential (V)
E_{pa}	anodic peak potential (V)
E_{pc}	cathodic peak potential (V)
F	the Faraday constant (96485 C mol^{-1})
i	current (A)

i_L	limiting current (A)
i_p	peak current (A)
i_{pa}	anodic peak current (A)
i_{pc}	cathodic peak current (A)
j	current density (A m^{-2})
$\vec{j}$	partial cathodic current density (A m^{-2})
$\overleftarrow{j}$	partial anodic current density (A m^{-2})
j_o	exchange current density (A m^{-2})
j_L	limiting current density (A m^{-2})
j_{LA}	limiting current density for anodic reaction (A m^{-2})
j_{LC}	limiting current density for cathodic reaction (A m^{-2})
$\vec{k}$	rate constant for cathodic reaction (m s^{-1})
$\overleftarrow{k}$	rate constant for anodic reaction (m s^{-1})
$\vec{k}_o$	rate constant for electron transfer when the potential is zero versus a defined reference; cathodic reaction (m s^{-1})
$\overleftarrow{k}_o$	rate constant for electron transfer when the potential is zero versus a defined reference; anodic reaction (m s^{-1})
k_m	mass transfer coefficient (m s^{-1})

k_s	standard rate constant for a redox couple (m s^{-1})
M	molar concentration (mol dm^{-3})
MM	molar mass (g mol^{-1})
n	number of electrons involved in electrode reaction (dimensionless)
O	refers to species O in the reaction $O + ne^- \leftrightarrow R$
$[O]_{x=0}$	concentration of species O at electrode surface (mol dm^{-3})
R	gas constant (8.316 J K^{-1} mol^{-1}), or species R in the reaction $O + ne^- \leftrightarrow R$
R_u	uncompensated resistance (Ω)
$[R]_{x=0}$	concentration of species R at electrode surface (mol dm^{-3})
R^2	coefficient of determination, used to assess the suitability of using a particular model, e.g. linear least squares to fit regression data; a value of one indicates an ideal fit (dimensionless)
t	time from commencement of experiment (s)
T	temperature (K)
α	electron transfer coefficient (dimensionless)
α_A	electron transfer coefficient for anodic reaction (dimensionless)
α_C	electron transfer coefficient for cathodic reaction (dimensionless)
δ	thickness of diffusion layer (m)

ΔG_{ADS}	free energy of adsorption (kJ mol^{-1})
η	overpotential (V)
ν	potential scan rate (mV s^{-1}), or kinematic viscosity (m^2 s^{-1})
ρ	resistivity (M Ω cm)
ω	rotation rate of Rotating Disc Electrode (radians s^{-1})

NOMENCLATURE

The acronyms and terms in this list are also defined when they first occur in the text of a new chapter.

4-M solution	solution containing iron, copper, palladium and platinum ions in a 0.1 M HCl matrix, with an approximate ratio of four parts iron, four parts copper, four parts palladium and one part platinum
AAS	Atomic Absorption Spectroscopy
active surface area	refers to electrochemically active surface area of a working electrode, i.e. surface where electron transfer occurs
Ag / AgCl	silver-silver chloride reference electrode
AR	Analytical Reagent grade chemical with certificate of analysis
ARC	Anglo Platinum Research Centre
BMR	Base Metals Refinery
CP	Chemically Pure grade chemical with assay indicated on product label
CV	Cyclic Voltammetry
Cu^{2+} / Cu^{+} (C)	refers to the redox couple associated with the reduction of Cu^{2+} to Cu^{+} on a graphite electrode surface (grade ET-10, Electrographite Carbon Co.) as described in Chapter 5

Cu^{+}/Cu^{0} (C+Cu)	refers to the redox couple associated with the reduction of Cu^{+} to Cu^{0} on a graphite electrode surface (grade ET-10, Electrographite Carbon Co.) after completion of the nucleation process, as described in Chapter 5
Cu solution	refers to a solution containing 191 mg l^{-1} Cu^{2+} in a background solution of 1 M NaCl, 1 M CH_3COONH_4, and 1 M CH_3COOH as described in Chapter 5
DME	Dropping Mercury Electrode
EQCM	Electrochemical Quartz Crystal Microbalance
$Fe(CN)_6^{3-}$ solution	refers to a solution containing 0.001 M $Fe(CN)_6^{3-}$ in a background solution of 0.1 M KCl (pH 3), as described in Chapter 5
GR	Guaranteed Reagent grade chemical with guaranteed product purity
HMDE	Hanging Mercury Drop Electrode
HOPG	Highly Oriented Pyrolytic Graphite
ICP-OES	Inductively Coupled Plasma - Optical Emission Spectrometry
ICP-MS	Inductively Coupled Plasma - Mass Spectrometry
$i-E$	refers to a plot of current (i) as a function of potential (E)
iR_u drop	refers to voltage obtained by the product of the current (i) and the uncompensated resistance (R_u) recorded across an electrode-solution interface, resulting in potential measurement errors

$j-E$	refers to a plot of current density (j) as a function of potential (E)
LSV	Linear Scan Voltammetry
M	refers to metal centres deposited on a cathode surface following the reaction $M^{n+} + ne^- \leftrightarrow M$
MFE	Mercury Film Electrode
$M-H$	refers to a bond between a particular cathode material (M) and a hydrogen atom (H)
M^{n+}	refers to metal ions present in solution for the reaction $M^{n+} + ne^- \leftrightarrow M$
MO	refers to a product formed on an electrode surface following adsorption, involving a metal (M) and oxygen (O)
MOH	refers to a product formed on an electrode surface following adsorption, involving a metal (M) and hydroxide (OH)
NHE	normal hydrogen electrode
NMR	Nuclear Magnetic Resonance
OA	Operational Amplifier
PGMs	Platinum Group Metals
PML	Palladium Mother Liquor, referring to a refinery stream generated at Anglo Platinum's Precious Metals Refinery
PMR	Precious Metals Refinery

PTFE	polytetrafluoroethylene, commonly known as Teflon
RDE	Rotating Disc Electrode
redox	refers to an electron transfer reaction involving either reduction or oxidation
RHE	reversible hydrogen electrode
RRDE	Rotating Ring Disc Electrode
SCE	saturated calomel electrode
SDME	Static Dropping Mercury Electrode
SEM	Scanning Electron Microscopy
SEM-EDS	a surface analytical technique employing a Scanning Electron Microprobe in combination with X-Ray Energy Dispersive Spectrometry
STM	Scanning Tunnelling Microscopy
UPD	underpotential deposition
UV-Vis	Ultraviolet-Visible Spectroscopy
voltammogram	refers to a current-voltage plot recorded during a voltammetric experiment
VRP	Values Recovery Process
XRD	X-Ray Diffraction
XPS	X-Ray Photoelectron Spectroscopy

1 INTRODUCTION

The Platinum Group Metals (PGMs) namely platinum, palladium, rhodium, iridium, ruthenium, and osmium form a distinctive group in the second and third transition rows of the periodic table. These metals have unique properties and are used in many applications.

Platinum and palladium bars are produced for the investment market, whilst various PGMs are used in the manufacture of jewellery. Apart from its precious and esoteric nature, PGMs also have unique physical and catalytic properties that are used in industry. Platinum, palladium and rhodium are used in the automotive industry as catalysts. The catalytic properties of these and other PGMs are also used in the chemical industry. One example is the catalytic oxidation of ammonia in the manufacture of nitric acid. The use of PGM catalysts in fuel cells also received much attention. In addition, the electronics and medical fields also make use of PGMs for a variety of purposes.

Due to the increasing demand for PGMs, production costs, and competition in the mining industry, continuous efforts are made to improve the technologies employed to produce pure metals from PGM bearing ores.

1.1 BACKGROUND

Considerable treatment of the original PGM bearing ore is required before a product suitable for final refining is obtained. At Anglo Platinum's operations, the processes involved in producing a feed material for the Precious Metals Refinery (PMR) include flotation, smelting, converting and Base Metal removal.

Initially the mined ore is reduced to a suitable size for further treatment.

This is achieved by means of various types of crushers and mills. A froth flotation process follows in order to separate the PGM particles from a liquid-ore mixture. The froth is created in flotation tanks by blowing air bubbles through the liquid-ore mixture. Suitable reagents are added to ensure that the PGM particles adhere to the air bubbles. The flotation concentrates are then sent to a smelter for further treatment.

At the smelter facilities flotation concentrates are dried and smelted to obtain a matte. Various fluxes are used to produce a matte that contains principally copper, nickel, iron and PGMs.

The matte is then treated in a converter by blowing oxygen to form a high grade matte containing Base Metals and PGMs. A slow cooling process allows the formation of a magnetic phase rich in PGMs within the matte. This material is crushed before the magnetic phase is separated. The magnetic phase is then subjected to a leaching step, and the remaining insoluble portion is sent to the PMR to serve as a feed material.

The non-magnetic portion is sent to the Base Metals Refinery (BMR) where copper, nickel and cobalt are recovered through various processes, including pressure leaching and electrowinning. The solid material remaining after Base Metal recovery is toll refined to recover the remaining PGMs.

1.1.1 The Refining Process

The refinery feed is dissolved to produce a liquor. Solvent extraction processes are used at the PMR, where PGMs are extracted from the dissolve liquor into an organic medium. The extracted PGMs contained in the organic phase are then stripped into an aqueous medium for final refining.

As a result of the refining process numerous effluents are generated. These effluents contain low concentrations of PGMs, typically in the mg l^{-1}

range, with varying quantities of other elements that were fed into the refining process via the starting material, or added as reagents. Given that large volumes of effluent are produced, it is essential to recover the PGMs from an economic and environmental point of view.

1.1.2 Values Recovery

The PGMs in the effluents are recovered via a Values Recovery Process (VRP). Effluents emanating from the refinery are combined and treated by means of a chemical reduction process. The PGMs are recovered in a solid form that can be recycled, whilst some of the unwanted impurity elements remain in solution for disposal to solar evaporation ponds. Three types of residues are produced, and are either recycled within the refinery or dispatched to the smelter

1.2 STATEMENT OF PROBLEM AND AIMS OF INVESTIGATION

There are several disadvantages associated with the current VRP. Some of the more important issues are listed:

- The possible formation of hydrogen gas under particular operating conditions. This may pose a safety hazard.
- Process inefficiencies that result in the re-treatment of some batches.
- The large VRP plant requires maintenance and engineering support, which contributes to the cost of recovering the PGMs.
- The volume of effluent increases after treatment via the VRP. These effluents have to be accommodated in solar evaporation ponds with limited capacity.
- The addition of chemicals complicates the refining process, as some of the solids recovered via the VRP have to be treated prior to recycling.

1.2.1 Aims of the Investigation

The general aim of the project was to investigate the feasibility of

recovering PGMs from refinery effluents via an electrochemical process instead of using the conventional VRP. This would involve the deposition of PGMs on a cathode material contained in an electrochemical reactor. The use of an electrochemical recovery technique would hold several advantages over traditional chemical reduction processes:

- Electrochemical treatment plants are normally orders of magnitude smaller than conventional chemical treatment plants.
- No volume increase in the treated effluent stream.
- Since electrochemical reduction processes do not require the addition of chemicals, the load in the treated effluent stream would not be increased. Aspects related to health, safety and the environment will also be addressed, since the handling and disposal of hazardous chemicals would not be required.
- The treatment of the recovered material prior to recycling may be simplified, as the resulting solid would not contain unwanted contaminants associated with conventional chemical reduction processes.
- Depending on the nature of the effluent, it may be possible to recover PGMs selectively.

Selection of effluent

In the conventional chemical reduction process, effluent streams are combined prior to treatment. Depending on the nature of the individual streams making up the batch to be treated, complications may arise which would make the recovery of PGMs inefficient.

The treatment of individual effluent streams instead of a combination of effluents would be advantageous for several reasons:

- The matrix of the stream will be *(i)* less complex and *(ii)* less variable, making it easier to predict which reactions would occur under specific

operating conditions.

- If the chemistry related to the treatment of a specific effluent can be predicted, efficient and robust recovery techniques may be developed. This could include the selective recovery of PGMs.
- If the effluent is treated at source, the recovered material may be recycled to the main refining process at the most appropriate stage instead of the start of the refining process. As a result, overall processing time and plant inventory will decrease. This will however only be possible if the recovered PGMs can be introduced to the main refining process in a suitable physical form.

The small footprint required for an electrochemical reactor in comparison to a conventional chemical reduction plant would make it ideal to treat refinery effluents at source. It was therefore decided to focus research activities on the treatment of a particular effluent instead of a combination of streams.

For the purpose of the project, the Palladium Mother Liquor (PML) generated at the PMR was used. This particular effluent was selected for three reasons:

- The recovery of PGMs via an electrochemical reactor must be beneficial from a financial point of view. In the context of refinery effluents, the PML contains relatively high concentrations of palladium (refer to Table 1.1), which would make the recovery of the metal viable.
- Concerns were raised with regards to the presence of stable amminated PGM complexes found in particular effluents. It was claimed that the stability of some of these complexes prevented the recovery of PGMs via chemical or electrochemical processes. These issues will be discussed in detail in the literature review section (Section 1.4). It was suspected that these stable complexes were also present in the PML solution. The study of PML solutions would

therefore provide the opportunity to quantify the effect of amminated PGM complexes on the efficiency of the proposed electrochemical reactor.

- Previous test work at the Anglo Platinum Research Centre (ARC) indicated that the electrochemical reduction of palladium and platinum on a cathode material may be feasible. It was also shown that the recovery of rhodium, iridium and ruthenium was more difficult. These investigations will be discussed in more detail in the literature review section.

  It was decided to select a stream containing palladium and platinum (i.e. the PML) instead of streams containing rhodium, iridium or ruthenium. The rationale was that it would be easier to focus initial studies on less complex systems. Experience and knowledge gained from this test work could then be used to investigate more complex systems involving rhodium, iridium and ruthenium in the future.

Detailed description of project aims

The aim of the project was to investigate the feasibility of removing PGMs from PML solutions via an electrochemical reactor to concentration levels that are equal to or lower than the current VRP specifications. The current VRP reduces the total PGM concentration in effluent streams to < 10 mg l^{-1}, with no single PGM present at concentrations > 2 mg l^{-1}. The concentrations of metals and major cations and anions found in a typical PML solution are provided in Table 1.1.

It was envisaged that the research methodologies developed in the course of this project would be used to assess the feasibility of removing PGMs from other PMR effluents in future projects.

Table 1.1 Components of a typical PML solution.

Component	Concentration
Major Metal Ions	
Cu	200 - 500 ($mg\ l^{-1}$)
Pd	100 - 200 ($mg\ l^{-1}$)
Pt	10 - 50 ($mg\ l^{-1}$)
Minor Metal Ions	
Au, Ag, As, Bi, Ir, Ni, Pb, Rh, Ru, Sb, Se, Sn, Te, Zn	$< 10\ (mg\ l^{-1})$
Other Major Ions	
$Na^+, NH_4^+, Cl^-, C_2H_3O_2^-$	$\approx 1\ (M)$

Note: Metal ion concentration ranges were based on routine analyses performed at the PMR in January and February 2002.

1.3 RESEARCH REQUIREMENTS

To develop a practical electrochemical reactor capable of removing PGMs from a PML solution, fundamental chemistry and chemical engineering contributions would be required. For this reason, two separate research projects were initiated. One research project focussed on the fundamental issues related to the interaction of metal ions at an electrode surface, whilst the second project focussed on engineering aspects related to the design of the electrochemical reactor. The fundamental research project is described in this dissertation.

A fundamental investigation associated with the electrochemical recovery of PGMs from a multi-component solution would involve many different areas of research. These include aspects related to thermodynamics, kinetics, electrode materials, and catalytic or inhibitive electrode processes

to name a few.

It was important to demonstrate the feasibility of PGM recovery via an electrochemical reactor within a reasonably short time period. The fundamental research project therefore focussed on the provision of information that was critical to the development of the electrochemical reactor. This information was used to assist in the design of the electrochemical reactor via the engineering research project.

The areas of research covered in the fundamental research project were therefore defined by issues related to the design of a practical electrochemical reactor. Due to the focus of the fundamental research project it was not possible to investigate the many complex fundamental issues in detail. The intention was to provide critical information required for the design of an electrochemical reactor, whilst identifying areas where additional fundamental research would be required. These issues could then be investigated via subsequent research projects if required.

Prior to the definition of specific objectives for the fundamental research project, a detailed literature review was conducted to assess the availability of relevant information.

1.4 LITERATURE REVIEW

Previous test work at ARC mainly concentrated on the feasibility of using commercially available electrochemical technologies to treat typical VRP solutions. This generally involved the use of electrochemical reactors with high surface area cathodes.

It was demonstrated that it may be possible to remove palladium and platinum from particular VRP streams in a quantitative manner, depending on the nature and composition of the effluent, and the particular electrochemical reactor used. The quantitative removal of rhodium, iridium and ruthenium could not be achieved from any of the VRP streams tested.

Due to the nature of the test work related to the commercial units, many of the projects involved empirical test work rather than fundamental research. Although these tests indicated that some of the PGMs could be recovered electrochemically, it was realised that a fundamental understanding of these processes would be required to effectively control any proposed electrochemical reactor used for the purpose of values recovery at PMR.

Since most of the commercially available technologies are patented, suppliers are not willing to divulge technical data. It was therefore necessary to review the information available in published journals in order to find research data that could contribute to the overall understanding of the processes that govern the interactions between metal ions, solution matrices and electrode materials relevant to the removal of PGMs from PMR effluents.

A summary of the literature review exercise is presented here. Since palladium and platinum were the major PGMs present in the PML effluents selected for the purpose of this study (refer to Section 1.2 and Table 1.1), the summary mainly focussed on references related to these metals.

1.4.1 Electrodeposition of Palladium and Platinum

The deposition of palladium and platinum from different solution matrices was investigated using a wide variety of substrates. Some of the more relevant journal papers in the context of the fundamental research project are subsequently discussed.

Highly Oriented Pyrolytic Graphite surfaces

Arvia and co-workers[1] investigated the kinetics and mechanisms of palladium island electroformation on Highly Oriented Pyrolytic Graphite (HOPG) from aqueous solutions containing $PdCl_2$. Voltammetric, Scanning Electron Microscopy (SEM) and Scanning Tunnelling Microscopy (STM) techniques were employed to investigate this system.

For voltammetric experiments a test solution containing 7.5×10^{-4} M $PdCl_2$, 5×10^{-2} M $NaClO_4$ and 5×10^{-3} M $HClO_4$ was utilised. All potentials were reported relative to a saturated calomel electrode (SCE). Voltammograms in the potential region 0.85 V to -0.35 V were recorded via Linear Scan Voltammetry (LSV) at a scan rate of 5 mV s^{-1}. Chronoamperometric experiments were also conducted in this potential range.

It was concluded that the initial deposition of palladium metal on the HOPG electrode between 0.38 V and 0.33 V proceeded under electron transfer controlled conditions via a $PdCl_2$ surface intermediate. At potentials more negative than that observed for the Tafel region, the deposition of palladium proceeded under diffusion controlled conditions. A cathodic peak (-0.18 V) was also observed just prior to the generation of a significant cathodic current due to the reduction of hydrogen ions. This peak was ascribed to the adsorption of hydrogen atoms on previously formed palladium islands.

The morphology of the palladium deposits was investigated via SEM and STM experiments. The aspect ratio of the deposited palladium islands, defined as the ratio of the maximum height of the island to the island radius, decreased as the cathodic overpotential shifted in a more negative direction, whereas the island density on the HOPG surface increased. It was concluded that the mechanism for palladium island formation and the aspect ratio depended on whether the cathodic potential was above or below the potential of zero charge of bulk palladium.

At potentials more positive than the zero charge potential (0.13 V used in experiments), compact rounded discs were formed. This growth mode was ascribed to the $PdCl_2$ intermediate produced during the deposition of palladium, which enhanced surface diffusion.

At potentials more negative than the zero charge potential (-0.10 V used in experiments), the palladium islands exhibited a branched two-dimensional growth pattern. This mechanism was explained by the presence of weak step-edge energy barriers at Pd(111) surfaces, where "111" refers to the crystal plane.

Arvia, with the aid of several other researchers[2] was also involved in studies related to the electrodeposition of platinum on HOPG. Similar research methodologies to that used for the study of palladium electrodeposition on HOPG were employed[1].

A test solution containing 3.86×10^{-2} M H_2PtCl_6 in a matrix of 1.1 M HCl was used to conduct LSV experiments with a HOPG working electrode. All potentials were reported relative to a reversible hydrogen electrode (RHE). The voltammograms were recorded between 0.75 V and 0.0 V using scan rate of 5 mV s^{-1}.

A small current plateau was observed between 0.68 V and 0.62 V (C1), followed by a broad cathodic peak at 0.33 V (C2) and a sharp peak at 0.05 V (C3).

The deposition of platinum in the potential range of C1 was investigated via ex-situ STM and SEM imaging, and complemented by electrochemical experiments involving Chronoamperometry, LSV and Cyclic Voltammetry (CV). It was concluded that the initial deposition of platinum occurred at defects in the HOPG surface, followed by disproportionation:

$$PtCl_6^{2-}(sol) + e^- \rightarrow PtCl_5^{2-}(HOPGD) + Cl^- \quad (1.1)$$

$$2PtCl_5^{2-}(HOPGD) \rightarrow 0.5Pt(HOPGD) + 1.5PtCl_6^{2-}(HOPGD) + Cl^- \quad (1.2)$$

where *sol* refers to the solution adjacent to the electrode surface, and *HOPGD* refers to defects in the HOPG surface.

The disproportionation reaction (Equation 1.2) was found to be the rate determining step. In addition to the reactions described in Equations 1.1 and 1.2, the simultaneous reduction of Pt^{4+} to Pt^{2+} was reported:

$$PtCl_6^{2-} + 2e^- \rightarrow PtCl_4^{2-} + 2Cl^- \quad (1.3)$$

It was also postulated that platinum electrodeposited in the potential region of C2 under diffusion control via the following reaction:

$$PtCl_6^{2-} + 4e^- \rightarrow Pt(s) + 6Cl^- \quad (1.4)$$

The reduction peak at C3 was attributed to three simultaneous reactions, namely the reduction of Pt^{4+} as described in Equation 1.4, the electrosorption of hydrogen atoms on platinum metal centres and the reduction of Pt^{2+} described in Equation 1.5:

$$PtCl_4^{2-} + 2e^- \rightarrow Pt(s) + 4Cl^- \quad (1.5)$$

The initial growth mechanism for the deposition of platinum in the potential range of C1 was characterised by the presence of small rounded nuclei, approximately 2 to 3 nm in size. These nuclei developed into large agglomerates with irregular and rough surfaces as the deposition time increased. Agglomerates were mainly found along HOPG surface steps.

Glassy carbon surfaces

Dong, Wang and co-workers[3] investigated the development of methodologies that could be used to produce highly dispersed palladium particles on glassy carbon surfaces. Large palladium surface areas are necessary for processes involving catalysis.

A solution containing 5×10^{-3} M $[PdCl_4]^{2-}$ in a 0.1 M K_2SO_4 matrix was analysed via CV, employing a glassy carbon working electrode and a SCE. A significant anodic peak was observed at 1.35 V.

It was concluded that the planar Pd^{2+} complex oxidised to form an octahedral Pd^{4+} complex through coordination to oxygen atoms of functional groups that were present on the glassy carbon surface. The presence of these surface octahedral complexes was confirmed by X-Ray Photoelectron Spectroscopy (XPS) experiments.

The glassy carbon electrode containing the Pd^{4+} surface complexes was placed in a solution containing 0.3 M H_2SO_4 prior to conducting CV experiments in a potential scan range of -0.4 V to 1.0 V. A significant cathodic current was observed at ca. 0.0 V during the initial cycle. It was concluded that the palladium surface complexes were reduced to metal particles.

XPS experiments confirmed the presence of palladium metal particles, whilst the application of STM revealed that the size of the palladium particles were in the nanometer range.

Carbon fibres

Georgolios, Jannakoudakis and Karabinas[4] investigated the deposition of platinum on carbon fibres from solutions containing 3×10^{-3} M H_2PtCl_6 or K_2PtCl_4 in a matrix of 0.5 M H_2SO_4. Experiments involving CV indicated that Pt^{4+} was reduced to its metallic form via well defined two-electron transfer reduction steps. The deposition of platinum metal centres via Pt^{2+} was observed at potentials $\leq$ 0.52 V versus a RHE.

From results obtained via Chronoamperomety, Chronopotentiometry and SEM analyses, it was concluded that the deposition of platinum involved an instantaneous nucleation process with hemispherical growth.

It was also demonstrated via CV analyses that hydrogen adsorption peaks only appeared when fairly thick platinum deposits were present on the electrode surface. When an electrolysis charge of 0.3 mC was applied for

every milligram of fibre contained in the working electrode (using a test solution of 3×10^{-3} M H_2PtCl_6 and 0.5 M H_2SO_4), no hydrogen adsorption peak was observed on the resulting platinum deposit.

Gold electrodes

Uosaki and co-workers[5] investigated the mechanism of palladium electrodeposition and the resultant characteristics of the deposit. A working electrode of Au(111) was employed with a background electrolyte consisting of 5×10^{-2} M H_2SO_4. The background electrolyte contained $[PdCl_4]^{2-}$ in concentrations between 1×10^{-5} M and 1×10^{-3} M, depending on the nature of the experiment. All potentials were referenced to a RHE.

Experiments involving an Electrochemical Quartz Crystal Microbalance (EQCM) and in situ STM analyses confirmed the formation of a $[PdCl_4]^{2-}$ adlayer on the Au(111) surface at 0.95 V.

EQCM and STM measurements also revealed the reduction of $[PdCl_4]^{2-}$ to Pd^0 on the Au(111) surface between 0.95 V and 0.35 V. From the data obtained it was concluded that palladium initially deposited on the Au(111) surface in a two-dimensional fashion via the $[PdCl_4]^{2-}$ adlayer. Once the Au(111) surface was covered by a Pd^0 monolayer, the next layer of metal was deposited on the existing monolayer. It was found that the deposition of palladium on existing Pd^0 monolayers also occurred via $[PdCl_4]^{2-}$ adlayers.

The two-dimensional or layer-by-layer growth of the palladium deposit was ascribed to differences in the stability of $[PdCl_4]^{2-}$ adlayers present on terraces or edges of deposited palladium islands. Since the interaction between the adsorbed species on the terraces of the palladium islands

were stronger compared to the edges, it was easier to deposit Pd^0 on the edges. This favoured the lateral two-dimensional growth of the palladium deposit.

The structure of the deposited palladium layer was examined by means of X-Ray Diffraction (XRD). It was concluded that a Pd(111) phase was deposited on the Au(111) substrate. The presence of Pd(111) was also confirmed via CV experiments. Voltammograms for the reduction of Cu^{2+} on the deposited palladium surface was compared to that obtained on a Pd(111) surface. Based on the similarities of the voltammograms, it was concluded that palladium was deposited as Pd(111).

Deposition from electroplating baths

Le Penven, Levason and Pletcher[6] investigated the deposition of palladium from standard electroplating baths containing $[Pd(NH_3)_2Cl_2]$ in NH_4Cl at a pH value of 8.9. The homogenous chemistry of $[Pd(NH_3)_2Cl_2]$ in these solutions was investigated, and the relative importance of oxygen reduction, hydrogen absorption and hydrogen evolution as competing cathode reactions were established.

Ultraviolet-Visible (UV-Vis) spectroscopy was employed to confirm the chemistry of $[Pd(NH_3)_2Cl_2]$ in aqueous NH_4Cl at various pH values. The pH values of the test solutions were adjusted with HCl or NH_3. It was found that Pd^{2+} stabilised as $[Pd(NH_3)_4]^{2+}$ at pH values between 5.0 and 13.6. At pH values below 5.0, $[Pd(NH_3)_2Cl_2]$ was formed, and at a pH value of 2.0 the major species was $[PdCl_4]^{2-}$.

Under the conditions prevailing in the electroplating bath (pH 8.9) $[Pd(NH_3)_4]^{2+}$ would therefore be present. In addition, no evidence of hydrolysis or other decomposition reactions related to this tetraammine complex was found.

Electroanalytical techniques involving potential sweep and potential step experiments at rotating and stationary working electrodes consisting of vitreous carbon and palladium surfaces were employed to investigate the deposition of palladium. Test solutions containing 1×10^{-2} M $\left[Pd(NH_3)_2Cl_2\right]$ in 1 M NH_4Cl were used. The pH of these solutions varied between 8 and 9. Potentials were reported relative to a SCE.

To produce a smooth, adherent palladium deposit via the electroplating bath, potentials in the range of -0.50 V to -0.55 V was applied. It was found that reactions involving hydrogen evolution and palladium hydride formation (absorption of H_2 in the growing palladium metal lattice) were only significant at potentials more negative than -0.67 V. Hence, under normal plating conditions, hydrogen evolution and palladium hydride formation would not be competing cathode reactions.

The reduction of oxygen however occurred at a mass transport controlled rate under the conditions employed in the electroplating bath. In a bath containing 1 g l^{-1} Pd^{2+}, the current efficiency was lowered by 20 % to 50 %, depending on the selected current density.

Data from experiments conducted with a Rotating Disc Electrode (RDE) indicated that convection increased the current density for palladium deposition. This lead to an increase in the rate of palladium deposition.

Le Penven, Levason and Pletcher also investigated the chemistry of a commercial electroplating bath for platinum[7], based on the use of a $Pt(NH_3)_4^{2+}$ in a phosphate buffer. The solution used throughout the investigation consisted of 2.6×10^{-2} M $Pt(NH_3)_4HPO_4$ in 2.8×10^{-2} M Na_2HPO_4 at pH values between 10 and 11.

Platinum-195 Nuclear Magnetic Resonance (NMR) spectra for the test solutions were recorded in the temperature range 293 K to 368 K. It was

confirmed that $Pt(NH_3)_4^{2+}$ was the only platinum species present in solution.

Potential sweep experiments were conducted using the same test solution. In terms of electroanalytical experiments the ionic strength of the solution was low, whilst convection became significant near the boiling point. A microelectrode was therefore used, since its response would be relatively undistorted by the effects of ohmic or iR_u drop and convection.

From the information obtained via microelectrode studies, a mechanism for the deposition of platinum in the electroplating bath was proposed. It was concluded that a ligand substitution reaction preceded an electron transfer step that resulted in the deposition of platinum:

$$Pt(NH_3)_4^{2+} + xH_2O \rightarrow Pt(NH_3)_{4-x}(H_2O)_x^{2+} + xNH_3 \qquad (1.6)$$

$$Pt(NH_3)_{4-x}(H_2O)_x^{2+} + 2e^- \rightarrow Pt(s) + (4-x)NH_3 + xH_2O \qquad (1.7)$$

It was noted that the efficiency of platinum deposition was very sensitive to temperature. At a temperature of 363 K the current efficiency for platinum deposition was 12 %. The current efficiency increased significantly at temperatures above 363 K. A current efficiency of 74 % was reported for the deposition of platinum using a temperature of 366 K. It was concluded that high temperature was essential to drive the slow ligand substitution reaction described in Equation 1.6.

Finally it was noted that the rate of platinum deposition may be increased if other PtL_4 complexes (L referring to a particular ligand), which are stable in solution but undergo ligand substitution at a more rapid rate compared to $Pt(NH_3)_4^{2+}$ could be identified.

The potential use of different types of PtL_4 complexes in electroplating baths was further investigated by Le Penven, Levason, Pletcher and other researchers[8]. Two different series of platinum complexes were evaluated, namely $Pt(NH_3)_{4-x}(H_2O)_x^{2+}$ and $PtCl_{4-x}(H_2O)_x^{(2-x)-}$. The ammonia complexes were present in a background electrolyte of 2.8×10^{-2} M Na_2HPO_4 (pH 10.3 to 10.6) at concentrations of 2.6×10^{-2} M Pt^{2+}. In the case of the chloro complexes, a background electrolyte of 1 M $HClO_4$ was employed. Platinum-195 NMR and potential sweep experiments were conducted.

It was reported that the ammonia complexes were extremely inert to ligand substitution reactions, and that these complexes were not directly electroactive. At pH 10.3 cathodic reactions occurred by a mechanism where ammonia ligands were displaced by water ligands. The rate of these ligand substitution reactions only became significant at temperatures above 368 K.

In turn it was found that the chloro complexes were far more susceptible to ligand substitution, and that these reactions occurred at room temperature. In addition, it was noted that the chloro complexes under investigation were reducible by direct electron transfer at room temperature.

It was however concluded that the major reaction pathway for the chloro complexes, as in the case for ammonia complexes, involved the displacement of the relevant ligand with water, followed by the electrochemical reduction of $Pt(H_2O)_4^{2+}$.

In conclusion it was noted that the dissolution of K_2PtCl_4 in water would be a facile way of producing Pt^{2+} in a readily reducible form. The presence of free chlorides in solution would however corrode the substrate in the electrochemical bath, making the use of such solutions impractical.

1.4.2 Electrochemistry of Palladium and Platinum Electrodes

Studies involving palladium and platinum electrodes contained in various solution matrices provide important information with regards to processes occurring at electrode-solution interfaces. Examples of such processes include metal oxide formation, hydrogen adsorption and absorption, and anodic dissolution mechanisms.

Palladium electrodes in sulphuric acid

Kim, Gossmann and Winograd[9] employed XPS techniques to study electrochemically oxidised palladium surfaces in 1 M H_2SO_4. Both PdO and PdO_2 were observed at potentials starting from 0.87 V versus a normal hydrogen electrode (NHE). These observations support Hoare's proposed mechanism for the formation of PdO_2[10] far below its equilibrium potential of 1.47 V. His scheme entailed *(i)* the formation of PdO at 0.87 V, *(ii)* the corrosion of palladium metal, *(iii)* the formation of PdO_2 on the electrode surface, and *(iv)* the slow decomposition of PdO_2 to form PdO. This proposed reaction mechanism is illustrated by the reactions shown in Equations 1.8 to 1.11:

$$Pd + H_2O \rightarrow PdO + 2H^+ + 2e^- \quad (1.8)$$

$$Pd \rightarrow Pd^{2+} + 2e^- \quad (1.9)$$

$$O_2 + Pd^{2+} + 2e^- \rightarrow PdO_2 \quad (1.10)$$

$$PdO_2 \rightarrow PdO + 0.5\,O_2 \quad (1.11)$$

At potentials more positive than 1.47 V, the palladium metal surface was directly oxidised to PdO_2:

$$Pd + 2H_2O \rightarrow PdO_2 + 4H^+ + 4e^- \quad (1.12)$$

Gossner and Mizerna[11] investigated the anodic behaviour of palladium

foil working electrodes in a 1 M H_2SO_4 matrix. Experiments involving CV and the measurement of the anodic and cathodic charges observed for the various voltammograms were employed during the investigation. All potentials were reported relative to a RHE.

The anodic behaviour of palladium was characterised by the corrosion of the metal at 0.80 V (Equation 1.13), followed by oxide formation at more positive potentials (Equation 1.14). The slow chemical dissolution of these oxide species in an acidic medium was also noted (Equation 1.15), whilst the formation of Pd^{4+} was also predicted at potentials more positive than 1.47 V (Equation 1.16):

$$Pd \leftrightarrow Pd^{2+} + 2e^- \quad (1.13)$$

$$Pd + H_2O \leftrightarrow PdO + 2H^+ + 2e^- \quad (1.14)$$

$$PdO + 2H^+ \leftrightarrow Pd^{2+} + H_2O \quad (1.15)$$

$$Pd + 2H_2O \leftrightarrow PdO_2 + 4H^+ + 4e^- \quad (1.16)$$

Anodic and cathodic charge amounts were interpreted in terms of metal dissolution, oxide formation, and diffusion of oxygen into bulk palladium. It was concluded that currents associated with each of these processes contributed to the overall anodic signal. The respective contributions of each of the mechanisms depended upon the applied potential.

In addition, it was found that the stability of the oxides formed on the palladium electrode surface depended on the switching potential used for a particular CV experiment, and the time the working electrode is held at a given potential. The degree of oxygen absorption was found to be dependent on the roughness of the palladium electrode surface.

Bolzán, Martins and Arvia[12] investigated the electrochemical behaviour of palladium electrodes in 1 M H_2SO_4 as a function of the perturbation

programme imposed on the working electrode. Various perturbation techniques were employed, including linear, triangular and repetitive triangular potential sweeps. All potentials were reported relative to a NHE.

It was found that the extent of electrode surface change depended on *(i)* the time scale of the potential perturbation, *(ii)* whether the PdO species formed are partially or completely reduced during the negative potential sweep, and *(iii)* the contribution of Pd^{2+} electrodeposition.

When repetitive triangular potential sweeps in the range $0.30\ V$ to $1.53\ V$ were applied to the palladium working electrode, it was found that the metal surface changed to a Pd_xO_y layer ($x >> y$). This was ascribed to the incomplete reduction of PdO species during the negative potential sweep of the perturbation. As a result, the anodic dissolution of palladium metal to Pd^{2+} was inhibited.

In addition it was noted that the deposition of Pd^{2+}, which also occurred during the potential perturbation programme, resulted in the presence of atoms at the metal surface that were not in equilibrium with the metal lattice:

$$Pd^{2+} + Pd_x(PdO) + 2e^- \rightarrow Pd^* Pd(PdO) \qquad (1.17)$$

where Pd^* denotes an electrodeposited palladium atom misfitting the equilibrium position in the metal lattice, and $x >> 1$.

After a prolonged repetitive triangular potential sweeps, sintering of the palladium surface was observed:

$$Pd^* Pd_x(PdO) \rightarrow Pd_{x+1}(PdO) \qquad (1.18)$$

The mechanism of oxide layer formation was also studied in detail. At potentials $< 1.1\ V$, the anodic charge was smaller than expected for the formation of an oxygen monolayer corresponding to one oxygen atom per

palladium atom at the electrode surface. It was concluded that a Pd(OH) layer formed under these conditions. The formation of $Pd(O)$, and the aging of the resulting oxide film (occurring via a place-exchange mechanism) was observed at potentials $< 1.5\ V$.

A thickening of the oxide layer was reported in the potential range $1.0\ V$ to $1.5\ V$ in a non-stoichiometric fashion, as illustrated in Equation 1.19:

$$Pd_x Pd(O) + (n+y)H_2O \leftrightarrow Pd_{x+1}O_{y+1}.nH_2O + 2yH^+ + 2ye^- \quad (1.19)$$

where $y > x$, and n indicates the number of hydration water molecules in the film.

It was also concluded that a new oxide species formed at potentials exceeding $1.2\ V$:

$$PdO + H_2O \rightarrow PdO_2 + 2H^+ + 2e^- \quad (1.20)$$

In a subsequent journal paper Bolzán, Martins and Arvia[13] continued their research related the electrodissolution of palladium electrodes immersed in $1\ M\ H_2SO_4$. In addition to the experimental techniques described in the previous journal article[12], repetitive triangular potential sweeps and combined perturbation functions were investigated by using of a Rotating Ring Disc Electrode (RRDE). The electrode was prepared by electroplating palladium on the disc and ring of a commercial platinum electrode.

It was reported that the formation of soluble Pd^{2+} in the low potential range ($< 1.0\ V$ relative to the RHE) could be explained on the basis of a competitive process involving a $Pd(OH)$ intermediate formed by the reversible oxidation of water:

$$Pd + H_2O \leftrightarrow Pd(OH) + H^+ + e^- \quad (1.21)$$

The $Pd(OH)$ intermediate formed via Equation 1.21 could either be involved in an electrodissolution process (Equations 1.22 and 1.23), or the electroadsorption of oxygen (Equation 1.24):

$$Pd(OH) \rightarrow Pd(OH)^{+} + e^{-} \quad (1.22)$$

$$Pd(OH)^{+} \leftrightarrow Pd^{2+} + OH^{-} \quad (1.23)$$

$$Pd(OH) \rightarrow Pd(O) + H^{+} + e^{-} \quad (1.24)$$

It was also concluded that the adsorption of HSO_4^- anions led to the formation of highly soluble $PdSO_4$, which enhanced the dissolution of palladium metal.

Burke and Casey[14] conducted research related to the development of an efficient cathode for a methanol/air fuel cell. This necessitated a study of the electrochemical behaviour of palladium electrodes in 3 M H_2SO_4. A palladium wire was employed as the working electrode, and for particular experiments the smooth electrode surface was coated with palladium black. All potentials were reported relative to a RHE.

From CV experiments conducted with a palladium black working electrode, it was found that the formation of an adsorbed hydroxide layer commenced at ca. 0.75 V when the potential sweep progressed to more positive potentials. At potentials more positive than 0.75 V, the formation of a place exchanged PdO film was reported. In addition, a small oxidation peak, ascribed to the formation of traces of PdO_3, was observed at 1.04 V.

On the return sweep of the CV plot, a reduction peak at 0.75 V was observed. This peak was associated with the reduction of the PdO monolayer formed on the preceding potential sweep. An additional broad and flat reduction peak was also observed at ca. 0.40 V. It was concluded

that the peak formed as a result of the reduction of incipient (i.e. low surface coverage) hydrous oxide species that are stable at potentials well below that observed for the reduction of normal PdO monolayers.

The formation of these stable hydrous oxide species was ascribed to the slow reaction of adatom species, i.e. metal atoms with a low bulk coordination number, with water molecules contained in the background electrolyte:

$$Pd^{*} + 6H_2O \rightarrow [Pd\,(OH)_6^{2-}]_{ads} + 6H^{+} + 6e^{-} \qquad (1.25)$$

where Pd^{*} refers to an adatom, and the subscript *ads* indicates an adsorbed species.

Palladium electrodes in sodium hydroxide

In addition to the research conducted in a 3 M H_2SO_4 matrix[14], Burke and Casey also investigated the phenomenon of incipient hydrous oxide or pre-monolayer formation in 1 M $NaOH$[15]. Apart from using a different background electrolyte, the experimental conditions were identical. The working electrode consisted of a palladium wire coated with palladium black, and all potentials were reported relative to a RHE.

It was found that pre-monolayer formation of $[Pd\,(OH)_6^{2-}]_{ads}$ also occurred in a basic background electrolyte. From CV analyses it was concluded that the pre-monolayer formation reaction could be observed on the forward sweep of the potential scan, i.e. progressing to a more positive direction, between 0.26 V and 0.68 V. It was also noted that this pre-monolayer oxidation process overlapped with the end of the hydrogen desorption region.

Bolzán[16] conducted a voltammetric study related to the electrochemical behaviour of palladium electrodes in 1 M $NaOH$. Chronoamperometry and CV experiments were used to characterise the electrosorption of

hydrogen and oxygen atoms. Fast reduction-oxidation (redox) systems and electrodissolution reactions were detected via modulated voltammetry and RRDE experiments.

A palladium wire was employed as the working electrode during voltammetric experiments, whilst the RRDE consisted of a gold ring and palladium disc. Potentials were reported relative to a RHE.

Potentiodynamic profiles obtained within the potential range applicable to the thermodynamic stability of water were divided into two regions. The first potential region involved reactions related to the electroadsorption and desorption of hydrogen atoms. In addition, the diffusion of hydrogen into bulk palladium was observed. A second potential region involved the electroformation and reduction of palladium oxide layers.

The sorbed hydrogen atom region was observed in the potential range 0.0 V to 0.60 V when a scan rate of 100 mV s^{-1} was employed during CV experiments. It was reported that hydrogen adsorption on the palladium surface preceded the absorption of hydrogen inside the metal lattice. The voltammetric desorption of hydrogen from bulk palladium was found to occur under mixed control, i.e. the process involved the diffusion of hydrogen to the electrode surface, followed by oxidation of the surface hydrogen.

It was also concluded that the initial stages of oxide layer formation on the palladium electrode surface commenced at potentials of ca. 0.68 V, and involved the formation of two distinguishable surface states. The initial layer consisted of $Pd(OH)$, which subsequently deprotonated to form a PdO species. Formation of a monolayer was concluded at a potential of 1.25 V. The oxide film at the monolayer level was also irreversibly transformed into a more stable structure via a place exchange mechanism. At potentials more positive than 1.25 V, the growth of a second oxide

layer consisting of PdO_2 commenced.

It was reported that the electrodissolution process related to the formation of Pd^{2+} involved the formation of a $Pd(OH)$ intermediate similar to that observed in a 1 M H_2SO_4 matrix (refer to Equations 1.22 and 1.23). The process in the alkaline medium was however hindered by the high OH^- concentration which stabilised the $Pd(OH)$ species.

Palladium oxide film formation as a function of pH

Burke and Roche[17] investigated the formation of oxide films on palladium metal electrodes as a function of pH. The mechanism of oxide growth was investigated via CV experiments, employing test solutions containing H_2SO_4 and NaOH. It was found that the potential for the onset of surface oxidation decreased with increasing pH. A decrease of ca. 13 mV per unit increase in solution pH over the range 2.0 to 13.5 was reported.

The potential shift in a more negative direction with increasing pH was ascribed to the formation of anionic species during the initial stages of surface oxidation:

$$Pd + (x+1)H_2O \rightarrow [PdO.xH_2O]^- + 2H^+ + e^- \qquad (1.26)$$

It was also noted that the initial anionic species formed in Equation 1.26 underwent a place-exchange type of reaction to form a more neutral deposit. The presence of an aggregate $[Pd(OH_6)]^{2-}$ species on the palladium surface was reported.

Palladium electrodes in perchloric acid

Chierchie and Mayer[18] studied the anodic formation of oxide layers on a polycrystalline palladium electrode contained in a 0.5 M $HClO_4$ solution via CV and LSV experiments. Potentials were reported relative to a NHE.

CV experiments were conducted in the range 0.35 V to 1.45 V, with the forward sweep progressing towards more positive potentials. The cathodic peaks observed on the return sweep (as a result of the reduction of various oxide species formed on palladium) were analysed. These analyses included the establishment of relationships between reduction peak potentials and the anodic switching potential employed for a particular CV experiment. In addition, cathodic charges were plotted as a function of applied anodic switching potentials.

It was concluded that different oxide species formed on the palladium electrode, depending on the applied potential. At potentials < 1.05 V, the formation of a PdOH monolayer was predicted. The slow electrochemical transformation of PdOH to a more stable PdO layer was observed between the potentials 1.05 V and 1.35 V. At the same time, surface reconstruction, i.e. site exchange processes between adsorbed species and the substrate atoms was reported. In an earlier paper Gossner and Mizerna[11] reported that surface reconstruction constituted the initial step for the diffusion of oxygen into bulk palladium.

Platinum electrodes in hydrochloric acid

Hawkins and Nicol[19] investigated the dissolution and passivation of platinum in an acid chloride medium.

Results obtained from steady state potentiostatic experiments were used to propose mechanisms for the dissolution of platinum and the evolution of chlorine. All potentials were reported relative to a NHE. The matrix of the solutions used for the steady state experiments varied between 1.75 M HCl and 6.08 M HCl. At potentials more positive than 1.10 V, the dissolution of platinum and the evolution of chlorine occurred simultaneously.

In order to propose mechanisms for these reactions, it was essential to separate the anodic current into partial currents due to platinum dissolution

and chlorine evolution. This was achieved via experiments involving *(i)* a flow cell method combined with spectrophotometric analyses, and *(ii)* the use of an electrode consisting of a platinum disc and a vitreous graphite ring.

It was concluded that the platinum dissolution reaction is first order in chloride, and that the transfer of the first electron is rate determining:

$$Pt + Cl^- \rightarrow PtCl^- + e^- \qquad (1.27)$$

A series of fast electron transfer steps would then produce a stable $PtCl_4^{2-}$ complex which would be oxidised to $PtCl_6^{2-}$ at more positive potentials.

It was also noted that the platinum dissolution rate decreased at potentials more positive than $1.15\ V$ when solutions containing between $2\ M\ HCl$ and $5\ M\ HCl$ were used. Steady state and CV experiments indicated that the passivation of the platinum surface occurred as a result of a slow oxide formation reaction at potentials more positive than $1.15\ V$. The low rate of oxide formation in chloride solutions relative to sulphate based solutions was ascribed to the slow desorption of chloro complexes which originally formed at more negative potentials relative to the oxide formation reaction.

Oxidation of an adsorbed $PtCl_4^{2-}$ complex at a potential of $1.01\ V$ was observed when a solution containing $2\ M\ HCl$ was used, whilst the same oxidation peak was observed at $0.74\ V$ in a $12\ M\ HCl$ matrix. The relative proportions of the products of this oxidation reaction were dependent on the chloride concentration. In solutions containing $12\ M\ HCl$, the $PtCl_6^{2-}$ complex predominated, whilst the $PtCl_5(H_2O)^-$ complex was found in $2\ M\ HCl$. It was noted that the formation of adsorbed chloro complexes resulted in the partial inhibition of the platinum dissolution process.

Platinum electrodes in sulphuric acid

Arvia, Folquer, Zerbino and Tacconi[20] investigated changes in the characteristics of oxygen monolayers on a platinum surface (aging) after treatment via a dynamic potentiostatic perturbation program. A platinum wire was used as a working electrode, and background electrolytes containing 0.1 M H_2SO_4 or 3.7 M H_2SO_4 were employed.

It was reported that the original oxygen bonds to platinum metal centres were modified to form more stable species during the dynamic aging process. The possible penetration of oxygen into the metal due to the reconstruction of the electrode surface by dynamic aging was also proposed. This was achieved by the redistribution of surface metal atoms resulting from the formation and breaking platinum-oxygen bonds.

Adsorption of oxygen on platinum in acid and alkaline media

Ragotzky and Tarasevich[21] proposed a mechanism for the electrochemical adsorption of oxygen on platinum surfaces in acid and alkaline pH ranges. The reaction scheme was based on the formation of MO products, via the formation of an intermediate product MOH, where M, O, and OH refers to the platinum metal surface, oxygen and hydroxide respectively. It was concluded that the formation of the MOH intermediate may result from an electrochemical reaction involving either water molecules or hydroxide ions as described in Equations 1.28 and 1.29:

$$M + H_2O \rightarrow MOH + H^+ + e^- \qquad (1.28)$$

$$M + OH^- \rightarrow MOH + e^- \qquad (1.29)$$

The formation of MO form the MOH intermediate was reported to proceed via three possible reactions involving *(i)* a dismutation process (Equation 1.30), *(ii)* an electrochemical reaction in the absence of hydroxide ions (Equation 1.31), or *(iii)* an electrochemical reaction with the

participation of hydroxide ions (Equation 1.32):

$$2MOH \rightarrow MO + M + H_2O \quad (1.30)$$

$$MOH \rightarrow MO + H^+ + e^- \quad (1.31)$$

$$MOH + OH^- \rightarrow MO + H_2O + e^- \quad (1.32)$$

The process was described quantitatively by incorporating data from potentiodynamic experiments into a mathematical model.

1.4.3 Anodic Dissolution of Precious Metals

Rand and Woods[22] studied the anodic dissolution of platinum, palladium, rhodium and gold electrodes in 1 M H_2SO_4 via CV. Following the CV experiments, background electrolytes were analysed for metal content (platinum, palladium, rhodium or gold depending on the electrode employed) by means of Atomic Absorption Spectroscopy (AAS) or spectrophotometric analyses.

Based on the difference between the anodic and cathodic charges recorded for each CV cycle, it was concluded that the anodic dissolution of platinum, palladium, rhodium and gold occurred in a 1 M H_2SO_4 matrix.

Evidence of anodic rather than cathodic dissolution (e.g. reduction of PtO_2 to Pt^{2+}) was derived from experiments involving the variation of dissolution rates with both potential and temperature.

Styrkas and Styrkas[23] investigated the electrochemical dissolution of platinum and palladium electrodes in acidic chloride and bromide electrolytes. It was concluded that dissolution of the electrodes or metal powders could be achieved via the application of an alternating current. The successful application of this technique resulted from the fact that passivating oxide layers, which formed during anodic polarisation was removed. The dissolution palladium and platinum was particularly efficient

in the presence of halides.

1.4.4 Voltammetric Study of Palladium at Carbon Paste Electrodes

Lubert, Guttmann and Beyer[24] investigated the voltammetric behaviour of Pd^{2+} in chloride solutions using a carbon paste working electrode.

The background electrolyte consisted of KCl at concentrations between 0.5 M and 1.0 M. In some cases HCl was added to adjust the pH, which varied between 2.1 and 5.5. The concentration of the analyte, $Na_2[PdCl_4]$, varied between 1×10^{-5} M and 1×10^{-4} M.

A carbon paste working electrode consisting of 5 g graphite powder (RWB, Ringsdorff) and 2.25 g paraffin oil was used. The reference was a silver-silver chloride electrode (Ag/AgCl) containing saturated KCl.

The application of CV revealed the presence of two reduction peaks (C1, C2), and two oxidation peaks (A1, A2). Peaks C1 and C2 were observed at ca. -0.2 V and ca. -0.8 V respectively. In the case of the anodic peaks A1 was observed at ca. -0.4 V, whilst A2 was observed at ca. 0.6 V.

The presence of Peak C1 was ascribed to the reduction of Pd^{2+} to Pd^0, or the combined reduction of Pd^{2+} and functional groups on the carbon surface. It was also noted that these reduction reactions were catalysed by the presence of palladium metal on the surface of the working electrode. Peak C2 was attributed to the possible reduction of carbonyl surface groups present on the working electrode. It was also noted that protons participated in the reaction.

Peak A1 was related to the oxidation of molecular hydrogen present at palladium metal surfaces deposited on the working electrode. It was reported that Peak A2 only appeared at pH $<$ 3, or pH 5.5 after potentiostatic treatment. Peak A2 was ascribed to *(i)* the oxidation of

deposited palladium or *(ii)* the oxidation of surface bound palladium complexes as illustrated in Equations 1.33 and 1.34:

$$Pd^{0} + 4Cl^{-} \rightarrow [PdCl_4]^{2-} + 2e^{-} \quad (1.33)$$

$$[Pd^{Y}Cl_m]^{2-} + (4-m)Cl^{-} \rightarrow [PdCl_4]^{2-} + (2-Y)e^{-} \quad (1.34)$$

where $|Y| \leq 2$ and $m \leq 4$.

An electroanalytical procedure for the determination of Pd^{2+} in solution was also proposed. It was suggested that palladium complexes may be immobilised at the carbon paste electrode surface via a polarisation step at 0.0 V. The exact structure and nature of the palladium complex could however not be elucidated from experimental data. During an anodic scan the surface bound palladium is oxidised at ca. 0.6 V. The oxidation peaks may then be used to determine the concentration of palladium immobilised on the electrode surface.

The amount of metal immobilised on the electrode surface depends on the composition of the test solution, polarisation time and stirring.

Lubert, Guttmann and Beyer[25] also investigated mechanisms related to the reduction of hydrogen ions and the subsequent oxidation of molecular hydrogen in the presence of $[PdCl_4]^{2-}$ via CV and potentiostatic pre-treatment experiments, using a carbon paste electrode.

A carbon paste electrode identical to that described in the previous journal paper[24] was used. The background electrolyte consisted of 0.5 M or 1.0 M KCl. The pH of the background electrolyte ranged between 3 and 7. The concentration of $[PdCl_4]^{2-}$ varied between 2×10^{-5} M and 3×10^{-4} M. A SCE was used in all cases, except for experiments involving potentiostatic pre-treatment, where a Ag/AgCl (saturated KCl) reference was utilised.

It was concluded that the reduction of hydrogen ions proceeded via different mechanisms, depending on the pH of the test solution. At a pH value of 3, a reduction peak at -0.75 V was observed. This peak was ascribed to the reduction of protonated chloropalladate species present on the surface of the carbon paste electrode:

$$[HPdCl_4]^- + 3e^- \rightarrow Pd^0_{sur} + H^0_{sor} + 4Cl^- \qquad (1.35)$$

where *sur* refers to the surface of the working electrode and *sor* refers to sorbed hydrogen, i.e. adsorbed and absorbed.

At pH values between 5 and 7 the reduction of hydrogen ions on deposited palladium metal centres was observed. It was concluded that hydrogen gas formed when palladium metal deposited between 0.25 V and 0.40 V.

The anodic peak observed at negative potentials was ascribed to the oxidation of molecular hydrogen present on deposited palladium metal centres. When test solutions with pH values between 5 and 7 containing higher $[PdCl_4]^{2-}$ concentrations (ca. 10^{-4} M) were used, two oxidation peaks resulted. It was concluded that the sorbed hydrogen was present at two energetically different states on the electrode surface under these conditions.

In a third paper Lubert, Guttmann and Beyer[26] concentrated on the anodic dissolution of palladium subsequent to its deposition on a carbon paste working electrode. The carbon paste electrode was again identical to that described in previous articles[24,25]. Background electrolytes consisting of 0.5 M KCl, adjusted to pH values between 3 and 6 by means of HCl were employed. The reference was a Ag/AgCl (saturated KCl) electrode.

Two anodic peaks were observed via CV experiments after the preceding

deposition of palladium metal. The first peak (A1) was observed at ca. 0.1 V , whilst the second peak (A2) was noted at ca. 0.5 V . It was concluded that Peak A1 indicated the anodic dissolution palladium present on the working electrode in monolayers or submomolayers. Peak A2 was ascribed to the anodic dissolution of a palladium multilayer.

It was suggested that several possible reaction mechanisms could be taking place if the working electrode containing deposited palladium metal was held at potentials > 0.8 V . The first reaction pathway would involve the formation of halide complexes on palladium metal centres in an initial dissolution step:

$$\left\{Pd^{0}\right\}_{Pd} + nCl^{-} \rightarrow \left\{\left[Pd^{II}Cl_{n}\right]^{-n+2}\right\}_{Pd} + 2e^{-} \qquad (1.36)$$

where the subscript *Pd* refers to localised palladium islands present on the original electrode surface.

The halide complexes would then undergo a desorption process to complete the dissolution step. This reaction pathway would give rise to Peak A2.

A second pathway involving the halide complexes formed via Equation 1.36 was also proposed. It was postulated that the application of potentials > 0.8 V resulted in the formation of carbon-chloride bonds at the carbon paste surface. The halide complexes present on localised palladium islands (illustrated in Equation 1.36) would then migrate to the "chlorinated" carbon regions by surface diffusion:

$$\left\{\left[Pd^{II}Cl_{n}\right]^{-n+2}\right\}_{Pd} \rightarrow \left\{\left[Pd^{II}Cl_{n}\right]^{-n+2}\right\}_{C} \qquad (1.37)$$

where the subscript *Pd* refers to localised palladium islands present on the original electrode surface, and subscript *C* denotes the carbon paste surface.

It was concluded that the halide complexes present on the carbon paste surface (refer to Equation 1.37) were reduced to Pd^0 or $\left\{\left[Pd^0Cl_n\right]^{-n}\right\}_C$ when the CV scan proceeded in a more negative direction. The associated reduction peak was noted at ca. 0.0 V. When the direction of the potential scan was reversed, the Pd^0 or $\left\{\left[Pd^0Cl_n\right]^{-n}\right\}_C$ was oxidised to form a halide complex on the carbon paste surface (refer to Equation 1.37). This reaction pathway would give rise to Peak A1.

1.4.5 Anion Interactions with Electrode Surfaces and Deposits

When the electrodissolution of palladium electrodes immersed in 1 M H_2SO_4 was investigated[13], it was noted that the presence of HSO_4^- anions led to the formation of highly soluble $PdSO_4$, resulting in an enhanced rate of metal dissolution.

Other journal papers related to the interaction of anions with a particular electrode material were encountered. Dunsch and co-workers[27] investigated the interaction of chloride ions with glassy carbon electrodes via ^{36}Cl radiotracer and galvanostatic experiments.

A strong interaction between chloride ions and the glassy carbon working electrode was reported at potentials more positive than 1.3 V on the RHE scale. It was concluded that a significant part of the chloride ions was chemically bonded to the surface of the glassy carbon electrode.

Attard and Al-Akl[28] characterised the structure of palladium films supported on a Pt(111) surface via the underpotential deposition (UPD) of copper. Experimental data was obtained from CV experiments. All UPD measurements were referenced to a copper wire (Cu^{2+}/Cu).

The nature of the anions in solution (HSO_4^-, Cl^-, Br^-) was reported to influence the stability of the palladium islands deposited on Pt(111)

surfaces. Palladium films in sulphuric acid were stable up to a potential limit of 0.6 V. At potentials more positive than 0.8 V palladium was stripped form the Pt(111) surface. In the case of the strongly adsorbed Cl^- and Br^- anions, palladium films were found to be stable up to potential of 0.3 V.

It was concluded that the desorption of multilayer palladium ions may be catalysed by the Cl^- and Br^- ions to produce an ordered palladium monolayer. In the presence of copper, further anodic dissolution of the palladium monolayer led to the formation of a copper-palladium surface alloy. This occurred via a place exchange mechanism involving halide anions and the palladium monolayer, as well as copper UPD on the copper-palladium surface alloy. Continued oxidative desorption led to the formation of an alloy rich in copper relative to palladium.

1.4.6 Reduction of Ammonia Complexes of Palladium

Tsventarnyi and Kravtsov[29] investigated the mechanism and kinetics of the electroreduction of $Pd(NH_3)_4^{2+}$ on a palladium disc RDE. The study involved the application of steady state CV, pulsed galvanostatic, and pulsed potentiostatic experiments. Test solutions containing different concentrations of $Pd(NH_3)_4^{2+}$ and NH_3 in the presence of 0.1 M NaF were used. The pH of these solutions was varied between 5.8 and 12.8.

Hydrogen adsorption and absorption processes complicated the analysis of recorded voltammograms, except for solutions adjusted to pH values of 12.8. It was found that the adsorption of hydrogen on the palladium electrode hampered the reduction of $Pd(NH_3)_4^{2+}$.

Results also confirmed the absence of a preceding chemical stage or specific interactions between $Pd(NH_3)_4^{2+}$ and the electrode surface during palladium electrodeposition. The reduction of $Pd(NH_3)_4^{2+}$ was reported to

occur via an overall two-electron transfer process. Transfer of the first electron determined the overall rate of the reaction, similar to the reduction mechanism observed at a Dropping Mercury Electrode (DME).

1.4.7 Electrochemistry of Chloride Complexes of Platinum

Hubbard and Anson[30] investigated the electrochemical oxidation and reduction of $PtCl_4^{2-}$ and $PtCl_6^{2-}$. A micrometer thin platinum electrode was used to conduct LSV and CV experiments. The effects of acidity and halide concentration were evaluated.

It was reported that the reduction of $PtCl_6^{2-}$ led to the formation of $PtCl_4^{2-}$ in 1 M HCl solutions. When a 1 M $HClO_4$ solution was employed as the background electrolyte, the reduction of $PtCl_6^{2-}$ directly proceeded to platinum metal.

The oxidation of $PtCl_4^{2-}$ in 1 M chloride solutions produced a mixture of $PtCl_6^{2-}$ and $Pt(OH)_2Cl_4^{2-}$.

A method for the separation and quantitative determination of $PtCl_4^{2-}$ and $PtCl_6^{2-}$ by means of ion chromatography and ultraviolet absorption detection was developed by Nachtigall, Artelt and Wünsch[31].

Apart from the complexes containing only chloride ligands, $PtCl_4^{2-}$ and $PtCl_6^{2-}$ both form a number of species in diluted aqueous solutions containing chlorides. Depending on *(i)* the platinum and chloride concentrations, and *(ii)* pH and temperature, the chloride ligands can be exchanged for water molecules. The latter may lose protons resulting in the formation of platinum-hydroxo complexes.

An investigation of $PtCl_4^{2-}$ and $PtCl_6^{2-}$ stock solutions (equilibrated over a

period of three months) by means of ion chromatography and ultraviolet detection at 215 nm was carried out to obtain a qualitative measure of the number of hydrolysis products associated with each of the platinum species. Five hydrolysis products were identified for $PtCl_6^{2-}$, and three for $PtCl_4^{2-}$.

The hydrolysis kinetics of $PtCl_4^{2-}$ and $PtCl_6^{2-}$ standard solutions in water was evaluated by plotting the ultraviolet absorption peak areas of a freshly diluted standard (with water) against time. Equilibrium was reached after approximately nine and thirty hours for Pt^{2+} and Pt^{4+} respectively.

1.4.8 Stability of Platinum Complexes

Forsyth and co-workers[32] investigated the electrochemistry of platinum complexes in the form of $H_3Pt(SO_3)OH$. Platinum was electroreduced from a solution of this complex acid onto glassy carbon in preliminary experiments and then onto carbon black based electrodes as used in polymer electrolyte membrane fuel cells. The reduction was carried out in a 0.5 M H_2SO_4 matrix. In addition, comparisons of platinum electrodeposition from H_2PtCl_6 and $Pt(NH_3)_4Cl_2$ solutions in 0.5 M H_2SO_4 were provided.

Linear sweep electroreduction experiments involving a glassy carbon electrode and a SCE reference indicated that $H_3Pt(SO_3)OH$ was very stable in comparison to the other two platinum species investigated. It was reported that the platinum sulphite acid was reduced at potentials more negative than -0.4 V, compared to $Pt(NH_3)_4^{2+}$ and $PtCl_6^{2-}$ which were reduced at potentials more negative than 0.0 V and 0.2 V respectively. It was concluded that the complexing ability of sulphite ions contributed to the high stability observed for $H_3Pt(SO_3)OH$. It was also noted that the electroreduction of $Pt(NH_3)_4^{2+}$ was slow from a kinetic point of view.

1.4.9 General Comments

From discussions related to the references provided under the preceding sub-headings it is clear that the interaction between particular PGMs and a selected cathode material is governed by a combination of aspects including speciation, the characteristics of the electrolyte, the solvent, the substrate, and the nature of the electrochemical perturbation applied to the working electrode.

These variables ultimately determine the mechanism for processes such as electrodeposition, electrodissolution, adsorption, absorption, catalysis and the inhibition of redox reactions. In order to develop an understanding of these processes in the context of the fundamental research project described via this dissertation, it would be necessary to conduct experiments with test solutions that reflect the characteristics of typical PML solutions.

Literature regarding the fundamentals of electrodepositing a combination of palladium and platinum on particular electrode materials, especially in systems approximating that of a PML solution, was generally unavailable. Methodologies for the study of electrodepostion mechanisms from multi-component solutions therefore had to be established.

1.5 FUNDAMENTAL RESEARCH OBJECTIVES

Based on limited availability of information in the literature, the overall aims of the project (Section 1.2), and research requirements (Section 1.3), the following objectives were defined for the fundamental research project:

- Establish methodologies that can be used to develop a qualitative understanding of the interactions occurring at an electrode-solution interface. The interaction between metal ions found in a typical PML solution, and a selected cathode material will be investigated. Special attention will be given to reactions involving the deposition of metals on a particular cathode, as well as factors that will catalyse or inhibit

certain redox reactions. Although issues related to the possible anodic dissolution of metals deposited on a cathode will receive some attention, the emphasis will be placed on the recovery of PGMs, as stated in the aims of the investigation.

- Use the established methodologies to assess the feasibility of recovering palladium and platinum from the PML using a particular cathode material in the proposed electrochemical reactor.
- If qualitative investigations indicated that the use of a particular cathode material was feasible, quantify the level of PGM reduction in the PML solution. This will confirm if the use of the proposed cathode material would result in the removal of the total PGMs present in the PML solution to concentrations < 10 mg l^{-1}, with no single PGM present at concentrations > 2 mg l^{-1}, as described in Section 1.2.1.
- Quantify the possible influence of amminated PGM complexes on the overall recovery of PGMs from a typical PML solution.
- Establish methodologies that may be used to determine kinetic parameters associated with a particular redox couple. These parameters include exchange current densities, electron transfer coefficients, standard rate constants and mass transfer coefficients.
- Use the established methodologies to determine kinetic parameters for selected redox couples. This data will quantify the rate at which the reactions take place at the electrode-solution interface, and can also be used for future engineering modelling purposes.

1.6 SUMMARY OF CHAPTERS

This dissertation contains six chapters, including the current chapter. In this chapter the overall aims of the investigation, a detailed literature review, and the objectives of the fundamental research project were provided.

In Chapter 2 (Experimental) the theory associated with the analytical techniques and instrumentation employed for the experiments described in the dissertation were discussed. The instrumentation, electrodes and equipment used were listed, and a general experimental procedure employed to perform voltammetric experiments was described.

To achieve the objectives stated in Section 1.5, research activities were carried out in three phases (Chapters 3 to 5):

- Phase 1 involved the establishment of qualitative methodologies to investigate the interaction between metal ions found in a PML and a particular cathode material. This was described in Chapter 3 (Qualitative Methodology).
- Phase 2 involved the application of established methodologies to assess the feasibility of recovering palladium and platinum from PML solutions via a particular cathode material. Where feasible, the level of PGM recovery was quantified. The potential influence of amminated PGM complexes on the overall recovery of PGMs from PML solutions was also quantified. This was discussed in Chapter 4 (Evaluation of Selected Cathode Material).
- Phase 3 involved the establishment of methodologies to determine exchange current densities, electron transfer coefficients, standard rate constants and mass transfer coefficients and the application of these methodologies to selected redox couples. This was described in Chapter 5 (Kinetic Parameters).

Chapters 3 to 5 contain introductory and concluding sections where the objectives and conclusions associated with each of the chapters were discussed. The concluding sections also contain a sub-section where future research activities were proposed. Each chapter includes a section where the experiments associated with a particular phase of the research project were described in detail. In some cases additional theoretical

information was provided to facilitate the discussion of results obtained for some of the experiments.

In Chapter 6 (Conclusions) the objectives of the research project were restated. It was shown how the objectives were achieved via the experiments conducted in Chapters 3 to 5. An overall summary of proposed future research activities was also provided.

Selected results were also presented in *Appendices A* and *B*.

Acronyms and selected terms used throughout the dissertation were defined in the *Nomenclature*. These acronyms and terms were also defined when they first occurred in the text of a particular chapter.

Details regarding the sign convention, units of expression and data presentation were provided at the start of each individual chapter.

2 EXPERIMENTAL

This chapter provides the following information related to experiments described in the dissertation:

- A statement regarding the sign convention adopted, and the units in which the various symbols and parameters were expressed.
- A discussion of the main analytical techniques employed, namely Cyclic Voltammetry (CV), Linear Scan Voltammetry (LSV), Chronoamperometry, and Rotating Disc Electrode (RDE) experiments in order to facilitate the interpretation of results presented in later chapters.
- Description of the instrumental set-up, electrodes and other components used to conduct the experiments, and the provision of a brief overview of the functioning of each of these components.
- A list of the make and model of instrumentation, electrodes and equipment used to conduct experiments involving the above-mentioned analytical techniques.
- A general procedure used to perform voltammetric experiments.

2.1 SIGN CONVENTION AND UNITS OF EXPRESSION

Unless otherwise stated, the following sign convention was used:

- Anodic currents are positive, and cathodic currents are negative.
- Making the potential more positive will increase the driving force for oxidation, whilst making the potential more negative will increase the driving force for reduction.

The units in which the various symbols and parameters in this dissertation are expressed correspond to the units indicated in the *List of Symbols*. In

cases where the units of expression are different to those stated in *the List of Symbols*, the relevant units are provided in the text.

2.2 ANALYTICAL TECHNIQUES

2.2.1 Introduction to Voltammetry

A wide variety of electroanalytical procedures are in use today. Interfacial methods are based on processes occurring at the interface between an electrode surface and a thin layer of solution adjacent to the surface. In turn, interfacial methods may be divided into two categories namely static and dynamic techniques. Static techniques involve potentiometric measurements where the potential of an electrochemical cell is recorded in the absence of appreciable current. In dynamic techniques the current produced in the electrochemical cell is of interest.

Voltammetry may be categorised as an interfacial dynamic technique. Information related to the analyte is obtained from the measurement of current as a function of applied potential under conditions that encourage the polarisation of a working electrode[33a], i.e. the electrode where the reaction of interest is taking place.

An ideal polarised electrode maintains a constant current and is independent of potential over a considerable range. The degree of polarisation is measured by overpotential (η). In order to encourage polarisation, working electrodes with typical surface areas of a few square millimetres are used. These electrodes are referred to as microelectrodes.

In summary, voltammetry may be defined as a technique where a variable potential is imposed on an electrochemical cell containing a polarisable microelectrode. The resulting current response is recorded as a function of the varied potential.

2.2.2 Cyclic Voltammetry

In CV, a cyclic linear potential sweep is imposed on a working electrode. A

current-voltage plot (voltammogram) is obtained by measuring the current at the working electrode during the potential sweep. The primary event is the oxidation or reduction of a chemical species at a working electrode.

CV is used extensively in the fields of electrochemistry, inorganic chemistry, organic chemistry and biochemistry. The technique can provide thermodynamic information as well as kinetic data related to electron transfer at an electrode-solution interface. In addition, CV can provide information related to the kinetics and mechanisms of chemical reactions subsequent to an electron transfer step. Some of the main advantages of CV are based on the fact that a wide potential range can be scanned rapidly for reducible and oxidisable species. These experiments can also be performed with variable time scales by applying different potential scan rates.

The shape of a typical voltammogram obtained after a CV experiment can best be explained by referring to the example in Figure 2.1, where the electrochemical behaviour of $K_3Fe(CN)_6$ was investigated[34a,35]. The potential scan is initiated at point a, and proceeds to more negative potentials (forward direction). When the potential is sufficiently negative to reduce $Fe(CN)_6^{3-}$, a cathodic current is evident (b) due to the following electrode process:

$$Fe(CN)_6^{3-} + e^- \rightarrow Fe(CN)_6^{4-} \qquad (2.1)$$

The cathodic current increases rapidly ($b - d$) until the current peaks at point d, the cathodic peak potential (E_{pc}). At this stage mass transport becomes the rate determining step. As the forward sweep proceeds from E_{pc} towards a more negative potential, the concentration gradient at the electrode-solution interface continues to decrease, resulting in a reduced rate of mass transport. This causes the current to decay ($d - f$).

The scan direction is switched to a positive direction at point *f* (switching potential) for the reverse scan. At this stage the potential is still sufficiently negative to reduce $Fe(CN)_6^{3-}$, and the cathodic current continues even though the potential scan is now proceeding in a positive direction.

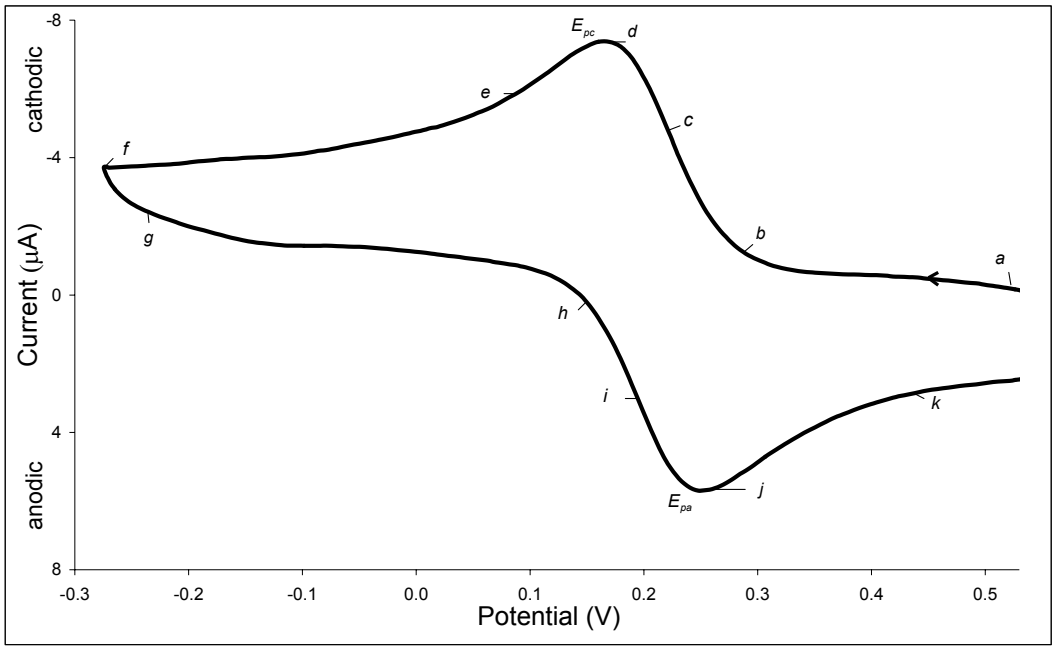

Figure 2.1 Cyclic voltammogram of 1 mM $K_3Fe(CN)_6$ in 0.1 M KCl (pH 3.0). Scan initiated at 0.6 V versus a Ag/AgCl (3 M KCl) reference electrode in a negative direction at 250 mV s^{-1}. Glassy carbon working electrode with disc diameter of 2 mm.

When the electrode becomes a sufficiently strong oxidant, $Fe(CN)_6^{4-}$, which has been accumulating adjacent to the electrode, can now be oxidised by the following electrode process:

$$Fe(CN)_6^{4-} \rightarrow Fe(CN)_6^{3-} + e^- \qquad (2.2)$$

This process produces an anodic current at point *h*. The anodic current rapidly increases ($h - j$) until the anodic peak potential (E_{pa}) at point *j* is reached, where mass transport becomes the rate determining step. The current then decays ($j - k$) as the solution surrounding the electrode is

depleted of $Fe(CN)_6^{4-}$. It should be noted that when the current decays beyond E_{pc} and E_{pa}, its magnitude becomes a function of time and is independent of the applied potential.

The first cycle of the CV experiment in this example is completed when the potential at point *a* is again reached. This cycle can now be repeated a number of times if required. In many cases the repeat cycles will provide valuable information regarding the processes taking place at the electrode surface. The use of multiple scans will be discussed separately in this section.

Reversible systems

Electrochemical reversibility refers to electron transfer reactions that are fast enough to maintain the concentrations of oxidised and reduced forms in equilibrium with each other at the electrode surface. The proper equilibrium ratio at a given potential is determined by the Nernst equation:

$$E_e = E^\circ - \frac{RT}{nF} \ln \left(\frac{[R]}{[O]} \right)_{x=0} \qquad (2.3)$$

where the standard electrode potential, E°, may be described as the half-cell potential with respect to the standard hydrogen electrode when the reactants and products are at unit activity and pressure.

It should be noted that the Nernst equation is theoretically expressed in activities rather than concentrations. Activity coefficient data for electrochemical work are limited, and consequently concentrations must be used. Although this approach is acceptable for test solutions approaching infinite dilution, appreciable errors may be encountered in the calculation of potentials for solutions at higher ionic strengths. Further deviations between molar concentrations and activities may be encountered due to solvation, association, dissociation, and complex

formation reactions involving the species of interest.

The peak current (i_p) for a reversible system is described by the Randles – Sevčik equation. Assuming that the forward sweep of the first cycle of a CV experiment is recorded at 298 K, then:

$$i_p = \left(2.69 \times 10^5\right) n^{3/2} A D^{1/2} \nu^{1/2} c \qquad (2.4)$$

where A = electrode area (cm^2); D = diffusion coefficient ($\text{cm}^2\ \text{s}^{-1}$); ν = potential scan rate ($\text{V}\ \text{s}^{-1}$); c = concentration of the reactive species in bulk solution ($\text{mol}\ \text{cm}^{-3}$).

Accordingly, the peak current for a reversible system is proportional to the square root of the scan rate, and directly proportional to the concentration of species present in the bulk solution.

The following diagnostic checks may be used to check for reversibility:

- The ratio of the anodic peak current (i_{pa}) and the cathodic peak current (i_{pc}) should be 1.
- The position of E_{pa} and E_{pc} will be independent of the scan rate.
- When the number of electrons transferred in the electrode reaction of a reversible couple at 298 K equals one, the separation between E_{pa} and E_{pc} will be between 57 mV and 60 mV.

The formal potential for a reversible reduction-oxidation (redox) couple is centered between E_{pa} and E_{pc}:

$$E^{\circ\prime} = \frac{E_{pa} + E_{pc}}{2} \qquad (2.5)$$

where the formal potential, $E^{\circ\prime}$, may be described as the half-cell

potential with respect to the standard hydrogen electrode when the concentrations of reactants and products are 1 M, and the concentrations of any other constituent of the solution are carefully specified.

The formal electrode potential was introduced as an alternative to the use of standard electrode potentials for the calculation of electrode potentials in an attempt to compensate for activity effects, as discussed with Equation 2.3.

Irreversible systems

Electrochemical irreversibility is caused by slow electron exchange of a particular species with the working electrode. In the case of irreversible systems, the Nernst equation is not obeyed. A reduction or oxidation reaction may be termed reversible or irreversible depending on the time domain of an electrochemical experiment. In the case of a CV experiment, a system will be irreversible if electron exchange is slow in comparison with the scan rate.

For an irreversible system, E_{pa} and E_{pc} will move further apart as the scan rates employed for a CV experiment are increased. As the scan rate is increased, E_{pa} will move to more positive potentials, whilst E_{pc} will move to more negative potentials. This is due to the fact that slow electron transfer reactions are driven by overpotential. Voltammograms for irreversible systems will therefore have a more drawn out shape compared to reversible systems.

Multi-electron transfer

Consider the following reversible two-electron transfer reaction:

$$Species\ 1 + e^- \leftrightarrow Species\ 2 \quad \left(E^{\circ'}1\right) \tag{2.6}$$

$$Species\ 2 + e^- \leftrightarrow Species\ 3 \quad \left(E^{\circ'}2\right) \tag{2.7}$$

Two scenarios regarding the formal potentials are possible. One possibility is that $(E^{\circ\prime}1) > (E^{\circ\prime}2)$, or alternatively $(E^{\circ\prime}1) < (E^{\circ\prime}2)$. Each of these scenarios will influence the characteristic shape of the voltammogram obtained from a CV experiment, as illustrated in Figure 2.2[36a].

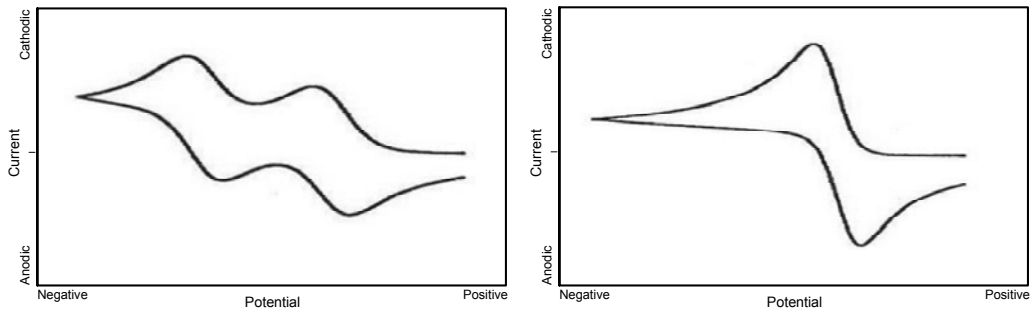

Figure 2.2 Characteristic shapes of voltammograms obtained for a two-electron transfer reaction. A double peak (voltammogram on the left) will result if $E^{\circ\prime}1 > E^{\circ\prime}2$, whilst a single overlapped peak (voltammogram on the right) will result if $E^{\circ\prime}1 < E^{\circ\prime}2$.

Multiple scans

Coupled homogenous reactions involve an electron transfer step leading to species that react with components of the particular medium where the electron transfer step occurred. One of the strengths of CV is to investigate these coupled homogenous reactions by generating a species during one scan, and following its response with subsequent scans.

Multiple scans may also be used to indicate changes in the properties of cathode materials. If for example metal ions in solution are reduced to their metallic state on an existing cathode material, it would be possible to monitor changes in the properties of the cathode via subsequent CV scans.

Adsorbed species

In some cases species can adsorb onto the electrode surface. Adsorption will be indicated by characteristic symmetrical peaks, as illustrated in Figure 2.3.

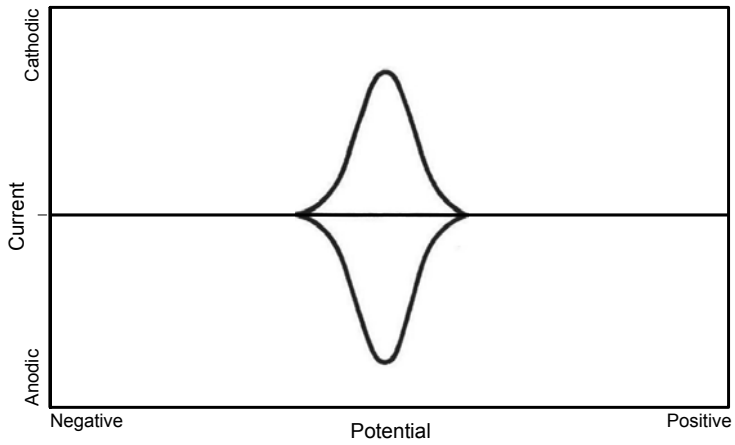

Figure 2.3 Cyclic voltammogram for the oxidation of an adsorbed reactant, assuming a reversible reaction.

The following diagnostic checks may be used to confirm the presence of adsorption peaks for a reversible electron transfer couple[37a]:

- Currents of the symmetrical adsorption peaks drop to zero once the reactant is fully consumed. The magnitude of these currents is dependent on the number of sites on the electrode surface where adsorption can occur.
- Adsorption peak currents are proportional to the potential scan rate.
- Separation between the forward and reverse peaks is 0 mV .

Consider the following oxidation reaction involving species R and O:

$$R - ne^{-} \leftrightarrow O \qquad (2.8)$$

If species R is strongly adsorbed to the electrode, the adsorption peak will appear at a more positive potential compared to the normal expected peak potential, since a higher overpotential would be required to oxidise the adsorbed species on the electrode surface. An example of a typical voltammogram obtained where species R is adsorbed onto the electrode surface is provided in Figure 2.4[37b].

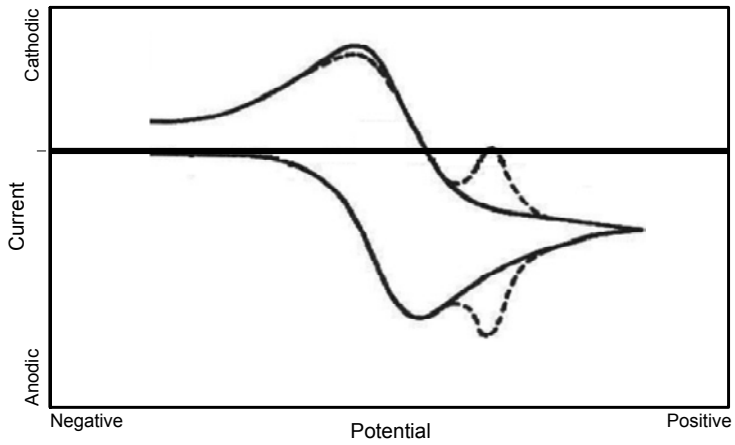

Figure 2.4 Voltammogram for the oxidation of species R. The dashed line shows the expected voltammogram with adsorption, whilst the solid line denotes a normal reversible reaction without adsorption.

The proportion of a particular species adsorbed onto a given electrode surface is determined by the total number of active sites available.

Phase formation

When metal ions are reduced to their respective metallic states, characteristic voltammograms indicating phase formation will result. A typical voltammogram illustrating this phenomenon is shown in Figure 2.5.

A metal ion M^{n+} is reduced to its metallic form M during the forward scan. For the reverse scan, it is noted that there is a potential range where the cathodic current density is higher than that for the forward scan. This is explained by the fact that metal nuclei of the species M need to be present to facilitate the deposition of metal ions M^{n+} at an appreciable rate. In order to form the nuclei an overpotential is required, which would explain the low current density observed for the forward scan. Nucleation and phase growth continues, and when the reverse scan commences conditions for the deposition of species M^{n+} are favourable from a thermodynamic and kinetic point of view.

A higher current density on the reverse scan will therefore result in the potential range where it is thermodynamically and kinetically feasible to deposit the metal species M.

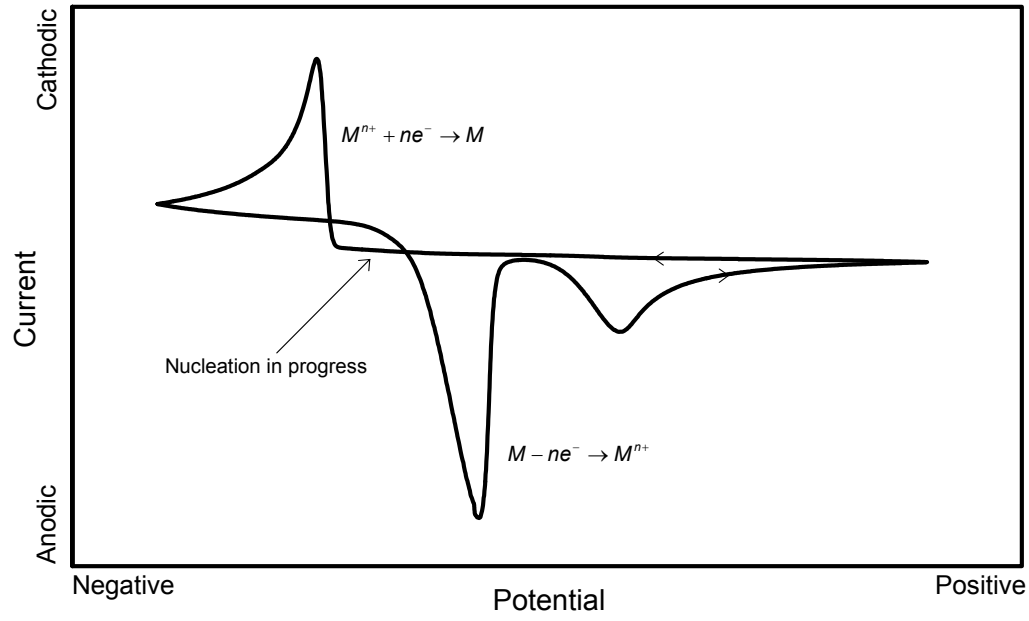

Figure 2.5 Cyclic voltammogram for the deposition of species M on an inert cathode, and the resulting oxidation of species M to M^{n+} ions.

As the reverse scan proceeds to more positive potentials a sharp symmetrical anodic peak (stripping peak) is observed as the metal layer deposited on the electrode is removed. The peak is symmetrical due to the fact that the metal is present on the electrode, as opposed to the normal means of transport to the electrode by diffusion. For the same reason the current for the stripping peak will be high relative to peaks obtained where transport to the working electrode occurs via diffusion.

2.2.3 Linear Scan Voltammetry

In CV, a cyclic linear potential sweep is imposed on a working electrode. A voltammogram is obtained by measuring the current at the working electrode during the potential sweep. The same principle is employed in LSV, except for the fact that the linear potential sweep is not cyclic. In

other words, the LSV curve will consist of a forward sweep only, compared to a forward and reverse sweep observed for CV.

In the course of the project described in this dissertation, LSV was mainly used to perform slow potential sweep experiments. The resulting $i-E$ plots were used for the calculation of kinetic parameters. More information regarding the calculation of kinetic parameters will be provided in Chapter 5.

2.2.4 Chronoamperometry

Chronoamperometry is defined as a potential step experiment. In a potential step experiment, the potential of the electrode is changed rapidly (effectively instantaneously) from a value where no current passes, i.e. no chemical change occurs at the surface, to one where the electrode reaction of interest takes place. Potential step experiments are well suited for determining exact kinetic parameters when a reaction mechanism is fully understood, but less suited for preliminary studies into reaction mechanisms.

In Chronoamperometry, the current versus time response is recorded subsequent to the potential step. Under diffusion controlled conditions, i.e. mass transport controlled with no additional stirring, the current (i) versus time (t) response is described by the Cottrell equation:

$$i = \frac{nFD^{½}cA}{\pi^{½}t^{½}} \tag{2.9}$$

where A = active electrode surface (cm^2); D = diffusion coefficient ($\text{cm}^2\ \text{s}^{-1}$); c = concentration of the reactive species in bulk solution (mol cm^{-3}).

In the context of the research project described in this dissertation, the Cottrell equation was used to calculate the electrochemically active

surface area of particular working electrodes. More information regarding the determination of active surface areas will be provided in Chapter 5.

2.2.5 Rotating Disc Electrodes

These electrodes consist of a disc of electronically conductive material surrounded by a sheath of insulating material with a diameter significantly larger than that of the disc. The faces of the disc and the sheath must be flush and the surfaces of both are polished flat. The rotation of the disc with its sheath leads to a well defined solution flow pattern.

The RDE acts as a pump by drawing the solution under study vertically upwards, before it is thrown outwards due to the fact that the solution cannot pass through the solid electrode surface.

A detailed mathematical discussion of the hydrodynamics of the RDE was provided by V G Levich and co-workers in the 1930s. The Nernst diffusion layer concept is extremely helpful in understanding experiments at the RDE. It may be used to derive equations needed to analyse experimental data, since Levich has deduced an expression relating the thickness of the hypothetical diffusion layer to experimental variables including the rotation rate (ω) of the disc electrode:

$$\delta = \frac{1.61\ \nu^{0.166} D^{0.33}}{\omega^{0.5}} \tag{2.10}$$

where δ = diffusion layer thickness (m); ν = kinematic viscosity ($m^2\ s^{-1}$).

The Nernst diffusion layer concept permits the derivation of the current density at a RDE for potentials where the electrode reaction is mass transport controlled. This derivation is known as the Levich equation:

$$i_L = 0.62\ nFD^{0.67} A \nu^{-0.166} c\omega^{0.5} \tag{2.11}$$

where c = concentration of species in bulk solution (mol m^{-3}); ν = kinematic viscosity (m^2 s^{-1}).

A test for mass transport control is therefore a plot of i_L versus $\omega^{0.5}$ (at a fixed applied potential) that is linear and passes through the origin.

The Levich equation assumes a laminar flow regime, i.e. the solution moves toward the electrode in a highly organised manner so that it may be considered to consist of a series of separate non-mixing layers. This is the case only below a critical rotation rate. With higher rotation rates a turbulent flow regime is achieved, and under these conditions the Levich equation will not be valid. Maximum rotation rates for RDE experiments are in the region of 6000 rotations per minute (rpm), depending on experimental factors such as the eccentricity of the rotation of the RDE support. There is also a minimum rotation rate for the equation to hold because it is necessary that forced convection dominate diffusion as well as natural convection. Normally a minimum rotation rate of 100 rpm is allowed.

2.3 INSTRUMENTATION AND ELECTRODES

A three-electrode cell configuration with potentiostatic control was used to conduct experiments involving the analytical procedures discussed in Section 2.2. In this configuration, the external circuit is arranged to maintain potential control between a working and a reference electrode. Current is measured between the working electrode and an auxiliary electrode. The use of a three-electrode system allows control of the working electrode potential relative to a reference electrode whilst the cell current is recorded.

A three-electrode electrochemical cell is made up of working, reference and auxiliary electrodes immersed in a supporting or background electrolyte containing the analyte. A brief description of the functioning and

characteristics of the most important electronic components, the various electrodes, and the cell design is provided in Sections 2.3.1 to 2.3.3.

2.3.1 General Principle of Potentiostatic Control

The purpose of a potentiostat is the accurate application of a desired potential to a working electrode. In general terms, the potential difference between a working and reference electrode is measured and compared against the desired potential. Based on the difference between the actual and desired potential, a current will be forced to flow between an auxiliary electrode and the working electrode. This current will cause the potential of the working electrode to shift towards the desired potential. The time taken to achieve this potential shift is in the microsecond domain.

In practice, potentiostatic control is achieved by means of operational amplifiers (OAs). A source voltage is connected to the positive input of an OA with negative feedback[38], as shown via OA-1 in Figure 2.6.

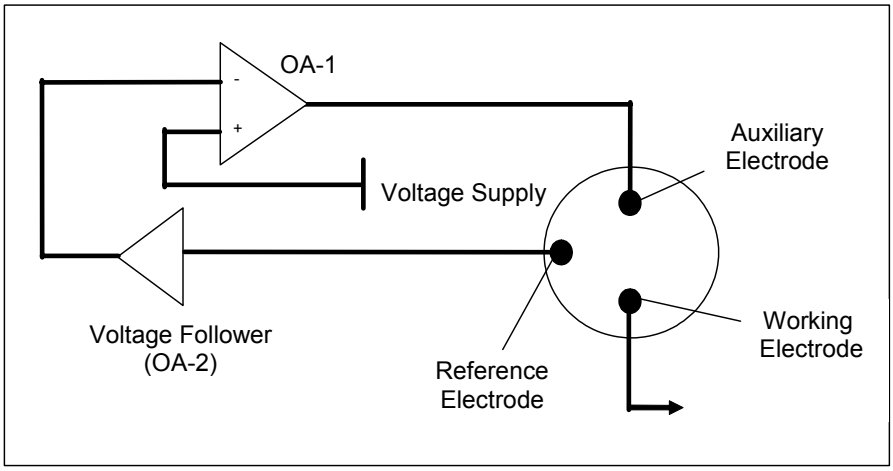

Figure 2.6 Schematic diagram of a potentiostat.

A feedback amplifier in the form of a buffer of unity voltage gain (voltage follower) is placed in the feedback loop as illustrated via OA-2 in Figure 2.6. The output from the reference electrode, which is a high impedance source, is connected to the voltage follower in order to produce a low impedance signal capable of producing considerable current. This allows

measurement of the potential difference between a working electrode and the buffered reference electrode.

The voltage follower (OA-2) consists of a circuit in which the input from the reference electrode is fed into the non-inverting and high impedance positive terminal, and the feedback loop is provided from the output to the inverting input of OA-1[33b]. Current at the output of OA-2 is drawn from the internal circuitry of the amplifier.

A typical three-electrode electrochemical cell is normally operated via the combination of a signal generator, a potentiostat and a current to voltage converter. The signal generator and current converter also function by means of OAs connected in different configurations. A schematic diagram of a typical electrochemical cell[33c] is illustrated in Figure 2.7.

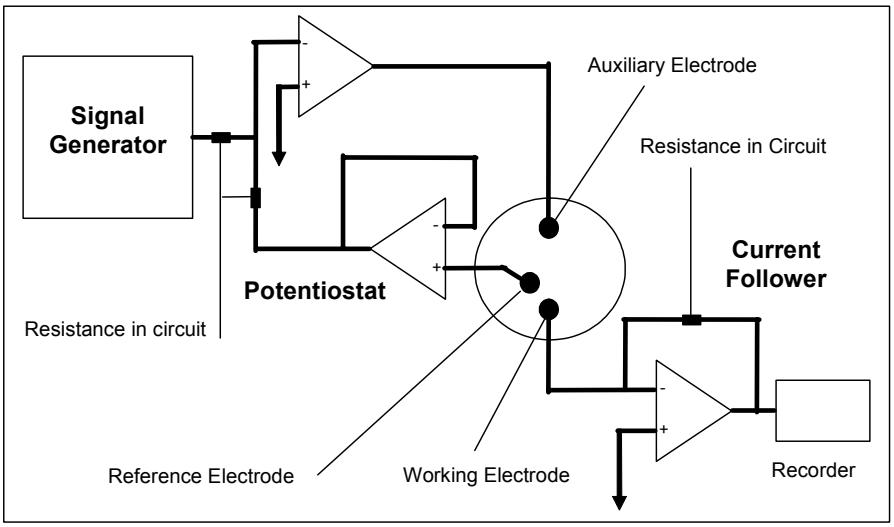

Figure 2.7 Schematic diagram of a typical three-electrode electrochemical cell.

The signal generator applies a variable potential output signal, which is fed into a potentiostatic control circuit. Typical waveforms include linear, differential pulse, square wave, and triangular excitation signals. The current flowing between the working electrode and the auxiliary electrode as a function of variable potential is measured by the current to voltage converter, also referred to as a current follower. In the current follower

mode, the current flows around the operational amplifier through a resistance. The voltage measured at the output is then proportional to the current and the resistance of the amplifier.

2.3.2 Electrodes

Working electrodes

The reaction of interest is studied via reduction or oxidation steps taking place at the working electrode. A large variety of working electrodes have been used in voltammetry. Solid electrode materials include glassy carbon, carbon paste, platinum, copper, silver, bismuth and gold available in different geometries, most commonly discs, wires or rings.

In polarography, a Static Dropping Mercury Electrode (SDME) is employed. Other mercury electrodes used for voltammetric experiments include the Hanging Mercury Drop Electrode (HMDE) and the Mercury Film Electrode (MFE).

One of the advantages of using mercury electrodes is the negative potential range that can be used prior to the reduction of hydrogen ions to hydrogen gas. The solid electrodes mentioned above are generally used in positive potential ranges where mercury will oxidise.

The main advantage of using a mercury electrode instead of a solid electrode is associated with the fact that memory effects, surface fouling and oxidation of the electrode surface can be eliminated by reproducing a fresh mercury layer.

Reference electrodes

The purpose of the reference electrode is to provide a known, constant half cell potential when used with the working electrode. In addition, the electrode should be insensitive to the composition of the solution under study. An ideal reference electrode must *(i)* be reversible and obey the Nernst equation, *(ii)* exhibit a potential that is constant with time *(iii)* return

to its original potential after being subjected to small currents and *(iv)* exhibit little hysteresis with temperature cycling[33d]. Since the current drawn from the reference electrode will be negligible, the required surface need not be large.

The two most commonly used references are the saturated calomel (SCE) and silver-silver chloride (Ag/AgCl) electrodes.

Auxiliary electrodes

Reactions at the auxiliary electrode are driven by the potentiostatic circuit to balance the faradaic process at the working electrode. If reduction takes place at the working electrode, oxidation will take place at the auxiliary electrode[36b]. The reactions at the auxiliary electrode should not affect or limit the reactions taking place at the working electrode in any way. If necessary, the anolyte and catholyte may be separated with a glass sinter or ion permeable electrode.

In order to ensure that the reactions taking place at the auxiliary electrode do not limit the current, the surface area is normally large in comparison to that of the working electrode.

In many cases the auxiliary electrode will consist of a glassy carbon rod or a platinum wire.

2.3.3 Electrochemical cell design

Different cell configurations, shapes and sizes are employed, depending on the nature and purpose of the experiments performed. A general purpose electrochemical cell for voltammetric measurements was used for the experiments discussed in the present document. This design will subsequently be described.

The reaction vessel consisted of a heavy walled glass container that tapered to the bottom. This allowed the analysis of different volumes of

sample. The glass container was jacketed to allow coupling to a constant temperature water bath.

Dissolved oxygen reduction waves often interfere with the analysis of other species present in the analyte solution. For this reason, the cell was fitted with a purge tube in order to bubble nitrogen gas through the analyte solution. The stream of nitrogen gas removed any dissolved oxygen present in solution.

In order to prevent complications due to substances leaking from the reference electrode, or fouling of the reference electrode interface in contact with the analyte solution, direct contact between the electrode and the solution was prevented. This was achieved by placing the reference electrode in a salt bridge, which only allows the flow of charged ions between the analyte solution and the electrolyte present in the salt bridge. In the majority of experiments the filling solution for the salt bridge had the same composition as the background electrolyte containing the analyte.

When the rates at which positively and negatively charged ions diffuse across a salt bridge junction are different, charge separation occurs. A junction potential develops, causing errors in the measurement of voltages applied to the working electrode. Junction potentials are minimised by using electrolyte ions such as K^+ and Cl^- which have similar diffusion coefficients[34b]. It should be noted that junction potentials also develop between the reference electrode and the electrolyte present in the salt bridge.

The accurate measurement of the potential between the reference and working electrodes will also be influenced by the ohmic or iR_u loss between the tip of the salt bridge and the working electrode. The voltage obtained by the product of the current (i) and the uncompensated resistance (R_u) is recorded across the electrode-solution interface,

resulting in potential measurement errors. To minimise iR_u drop, the tip of the salt bridge was placed as close as possible to the working electrode, and a background electrolyte of high conductivity was used.

2.4 LIST OF EQUIPMENT, ELECTRODES AND REAGENTS

The instrumentation, electrodes, equipment, reagents and solutions used to carry out the analytical procedures discussed in Section 2.2 are listed below.

2.4.1 Electroanalytical Equipment

- Autolab/PGSTAT10 (Eco Chemie, the Netherlands) connected to a 663 VA Stand (Metrohm, Switzerland) via an IME 663 interface (Eco Chemie) to obtain a three-electrode cell configuration with potentiostatic control.
- GPES 4.7 software for control of the equipment, real time monitoring of experiments and subsequent data analysis (Eco Chemie).
- Jacketed reaction vessel (Metrohm, order no. 6.1418.220).
- Salt bridge with a ground glass sleeve (Metrohm, order no. 6.1245.000).
- Connector and driving shaft for solid working electrodes used on 663 VA Stand (Metrohm, order no. 6.1246.000).
- PTFE stirrer tip (Metrohm, order no. 6.1204.080).

2.4.2 Electrodes

- Glassy carbon auxiliary electrode rod (Metrohm, order no. 6.1247.000).
- Ag/AgCl (3 M KCl) reference electrode; (Metrohm, order no. 6.0278.000).
- Glassy carbon tip working electrode with disc diameter of 2 mm for 663 VA Stand (Metrohm, order no. 6.1204.110).

- Platinum tip working electrode with disc diameter of 2 mm for 663 VA Stand (Metrohm, order no. 6.1204.120).
- Custom made working electrodes manufactured from isostatically pressed graphite (Electrographite Carbon Co., grade ET-10). More information will be provided in relevant chapters.

2.4.3 Other Equipment and Consumables

- Stereo microscope (Micro Met Scientific, FST 652 stereo).
- Compound microscope (Micro Met Scientific, Nova IN 713).
- Camera used with stereo or compound microscopes (JVC, model C721EG).
- Software for microscopes (Archive4Images).
- Constant temperature water bath (Labcon, CPE 100 circulator).
- Ultrasonic bath, with output frequency of 0 – 50 Hz (Integral Systems).
- Polishing wheel (Struers, DAP-2).
- Polishing cloth with 203 mm diameter for use on DAP-2 polishing wheel (IMP, IMPCLOTH, PSA, part no. 080344).
- Synthetic diamond paste with 1 μm particle size for use on IMPCLOTH (IMP, part no. 010172).
- Diamond extender blue, used as lubricant with synthetic diamond paste (IMP, part no. 070031).
- Magnetic stirrer motor (Metrohm, E549).
- Magnetic stirrer bar, PTFE, length 1 cm.
- Magnetic retriever rod, PTFE, length 30 cm.
- pH meter (Beckman, Φ72).

- pH combination electrode (Metrohm, pH 0 – 14, 80 °C, order no. 6.0234.100).
- Water supply system, capable of producing ultra pure water with a resistivity (ρ) of 18.2 M Ω cm (Millipore, Milli-Q Synergy).
- Nitrogen gas (Afrox, ultra high purity, 99.999 %).
- Fume hood covering electrochemical cell.
- Filter paper circles, diameter 110 mm (Schleicher & Schüll, reference no. 311610; or Whatman no. 1).
- Polishing kit consisting of aluminium oxide powder and polishing matte for use with glassy carbon and platinum tip working electrodes (Metrohm, order no. 6.2802.000).
- Hand held autopipettes with disposable tips. Three separate pipettes were used covering the volume ranges 1 – 100 μl ; 100 – 1000 μl and 1 – 5 ml (Genex Beta).
- Top pan balance, 2 decimal places in gram units (Precisa 300 C).
- Analytical balance, 4 decimal places in gram units (Precisa 180 A).
- Drying oven, maximum temperature 250 °C (Scientific, Series 2000).

2.4.4 Reagents and Solutions

- Potassium chloride, KCl , MM = 74.55 g mol^{-1}, Analytical Reagent (AR) grade; (Saarchem).
- 3 M KCl solution: A mass of 44.73 g KCl was weighed out, dissolved in ultra pure water and made up to a volume of 200 ml .
- Silver chloride, AgCl , MM = 143.34 g mol^{-1}, Laboratory Reagent, (BDH).
- Hydrochloric acid, HCl , 32 % , MM = 36.46 g mol^{-1}, AR grade, (NT

Laboratory Supplies).

- 0.1 M HCl solution: The solution was prepared by diluting a volume of concentrated AR grade acid by a factor of ten, using ultra pure water.
- 6 M HCl solution: The solution was prepared by diluting a volume of concentrated AR grade acid by a factor of 1.6, using ultra pure water.
- pH 4 buffer solution (Metrohm, order no. 6.2037.100).
- pH 7 buffer solution (Metrohm, order no. 6.2307.110).

2.5 EXPERIMENTAL PROCEDURE

Analytical techniques involving CV, LSV, Chronoamperometry and RDE experiments were carried out using a standard procedure. This entails *(i)* the storage of electrodes and related accessories, *(ii)* preparation and cleaning of electrodes and equipment, *(iii)* connection of the various components of the three-electrode electrochemical cell, and *(iv)* general steps followed when conducting a specific experiment.

The electrodes, equipment, consumables, reagents and solutions referred to are described in detail in Section 2.4.

2.5.1 Storage

Salt bridge

Between different sets of experiments the cleaned salt bridge (ground glass sleeve loosened) was stored in a 0.1 M HCl solution. A fresh storage solution was prepared weekly.

Reference electrode

The cleaned Ag/AgCl (3 M KCl) reference electrode was stored in a solution of 3 M KCl to which a small amount of AgCl salt was added. A fresh storage solution was prepared weekly.

Auxiliary electrode

To prevent unnecessary handling of the fragile glassy carbon rod, the electrode was fitted to the auxiliary electrode holder in the 663 VA Stand assembly on receipt, and was not removed after a set of experiments. The clean electrode was stored inside the empty reaction vessel of the 663 VA stand, still attached to the holder in the stand assembly.

Working electrode

The cleaned solid working electrodes were either stored in the containers in which they were delivered after purchase, or a custom built Perspex holder.

Stirrer tip

The cleaned stirrer tip was stored in the container in which it was delivered after purchase.

2.5.2 Preparation and Cleaning

Reaction vessel, stirrer bar, auxiliary electrode and salt bridge

Prior to a new set of experiments, the following procedure was followed:

Preparation step 1. The auxiliary electrode, already connected to the 663 VA Stand was thoroughly rinsed with ultra pure water and carefully dried with a clean filter paper circle.

Preparation step 2. The reaction vessel cover was rinsed with ultra pure water. Subsequently the reaction vessel itself was emptied and rinsed with ultra pure water at least three times before drying the vessel and cover with a clean filter paper circle.

Preparation step 3. The salt bridge assembly was thoroughly rinsed with ultra pure water (ground glass sleeve loosened). The empty salt bridge was dried with a filter paper circle.

Preparation step 4. The magnetic stirrer bar was rinsed with ultra pure

water at least three times before it was dried with a filter paper circle. The dried stirrer bar was placed in the clean reaction vessel.

Preparation step 5. The stirrer tip (if used for a particular set of experiments) was rinsed with ultra pure water at least three times before it was dried with a filter paper circle. The dried stirrer tip was connected to driving shaft for solid electrodes used on the 663 VA Stand.

General note. Preparation steps 1 to 5 were carried out on the assumption that the cleaning steps (as described below) were followed after a set of experiments.

After a set of experiments, the following procedure was followed:

Cleaning step 1. The reaction vessel cover was lifted before the auxiliary electrode, salt bridge assembly, working electrode and stirrer tip connected to the 663 VA Stand were thoroughly rinsed with ultra pure water and carefully dried with a clean filter paper circle.

Cleaning step 2. The salt bridge assembly was taken out of the reaction vessel cover and the reference electrode was removed. Following this, the electrolyte solution remaining in the salt bridge was discarded and the ground glass sleeve of the salt bridge loosened, before rinsing the vessel with ultra pure water. The rinsing step was repeated at least three times before the salt bridge was carefully dried with a filter paper circle.

Cleaning step 3. The magnetic stirrer bar was recovered from the reaction vessel via a magnetic retriever rod. Both the stirrer bar and retrieving rod were thoroughly rinsed with ultra pure water before the bar was dried with a filter paper circle.

Cleaning step 4. The stirrer tip was rinsed with ultra pure water at least three times before it was dried with a filter paper circle.

Cleaning step 5. The solution in the reaction vessel was discarded. The vessel was rinsed at least three times with ultra pure water before it was

dried with a filter paper circle, and returned to the stand.

Cleaning step 6. The stirrer bar and salt bridge (sleeve loosened) was placed back in the reaction vessel cover, which still contained the auxiliary electrode and the stirrer tip. The fume hood covering the reaction vessel and experimental assembly was switched on. The reaction vessel was filled with 6 M HCl, and the cover was lowered onto the vessel. The HCl solution was stirred via the connector and driving shaft for solid working electrodes (rotating electrode option, using the stirrer tip) for approximately ten minutes.

Cleaning step 7. Following the acid cleaning step, the auxiliary electrode, salt bridge, stirrer tip and reaction vessel cover was thoroughly rinsed with ultra pure water before drying with a filter paper circle. The stirrer bar was recovered via a magnetic retriever rod. Both the stirrer bar and retrieving rod was thoroughly rinsed with ultra pure water before the bar was dried with a filter paper circle.

Cleaning step 8. The reaction vessel containing the 6 M HCl was emptied and rinsed at least three times with ultra pure water before drying with a filter paper circle.

Cleaning step 9. The stirrer bar was wrapped in paper towel and stored in a drawer, whilst the auxiliary electrode, reference electrode, salt bridge and stirrer tip was stored as described in Section 2.5.1, until the next set of experiments commenced.

Reference electrode

The Ag/AgCl (3 M KCl) reference electrode was removed from its storage solution and rinsed with ultra pure water prior to use. The electrode was carefully dabbed dry, using a clean filter paper circle.

On completion of experimental work, the electrode was again rinsed, dried and placed back into its storage solution.

Solid working electrodes

Prior to and after a particular set of experiments, the working electrode was rinsed at least three times with ultra pure water before it was dried with a filter paper circle. Following the rinsing step, one of four preparation techniques was employed:

Method 1. Three filter paper circles were placed on top of each other on a Perspex plate. A few drops of ultra pure water were dispensed on the filter papers. The electrode surface was polished on the filter paper surface using small circular motions. Polishing of the electrode surface was alternated between the dry and wet parts of the filter papers. The entire area on the filter paper was utilised in order to prevent polishing of the surface on areas containing contaminants previously removed from the electrode. Finally the electrode was rinsed with ultra pure water and dabbed dry with a clean filter paper circle.

Method 2. The electrode surface was polished using an aluminium oxide powder and matte kit. The electrode was then rinsed with ultra pure water and placed in a 100 ml glass beaker containing ultra pure water. The glass beaker containing the electrode was placed in an ultrasonic bath for approximately two minutes. Following this, the electrode was prepared as described in Method 1.

Method 3. The electrode surface was prepared on a polishing wheel, using a cloth impregnated with synthetic diamond paste and a lubricant. The polishing wheel was rotated at 125 rpm. A custom built Perspex holder was used to keep the electrode in place on the polishing wheel. Following the polishing step, the electrode was rinsed with ultra pure water and dabbed dry with a clean filter paper circle.

Method 4. In the case of custom made electrodes (isostatically pressed graphite), the active surface was prepared by sanding the surface with a fine emery paper. The electrode was then rinsed with ultra pure water and dabbed dry with a filter paper circle. More information regarding the

preparation of custom built electrodes will be provided in the relevant chapters.

2.5.3 Assembly and General Procedure

Prior to a new set of experiments, the electrodes and equipment were connected and operated in a specific sequence.

Assembly

Step 1. The reaction vessel cover was lifted to facilitate the installation of the necessary components.

Step 2. The salt bridge was filled with a suitable electrolyte. Normally the electrolyte was identical to the background electrolyte in the reaction vessel.

Step 3. The reference electrode was fitted to the salt bridge, and the salt bridge-reference electrode assembly placed into the reaction vessel cover. The reference electrode was then connected to the VA Stand assembly.

Step 4. The auxiliary electrode (left in reaction vessel cover after cleaning) was connected to the VA Stand assembly.

Step 5. The working electrode was fitted to the reaction vessel cover and connected to the VA Stand assembly.

Step 6. The stirrer tip (if required for the particular experiment) was fitted to the stirrer motor drive shaft.

General procedure

Step 1. A magnetic stirrer bar was placed into the clean reaction vessel, before a suitable background electrolyte was added. The volume of electrolyte added was normally between 10 ml and 20 ml. If actual refinery effluents were analysed, a suitable volume was added directly to the reaction vessel.

Step 2. The reaction vessel cover, in which the various electrodes and components were fitted, was lowered onto the reaction vessel in order to establish contact between the electrodes and the solution in the vessel.

Step 3. The constant temperature water bath, already connected to the jacketed reaction vessel was switched on. The temperature was regulated between 24.9 °C and 25.1 °C, and all experiments were conducted within this range. Sufficient time was allowed (approximately 30 minutes) to ensure that the solution in the reaction vessel reached the temperature maintained by the water bath.

Step 4. The stirrer motor situated below the reaction vessel was switched on to facilitate mixing via the magnetic stirrer bar. If the stirrer tip was fitted, the motor for the stirrer tip drive shaft was switched on and set to a speed suitable for the particular experiment.

Step 5. The nitrogen gas supply was opened to purge oxygen from the solution contained in the reaction vessel. A minimum time of 15 minutes was allowed for the purging step.

Step 6. The appropriate electroanalytical technique was selected via the instrument software. The relevant information and parameters required for the experiment was entered.

Step 7. A background electrolyte was analysed via the selected electroanalytical technique, using a suitable potential range. This experiment was used to check for *(i)* the absence of any impurities in the background electrolyte, *(ii)* the presence of memory effects associated with the working electrode, or *(iii)* any anomalies associated with the experimental set-up. If any abnormalities associated with the above-mentioned checks were observed, the preparation and cleaning procedure described in Section 2.5.2, or the assembly procedure in Section 2.5.3 was repeated, depending on the nature of the problem identified whilst analysing the background electrolyte. Following the repeat of procedures described Section 2.5.2 or Section 2.5.3, the background electrolyte was

analysed again to check if the original abnormality was corrected.

Step 8. Following the satisfactory analysis of the background electrolyte, suitable aliquots of metal ion solutions (depending on the objective of the experiments) were added to the background electrolyte contained in the reaction vessel by means of hand held pipettes with disposable tips. Different experiments were conducted after the addition of a particular metal ion or combination of metal ions to the background electrolyte (e.g. different scan rates or potential ranges), again depending on the objective of the set of experiments. All results were recorded and stored via the instrument software control package.

Step 9. If refinery effluents were analysed, the background electrolyte was discarded if no abnormalities were observed (Step 6), and replaced with the particular effluent. Oxygen was purged from the effluent prior to conducting the planned set of experiments.

General note. Between different experiments, the solution in the reaction vessel was stirred, with the nitrogen gas supply turned on to ensure the continued removal of oxygen.

2.6 GENERAL

This chapter provided a general description of the analytical techniques employed, instrumental set-up and electrode requirements, equipment and reagents used, and general procedures followed to conduct electroanalytical procedures. Where applicable, additional detailed information regarding a particular phase of the project will be provided in the relevant chapter. This will include the following aspects:

- Different types of working electrodes were employed at different stages of the project. Some of the electrodes were commercially available, whilst other had to be constructed in-house. The type and construction of the different working electrodes will be specified in the relevant chapters of the dissertation.

- Where necessary, additional theoretical information will be provided with regards to the application of electroanalytical procedures to address a particular phase of the research project.
- The experimental design, calculations and data handling procedures used in each of the project phases will be described with the applicable chapter of the dissertation.
- Information regarding particular reagents and solutions not mentioned in this chapter will be provided where applicable.

3 QUALITATIVE METHODOLOGY

3.1 INTRODUCTION

In Chapter 1 the overall objectives of the project, namely the electrochemical recovery of Platinum Group Metals (PGMs) from refinery effluents were discussed. The rationale for using the Palladium Mother Liquor (PML) in studies related to the project was also explained. In addition, the need to conduct two different research projects covering fundamental research and engineering aspects in order to obtain the overall objectives of the project was highlighted.

The first phase of the fundamental research project described in this dissertation involved the development of a qualitative understanding of the interactions of the different metal ions found in the PML with a particular cathode material. This information was used to evaluate the cathode material selected for the electrochemical reactor, developed as part of the engineering project[39].

3.1.1 Cyclic Voltammetric Experiments

A survey of the different available electroanalytical techniques indicated that Cyclic Voltammetry (CV) could be used as a powerful tool in the interpretation of reactions occurring at an electrode-solution interface. Details regarding the principles and applications of CV are provided in Chapter 2.

Although CV could potentially provide valuable qualitative information with regards to the interaction between ions and a solid electrode, the current-voltage plots (voltammograms) obtained from these experiments may become difficult to interpret. This is especially true where multi-component solutions such as the PML are involved, due to the overlap of different cathodic and anodic peaks.

The interpretation of voltammograms becomes even more difficult where metal ions are reduced to their metallic states on the working electrode employed for the experiment. The presence of metal centres on a working electrode will change the overall characteristics of the electrode, and therefore influence the thermodynamic and kinetic information obtained at the electrode-solution interface. In addition, the presence of particular active metal centres, or combinations of different metal centres can potentially catalyse or inhibit a given reduction-oxidation (redox) reaction. Based on the objectives of the project, namely to remove PGMs from refinery effluents, it was clear that a study of the PML would include the reduction of metal ions to their metallic states on a working electrode.

The fact that CV involves the study of a dynamic system also has to be considered when voltammograms are interpreted. In other words, it should be kept in mind that the reactions taking place at the working electrode-solution interface at any given instance during a particular experiment depend on a number of variable conditions and parameters. The most important variables are listed below:

- The potential of the working electrode.
- The physical state and condition of the working electrode.
- The presence, quantity and morphology of active metal centres on the original working electrode surface.
- The ratio and concentration of electrochemically active components present in the bulk solution.
- The nature of the background electrolyte and other complexing agents present in the bulk solution.

The inherent difficulties associated with the interpretation of voltammograms involving multi-component solutions and metal deposition would therefore make the study of a solution such as the PML (refer to

Table 1.1) very difficult. This fact is confirmed if the voltammogram of a typical PML solution shown in Figure 3.1 is studied.

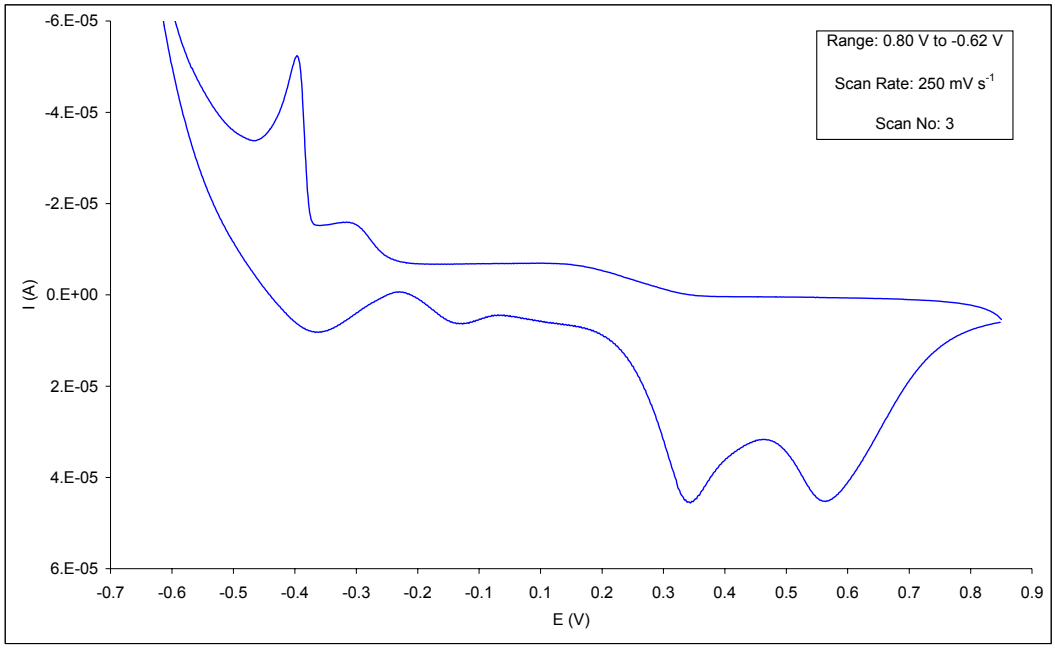

Figure 3.1 Cyclic voltammogram of a typical Palladium Mother Liquor solution. Scan initiated at 0.80 V versus a Ag/AgCl (3 M KCl) reference electrode in a negative direction. Glassy carbon working electrode with disc diameter of 2 mm.

The complexity of the PML voltammogram is further highlighted when it is compared to a voltammogram obtained for a simple redox couple involving $Fe(CN)_6^{3-}/Fe(CN)_6^{4-}$ as shown in Figure 2.1.

It became clear that if CV was to be used as a tool to understand the interactions between metal ions contained in the PML and a selected cathode, suitable methodologies with regards to the interpretation of the resulting voltammograms had to be found.

3.1.2 Objectives

The objective of the research data presented in this chapter was to develop the necessary methodologies required to interpret

voltammograms involving multi-component solutions and metal deposition. If successful, these methodologies would establish the use CV as a tool in the qualitative study of the interaction between metal ions contained in the PML and a proposed cathode material. An added advantage of establishing the methodologies required for the interpretation of voltammograms involving PML solutions is that these techniques could also be applied to future studies of other refinery streams for the purpose of electrochemical metal removal.

In Chapter 1 it was stated that the nature of the project necessitated confirmation of the feasibility of removing PGMs from refinery effluents in a relatively short period of time, considered from a research point of view. It was also explained that fundamental research activities were focussed on the provision of information that could be used in the development of a practical electrochemical reactor. As a consequence, time and resources that could be allocated to different aspects of the research project was limited. It was therefore not the intention to investigate the many complex reaction mechanisms taking place at the working electrode in detail. The large data base obtained during this phase of the project would however provide a solid foundation for future detailed fundamental studies.

3.2 EXPERIMENTAL DESIGN AND DATA PRESENTATION

3.2.1 Working Electrode

In the majority of cases, a glassy carbon working electrode was employed for experiments described in this chapter. The glassy carbon electrode was selected for several reasons. Although the design of the proposed electrochemical reactor (engineering project) was not finalised when the first phase of this research project commenced, it was clear that a three-dimensional cathode configuration would be required to deal with the low concentrations of PGMs typically contained in PML solutions (refer to Table 1.1). This design normally involves the use of particulate cathode materials. At the time, the engineering project team indicated the possible

use of carbon or graphite. The major reason for using a glassy carbon electrode was therefore to exploit possible similarities in the behaviour of this commercially available electrode, and the actual cathode materials proposed for the electrochemical reactor.

In addition, literature revealed that glassy carbon electrodes were used in electroanalytical studies associated with PGMs and metal deposition. Details of the literature review are supplied in Chapter 1. It was reasoned that relevant literature could be used to assist in understanding the resulting voltammograms obtained whilst using a glassy carbon working electrode.

3.2.2 Experimental

In order to interpret the complex voltammograms obtained from typical PML solutions, the influence of major and minor metal ions found in a typical PML solution was investigated.

Major metal ions

- Single component synthetic solutions of the major metal ions found in the PML namely copper, palladium and platinum were prepared. Details regarding the preparation of these solutions are provided in Section 3.3.

- The voltammograms resulting from these single metal ion interactions with a glassy carbon electrode in an acid chloride matrix (0.1 M HCl) were recorded and analysed. The final concentration of a particular metal ion in solution approximated that found in a typical PML solution. Details regarding the dilution of the synthetic single metal ion solutions are provided in Section 3.3.

- Once a qualitative understanding of the behaviour of a single metal ion at the glassy carbon electrode-solution interface was established, the complexity of the solutions analysed via CV was increased gradually. Voltammograms of different combinations of copper, palladium and

platinum in a matrix of 0.1 M HCl were recorded and analysed. The final concentration and ratios of the different metal ions in solution approximated that found in a typical PML solution. Details regarding the addition of different synthetic single metal ion solutions are provided in Section 3.3.

Particular emphasis was placed on the identification of peaks associated with the reduction of a particular metal ion to its metallic state and the possible anodic dissolution of the resulting metal centres found on the original working electrode surface. Processes related to hydrogen gas formation and inhibition also received special attention.

Minor metal ions

Following experiments involving the three major metal ions found in the PML, the possible influence of the remaining minor metal ions was investigated:

- Single component synthetic solutions of the minor metal ions found in a typical PML solution, namely antimony, arsenic, bismuth, gold, iridium, lead, nickel, rhodium, ruthenium, selenium, silver, tellurium, tin and zinc were prepared. Details regarding the preparation of these solutions are provided in Section 3.3.

- The voltammograms of the interaction between these single metal ions and a glassy carbon electrode in an acid chloride matrix (0.1 M HCl) were recorded and analysed. The final concentration of a particular metal ion in solution was ca. 50 mg l^{-1}. Details regarding the dilution of the synthetic single metal ion solutions are provided in Section 3.3.

- Voltammograms of different combinations of copper, palladium, platinum, and a particular minor metal ion in a matrix of 0.1 M HCl were recorded and analysed. The final concentration and ratios of the major metal ions in solution approximated that found in a typical PML solution, whilst the concentration of the minor metal ion was ca. 50

mg l^{-1}. Details regarding the addition of different synthetic single metal ion solutions are provided in Section 3.3.

The emphasis regarding the study of the electrochemical behaviour of the minor metal ions with a glassy carbon electrode was different compared to the approach followed for the major metal ions. Concentrations of the minor metal ions in the PML was very low in relation to the three major metal ions (refer to Table 1.1). It was reasoned that the influence of the minor components in the PML on the overall interaction of metal ions with the glassy carbon electrode will be associated with catalytic or inhibitive processes induced by the presence of active metal centres (even in small quantities) on *(i)* the original electrode surface or *(ii)* other active metal centre surfaces.

Attention was therefore focussed on the possibility of reducing the minor metal ions to their metallic states in the potential region utilised for a 0.1 M HCl matrix. If metal deposition was feasible, it follows that catalytic or inhibitive processes were possible.

The final minor metal ion concentration used in CV experiments was ca. 50 mg l^{-1} instead of concentrations of < 10 mg l^{-1} normally found in a typical PML solution. This was done to prevent possible interpretational errors due to issues related to detection limits or the inherent sensitivity of the technique.

Interpretational techniques

To interpret the complex voltammograms obtained when a typical PML was analysed, a systematic process was adopted. Synthetic solutions of all the metal ions found in the PML were prepared and analysed individually. The complexity of the test solutions was then gradually increased to approximate that of a typical PML. This approach alone could however not provide a suitable qualitative explanation of the interactions

taking place at the working electrode. Several additional interpretational approaches had to be employed, and are listed below:

- Variation of the potential ranges used for a particular CV experiment.
- The use of Fe^{3+} as a witness ion.
- Using a platinum disc working electrode in addition to the glassy carbon electrode.

The use of these interpretational techniques will be discussed, where applicable, in Section 3.5.

3.2.3 Data Presentation

The sign convention and units of expression defined in Chapter 2 (Section 2.1) also applies to the current chapter.

It should be noted that the voltammograms illustrated in Figures 3.1 to 3.22 represent the raw data obtained from a particular experiment, without additional background subtraction or smoothing operations. The peaks in Figures 3.2 to 3.22 that are labelled with the letter “C” denote cathodic peak potentials (E_{pc}) recorded during a particular experiment, whilst peaks labelled with the letter “A” refer to anodic peak potentials (E_{pa}). If more than one voltammogram was shown in a particular figure, differentiation was achieved via line colour and thickness.

Where multi-component metal ion solutions were analysed, the sequence of metal addition will be indicated via a text box associated with the particular illustration. If for example, a solution containing both copper and palladium ions was analysed, and the copper was added to the background electrolyte prior to palladium, the text box will indicate “Cu + Pd”.

The first potential scan of each CV experiment progressed to more

negative potentials, compared to the starting potential. All experimental potential values were measured relative to a silver-silver chloride (Ag/AgCl) reference electrode containing a 3 M KCl solution. The active surfaces of all working electrodes employed for the various experiments described in this chapter had a disc diameter of 2 mm.

Where Fe^{2+}, Fe^{3+}, Cu^{+} or Cu^{2+} is mentioned in the text, reference is made to the oxidation state of the metal ion as opposed to a particular species present in the test solution.

3.3 ELECTRODES, REAGENTS AND PROCEDURES

The information provided in Section 2.4 (equipment, electrodes, reagents) and Section 2.5 (experimental procedure) is also applicable to experiments described in this chapter. Additional information particularly relevant to experiments discussed in the subsequent sections of Chapter 3 is provided here.

3.3.1 Electrodes

A commercial glassy carbon tip working electrode with a disc diameter of 2 mm (Metrohm, order no. 6.1204.110) was used. In some cases a commercial platinum tip working electrode with a disc diameter of 2 mm (Metrohm order no. 6.1204.120) was employed.

3.3.2 Reagents, Solutions and Sample Addition

Major metal ions

Stock solutions for copper, palladium and platinum were prepared in an acid chloride medium.

Copper stock solution. A mass of 0.36 g Analytical Reagent (AR) grade $CuSO_4.5H_2O$, supplied by Merck, was dissolved in 0.1 M HCl and made up to a volume of 10 ml, using the same acid. This produced a solution with a copper ion content of 9.1 g l^{-1}.

In the majority of cases 0.20 ml of the copper stock solution was added to the reaction vessel (described in Section 2.4.1) used for CV experiments. Normally the 0.20 ml aliquots of the stock solution were added to 10 ml of background electrolyte present in the reaction vessel to produce a final copper metal ion concentration of 178 mg l^{-1}. Additions were made by means of hand held autopipettes described in Section 2.4.3.

Palladium and platinum stock solutions. Stock solutions of 10 g l^{-1} palladium and 10 g l^{-1} platinum in a 20 % HCl matrix were obtained from the Anglo Platinum Research Centre (ARC). These solutions were prepared by dissolving the relevant metal ($>$ 99.99 % purity) in a mixture of ultra pure hydrochloric and nitric acids. The nitric acid remaining after the dissolution step was decomposed and boiled off. The remaining solution was diluted with ultra pure water to produce the appropriate metal and hydrochloric acid concentrations.

In the majority of cases 0.20 ml of the palladium stock solution was added to the reaction vessel used for CV experiments. Normally the 0.20 ml aliquots of the stock solution were added to 10 ml of background electrolyte present in the reaction vessel to produce a final palladium metal ion concentration of 196 mg l^{-1}. Additions were made by means of hand held autopipettes described in Section 2.4.3.

In most cases 0.05 ml of the platinum stock solution was added to the reaction vessel. Normally the 0.05 ml aliquots of the stock solution were added to 10 ml of background electrolyte present in the reaction vessel to produce a final platinum metal ion concentration of 50 mg l^{-1}. Additions were made via hand held autopipettes described in Section 2.4.3.

Minor metal ions

Minor metal ion stock solutions were obtained from ARC. The precious metal ion stock solutions (gold, rhodium, iridium, ruthenium) were prepared from their respective pure metals ($>$ 99.99 %), whilst the

remainder of the stocks were obtained by the dilution of commercial ampoules. Details regarding the preparation of these stocks are provided in Table 3.1.

Table 3.1 Preparation of minor element stock solutions.

Element	Original Matrix	Preparation
Ag	Ampoule - 5 % HNO_3	Dilute with H_2O
As	Ampoule - H_2O	Dilute with H_2O
Au	Metal	Aqua Regia Dissolution
Bi	Ampoule - 20 % HCl	Dilute with 20 % HCl
Ir	Metal	Pressure Dissolution
Ni	Ampoule - H_2O	Dilute with H_2O
Pb	Ampoule - H_2O	Dilute with H_2O
Rh	Metal	Pressure Dissolution
Ru	Metal	Pressure Dissolution
Sb	Ampoule - 24 % HCl	Dilute with 20 % HCl
Se	Ampoule - 6.3 % HNO_3	Dilute with H_2O
Sn	Ampoule - 24 % HCl	Dilute with 20 % HCl
Te	Ampoule - 50 % HCl	Dilute with 20 % HCl
Zn	Ampoule - 0.06 % HCl	Dilute with 20 % HCl

Note: The final concentrations of all solutions were 1 g l^{-1}, except for gold, which had a final concentration of 5 g l^{-1}.

Aliquots of 0.50 ml of the minor element stock solutions were added to the reaction vessel used for CV experiments. Normally the 0.50 ml aliquots of the stock solution were added to 10 ml of background electrolyte present

in the reaction vessel to produce a metal ion concentration of 48 mg l^{-1}. Additions were made by means of hand held autopipettes, as described in Section 2.4.3.

Other solutions

Iron stock solution. A mass of 2.75 g AR grade $FeCl_3.6H_2O$, supplied by Saarchem, was dissolved in 0.1 M HCl and made up to a volume of 100 ml, using the same acid. This produced a solution with an iron content of 5.7 g l^{-1}. Aliquots of 0.20 ml of the iron stock solution were added to the reaction vessel, normally containing 10 ml of background electrolyte to produce a final metal ion concentration of 111 mg l^{-1}. Additions were made by means of hand held autopipettes.

Background electrolyte. A 0.1 M HCl solution was used as the background electrolyte. The preparation of this solution is described in Section 2.4.4. The background electrolyte was added to the reaction vessel by means of a hand held autopipette, described in Section 2.4.3.

3.4 ELECTRON TRANSFER AT THE ELECTRODE SURFACE

Knowledge of the variables influencing the electron transfer event occurring at a solid electrode-solution interface is essential in fundamental studies. These variables include characteristics associated with the electrode and electrolyte solution. In addition, the reactants, intermediates and products (present in solution) that are associated with electron transfer reactions will be influenced by factors such as solvation and complexation.

A short theoretical discussion related to the aspects highlighted above, as well as a brief explanation of important processes in the context of this research project, namely adsorption, metal deposition and the catalytic generation of hydrogen gas in an acid medium will be provided here[37c,40,41].

The information supplied in this section is intended to provide the basic background required to support and clarify statements in Section 3.5. Additional detailed information related to issues involving reactions taking place at the electrode-solution interface is provided in the literature review section found in Chapter 1.

3.4.1 Solid Electrodes

Two types of electrodes are important in terms of the project described in this dissertation. These are carbon based electrodes and metal electrodes.

Carbon based electrodes

Carbon materials are used widely in electrochemical manufacturing processes due to a number of reasons:

- High thermal and electrical conductivity.
- Availability in compact and disperse forms.
- Chemical and electrochemical stability.
- Raw material available at low cost.

Examples of some of these manufacturing processes include chlorine and fluorine production, and electrometallurgical processes in melts and aqueous solutions.

From an electroanalytical point of view, carbon electrodes allow the study of reactions normally not accessible at a mercury electrode. Carbon also meets the practical requirements for the use and production of solid electrodes for electroanalytical purposes, namely a large useful potential range, ability to be incorporated into an electrode, and surfaces that can be refreshed (polished).

Carbon is mainly found in nature as graphite, diamond and fossil fuel. Artificial forms of carbon include activated carbon, carbon blacks, pyrolytic

graphite, glassy carbon and various fibres, fabrics and thick felts. The different physical and physicochemical properties associated with each of these forms of carbon can be ascribed to the fact that the atom can be in different states of hybridization, and therefore form various types of bonds.

Glassy carbon. Since a glassy carbon working electrode was used in many of the experiments described in this chapter, the properties of the material will be described briefly. Glassy carbon crystals of approximately 100 Å consist of two types of carbon, namely a tetrahedral modification (diamond structure) and a trigonal modification (graphite structure). The tetrahedral structure contributes to the inherent hardness of glassy carbons. Glassy carbon has both closed and open porosity with an average pore size of 20 Å. The glassy carbon structure may be described as containing ribbons of thin carbon sheets resembling graphite, with some cross linking.

Glassy carbon is impermeable to gas and highly resistant to chemical attack, although mixtures of sulphuric acid and nitric acids can decompose the material.

Surface chemistry of carbon electrodes. The carbon surface can bind to elements such as nitrogen, halogens, sulphur and oxygen to form surface compounds. Some examples describing the bonds between different elements and carbon surfaces are provided:

- Activated carbon will form bonds with nitrogen if treated with ammonia at temperatures between 750 °C and 900 °C. Nitrogen can also be incorporated into carbon material during its preparation stage by using particular raw materials. The presence of carbon-nitrogen bonds were reported after the preparation of graphite fibres from polyacrylonitrile.
- The halogens form stable complexes with carbon surfaces. The stability of the bonds decrease in the series $Cl > Br > I$.
- If carbon materials are heated at temperatures between 700 °C and 900 °C in the presence of hydrogen sulphide or sulphur dioxide,

carbon-sulpur bonds will form.

- Surface bonds involving oxygen are formed in the manufacturing process or activation of carbon materials, and upon adsorption of molecular oxygen on the surface. Some of the main oxygen containing functional groups found on carbon surfaces includes carboxylic, phenolic, carbonylic and lactonic groups.

  It was reported that glassy carbon contained many oxygen functional groups after electrochemical pre-treatment[3]. The pre-treatment involved potential cycling of the glassy carbon electrode between 0.40 V and 1.5 V versus a Saturated Calomel Electrode (SCE), in a 0.1 M K_2SO_4 matrix.

From the examples it is clear that the presence of surface compounds on carbon electrodes is a function of the starting material, the manufacturing process and the conditions used to operate these electrodes. It should be noted that the characteristics of the solution in contact with the electrode surface contribute to the overall operating conditions. The quantity and characteristics of surface compounds will play a significant role in electron transfer processes taking place at the electrode surface.

It should also be noted that the carbon electrode itself could undergo oxidation, depending on the applied potential[42a].

Metal electrodes

The bulk structure of metals is determined by the packing arrangement of its constituent atoms. Three arrangements are common, namely the hexagonal closed packed lattice (e.g. zinc), the face centred cubic lattice (e.g. copper, gold, nickel and platinum) and the body centred cubic lattice (e.g. iron). Bulk metals are formed by the continuous repetition of a particular fundamental unit.

The surfaces of metal electrodes play an important part in reactions taking place at the electrode-solution interface, especially in the case of

adsorption. Normal metal electrodes are polycrystalline and consist of a combination of crystal planes. A single crystal plane is exposed by cutting through a particular crystal lattice (e.g. face centred cubic lattice) at a specific angle. These crystal planes are described by means of Miller indices.

The crystal planes have a characteristic arrangement of atoms and exhibit different catalytic activities. The difference in catalytic activity can be ascribed to *(i)* the ability of a particular surface to interact with polyatomic molecules, *(ii)* the possibility that several adsorption sites can interact with a single adsorbed species, *(iii)* the fact that two or more species present on the electrode surface can interact with each other.

The sum of all the reactions taking place at a polycrystalline metal electrode will therefore be a function of the characteristics of the different exposed crystal planes. Defects in a crystal lattice may also influence the reactions taking place at the electrode surface.

Exposed surfaces of most metals are oxidised if it is in contact with air, or in solution if held at potentials favourable for oxidation. The stability of many of these metal surfaces to anodic dissolution is due to the presence of a passivating oxide layer. If oxide layers are present on a metal surface, its characteristic adsorptive and chemical properties will also change.

The influence of surface oxides on the thermodynamics and kinetics of electrode transfer processes will be determined by the thickness of the oxide layer and the properties of the oxides.

3.4.2 Electrolyte Solutions

Solutions used for electrochemical experiments consist of a solvent, an electrolyte and an electroactive species.

Solvents

The purpose of the solvent is to dissolve the electrolyte in order to produce a solution with conductivities suitable for electrochemical experiments. Water is the most common solvent and was also used in the research activities described in this chapter. Water is a good solvent for acids, bases and salts. The following properties of water contribute to its effectiveness as a solvent:

- Water molecules form hydrogen bonds with other water molecules, resulting in the formation of oligomers. It should however be noted that the structures formed are not rigid, due to the continuous breaking and formation of hydrogen bonds.
- Water molecules are easily polarised, and interact electrostatically with charged species. Ions are therefore readily solvated.
- Water can act as a proton donor or a proton acceptor.

Electrolytes

The electrolyte, if ionised to a high degree, will serve the following purpose:

- Make the activity coefficients of the reactant and product equal, allowing for the cancellation of these terms when applied to the Nernst equation.
- Minimise the effects of the electrical double layer.
- Minimise ohmic or iR_u drop between the tip of the salt bridge and the working electrode when conducting electroanalytical experiments.

3.4.3 Reactants, Intermediates and Products

The thermodynamics and kinetics of reactions involving electron transfer are influenced by the interaction of reactants, intermediates and products with the various components that are contained in the solution in which

they are present.

Interactions involving the stabilisation of a particular reactant, intermediate or product in solution will make the subsequent reduction or oxidation of these species more difficult. This will result in the shift of formal potentials for reduction reactions to more negative potentials. In the case of oxidation reactions, formal potentials will shift to more positive potentials.

When reactants are transformed into products, or products are formed via intermediates, the rate of product formation will be determined by the degree to which the structures of the reactants or intermediates are altered to form the product. The kinetics of a particular redox couple will decrease if *(i)* changes to the geometry, *(ii)* changes to the number of ligands *(iii)* ligand substitution, or *(iv)* large changes in bond lengths or bond angles occurred when the product was formed.

Transition metals in an aqueous medium, including those formed by PGMs, have several characteristic features:

- The metals are present as solvated cations. The cations are surrounded by tightly bound water molecules (in many cases six). These hydrated complexes are stable in acid solutions. As the pH of the solution is increased, a stepwise replacement of water molecules by hydroxide ions will take place, and eventually a metal hydroxide will precipitate.
- The transition metals may form stable metal-ligand complexes, for example $Fe(CN)_6^{3-}$ and $Fe(CN)_6^{4-}$. The Fe^{3+} and Fe^{2+} metal ions are surrounded (octahedrally) by six cyanide ligands. These complexes are very stable and no ligand dissociation occurs, even in the absence of other cyanide ligands. Since the solvent is not directly involved in bonding to the metal centre, the redox potential will be independent of the solvent. In addition, it can be predicted that the kinetics associated

with the $Fe(CN)_6^{3-}/Fe(CN)_6^{4-}$ couple will be rapid, due to the absence of significant structural changes during the redox process.

- Many metal-ligand complexes involving a series of equilibria may be formed:

$$M(H_2O)_6^{n+} + L \leftrightarrow M(H_2O)_5L^{n+} + H_2O \quad (3.1)$$

$$M(H_2O)_5L^{n+} + L \leftrightarrow M(H_2O)_4L_2^{n+} + H_2O \quad (3.2)$$

. .

. .

. .

$$M(H_2O)L_5^{n+} + L \leftrightarrow ML_6^{n+} + H_2O \quad (3.3)$$

where L denotes a particular monodentate ligand.

The extent of complexation of the metal ion may be calculated from the stability constants of the particular metal-ligand complex. In general, the formation of a metal-ligand complex will shift the reduction potential to a more negative potential.

- The transition metal may form ion pairs with anions in solution. In this case the cation and anion retain their hydration shells, and the interaction is based on electrostatic forces. Ion pair formation is common in electroanalytical chemistry due to the presence of high concentrations of electrolytes present in the test solution. The influence of ion pair formation on the redox potential of a particular couple is small, due to the weak electrostatic forces.

3.4.4 Adsorption

Adsorption involves the interaction of species in solution with an electrode surface. The species may include the reactant, an intermediate, a product,

the solvent, or ions from the background electrolyte. Both neutral molecules and ions may be adsorbed.

The nature of the adsorption process may vary. Mechanisms may range from the formation of covalent bonds to electrostatic interactions. All these processes may either be reversible or irreversible.

Depending on the material of construction, composition of the solution, and applied potential, the electrode surface will have a characteristic charge. This surface charge will attract ions, dipoles and π-electron systems. Dipoles may also be induced by the electrical field at the electrode-solution interface.

The tendency of a species to adsorb on a particular surface is expressed as the free energy of adsorption, ΔG_{ADS}. This value depends on the extent to which a potential adsorbate is stabilised by other interactions in solution, in addition to its affinity for a particular electrode surface. It is therefore apparent that adsorption effects will be a function of the matrix of the solution in which the potential adsorbate is contained.

The presence of an adsorbed species may influence the rate and mechanism of electrode reactions. Two of the major processes involving adsorbed species are electrocatalysis and the inhibition of electron transfer.

Catalysis involves an increase in the rate of a reaction via a species not consumed in the overall reaction. In the case of electrocatalysis an adsorbed species will play a role in the provision of an alternative pathway (lower energy of activation) for the conversion of reactants to products. An increase in reaction rate will be characterised by an increase in current density at a fixed potential, or a decrease in the overpotential required to achieve a particular current density.

Adsorbed species that are not directly involved in a particular redox process may inhibit electron transfer in two ways. In the first case, the adsorbed species may be seen as occupying sites on the electrode surface, thereby reducing the sites available for electron transfer. Secondly, the adsorbate may be seen as covering the entire electrode surface, making the distance for electron transfer between the reactant and the electrode surface greater.

3.4.5 Phase Formation

Examples of phase formation reactions include the cathodic deposition of metals and the anodic formation of metal oxide layers. In the case of metal deposition, the phase formation process can be summarised in a series of steps. Metal deposition occurs as a result of *(i)* the transport of the solvated metal ion to the electrode surface, *(ii)* electron transfer at the electrode surface, *(iii)* formation of an adatom, *(iv)* surface diffusion of adatoms to form a stable nucleus, and *(v)* growth of the nucleus by the incorporation of adatoms.

Nucleation and growth mechanism

Small metal centres are not thermodynamically stable and will re-dissolve. In order to form stable metal nuclei, a critical size must be reached via the rapid accumulation of adatoms. This can only be achieved by the application of a sufficient overpotential.

Once a stable nucleus is formed on the electrode surface, a growth process will commence. Growth may either be two-dimensional (monolayer) or three-dimensional (hemisphere or cone). The process occurs by incorporation of adatoms to the perimeter of the monolayer, or the surface of a hemisphere or cone.

As more metal is deposited via this growth process, the rate of metal deposition will increase due to the greater area available for metal reduction. Individual metal nuclei will continue to grow until physical

overlap between the nuclei occurs. When overlap between individual metal centres has occurred over the whole surface of the cathode, the metal layer will start to thicken. The rate determining step at this stage may either be electron transfer or mass transport.

3.4.6 Hydrogen Gas Evolution and Oxidation

The evolution of hydrogen gas in an acid solution will be discussed, since all the experiments related to this chapter were conducted in a hydrochloric acidic medium.

Hydrogen evolution is facilitated by an electrocatalytic process involving the adsorption of a hydrogen atom:

$$H^+ + M + e^- \rightarrow M - H \tag{3.4}$$

where M denotes a particular cathode material.

Following the adsorption step, two possible reaction pathways are possible:

$$2M - H \rightarrow H_2 + 2M \tag{3.5}$$

$$M - H + H^+ + e^- \rightarrow H_2 + M \tag{3.6}$$

The faster of the two reactions will dominate, and therefore determine the overall mechanism. The rate of a particular reaction will in turn be determined by the characteristics and morphology of the selected cathode material.

The overall reaction for the generation of hydrogen gas in an acid solution is therefore expressed as follows:

$$2H^+ + 2e^- \rightarrow H_2(g) \tag{3.7}$$

Catalysis is most efficient for intermediate free energies of adsorption.

When the $M-H$ bonds are weak, coverage of the surface will be low, resulting in low rates of hydrogen evolution. If on the other hand the $M-H$ bonds are too strong, it will be difficult to break via Equations 3.5 and 3.6.

The high exchange current densities associated with hydrogen evolution on PGM surfaces is due to the formation of $M-H$ bonds with intermediate energies of adsorption.

The electrochemical oxidation of molecular hydrogen in an acid solution is initiated by chemisorption on the surface of an electrocatalyst. This step is followed by the oxidation of the chemisorbed hydrogen. The overall reaction will be the reverse of the process shown in Equation 3.7.

The electrochemical oxidation of molecular hydrogen on platinum and palladium surfaces is rapid, and occurs at low overpotentials. Although the chemisorption of hydrogen on carbon surfaces is well documented, carbon does not exhibit electrocatalytic activity for the oxidation of molecular hydrogen[42b].

3.5 RESULTS AND DISCUSSION

The interaction of the major and minor metal ions found in a typical PML solution with a glassy carbon working electrode was investigated as described in Section 3.2.2. More than 600 CV experiments were conducted during this phase of the research project. The most important voltammograms will be shown to support subsequent discussion.

3.5.1 Background Electrolyte

The background electrolyte determined the potential range available for CV studies. A 0.1 M HCl solution was employed after removing oxygen via a nitrogen gas purge. The oxidation of chloride ions ($E^\circ = 1.36$ V) and water ($E^\circ = 1.23$ V), and the reduction of hydrogen ions ($E^\circ = 0.00$ V) were the limiting factors:

$$2Cl^- - 2e^- \rightarrow Cl_2(g) \quad (3.8)$$

$$2H_2O - 4e^- - 4H^+ \rightarrow O_2(g) \quad (3.9)$$

The overall reaction for the evolution of hydrogen gas in an acid medium was provided in Equation 3.7.

Discussion of results

A typical voltammogram of the 0.1 M HCl background electrolyte is shown in Figure 3.2. The rapid increase in the cathodic current observed at potentials more negative than -0.30 V is due to the formation of hydrogen gas at the interface between glassy carbon and the electrolyte, as described in Equation 3.7.

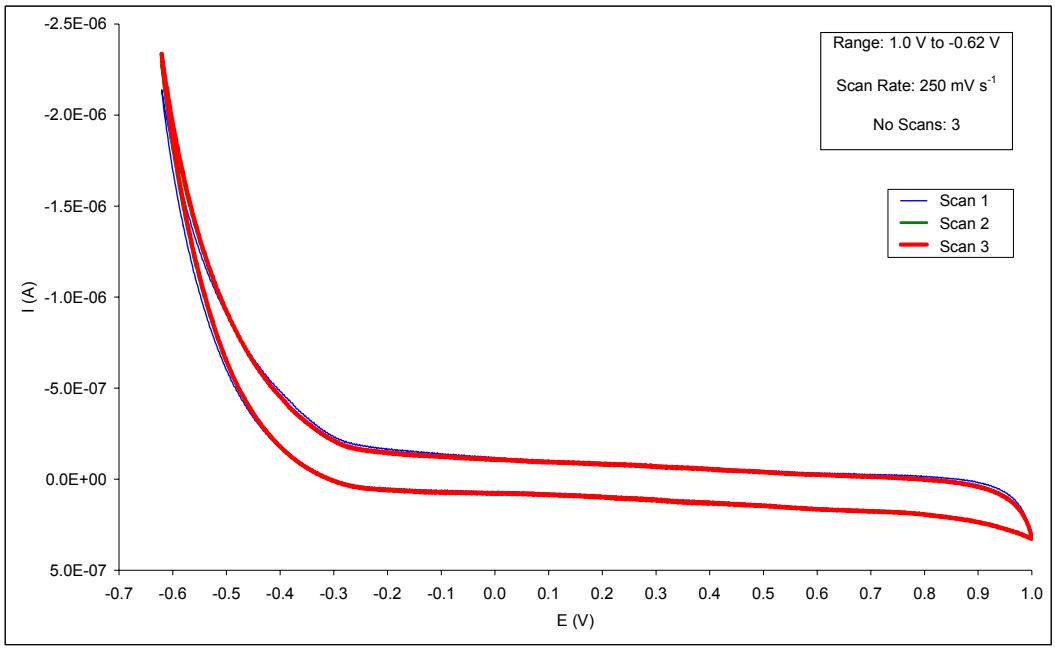

Figure 3.2 Cyclic voltammograms of a 0.1 M HCl background electrolyte, using a glassy carbon working electrode.

The anodic current, reaching a maximum value of 0.30 μA at 1.0 V may be ascribed to *(i)* oxidation reactions as provided in Equations 3.8 and 3.9,

(ii) oxidative processes involving the glassy carbon working electrode, or a combination of the above-mentioned factors.

The voltammograms obtained for the background electrolyte, or for that matter any other test solution used in this research project could never be reproduced exactly. In the case of the background electrolyte for example, the potential at which the generation of hydrogen gas became significant could vary by 0.10 V. The variation is to be expected due to the porous nature of the glassy carbon electrode. In addition, the cleaning and preparation of the working electrode prior to a set of experiments, and the nature of work within a set of experiments will also influence the response of the working electrode.

3.5.2 Reactions Involving Iron

As noted in Section 3.2.2, iron was used to assist with the interpretation of voltammograms. The preparation of a ferric chloride solution for this purpose was also described in Section 3.3.2. Interactions of the Fe^{3+}/Fe^{2+} redox couple with glassy carbon and platinum working electrodes are described here to facilitate later discussions involving the redox couple as an interpretational tool.

Discussion of results

In Figure 3.3, the voltammogram of a background solution containing 110 mg l^{-1} iron is compared to a 0.1 M HCl background electrolyte. Peak C1 (ca. -0.10 V) is indicative of the reduction of Fe^{3+} :

$$Fe^{3+} + e^{-} \rightarrow Fe^{2+} \qquad (3.10)$$

As the scan proceeds to potentials more negative than Peak C1, the formation of hydrogen gas is initiated. When the cathodic currents for voltammograms of the background solution and the solution containing iron are compared, it is noted that the magnitude of each of the currents at -0.62 V is similar (ca. 10 μA). This implies that the working electrode

surface had similar properties at the end of the forward sweep of each experiment, confirming the absence of any metal deposition. If iron metal deposition did occur, the magnitude of the cathodic current due to hydrogen evolution and the potentials at which the cathodic current became significant would be different when compared to the voltammogram of the background electrolyte.

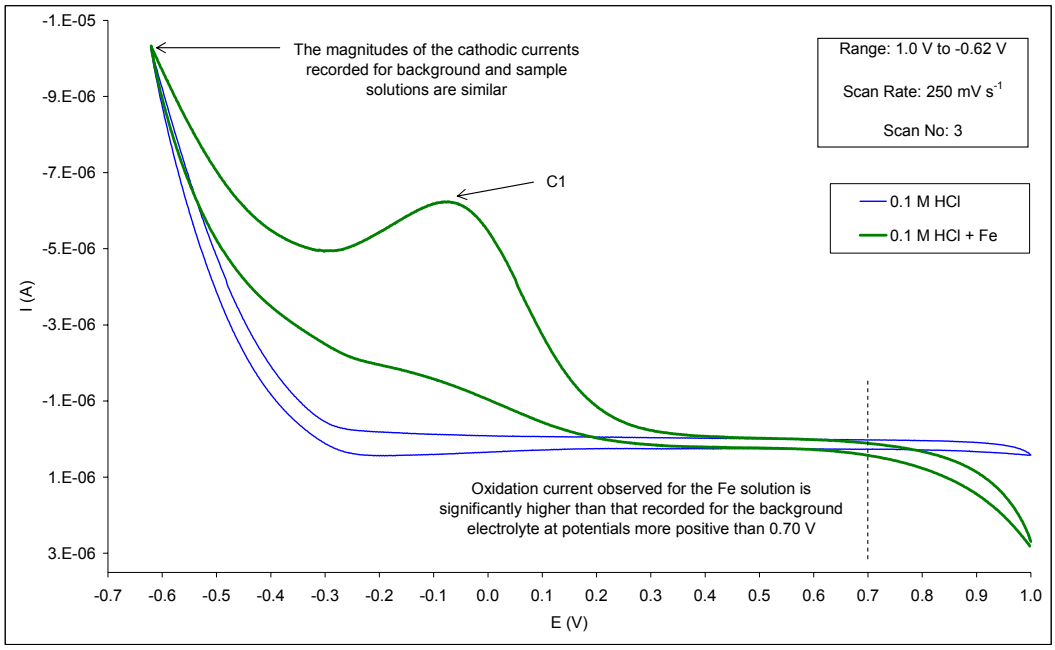

Figure 3.3 Cyclic voltammograms of a 0.1 M HCl background electrolyte, and the background electrolyte containing 110 mg l^{-1} iron, using a glassy carbon working electrode.

The fact that Fe^{3+} is not reduced to its metallic state on the glassy carbon electrode forms the basis of its use as a witness ion. If another metal ion in solution is reduced to its metallic state and remains on the electrode surface until the Fe^{3+} ions are reduced, the characteristic peak position (E_{pc}) and current normally observed for the reduction step will change. The degree of change in peak potential and current depends on the characteristics and amount of the new active metal centres formed on the electrode surface. The witness ion will therefore confirm the deposition of different metals whilst not interfering with the processes occurring at the

electrode-solution interface.

From Figures 3.3 and 3.4 it is evident that no peak for the oxidation of Fe^{2+} to Fe^{3+} is observed. In CV experiments, this would normally indicate the existence of a coupled homogenous reaction.

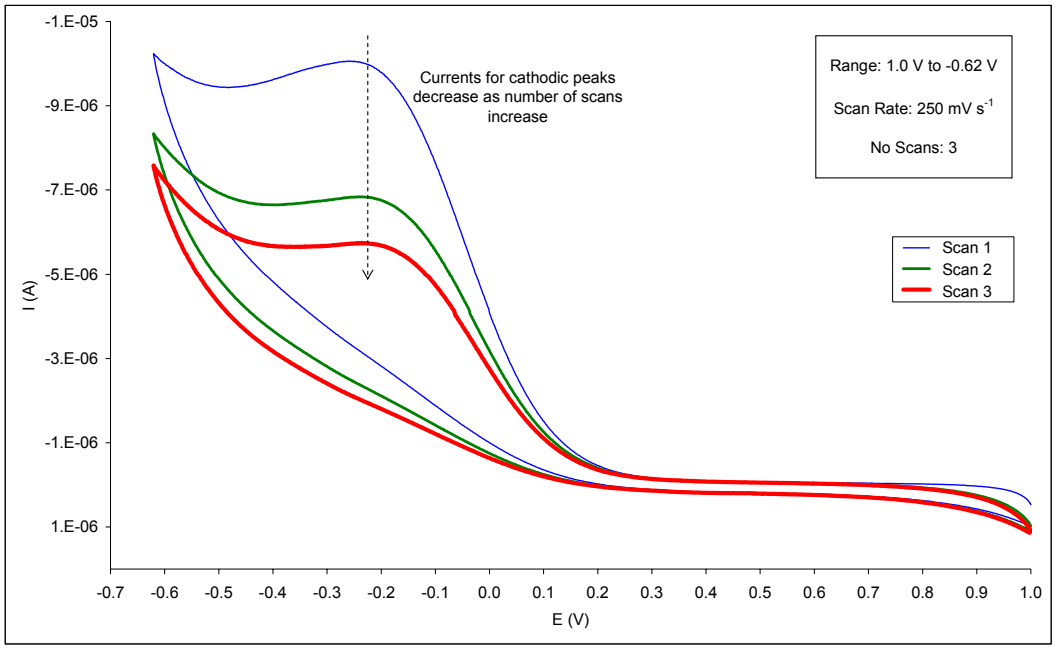

Figure 3.4 Cyclic voltammograms of a solution containing 110 mg l^{-1} iron in a 0.1 M HCl background electrolyte, using a glassy carbon working electrode.

When the same solution is however analysed using a platinum disc electrode, as shown in Figure 3.5, cathodic and anodic peaks (Peaks C1 and A1) are observed. This provides evidence that the absence of a peak for the oxidation of Fe^{2+} to Fe^{3+} is due to an interaction involving the glassy carbon electrode itself, rather than a coupled homogenous reaction.

The comparison of voltammograms for the reduction of Fe^{3+}, obtained on a glassy carbon electrode and a platinum disc electrode also illustrated the application of a witness ion.

Due to the varying electrocatalytic properties of the electrode surfaces, the characteristic potentials and currents of the reduction peaks were different.

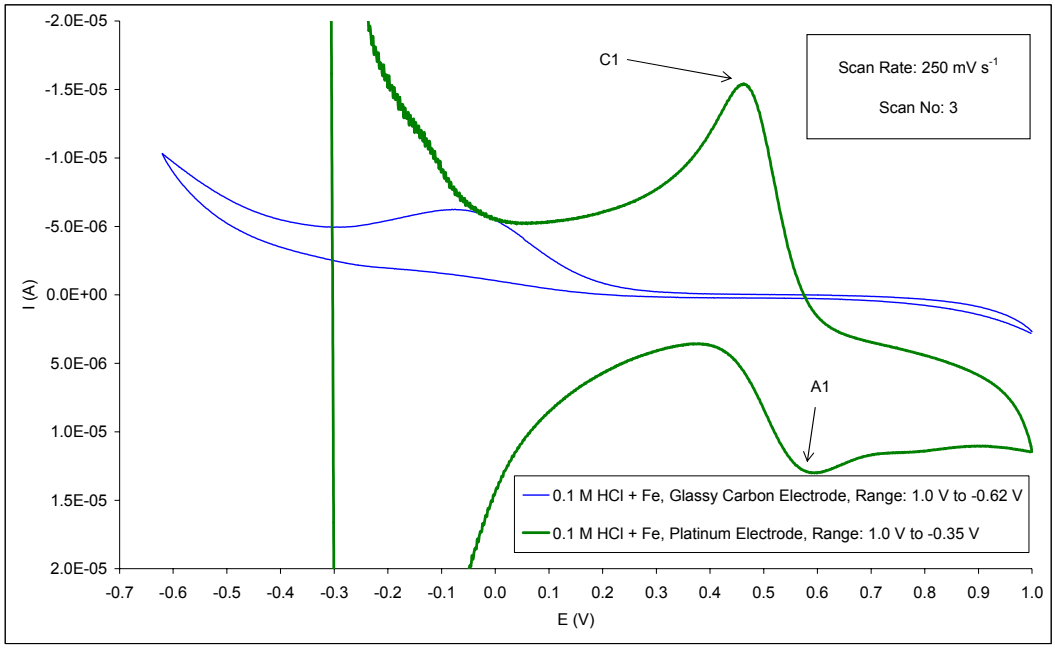

Figure 3.5 Cyclic voltammograms of a solution containing 110 mg l^{-1} iron in a 0.1 M HCl background electrolyte, using glassy carbon and platinum disc working electrodes.

In Figure 3.3 it was observed that the oxidation current recorded for the iron test solution is significantly higher than that observed for the background electrolyte at potentials more positive that 0.70 V. From Figure 3.4 it is also evident that the current observed for the reduction of Fe^{3+} diminishes as the number of potential scans increase. The above-mentioned facts support the conclusion that the glassy carbon electrode surface itself is involved in a reaction if a Fe^{3+}/Fe^{2+} redox couple is present in a 0.1 M HCl matrix.

The exact mechanism involving the Fe^{3+}/Fe^{2+} redox couple and a glassy carbon surface could not be confirmed. From the experimental data, and available literature information, two possible mechanisms may be suggested[41,42c]:

1st proposed mechanism. Functional groups present on the glassy carbon surface are oxidised at potentials more positive than ca. 0.10 V. When Fe^{2+} is generated on the forward sweep of the CV, the ions rapidly react with the oxidised surface by donating an electron to neutralise the positive charge of the surface. Since the Fe^{2+} ions all react prior to potentials at which its oxidation would be feasible from a thermodynamic and kinetic point of view, no peak is observed. The overall process also influences the electrocatalytic properties of the working electrode, with the Fe^{3+} reduction currents decreasing as the number of sweeps increase (Figure 3.4).

2nd proposed mechanism. At potentials more positive than ca. 0.10 V, Fe^{3+} acts as an oxidant. The Fe^{2+} ions formed in this process are then oxidised at potentials > ca. 0.70 V, resulting in the anodic current observed in Figure 3.3:

$$4Fe^{3+} + C + 2H_2O \rightarrow CO_2 + 4Fe^{2+} + 4H^+ \quad (3.11)$$

$$Fe^{2+} - e^- \rightarrow Fe^{3+} \quad (3.12)$$

The fact that reactions involving the electrode was occurring did however not hamper the use of the Fe^{3+} reduction peak as an interpretational tool.

3.5.3 Major Metal Ions

In Section 3.2.2, the matrix of a typical PML solution was described in terms of major metal ions (copper, palladium and platinum), and the remaining minor metal ions present in concentrations of < 10 mg l^{-1}. The preparation of synthetic single stock solutions for these metals is described in Section 3.3.2. A discussion of the behaviour of the major metal ions is presented in this section.

Reactions involving palladium

Discussion - Figure 3.6. The reduction of palladium ions to its metallic state is illustrated via the voltammogram in Figure 3.6.

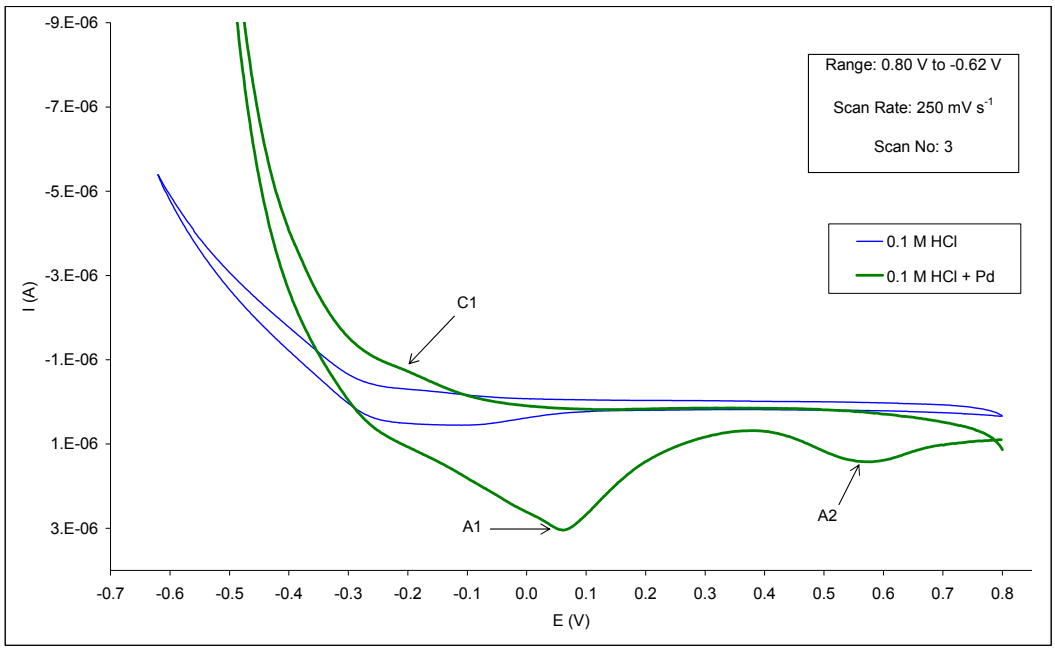

Figure 3.6 Cyclic voltammograms of a 0.1 M HCl background electrolyte, and the background electrolyte containing 110 mg l^{-1} palladium, using a glassy carbon working electrode.

Peak C1 is indicative of the reduction of the palladium ions to metal. The increase in the slope and magnitude of the hydrogen ion reduction current recorded for the test solution containing palladium compared to that obtained for the background electrolyte confirms the catalytic generation of hydrogen gas on active palladium metal centres.

Peak A1 is ascribed to the oxidation of molecular hydrogen on the deposited palladium metal centres. It was noticeable that the potential of this peak, E_{pa}, was only recorded at ca. 0.05 V. A high overpotential is therefore required to oxidise molecular hydrogen on the palladium metal centres. This is due to the strong interaction between palladium metal and the chemisorbed hydrogen atoms (refer to Section 3.4.6).

The oxidation of palladium metal to ions is observed at Peak A2. Normally an anodic stripping peak is symmetrical, and its current is high compared to normal diffusion peaks (refer to phase formation reactions described in Section 2.2.2). Peak A2 does not exhibit these characteristics. The drawn

out shape of the peak may be ascribed to the nature of the background electrolyte (0.1 M HCl) employed for the experiment. It was shown that the concentration of halide ions will have a major impact on the stripping efficiency of palladium[28].

The chloride concentration may therefore be important when an attempt is made to recover palladium metal from a cathode after the treatment of a PML solution. As this research project focussed on the removal of PGMs from PML solutions, time and resources did not allow further test work with regards to the effect of chloride concentration on the anodic stripping of palladium metal from cathode materials. This should however form part of future studies where the emphasis will shift to the recovery of PGMs from cathode materials.

Discussion - Figure 3.7. It was noted that higher concentrations of palladium in solution (196 mg l^{-1} versus 99 mg l^{-1}) would result in the observation of higher reduction and oxidation currents, as illustrated in Figure 3.7. This is to be expected, since the rate of transport of palladium ions to the electrode-solution interface will increase. The same effect will be noticeable if the potential scan rate of the experiments is increased, or the potential range of the experiments is extended to more negative potentials.

No proportionality was noted between the peak currents (C1, A1, A2) and the concentration of palladium ions added to the test solutions. This phenomenon is important in terms of understanding the reactions taking place at the glassy carbon surface when other metal centres have formed on the surface. The voltammograms obtained from such experiments represent the sum of all reactions taking place at the electrode-solution interface.

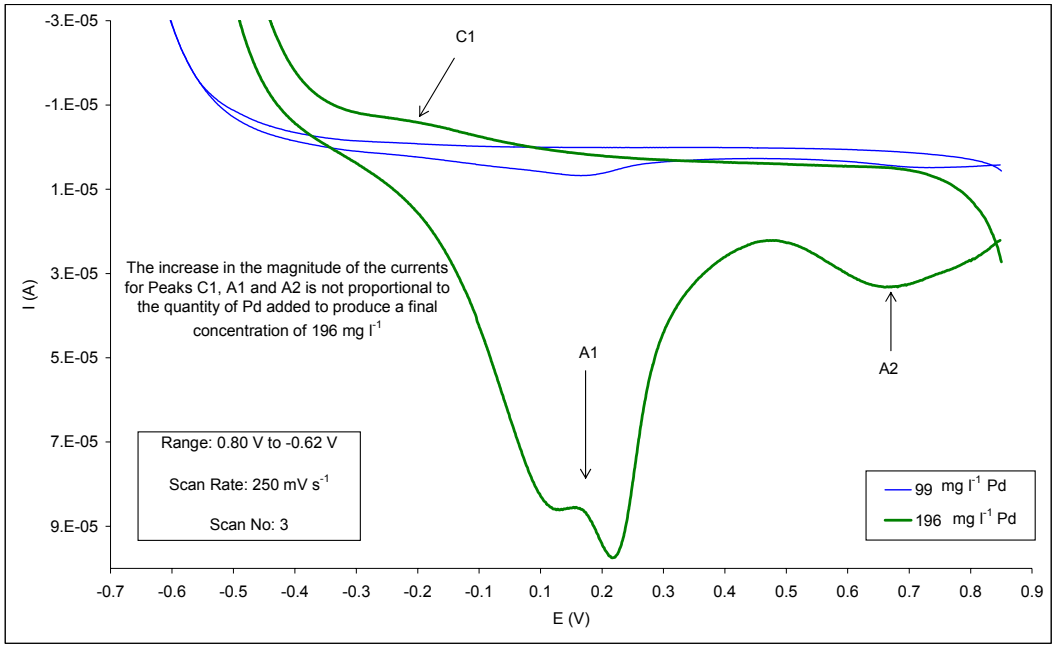

Figure 3.7 Cyclic voltammograms of solutions containing *(i)* 99 mg l^{-1} or *(ii)* 196 mg l^{-1} palladium in a 0.1 M HCl background electrolyte, using a glassy carbon working electrode.

Since the exchange current densities (j_o) for the reduction of hydrogen and other metal ions on PGM metal centres are normally orders of magnitude greater than that of a carbon based substrate[41,37d], the overall characteristics of the electrode will tend to approximate that of a PGM electrode, even when a small amount of active PGM metal centres relative to the carbon substrate is present.

The double peak (A1) observed for the solution containing 196 mg l^{-1} palladium also confirms the oxidation of molecular hydrogen[3]. If molecular hydrogen is present on the glassy carbon working electrode, the chemical and electrochemical reduction of palladium ions to metal may simultaneously occur at the electrode surface. It is also possible that the overall mechanism for the reduction of palladium ions to metal takes place via a combination of chemical and electrochemical processes. The exact mechanism of the palladium reduction process was not investigated in detail, due to the focus and nature of the project, as described in Section

3.1.2.

Discussion - Figure 3.8. In order to provide final confirmation regarding the deposition of palladium ions on a glassy carbon working electrode whilst employing a 0.1 M HCl background electrolyte, a witness ion (Fe^{3+}) was used. In Figure 3.8, voltammograms illustrating the behaviour of a solution containing 107 mg l^{-1} iron and 188 mg l^{-1} palladium are shown for three successive scans.

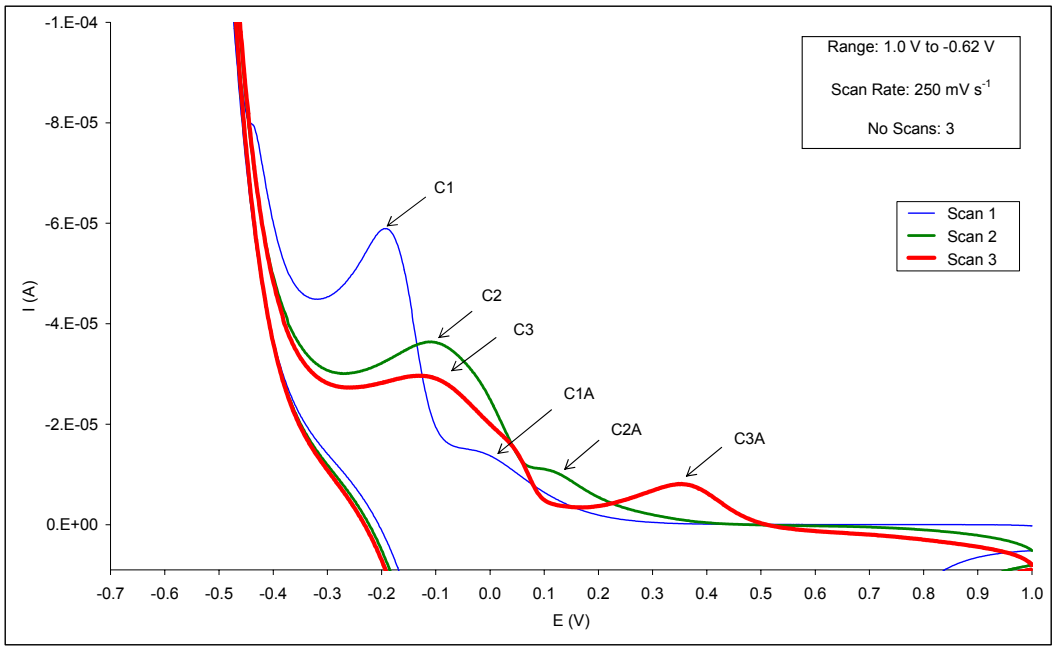

Figure 3.8 Cyclic voltammograms of a solution containing 107 mg l^{-1} iron and 188 mg l^{-1} palladium in a 0.1 M HCl background electrolyte, using a glassy carbon working electrode.

Initially, for Scan 1, a peak potential of ca. -0.22 V (C1) was recorded for the reduction of palladium ions to metal. For Scans 2 and 3 the peak potential values shifted to -0.13 V (C2, C3), suggesting a change in the electrocatalytic properties of the working electrode due to the deposition of palladium metal centres. Confirmation of metal deposition is provided by the fact that the peak potential values for the reduction of Fe^{3+} to Fe^{2+} progressively shifted from -0.10 V (Peak C1A) for Scan 1 to 0.11 V and then to 0.33 V (Peaks C2A, C3A) for Scans 2 and 3 respectively.

Reactions involving platinum

Discussion - Figure 3.9. Voltammograms shown in Figure 3.9 compare the interaction of a 0.1 M HCl background electrolyte to that of the same background solution containing 196 mg l^{-1} platinum. The cathodic peak at ca. -0.18 V (labelled C1), is indicative of the deposition of platinum metal centres on the glassy carbon electrode surface. At potentials more negative than ca. -0.25 V , a significant current was generated due to the catalytic generation of hydrogen gas on the platinum metal centres.

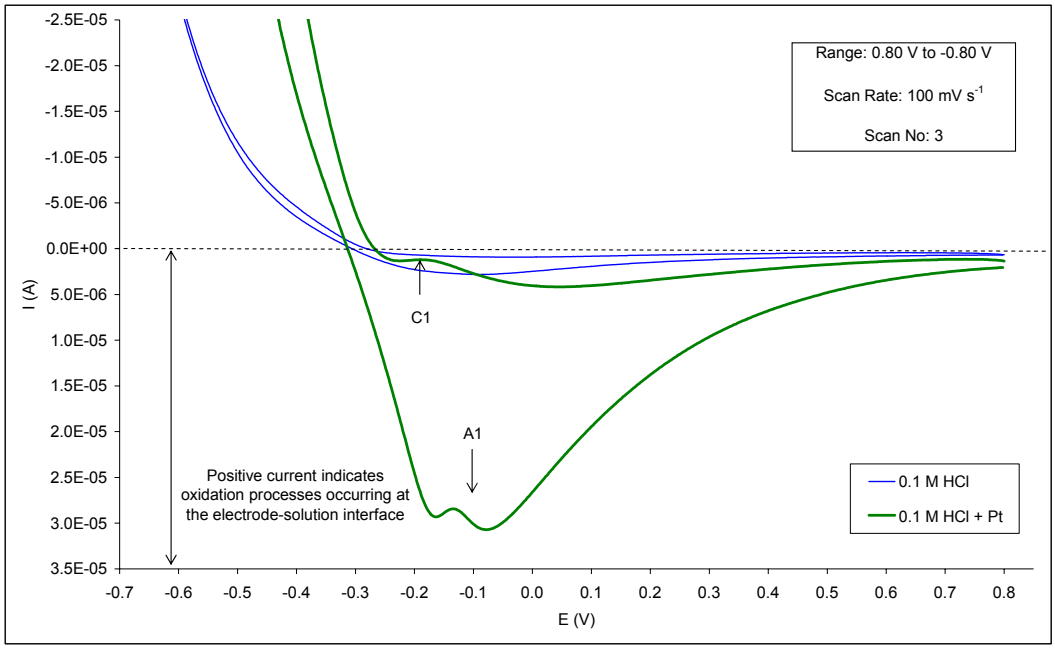

Figure 3.9 Cyclic voltammograms of a 0.1 M HCl background electrolyte, and the background electrolyte containing 196 mg l^{-1} platinum, using a glassy carbon working electrode.

The broad asymmetrical anodic peak at A1 is ascribed to the oxidation of molecular hydrogen on the electrode surface, as shown in Equation 3.7. If this peak potential is compared to the oxidation potential of molecular hydrogen on a palladium substrate (Figure 3.7) a significant difference is noted. The oxidation of molecular hydrogen on a platinum substrate occurs at ca. -0.10 V , compared to ca. 0.10 V for a palladium substrate.

Differences in oxidation potentials are ascribed to the varying stabilities of

the chemisorbed hydrogen atom interactions (refer to Section 3.4.6) with a particular substrate. The fact that the peak potentials for the oxidation of molecular hydrogen differ is useful from an interpretational point of view. The presence of a particular peak would indicate the type of active metal centres present on a working electrode surface.

No evidence was found for the oxidation of platinum metal centres to ions under the experimental conditions employed. The possible anodic dissolution of platinum metal should however not be ignored. When the oxidation of palladium metal was discussed earlier in this section, the influence of the matrix on overall dissolution characteristics was highlighted. It may also be possible that platinum metal is oxidised to ions at a very slow rate due to kinetic considerations.

In addition, platinum metal centres in an acidic medium are prone to oxidation, depending on the potential applied:

$$Pt + H_2O - 2e^- \leftrightarrow PtO + 2H^+ \tag{3.13}$$

The presence of oxides further complicates the anodic dissolution process. Factors influencing the formation of metal oxide deposits and the anodic dissolution of metals found in these oxide layers are discussed in detail in the literature review section of Chapter 1.

No additional test work was carried out with regards to the anodic stripping of platinum metal from cathode materials due to the nature of the project, time, and resources as pointed out in Section 3.1.2. This should however form part of future studies where the emphasis will shift to the recovery of PGMs from cathode materials.

The current on the forward sweep of the voltammogram recorded for the platinum solution was positive (implying an oxidation process) up to a potential of ca. -0.25 V. A reduction current was observed at more negative potentials. Although not shown in Figure 3.9, it was also noted that the magnitude of the oxidation current increased as the number of

potential scans increased. The potential at which an overall reduction current was noted also shifted to more positive values, reaching ca. -0.25 V on the third scan. A number of explanations could be provided to explain this phenomenon.

If the potentials recorded for this voltammogram are converted to reflect the values relative to a standard hydrogen electrode, it is noted that the switch between positive and negative currents occur close to a value of 0 V. It may therefore be feasible that the behaviour of the glassy carbon electrode with finely dispersed platinum metal centres present on its surface approximate the characteristics of a hydrogen electrode. Hence, hydrogen ions will be reduced at potentials more negative than 0 *V* versus this pseudo hydrogen electrode, whilst an oxidation current for the formation of hydrogen ions from molecular hydrogen will be observed at more positive potentials. As the number of cycles for a particular CV experiment is increased, more finely divided platinum metal centres are deposited, until there are enough present on the electrode surface to approximate the behaviour of a hydrogen electrode.

The overall response observed for the interaction between a glassy carbon working electrode and a solution containing platinum ions, would most likely be a combination of a number of simultaneous reactions taking place at any given time during a CV experiment. Apart from reactions involving the so-called pseudo hydrogen electrode, deposition of platinum on the electrode surface will continue at favourable potentials. Other possible reactions include the oxidation of platinum metal to PtO (Equation 3.13), and the subsequent reduction of this oxide. The formation and reduction of platinum oxides other than PtO may also be possible.

Discussion - Figure 3.10. Final confirmation of the reduction of platinum ions on a glassy carbon working electrode, employing a 0.1 M HCl background electrolyte was provided by using a Fe^{3+} witness ion.

In Figure 3.10, voltammograms illustrating the behaviour of a solution

containing 105 mg l^{-1} iron and 47 mg l^{-1} platinum are shown for three successive scans.

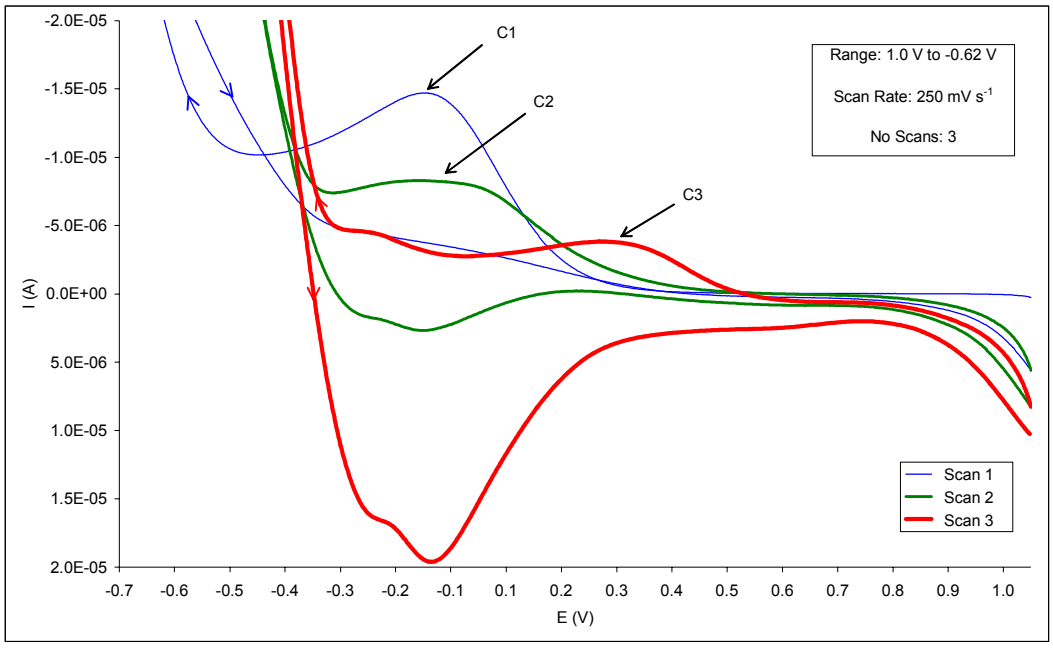

Figure 3.10 Cyclic voltammograms of a solution containing 105 mg l^{-1} iron and 47 mg l^{-1} platinum in a 0.1 M HCl background electrolyte, using a glassy carbon working electrode.

As the CV experiment progressed from Scans 1 to 3, the slope of the currents due to the generation of hydrogen gas increased, suggesting an increase in the number of active metal centres present on the glassy carbon surface.

When the hydrogen reduction currents on the forward and reverse sweeps of Scan 1 were compared, it was noted that the reverse sweep current appeared at more positive potentials relative to the forward sweep. This pointed to the fact that platinum metal centres formed, and that hydrogen was generated on platinum metal centres when the reverse sweep was recorded. The potentials at which the hydrogen reduction currents were observed continued to shift in a positive direction as more scans were recorded, indicating the continued deposition of platinum metal centres. By the time that Scan 3 was recorded the relative potentials of the hydrogen

reduction currents on the forward and reverse sweeps were much closer compared to the differences noted for Scan 1. This indicated that a significant amount of platinum metal centres were present on the glassy carbon surface on the completion of Scan 3.

The magnitude of the resultant molecular hydrogen oxidation peaks also increased, presumably in relation to the volume of gas generated on the forward sweep of the CV experiment.

Confirmation of metal deposition was also provided by observing a shift in the reduction potential for Fe^{3+} ions. Initially, the peak potential for the reduction process was observed at ca. -0.15 V (C1), consistent with previous experiments (Figure 3.3) involving a solution containing Fe^{3+} only. As the CV experiment involving a combination of iron and platinum metal ions progressed to Scans 2 and 3, the reduction peaks (C2, C3 in Figure 3.10) shifted to more positive potentials, indicating a change in the electrocatalytic properties of the electrode. This confirmed the presence of platinum on the electrode surface. The peak potential for the reduction of Fe^{3+} on the third CV scan was ca. 0.30 V, compared to 0.45 V obtained for the reduction on a platinum disc electrode (Figure 3.5).

If more scans were carried out for the experiment involving iron and platinum ions as shown in Figure 3.10, the peak potential for the reduction of Fe^{3+} would approximate a value of 0.45 V when the entire glassy carbon surface is covered by platinum. It should be noted that the physical characteristics of the deposited platinum (powder versus metal sheet) will have an influence on the final reduction potential of Fe^{3+}.

Reactions involving copper

Discussion - Figure 3.11. The characteristics of a voltammogram obtained for a reaction involving metal deposition was described in Section 2.2.2. The same characteristics are evident in Figure 3.11. Peak C1 at ca. -0.35 V is indicative of the reduction of copper ions to metal via a nucleation

process. It was also noted that the slope of the reduction current leading to Peak C1 was much steeper compared to other reactions involving a one-electron transfer process, for example the Fe^{3+}/Fe^{2+} redox couple described in Figure 3.5. The slope of this reduction current may be ascribed to a multi-electron transfer process involving the overall reduction of Cu^{2+} ions to metal. Multi-electron transfer processes were described in detail in Section 2.2.2.

Another possible explanation for the characteristic slope observed during the reduction of copper ions is that the process is catalysed by the presence of copper metal nuclei on the glassy carbon working electrode. This will lead to the development of significant reduction currents at low overpotentials. Evidence of such a catalytic process was provided by comparing the voltammograms of Scans 1 and 3 (range 1.0 V to -0.80 V) recorded for a synthetic solution containing copper ions, as illustrated in Figure 3.11. It was noted that the onset of a significant reduction current for Scan 3 occurred at more positive potentials relative to Scan 1.

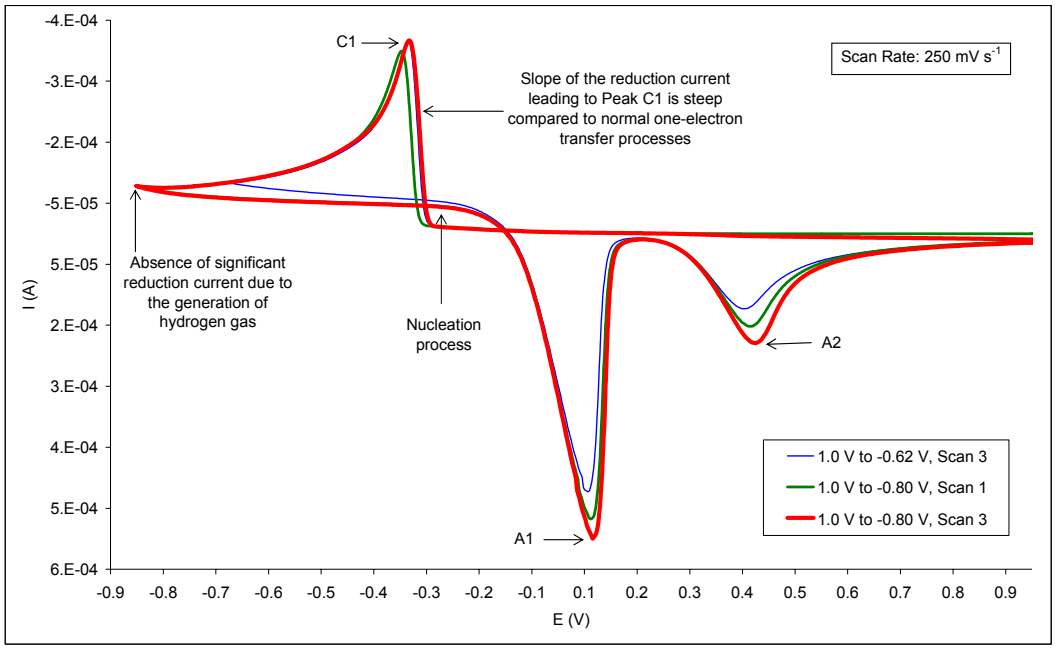

Figure 3.11 Cyclic voltammograms of a solution containing 431 mg l^{-1} copper in a 0.1 M HCl background electrolyte, using a glassy carbon working electrode.

It was concluded that the shift in the potential at which the current for the overall reduction of Cu^{2+} was observed occurred due to the presence of copper metal centres on the graphite electrode. Although the majority of the copper metal centres that were deposited during Scans 1 and 3 were stripped anodically (refer to next paragraph for discussion of anodic dissolution process), some of the centres remained on the glassy carbon surface resulting in the catalytic reduction of Cu^{2+}.

The oxidation peak observed at A1 (ca. 0.10 V) exhibits all the characteristics of a typical anodic dissolution process. It was concluded that copper metal formed on the glassy carbon surface was anodically dissolved as indicated by Peak A1. These dissolved copper ions were then oxidised to a higher oxidation state at potentials of ca. 0.40 V (Peak A2).

The oxidation current for Peak A2 was smaller relative to the oxidation currents observed for the anodic stripping peak, and was ascribed to the fact that copper ions stripped from the electrode surface diffused away from the electrode surface as soon as they were formed. When the subsequent oxidation of the copper ions occurred at ca. 0.40 V, the concentration of the ions at the electrode surface was lower relative to the concentrations present on the electrode surface during the anodic stripping process, resulting in lower oxidation currents.

Based on the evidence obtained from the voltammograms in Figure 3.11, it was concluded that copper metal was possibly oxidised to Cu^{+} at ca. 0.10 V, followed by the oxidation of Cu^{+} to Cu^{2+} at ca. 0.40 V. Confirmation of the relationship between Peaks C1, A1 and A2 were obtained by employing two different potential ranges, as shown in Figure 3.11. The absence of a significant reduction current due to hydrogen evolution, even at potentials as negative as -0.80 V was also noted. This fact should be kept in mind in situations where the generation of hydrogen gas via the proposed electrochemical reactor (refer to Chapter 1 for discussion of project objectives) could potentially become problematic from a safety and operational point of view.

Discussion - Figure 3.12. Although the cathodic peak potential (E_{pc}) for the reduction of copper ions to metal was observed at ca. -0.35 V, employing the experimental conditions provided in Figure 3.11, it should be noted that the actual deposition of copper is initiated at more positive potentials. In Figure 3.12 a cathodic current due to the formation of copper metal nuclei is already observed at ca. 0.25 V.

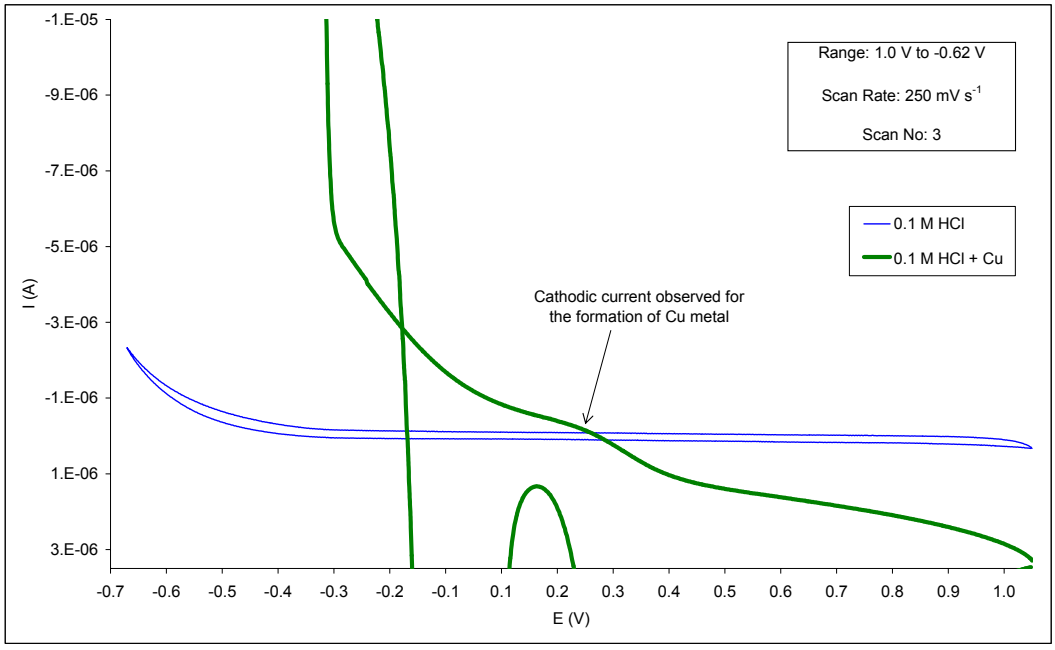

Figure 3.12 Cyclic voltammograms of a 0.1 M HCl background electrolyte, and the background electrolyte containing 178 mg l^{-1} copper, using a glassy carbon working electrode.

Reactions involving copper and palladium

Once a qualitative understanding of the interactions of single component synthetic solutions of the major metal ions in a typical PML solution was developed (as described thus far in Section 3.5.3), the complexity of the test solutions was increased. The combined interaction of copper and palladium ions with a glassy carbon electrode in a background solution of 0.1 M HCl is described here.

Discussion - Figures 3.13 to 3.15. In Figure 3.13 a voltammogram recorded for a solution containing iron, copper and palladium ions (Peaks

C1, C2, A1, A2, A3, A4) is compared to that obtained for a solution containing iron and copper ions (Peaks C1A, A1A, A2A).

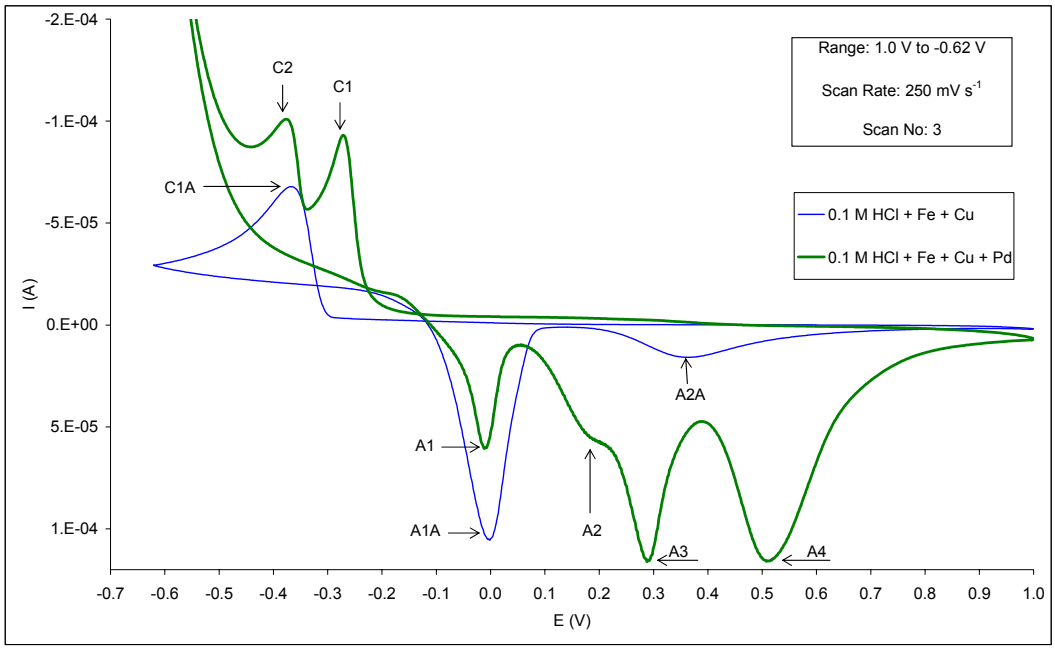

Figure 3.13 Cyclic voltammograms of solutions containing *(i)* 108 mg l^{-1} iron, 174 mg l^{-1} copper and *(ii)* 108 mg l^{-1} iron, 171 mg l^{-1} copper, 189 mg l^{-1} palladium in a 0.1 M HCl background electrolyte, using a glassy carbon working electrode.

The interaction of a synthetic solution containing iron and copper with a glassy carbon electrode was described under the preceding sub-heading "Reactions involving copper" (Section 3.5.3).

The anodic peaks in Figure 3.13 labelled A1 and A1A as well as those labelled A3 and A2A correspond. When the behaviour of copper was studied, Peak A1A was attributed to the oxidation of copper metal to Cu^{+}, and Peak A2A was ascribed to the oxidation of these ions to Cu^{2+}. The corresponding peaks provide evidence that copper is also deposited as a metal when a mixture of copper and palladium ions interact with a glassy carbon working electrode at specific potentials, and that the deposited copper metal is dissolved anodically at favourable potentials.

When the potentials of the cathodic peaks labelled C1 and C2 were compared to the peak labelled C1A, the initial conclusion was that C2 could be ascribed to the reduction of copper ions to metal. Upon further investigation a significant hydrogen reduction current was noted at potentials more negative than Peak C2. This implied that the formation of Peak C2 could be due to the reduction of palladium ions to metal, as experiments involving single component solutions of this metal ion (refer to Figure 3.6) indicated the catalytic generation of hydrogen on active palladium metal centres. It was also shown in Figure 3.11 that the deposition of copper metal was not characterised by the generation of large amounts of hydrogen gas, even at potentials as negative as -0.80 V .

In order to confirm the identification of Peaks C1 and C2, a series of CV experiments were carried out, using different potential ranges, as shown in Figures 3.14 and 3.15.

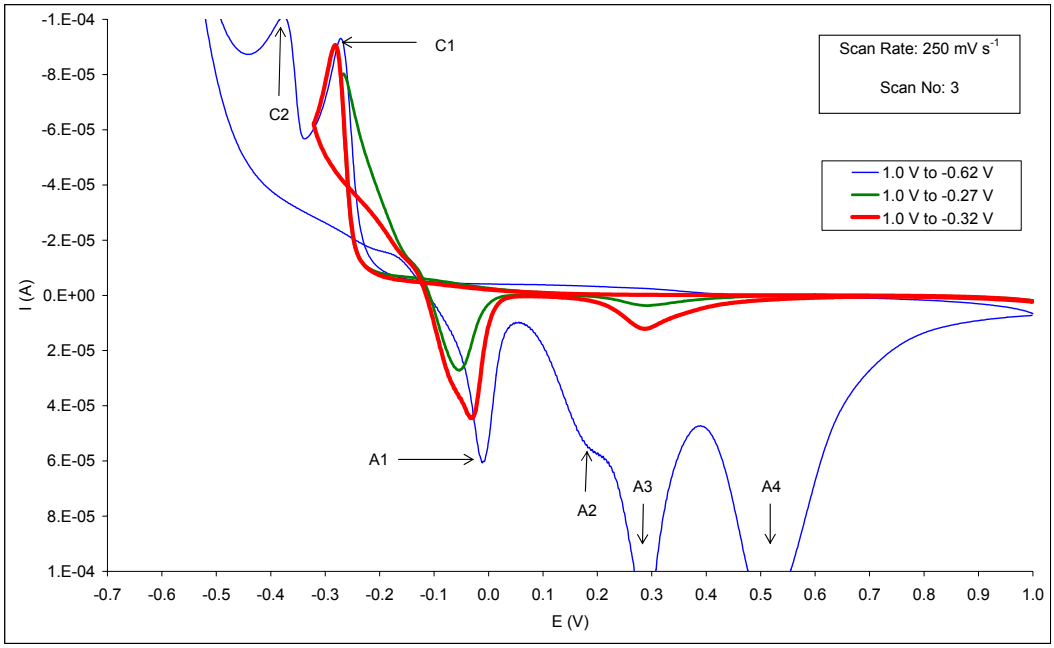

Figure 3.14 Cyclic voltammograms of a solution containing 106 mg l^{-1} iron, 171 mg l^{-1} copper and 189 mg l^{-1} palladium in a 0.1 M HCl background electrolyte, showing experiments where different potential ranges were utilised. A glassy carbon working electrode was employed.

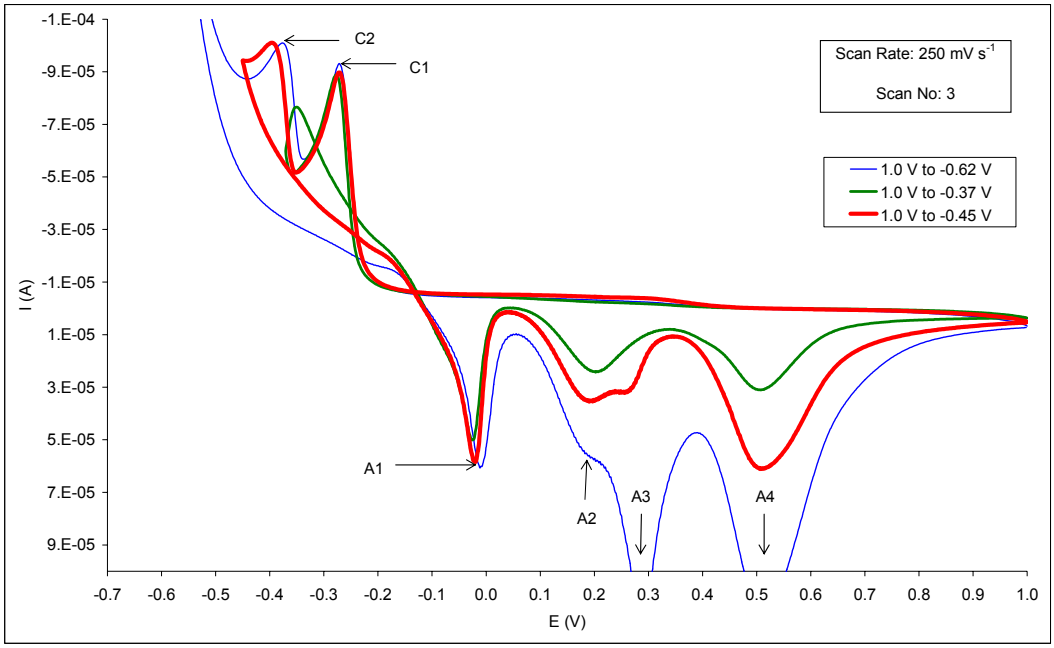

Figure 3.15 Cyclic voltammograms of a solution containing 106 mg l^{-1} iron, 171 mg l^{-1} copper and 189 mg l^{-1} palladium in a 0.1 M HCl background electrolyte, showing experiments where different potential ranges were utilised (in addition to those shown in Figure 3.14). A glassy carbon working electrode was employed.

Peak C1 was associated with the characteristic anodic stripping peak for copper metal at A1. This pointed to the association of Peak C2 with the reduction of palladium ions to metal.

Discussion - Figure 3.16. From the discussion involving Figures 3.13 to 3.15, the deposition of copper and palladium was confirmed. In addition, the anodic dissolution of copper from a glassy carbon electrode surface containing both copper and palladium metal was indicated. The issue regarding the possible anodic dissolution of palladium metal, or the absence thereof was however not confirmed.

In Figure 3.16 a voltammogram recorded for a solution containing iron, copper and palladium ions (Peaks C1, C2, A1, A2, A3, A4) is compared to that obtained for a solution containing palladium ions only (Peaks A1A, A2A).

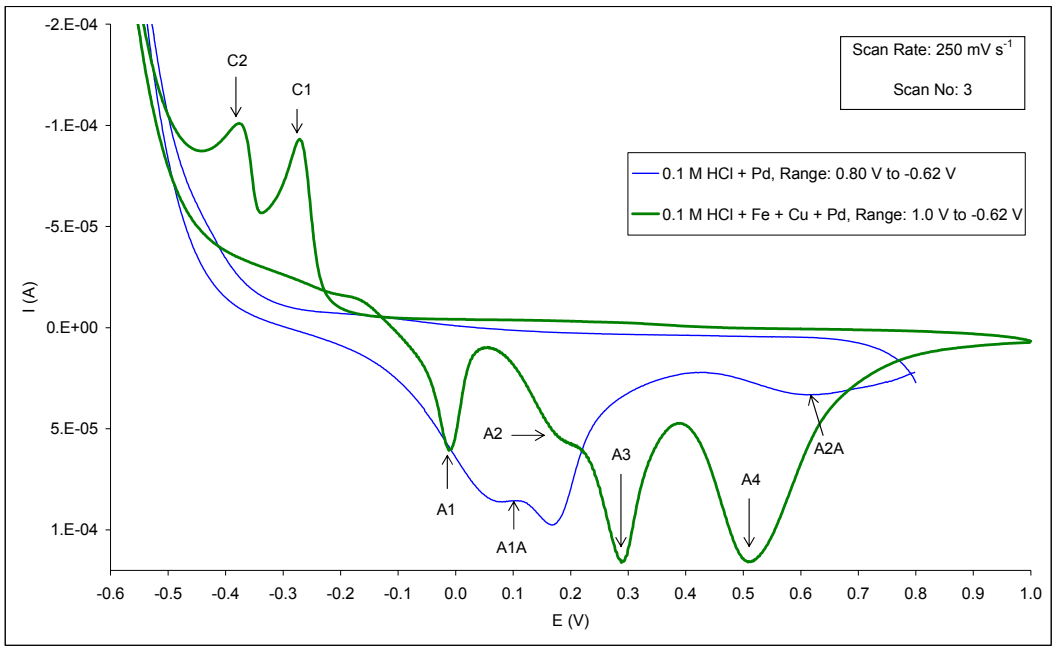

Figure 3.16 Cyclic voltammograms of solutions containing *(i)* 196 mg l^{-1} palladium and *(ii)* 106 mg l^{-1} iron, 171 mg l^{-1} copper, 189 mg l^{-1} palladium in a 0.1 M HCl background electrolyte, using a glassy carbon working electrode.

The interaction of a synthetic palladium ion solution with a glassy carbon electrode was described under the sub-heading “Reactions involving palladium” in this section (Section 3.5.3).

The anodic peaks in Figure 3.16 labelled A4 and A2A correspond. When the behaviour of palladium was studied, Peak A2A was attributed to the oxidation of palladium metal to ions. The corresponding peaks confirm that palladium metal is anodically stripped from a glassy carbon electrode surface containing both copper and palladium metal centres if favourable potentials are applied.

In addition, corresponding Peaks A2 and A1A indicated the oxidation of molecular hydrogen to hydrogen ions on a glassy carbon electrode containing both copper and palladium metal centres.

General discussion. When the peak potentials for the reduction of copper and palladium in a solution containing both of these ions were compared

to the peak potentials recorded for the reduction of copper or palladium in a single component solution, it was noted that the relative potential values had shifted. For the solution containing both copper and palladium ions, the reduction peak potentials shifted by ca. 0.10 V relative to the potentials recorded for the single component solutions. In the case of copper reduction, the peak potential had shifted in a more positive direction, whilst the peak potential for the reduction of palladium had shifted in a more negative direction.

The difference in the peak potentials for the reduction of a combination of copper and palladium ions in solution, compared to those obtained for the respective ions in single component solutions can be ascribed to changes in the overall characteristics of the glassy carbon electrode surface. As the CV experiment progress to more negative potentials, copper and palladium active metal centres are formed on the glassy carbon electrode surface. The nucleation process will change the overall exchange current density values (j_o) for the reduction of copper and palladium ions on the glassy carbon electrode surface. This will influence the rate of reduction, resulting in a shift of peak potentials.

If the oxidation peaks of voltammograms recorded for a mixture of copper and palladium ions in solution are compared to that obtained of voltammograms recorded for solutions containing only copper or palladium ions, similarities and differences are noted.

The stripping peak potentials for the anodic dissolution of copper metal remains the same irrespective of the fact that multi-component or single component solutions were analysed. This may indicate that *(i)* discrete copper metal centres formed on the glassy carbon surface, separate from the any palladium metal centres, *(ii)* that metal centres containing a mixture of copper and palladium are present with a very high ratio of copper, or *(iii)* that a combination of discrete copper metal centres and metal centres containing a mixture of copper and palladium are present.

In the case of palladium, the anodic stripping peak observed in the presence of both palladium and copper ions shifted ca. 0.10 V in a more negative direction relative to the stripping peak observed in the presence of palladium only. The shift in peak potential may be indicative of the presence of metal centres containing a mixture of copper and palladium.

From the discussion above, it is clear that the exact characteristics of the metals electrochemically deposited and stripped from the glassy carbon electrode cannot be elucidated from CV experiments alone. Additional surface analytical techniques, for example the use of a Scanning Electron Microprobe in combination with X-Ray Energy Dispersive Spectrometry (SEM-EDS) may be employed. The study of the composition and morphology of metals deposited onto a cathode material should form part of any additional in-depth studies that may follow on completion of the current research project.

Reactions involving palladium and platinum

Once a qualitative understanding of the combined interaction of copper and palladium ions with a glassy carbon electrode in a background solution of 0.1 M HCl was established, another combination of metal ions was investigated. The interaction of palladium and platinum ions under the conditions described above is described here.

Discussion - Figures 3.17 to 3.19. A voltammogram illustrating the interaction between a mixture of iron, palladium, and platinum ions and a glassy carbon working electrode is shown in Figure 3.17. The comparison between this experiment and a voltammogram recorded for a solution containing only palladium whilst employing a platinum disc working electrode is provided in Figure 3.18.

It was observed that the two voltammograms in Figure 3.18 (exhibiting characteristic hydrogen reduction and oxidation peaks) almost overlapped in the negative potential range. This led to the assumption that platinum ions are reduced to platinum metal centres on the glassy carbon electrode,

followed by the reduction of palladium ions on what is essentially a platinum cathode.

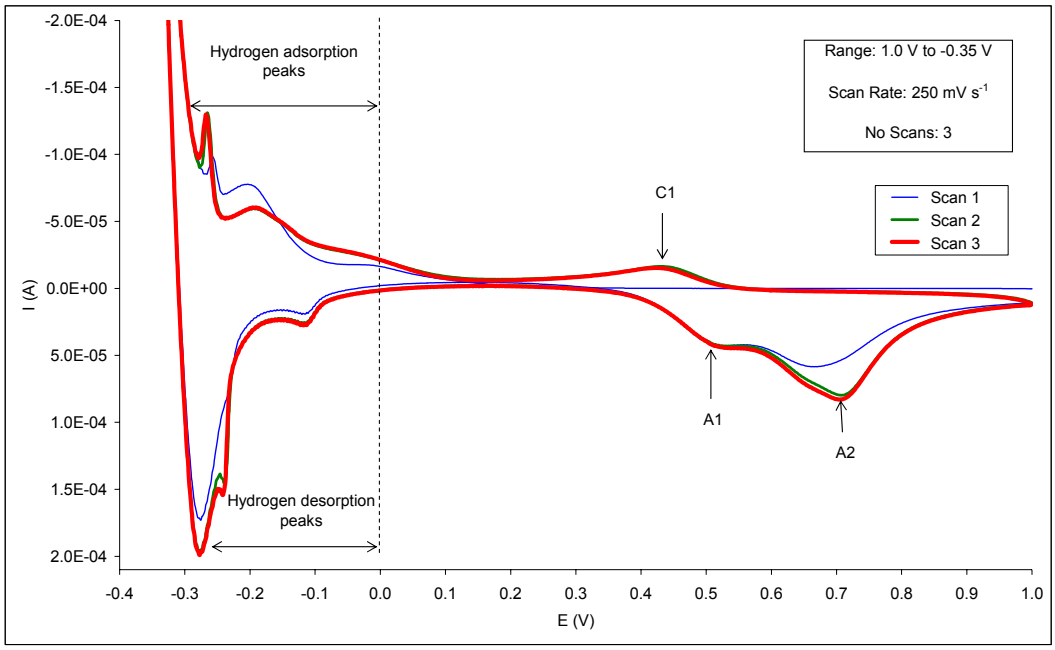

Figure 3.17 Cyclic voltammograms of a solution containing 105 mg l^{-1} iron, 188 mg l^{-1} palladium and 47 mg l^{-1} platinum in a 0.1 M HCl background electrolyte, using a glassy carbon working electrode.

In Figure 3.19, a voltammogram for the interaction of a mixture of iron, palladium and platinum ions with a platinum disc working electrode is shown. When the potentials of Peak C1 (ca. 0.45 V) and Peak A1 (ca. 0.55 V) shown in Figure 3.19 are compared to peaks with identical labels in Figures 3.17 and 3.18, it was noted that the positions correlated closely. Peaks C1 and A1 were identified as the reduction and oxidation peaks observed for the Fe^{3+}/Fe^{2+} redox couple observed on a platinum electrode surface after comparison to Figure 3.5.

Comparisons involving the use of a Fe^{3+} witness ion confirm the assumption that platinum metal centres are formed on the glassy carbon electrode, followed by the reduction of palladium ions on a platinum metal surface.

Evidence for the anodic dissolution of deposited palladium metal, as described under the sub-heading “Reactions involving palladium” in Section 3.5.3 was provided by *(i)* the presence of Peak A2 in Figures 3.17 and 3.19, and *(ii)* the presence of Peak A1A in Figure 3.18.

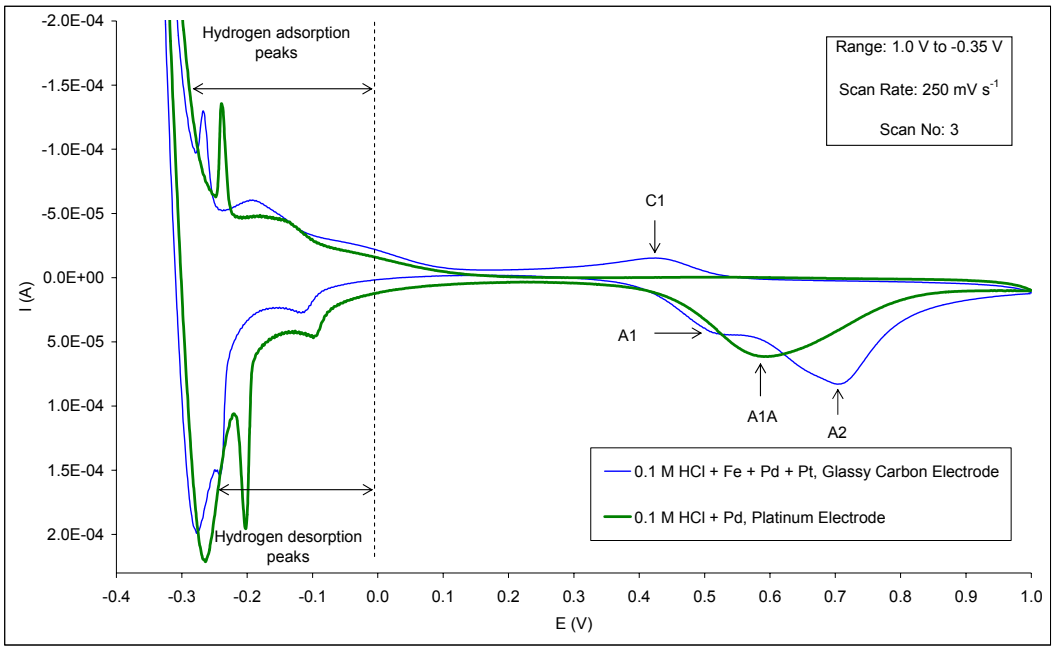

Figure 3.18 Cyclic voltammograms of a solution containing *(i)* 105 mg l^{-1} iron, 188 mg l^{-1} palladium, 47 mg l^{-1} platinum and *(ii)* 189 mg l^{-1} palladium in a 0.1 M HCl background electrolyte. Glassy carbon and platinum disc working electrodes were employed.

The first potential sweep in Figure 3.17 (labelled Scan 1) does not exhibit the peak due to the reduction of Fe^{3+} (Peak C1) on a platinum surface, pointing to the fact that significant quantities of platinum metal centres are only deposited at more negative potentials. Since no evidence of the anodic dissolution of significant amounts of platinum metal was found (see sub-heading “Reactions involving platinum”, Section 3.5.3), it would be reasonable to expect the presence of Peak C1 for the subsequent potential sweeps (Scans 2 and 3) as observed.

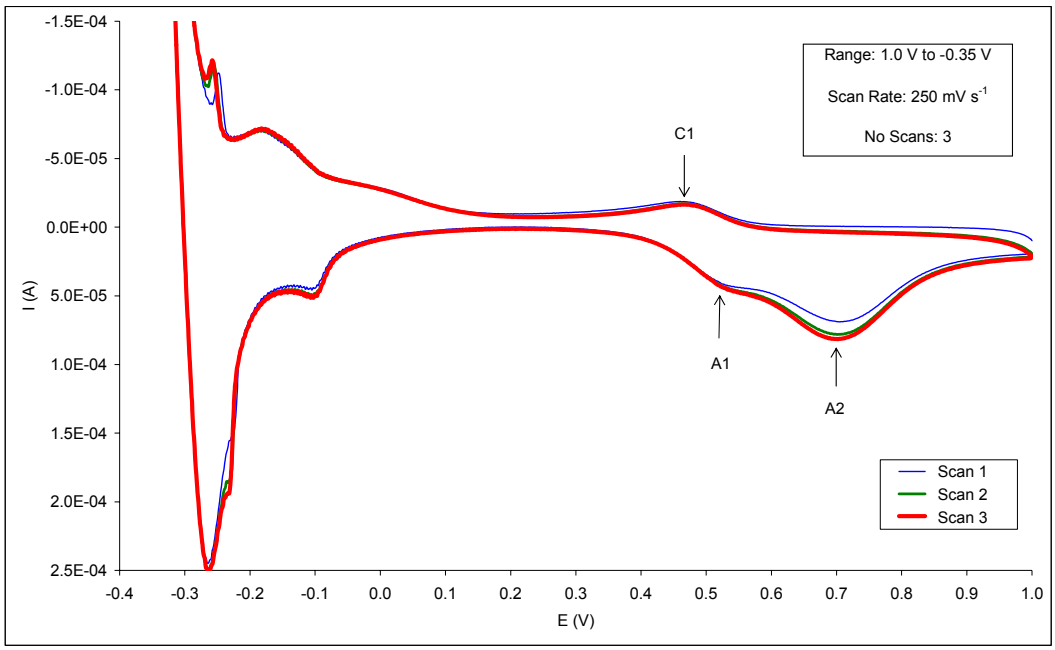

Figure 3.19 Cyclic voltammograms of a solution containing 105 mg l^{-1} iron, 188 mg l^{-1} palladium and 47 mg l^{-1} platinum in a 0.1 M HCl background electrolyte, using a platinum working electrode.

Reactions involving copper, palladium and platinum

Following the interpretation of voltammograms involving combinations of two of the major metal ions found in a typical PML solution, the complexity of the synthetic test solutions was increased to include three metal ions. The combined interaction of copper, palladium and platinum ions with a glassy carbon electrode in a background solution of 0.1 M HCl is described here.

Discussion - Figures 3.20 and 3.21. A comparison of voltammograms obtained for a solution containing *(i)* iron, copper, palladium and platinum ions (4-M solution) and *(ii)* a solution containing iron, palladium and platinum ions, using a glassy carbon working electrode is provided in Figure 3.20. Three major differences were noted in the negative potential range. The first difference relates to the absence of major hydrogen adsorption and desorption peaks for the analysis of the 4-M solution. Secondly, it was noted that the occurrence of the catalytic hydrogen

reduction wave for 4-M solutions shifted to more negative potentials by approximately 50 mV . Thirdly, an additional oxidation peak, labelled A1, was observed for the voltammogram of the 4-M solution.

The differences noted for the voltammograms in the negative potential region is ascribed to changes in the overall electrocatalytic properties of the working electrode when the two different solutions are analysed. In the case of the 4-M solution, it is assumed that the deposition of copper metal centres, in addition to the formation of palladium and platinum metal centres occur.

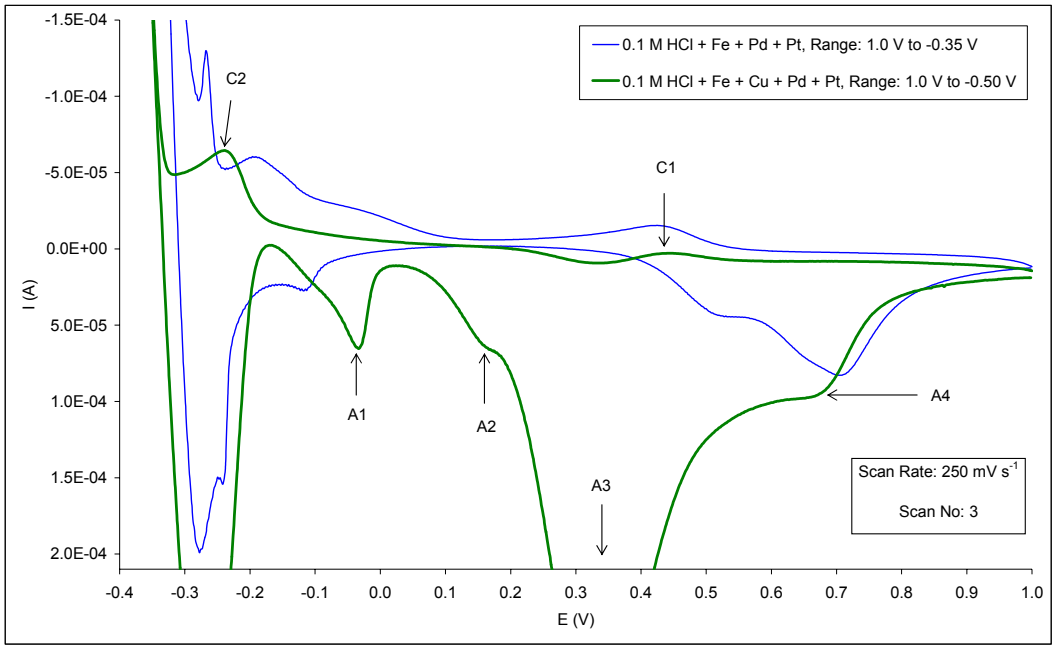

Figure 3.20 Cyclic voltammograms of solutions containing *(i)* 105 mg l^{-1} iron, 188 mg l^{-1} palladium, 47 mg l^{-1} platinum and *(ii)* 105 mg l^{-1} iron, 170 mg l^{-1} copper, 188 mg l^{-1} palladium, 47 mg l^{-1} platinum in a 0.1 M HCl background electrolyte, using a glassy carbon working electrode.

This assumption is confirmed by comparing a voltammogram recorded for a 4-M solution to that of a solution containing only copper ions, as shown in Figure 3.21, where it was noted that Peak positions A1 and A1A were similar.

Earlier in Section 3.5.3, under the sub-heading "Reactions involving copper" it was concluded that Peak A1A indicated the anodic dissolution of copper metal to Cu^{+}.

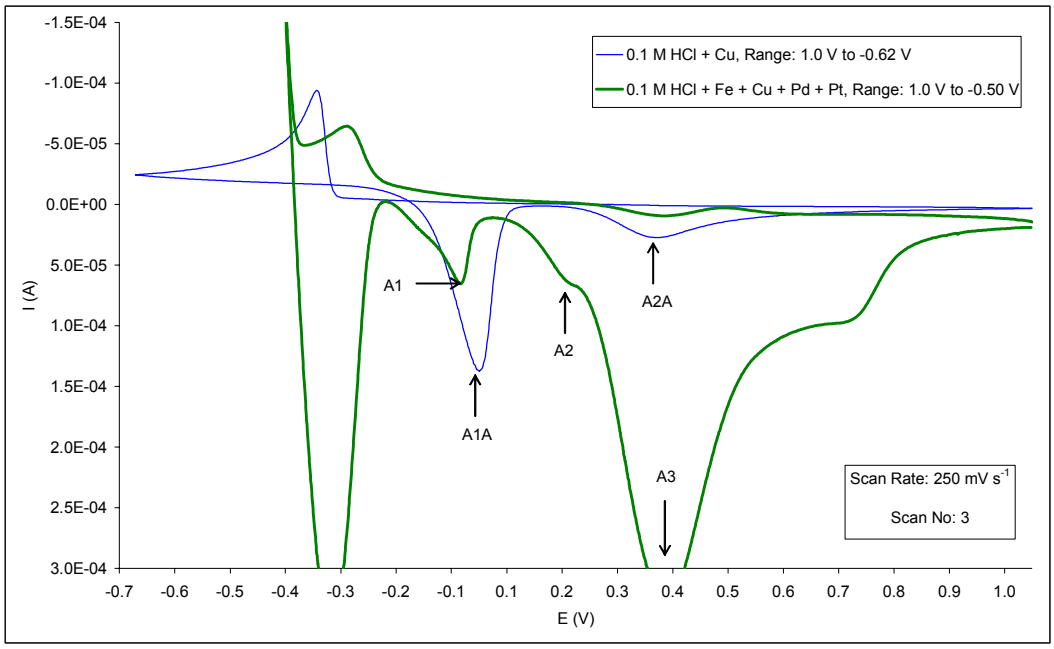

Figure 3.21 Cyclic voltammograms of solutions containing *(i)* 196 mg l^{-1} copper and *(ii)* 105 mg l^{-1} iron, 170 mg l^{-1} copper, 188 mg l^{-1} palladium, 47 mg l^{-1} platinum and in a 0.1 M HCl background electrolyte, using a glassy carbon working electrode.

Following the discussion under the previous sub-heading "Reactions involving palladium and platinum" (Section 3.5.3), Peak C1 in Figure 3.20 was ascribed to the reduction of Fe^{3+} on a platinum surface. The fact that the overall current on the forward sweep following Peak C1 is positive, i.e. indicating that oxidation is taking place, confirms the presence of platinum metal centres on the glassy carbon working electrode (refer to sub-heading "Reactions involving platinum", Section 3.5.3).

The formation of Peak C2 in Figure 3.20 is followed by a catalytic hydrogen ion reduction wave. Based on discussions earlier in Section 3.5.3 regarding the catalytic generation of hydrogen gas, it is clear that the presence of palladium, platinum or a combination of the two metals is

responsible for the reduction current.

The presence of platinum metal centres on the glassy carbon working electrode after conducting a CV experiment in the presence of a 4-M solution was already confirmed by Peak C1 in Figure 3.20. The presence of palladium metal centres was confirmed by Peaks A2 and A4 of the same voltammogram. Peak A2 is indicative of the oxidation of molecular hydrogen on palladium metal centres, as shown under the sub-heading "Reactions involving palladium" in this section (Section 3.5.3). Peak A4 was ascribed to the anodic stripping of palladium metal, after comparison to the voltammogram recorded for a solution containing iron, palladium and platinum ions, also shown in Figure 3.20.

Although the voltammograms are not shown here, potential ranges for CV experiments involving a 4-M solution and a glassy carbon electrode were varied between -0.27 V and -0.50 V in the negative potential range, after starting all experiments at 1.0 V. From these experiments it became apparent that significant quantities of copper metal centres are formed at more positive potentials compared to palladium and platinum.

When a voltammogram recorded for a 4-M solution was compared to that of a solution containing only copper ions, as shown in Figure 3.21, it was noted that peak positions A3 and A2A correlated. Earlier in Section 3.5.3, under the sub-heading "Reactions involving copper" Peak A2A was associated with the oxidation of Cu^{+} to Cu^{2+}. The magnitude of Peak A3 relative to Peak A2A did however indicate that an additional oxidation process must be occurring.

Due to the fact that copper, palladium and platinum metal centres were deposited on the glassy carbon working electrode, it is possible that alloys or combinations of metals formed on the electrode surface. The magnitude of the oxidation peaks labelled A3 in Figures 3.20 and 3.21 is therefore ascribed to the oxidation of copper metal centres possibly contained in *(i)* a deposit involving a combination of copper and palladium, or *(ii)* a deposit

consisting of a combination of copper, palladium and platinum. Since conditions for the oxidation of Cu^{+} to Cu^{2+} would be favourable at these potentials, any copper metal stripped from the electrode surface would instantaneously be converted to Cu^{2+}.

It was reasoned that two peaks for the anodic dissolution of copper were present. Peak A1 (Figures 3.20 and 3.21) was associated with the oxidation of copper metal centres to Cu^{+} where the metal was available on the surface of the glassy carbon working electrode, or the surface of other metal centres. Peak A3 was ascribed to the direct oxidation of copper metal centres contained in an alloy to Cu^{2+} ions, as described in the previous paragraph.

The conclusion that Peak A3 could be ascribed to the anodic stripping of copper metal centres from deposits consisting of a combination of different metals was supported by the fact that the magnitude of Peak A1A in Figure 3.21 is larger relative to the corresponding Peak A1. Originally Peak A1A was associated with the anodic dissolution of copper metal centres from deposits containing only copper metal, whilst Peak A1 was identified as the copper stripping peak where copper, palladium and platinum was present on the working electrode surface. It was concluded that the oxidation current associated with Peak A1 was reduced due to the fact that some of the copper originally present on the surface of glassy carbon electrode was now contained in an alloy with palladium or a combination of palladium and platinum.

Additional support for the argument that copper is anodically dissolved from deposits containing a combination of copper and palladium metal centres was also provided by the general discussion under the sub-heading “Reactions involving copper and palladium” of this section (Section 3.5.3). It was concluded that deposits containing a mixture of copper and palladium metal centres may be present on the glassy carbon electrode surface. The magnitudes of the peaks labelled A3 in Figures 3.13 to 3.16 also indicated that oxidation processes in addition to the

conversion of Cu^{+} to Cu^{2+} must be occurring, as pointed out earlier when Peak A3 of Figure 3.21 was discussed.

General discussion. The investigation related to the interaction of solutions containing copper, palladium and platinum ions with a glassy carbon electrode revealed that all the ions are reduced to metal on the electrode surface. By varying the potential ranges employed for different CV experiments, it was shown that significant quantities of copper metal was deposited at more positive potentials compared to palladium and platinum. As more negative potentials are imposed on the working electrode, the ratio of palladium and platinum metal centres relative to copper will increase, eventually resulting in the catalytic generation of hydrogen gas on the PGM metal centres.

It was also shown that copper and palladium metal centres were dissolved anodically. No evidence was found to indicate that platinum metal was dissolved anodically under the experimental conditions employed. This fact should be kept in mind when analysing successive CV scans. As the number of potential cycles increase, the amount of platinum metal centres on the electrode surface will increase, thereby influencing the overall characteristics of the working electrode.

As pointed out under the sub-heading “Reactions involving copper and palladium” in this section (Section 3.5.3), the exact characteristics of the metals electrochemically deposited and stripped from the glassy carbon electrode cannot be elucidated from CV experiments alone. Additional surface analytical techniques, for example SEM-EDS may be employed.

The study of the composition and morphology of metals deposited onto a cathode material should form part of any additional studies that may follow this research project.

Summary of reactions involving the major metal ions

The cathodic and anodic peak potentials (E_{pc}, E_{pa}) observed for the

deposition and anodic dissolution of different combinations of copper, palladium and platinum is provided in Table 3.2.

Table 3.2 Comparison of cathodic (E_{pc}) and anodic (E_{pa}) peak potentials for synthetic solutions containing combinations of the major metal ions found in a typical PML solution.

Matrix	Deposition E_{pc} (V)	Dissolution E_{pa} (V)	Reference
Pd - 99 mg l^{-1}	-0.23	0.59	Figure 3.6 (C1, A2)
Pt - 196 mg l^{-1}	-0.18 [(b)]	N/O [(a), (b)]	Figure 3.9 (C1)
Cu - 431 mg l^{-1}	-0.35	0.10	Figure 3.11 (C1, A1)
Pd - 171 mg l^{-1}	-0.39	0.52	Figure 3.13 (C2, A4)
Cu - 189 mg l^{-1}	-0.28	0.00	Figure 3.13 (C1, A1)
Pd - 188 mg l^{-1}	< ca. 0.10 [(c)]	0.72	Figure 3.17 (A2)
Pt - 47 mg l^{-1}	< ca. 0.10 [(c)]	N/O [(a)]	Figure 3.17
Pd - 188 mg l^{-1}	< ca. 0.20 [(d)]	0.68	Figure 3.20 (A4)
Pt - 47 mg l^{-1}	< ca. 0.20 [(d)]	N/O [(a)]	Figure 3.20
Cu - 170 mg l^{-1}	< ca. 0.20 [(d)]	-0.03	Figure 3.20 (A1)

[(a)] No peak observed.

[(b)] Scan rate of 100 mV s^{-1}.

[(c)] No discrete peaks observed. The approximate potential below which significant quantities of metal will deposit is supplied. Refer to sub-heading "Reactions involving palladium and platinum" in Section 3.5.3 for detailed discussion.

[(d)] No discrete peaks observed. The approximate potential below which significant quantities of metal will deposit is supplied. Refer to sub-heading "Reactions involving copper, palladium and platinum" in Section 3.5.3 for detailed discussion.

Unless stated otherwise, the potentials relate to experiments carried out at CV scan rates of 250 mV s^{-1}, with the potential value recorded on the third sweep. A glassy carbon working electrode, a Ag/AgCl reference electrode containing 3 M KCl, and a 0.1 M HCl background electrolyte was used at all times.

All the major metal ions, regardless of the combinations in which they were tested, deposited when a glassy carbon electrode was employed. Evidence of the anodic dissolution of deposited metal centres was found in the case of copper and palladium, again regardless of the combination of metals used for the particular experiment.

It should be kept in mind that the background electrolyte will influence the anodic stripping process of the various metals. The fact that a 0.1 M HCl background electrolyte was used may have contributed to the absence of a significant oxidation peak for the dissolution of platinum. Another possibility may be that the anodic dissolution was kinetically slow compared to the time scale of the CV experiments.

3.5.4 Palladium Mother Liquor (PML) Solutions

The voltammogram of a typical PML solution originally shown in Figure 3.1 was compared to voltammograms of synthetic solutions as illustrated in Section 3.5.3. If it could be shown that similarities did exist between voltammograms of synthetic solutions containing only combinations of copper, palladium and platinum in a 0.1 M HCl background electrolyte, and actual PML solutions with matrices similar to that indicated in Table 1.1, the interpretation of PML voltammograms would be simplified considerably. The objective was therefore to establish if these comparisons would assist in providing a qualitative explanation of the interaction of PML solutions with a particular cathode.

In Table 3.3 the actual metal content of the PML solution used for the

comparison is shown. The pH of this solution was 4.5, with major cation and anion concentrations similar to that indicated in Table 1.1.

Table 3.3 Actual metal content of PML solution used in the comparison of voltammograms recorded for refinery and synthetic solutions.

Element	**Concentration** (mg l^{-1})
Cu	494
Pt	19
Pd	171
Rh	6
Ru	3
Ag	3
Bi	4
Sb	1
Se	6
Te	3
Zn	2

Discussion of results

A comparison of voltammograms recorded for the PML solution described above and synthetic solutions containing *(i)* copper and palladium (refer to Figure 3.13) or *(ii)* copper, palladium and platinum ions (refer to Figure 3.20) is shown in Figure 3.22.

If the solutions used to obtain the voltammograms shown in Figure 3.22 are compared in terms of copper, palladium and platinum content, it is evident that the ratios of metals found in each case vary significantly.

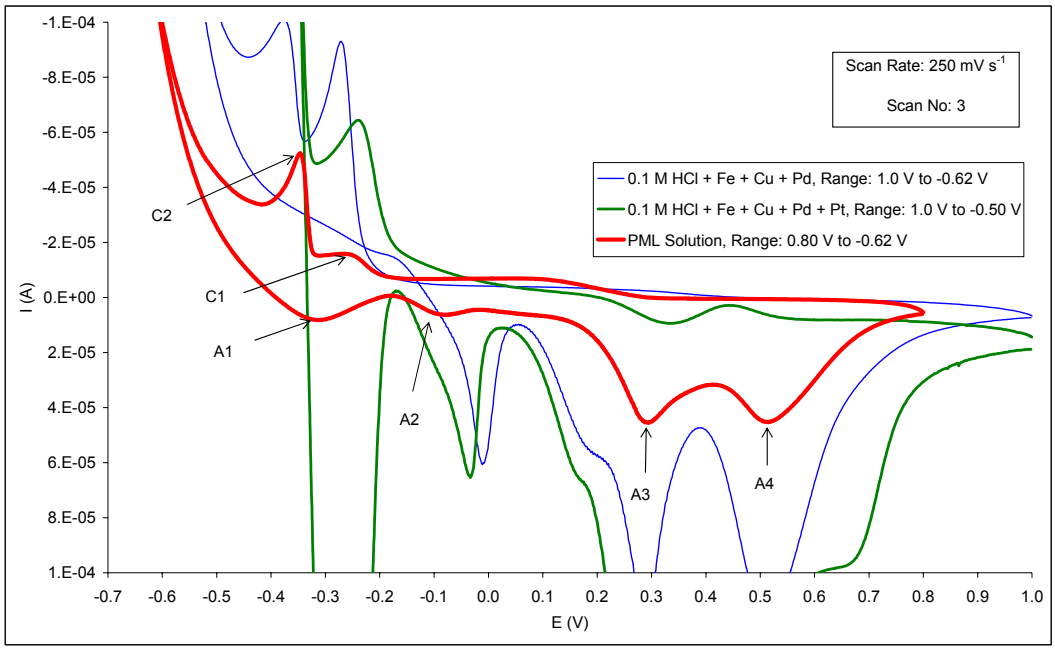

Figure 3.22 Cyclic voltammograms of *(i)* 106 mg l^{-1} iron, 171 mg l^{-1} copper and 189 mg l^{-1} palladium in a 0.1 M HCl background electrolyte, *(ii)* 105 mg l^{-1} iron, 170 mg l^{-1} copper, 188 mg l^{-1} palladium and 47 mg l^{-1} platinum in a 0.1 M HCl background electrolyte, and *(iii)* a PML solution. A glassy carbon working electrode was used in all cases.

For the synthetic solution containing copper and palladium, an approximate ratio of 1:1 was used, whilst an approximate metal ratio of 4 (Cu) : 4 (Pd) : 1 (Pt) was employed for the remaining synthetic solution. In contrast, the PML metal ratio was 25 (Cu) : 10 (Pd) :1 (Pt).

It may be argued that the metal ratios for the synthetic solutions should have been closer to that observed for the PML solution in order to reduce the number of variables when comparing the respective voltammograms. This will however not be practical due to the variability of a typical PML matrix in response to overall variability of the refining process. The best

approach would therefore be to use the ratios of metals in the synthetic solutions as a baseline, and to extrapolate the behaviour of these baseline solutions to explain the characteristics of voltammograms for PML solutions containing different ratios of metals.

This approach was used to interpret the PML voltammogram in Figure 3.22, where the amount of platinum was low compared to copper and palladium. It was noted that the PML voltammogram exhibited characteristics of both the synthetic solution voltammograms. Peaks C1 and C2 are similar to the peaks recorded for a synthetic solution containing only copper and palladium ions, whilst Peak A1 is similar to that observed for a solution containing copper, palladium and platinum ions. This provided evidence that the interaction between the PML solution and the working electrode involved copper, palladium and platinum ions.

The deposition of copper, palladium and platinum metal from a typical PML solution via a glassy carbon working electrode, and the subsequent anodic dissolution of copper and palladium metal was confirmed by comparing the anodic peak positions of the PML solution to those obtained for the synthetic solutions. Peak A1 was ascribed to the oxidation of molecular hydrogen on platinum metal centres (also refer to Figure 3.9). Peak A2 was associated with the oxidation of copper metal centres to Cu^{+} where the metal was present on the surface of the glassy carbon working electrode, or the surface of other metal centres (refer to Figure 3.21). Peak A3 was related to the oxidation of copper metal centres contained in an alloy (with palladium or a combination of palladium and platinum) to Cu^{2+} ions, as well as the oxidation of Cu^{+} to Cu^{2+} (refer to Figure 3.21). Peak A4 was indicative of the anodic dissolution of palladium metal centres (also refer to Figure 3.6).

It was also noted that the magnitude of Peaks C1 (deposition of copper metal centres) and A2 (oxidation of copper metal centres to Cu^{+} from surface deposits) for the voltammogram of the PML solution shown in

Figure 3.22 is small compared to the concentration of copper (494 mg l^{-1}) present in the sample. This may be attributed to the fact that alloys involving copper and palladium, or copper, palladium and platinum are formed, rather than pure copper deposits.

Based on the evidence presented, it was concluded that it is feasible to provide a qualitative explanation of the interaction between a typical PML solution and a glassy carbon electrode, using voltammograms recorded for synthetic solutions containing different combinations of copper, palladium and platinum.

3.5.5 Minor Metal Ions

In Section 3.2.2 it was noted that the emphasis of studies related to the influence of minor metal ions on the overall interaction of typical PML solutions with a glassy carbon electrode was different to the approach taken for the major metal ions. The concentrations of the minor metal ions in PML solutions were very low compared to the three major metal ions (refer to Table 1.1). As a consequence, the only way the presence of these metals was expected to alter the characteristics of voltammograms recorded for PML solutions was via catalytic or inhibitive processes induced by active metal centres of minor metals present on the electrode surface.

For this reason, attention was focussed on the possibility of reducing the minor metal ions to their metallic states in the potential region utilised for a 0.1 M HCl matrix and a glassy carbon working electrode. If metal deposition was feasible, it follows that catalytic or inhibitive processes were possible. A total of 14 synthetic single component solutions were analysed via CV, namely antimony, arsenic, bismuth, gold, iridium, lead, nickel, rhodium, ruthenium, selenium, silver, tellurium, tin and zinc.

It was determined that antimony, bismuth, gold, lead, rhodium, ruthenium and tellurium deposited within the potential range applicable to a 0.1 M

HCl matrix and a glassy carbon working electrode. The voltammograms recorded for single component solutions, and 4-M solutions in combination with one of these minor metals were studied in detail[43]. From these studies it became apparent that the characteristics of the voltammograms would not make a significant contribution to the process of interpreting voltammograms of typical PML solutions.

Copies of the voltammograms recorded for synthetic single component solutions involving metal deposition are shown in *Appendix A*. The sign convention and data presentation formats described in Section 3.2.3 also applies to Figures A1 to A7 presented in *Appendix A*.

Although studies involving the minor metals did not directly contribute to the development of methodologies to interpret voltammograms recorded for refinery effluents, several important facts were established. The presence of some of these metals on the glassy carbon electrode, in particular antimony, bismuth, lead, silver and tellurium, inhibited the occurrence of significant hydrogen ion reduction currents at potentials where this reaction would normally occur on a clean electrode. Although it is not likely that glassy carbon electrodes would be employed in the electrochemical reactor designed during the engineering component of the overall project (refer to Chapter 1 and Section 3.1), the possible advantages of inhibiting hydrogen gas generation via minor metal deposits on a given cathode material should be kept in mind.

It was also shown that it is possible to deposit other precious metals, namely gold, rhodium and ruthenium from synthetic single component solutions in a 0.1 M HCl matrix, utilising a glassy carbon electrode. This provided an indication that it may be feasible to remove these metals, in addition to palladium and platinum, from refinery effluents via carbon based cathode materials.

For the analysis of single component synthetic solutions involving iridium,

one cathodic and one anodic peak was observed. This was ascribed to the presence of a Ir^{4+}/Ir^{3+} redox couple. No evidence of metal deposition, described in literature[44] as a three-electron transfer reaction involving a Ir^{3+}/Ir redox couple (assuming a chloride medium), was found.

In the case of selenium, no evidence of redox behaviour was observed for single component synthetic solutions. When selenium was added to 4-M solutions, the resultant voltammograms were significantly different compared to voltammograms obtained for normal 4-M solutions. This observation led to the conclusion that selenium must react with the components in the 4-M solution, or deposited metal centres present on the glassy carbon electrode. Due to the scope of the project as described in Chapter 1 and Section 3.1.2 no further research related to the behaviour of selenium was conducted.

Of the synthetic single metal ions solutions tested arsenic, nickel, tin, and zinc did not exhibit redox behaviour in the potential range applicable to a 0.1 M HCl matrix and a glassy carbon electrode.

It should be noted that the behaviour of combinations of more than one minor metal ion in a 4-M solution, utilising a glassy carbon electrode was not investigated. The presence of different combinations of metals on the electrode surface will change the overall electrocatalytic properties of the electrode, influencing the thermodynamic and kinetic characteristics of the redox processes occurring on the electrode surface.

These issues should be investigated in more detail in later research projects, where the emphasis must be placed on fundamental mechanisms involved in metal deposition. Knowledge of these fundamental issues may assist in developing electrochemical metal recovery processes which, for example, will allow for the selective recovery of metal ions in solution.

3.6 CONCLUSIONS

A summary of the objectives of the research associated with this chapter, and the experiments conducted to achieve these objectives are provided. This is followed by a discussion of the main conclusions, and proposed future research activities.

3.6.1 Summary of Research Activities

In Section 3.1 it was stated that the first phase of the research project described in this dissertation involved a qualitative understanding of the interactions of the different metal ions found in typical PML solutions with a particular cathode material.

The potential use of CV as a tool to understand these interactions was discussed in Section 3.1.1. It was noted that the voltammograms recorded for multi-component solutions, especially where metal deposition was involved, were complex and difficult to interpret. The objective of the research activities described in this chapter was to develop the necessary methodologies required to interpret these complex voltammograms.

Section 3.2.2 described the approach that was adopted to develop the required methodologies. Single component synthetic solutions containing the metal ions normally found in a PML solution were prepared and analysed via CV. The resultant voltammograms were studied in order to understand the interaction of the single metal ion with a glassy carbon electrode on a qualitative level. Following the successful investigation of single component solutions, the complexity of the synthetic solutions was increased to contain different combinations of metal ions.

The approach of gradually increasing the complexity of synthetic solutions to approximate the composition of PML solutions was implemented in two phases. In the first phase the interaction of the major metal ions found in a typical PML solution, namely copper, palladium and platinum was investigated. The second phase involved a study of the minor metal ions

antimony, arsenic, bismuth, gold, iridium, lead, nickel, rhodium, ruthenium, selenium, silver, tellurium, tin and zinc. Synthetic single component solutions of the minor metal ions and combinations of a particular minor metal ion with copper, palladium and platinum were analysed in this phase.

Finally, the voltammograms recorded for synthetic solutions containing different combinations of metal ions were compared to the voltammogram of a PML solution. These comparisons led to a qualitative interpretation of the interaction between metal ions contained in PML solutions with a working electrode, in this case glassy carbon, when a particular potential is imposed on the electrode.

In order to assist in the interpretation of the various voltammograms, techniques related to *(i)* the variation of experimental potential scan ranges, *(ii)* the use of a witness ion, and *(iii)* the use of a platinum disc electrode were employed.

3.6.2 Reactions Involving Major Metal Ions

A summary of the peak potentials recorded for metal deposition (E_{pc}) and the anodic dissolution of deposited metal centres (E_{pa}) involving synthetic solutions containing combinations of the major metal ions found in a typical PML solution was provided in Table 3.2.

All the major metal ions, regardless of the combinations used, deposited when a glassy carbon electrode was employed. Evidence of the anodic dissolution of deposited metal centres was found in the case of copper and palladium, again regardless of the combination of metals used for the particular experiment.

It should be kept in mind that the background electrolyte will influence the anodic stripping process of the various metals. The fact that a 0.1 M HCl

background electrolyte was used may have contributed to the absence of a significant oxidation peak for the dissolution of platinum. Another possibility may be that the anodic dissolution was kinetically slow compared to the time scale of the CV experiments. Since the overall research project focussed on the removal, i.e. deposition of metals (refer to Chapter 1) the issue of anodic dissolution was not investigated in detail.

The interaction of synthetic solutions containing *(i)* a combination of palladium and platinum ions, and *(ii)* a combination of copper, palladium and platinum ions (0.1 M HCl matrix) with a glassy carbon electrode was discussed in Section 3.5.3.

After analysing solutions containing palladium and platinum ions, it was concluded that platinum metal centres deposited at potentials $<$ ca. 0.10 V. This was followed by the deposition of palladium metal centres on platinum metal surfaces. The peak potential for the anodic dissolution of palladium metal centres was observed at 0.70 V (refer to Table 3.2).

For solutions containing copper, palladium and platinum ions it was noted that the deposition of significant amounts of these metals occurred at potentials more negative than ca. 0.20 V. It was shown that significant quantities of copper metal centres formed at more positive potentials compared to palladium and platinum. As more negative potentials were imposed on the working electrode, the ratio of palladium and platinum metal centres relative to copper increased, eventually resulting in the catalytic generation of hydrogen gas on the PGM metal centres. Peak potentials of -0.03 V and 0.68 V respectively were observed for the anodic dissolution of copper and palladium (refer to Table 3.2).

3.6.3 Palladium Mother Liquor (PML) Solutions

Comparisons between voltammograms recorded for an actual PML solution and synthetic solutions (refer to Figure 3.22) were used to predict the behaviour of metal ions contained in the PML.

These comparisons indicated that copper, palladium and platinum ions in the PML solution were reduced to their metallic form on a glassy carbon electrode. The anodic dissolution of copper and palladium originally deposited from PML solutions was also observed.

It was noted that the behaviour of a typical PML solution containing a combination of many different metal ions and other cations and anions (refer to Table 1.1) could be interpreted by comparison to a synthetic solution containing only the three major metal ions in a 0.1 M HCl matrix.

3.6.4 Minor Metal Ions

A total of 14 synthetic single component solutions were analysed via CV, namely antimony, arsenic, bismuth, gold, iridium, lead, nickel, rhodium, ruthenium, selenium, silver, tellurium, tin and zinc.

It was determined that antimony, bismuth, gold, lead, rhodium, ruthenium and tellurium were deposited within the potential range applicable to a 0.1 M HCl matrix and a glassy carbon working electrode. The voltammograms recorded for single component solutions, and 4-M solutions in combination with one of these minor metals were also studied in detail.

Although studies involving the minor metals did not directly contribute to the development of methodologies to interpret voltammograms recorded for refinery effluents, important facts were established:

- Where antimony, bismuth, lead and tellurium were deposited, evidence of the inhibition of hydrogen gas evolution was found. The possible advantages of inhibiting the formation of hydrogen gas via minor metal deposits on the cathode of an industrial electrochemical reactor should be kept in mind.
- It was also shown that it is possible to deposit other precious metals, namely gold, rhodium and ruthenium from synthetic single component

solutions in a 0.1 M HCl matrix, utilising a glassy carbon electrode. This provided an indication that it may be feasible to remove these metals, in addition to palladium and platinum, from refinery effluents via carbon based cathode materials.

3.6.5 Future Research

Throughout this chapter it was emphasised that the research work described was not intended to provide a quantitative description of the many complex reaction mechanisms taking place at the working electrode.

The nature of the project necessitated confirmation of the feasibility of removing PGMs from refinery effluents, and provision of information that could be used in the development of a practical electrochemical reactor. As a consequence, time and resources that could be allocated to different aspects of the research project were limited.

Additional areas of research that will add to the overall fundamental understanding of processes occurring at the interface between a particular cathode material and a typical refinery effluent were identified throughout this chapter. These research requirements are listed below:

- Following the successful removal of PGMs from a refinery effluent via an electrochemical reactor, the metals need to be recovered from the cathode material. Research related to aspects involving the recovery of metals, in particular anodic dissolution will be required. The influence of factors related to the substrate, the presence of different metal-ligand complexes and characteristics of the sample matrix need to be investigated.

  Other methods of metal recovery, for example acid leaching, the in-situ generation of chorine gas to dissolve deposited metals, or the incineration of carbon based cathodes may also require consideration.

- Investigations into the morphology, mechanisms of formation and

composition of deposited metal centres will assist in the development of an electrochemical reactor capable of removing PGMs from refinery effluents.

- The inhibition of hydrogen gas formation via an electrochemical reactor will be important from a safety and efficiency point of view. It was noted that the deposition of antimony, bismuth, copper, lead, silver and tellurium metal centres on a glassy carbon working electrode, using a 0.1 M HCl matrix, inhibited the generation of significant quantities of hydrogen gas at potentials where this reaction would normally occur if palladium and platinum metal centres were present. Further research with regards to the factors and mechanisms inhibiting hydrogen gas generation would therefore be beneficial.

- It was pointed out that the quantity and ratio of different metal centres found on the electrode surface would influence the overall characteristics of the working electrode in terms of electrocatalytic activity. If an electrochemical reactor is used to remove palladium and platinum from PML solutions, the amount of PGMs on the cathode surface will increase with operation time.

  The CV experiments described in this chapter were conducted under conditions where the majority of active sites on the working electrode surface consisted of glassy carbon. It is expected that the proposed electrochemical reactor will be operated under conditions where the deposited PGMs will be recovered from the cathode surface at regular intervals to keep the metal inventory in the plant as low as possible. This implies that the original cathode surface will predominante under normal operating conditions.

  If operating requirements change and the accumulation of metals on the electrode is allowed to proceed to a stage approximating full coverage of the cathode surface, additional test work will be required to assess the overall influence on deposition.

- The behaviour of a single minor metal ion added to a mixture of copper, palladium and platinum (0.1 M HCl matrix) was investigated via a glassy carbon electrode. It was reported that the presence of minor metals in a PML solution did not have a significant impact on the overall characteristics of the resulting voltammograms. A study of the interaction of different combinations of these minor metal ions (antimony, arsenic, bismuth, gold, iridium, lead, nickel, rhodium, ruthenium, selenium, silver, tellurium, tin and zinc) and the major metal ions found in typical PML solutions (copper, palladium and platinum) may however provide valuable information with regards to electrocatalytic processes involving metal deposition or hydrogen gas generation.

Although the additional test work proposed above will be beneficial to the overall understanding of processes occurring at a glassy carbon working electrode surface, it may be more sensible to carry out this work on the cathode material finally selected for the proposed electrochemical reactor. If however, the characteristics of this substrate complicate the redox reactions taking place at the electrode surface, it may be advisable to first use a glassy carbon electrode before progressing to a more complex system.

In addition to CV, other analytical techniques such as spectroelectrochemistry, SEM-EDS and the use Rotating Ring Disc Electrode (RRDE) experiments would be required to obtain more detailed fundamental information regarding the processes occurring at a specific electrode-solution interface.

3.6.6 Final Comments

The objective to develop the necessary methodologies required to interpret voltammograms involving multi-component solutions and metal deposition was achieved. The principles applied to the interpretation of voltammograms recorded for PML solutions can in theory also be used for

other refinery streams.

The project now reached a stage where it was possible to assess the applicability of using a particular cathode material in the proposed electrochemical reactor.

4 EVALUATION OF SELECTED CATHODE MATERIAL

4.1 INTRODUCTION

The necessity to conduct two separate research projects covering fundamental and engineering aspects in order to develop an electrochemical reactor capable of removing Platinum Group Metals (PGMs) from refinery effluents was discussed in detail in Chapter 1.

As part of the engineering project, the use of an electrochemical reactor employing a packed particulate bed as the cathode was proposed[39]. The use of a three-dimensional cathode is most suitable for treatment of refinery effluents such as the Palladium Mother Liquor (PML), which contains low concentrations of PGMs (refer to Table 1.1), due to the high surface area per unit volume. Furthermore, the particles are good turbulence promoters, resulting in improved mass transport conditions.

A particulate bed was selected above other forms of three-dimensional cathodes such as screens or felts as no manual labour is required to load or discharge the reactor, allowing process automation. The pressure drop across the packed bed cathode is also lower compared to cathodes employing foams or felts.

It was also proposed that graphite particles be utilised in the packed bed in order to facilitate techniques involving the recovery of PGMs from the cathode material. The use of graphite for processes such as anodic stripping, leaching, and incineration will prevent complications due to the contamination of the recovered metals by the original cathode material.

From an engineering point of view, certain criteria had to be met before the proposed use of graphite particles would be feasible:

- Commercial availability of the selected material in particulate form.

- Low porosity of the material to prevent changes in the characteristics of the cathode, and inefficiencies related to recovery processes such as anodic dissolution.
- Resistance to chemical degradation.
- Availability of the material at a reasonable cost.

After considering the requirements for the particles listed above, the use of isostatically pressed graphite particles (grade ET-10, Electrographite Carbon Co.) was proposed. Although the cathode material met engineering requirements, the feasibility of recovering palladium and platinum from PML solutions had to be confirmed.

The second phase of the fundamental research project involved the evaluation of isostatically pressed graphite particles as a possible cathode material for the proposed electrochemical reactor, and is discussed in this chapter.

4.1.1 Objectives

In Chapter 3, qualitative methodologies were developed to interpret the interaction between metal ions found in a typical Palladium Mother Liquor (PML) and a glassy carbon working electrode. Experiments involving Cyclic Voltammetry (CV) were used to confirm the reduction of the major metal ions present in a PML namely copper, palladium and platinum to their respective metallic states on a glassy carbon surface. The anodic dissolution of copper and palladium metal centres present on a glassy carbon surface was also demonstrated.

The main focus of the research described in this chapter was to use the methodologies discussed in Chapter 3 to evaluate the viability of using the graphite particles identified via the engineering project as a cathode material.

If these qualitative investigations indicated that the use of graphite particles as a cathode were feasible, a quantitative evaluation of the level of PGM reduction in the PML solution would follow. This was necessary to confirm if the use of the proposed cathode material would result in the removal of the total PGMs present in the PML solution to concentrations $<$ 10 mg l^{-1}, with no single PGM present at concentrations of $>$ 2 mg l^{-1} as defined in the overall project objectives (refer to Chapter 1).

In addition, concerns were raised with regards to the presence of amminated PGM complexes found in particular refinery effluents, including the PML. It was claimed that the stability of some of these complexes prevented the recovery of PGMs via chemical or electrochemical processes. The exact nature of the different complexes was unknown, although $Pt(NH)_4^{2+}$ was identified as one of the stable species[45].

Since the presence of stable amminated complexes could potentially lead to inefficiencies when the proposed electrochemical reactor is used, the effect of NH_3 ligands on the overall recovery of PGMs from PML solutions had to be evaluated.

The detailed objectives of the research activities associated with Chapter 4 are listed below:

- Use methodologies developed in Chapter 3 to predict if palladium and platinum present in the PML solution could be reduced to their respective metallic states on the proposed cathode surface (isostatically pressed graphite, grade ET-10).
- If it was shown that palladium, platinum or a combination of the PGMs could be reduced to metal on the proposed cathode material, determine if the other major metal ion present in the PML solution (copper) would be deposited with the PGMs, resulting in the contamination of the final product.

- Validate predictions related to PGM recovery via a graphite electrode by depositing relevant metals on the proposed cathode material.
- If it was shown that copper, palladium, platinum or any combination of these metals could be deposited on the graphite surface, determine the extent of metal recovery from PML solutions.
- Evaluate the effect of NH_3 ligands on the overall recovery of PGMs from PML solutions.

4.2 EXPERIMENTAL DESIGN AND DATA PRESENTATION

4.2.1 Working Electrode

In order to evaluate the feasibility of using isostatically pressed graphite particles as a cathode material, a working electrode with an active surface consisting of the proposed material had to be used. Since working electrodes of this type (referred to as “graphite working electrodes” in the rest of the chapter) were not commercially available, they had to be constructed in-house. These working electrodes were used in all the experiments described in the present chapter. The in-house construction of the graphite working electrodes is described in Section 4.3.1.

4.2.2 Experimental

To meet the research requirements defined in Section 4.1.1, four different types of experiments were conducted. The first set of experiments involved investigations related to the feasibility of reducing palladium and platinum ions to their respective metallic states on a graphite working electrode, employing cyclic voltammetric methodologies. Detailed information is provided under the sub-heading “Feasibility studies” of this section.

For the second set of experiments the interpretation of particular voltammograms was validated by holding the graphite working electrode at potentials where a particular metal ion was predicted to be reduced to its

metallic form. Optical microscopy was utilised to confirm the presence of the particular metal on the electrode surface. Detailed information is provided under the sub-heading “Validation” of this section.

If the deposition of PGMs was confirmed, the degree of metal ion removal was quantified via a third set of experiments involving exhaustive electrolysis. The fourth set of experiments focussed on the effect of NH_3 ligands on the recovery of PGMs from PML solutions. Detailed information is provided under the sub-headings “Exhaustive electrolysis” and “Amminated complexes” of this section.

A three-electrode electrochemical cell with potentiostatic control, identical to the experimental set-up used in Chapter 2 was used to conduct the four different sets of experiments described above. For these experiments, a graphite working electrode was used instead of a glassy carbon or platinum disc working electrode.

Information provided in Section 2.4 (equipment, electrodes, reagents) and Section 2.5 (experimental procedure) also applies to experiments described in this chapter. The only differences are associated with the preparation and cleaning methods adopted for the graphite working electrode and the general procedure followed for each of the different sets of experiments.

Methods of preparing and cleaning the graphite working electrode are provided in Section 4.3.1, whilst the general procedure is described under the relevant sub-heading of the present section.

Feasibility studies

The interaction between the major metal ions found in a typical PML solution (copper, palladium and platinum) and a graphite working electrode was evaluated by performing experiments similar to those described in Section 3.2.2. The following general procedure was used:

- Single component synthetic solutions of the major metal ions found in the PML namely copper, palladium and platinum were prepared. Details regarding the preparation of these solutions were provided in Section 3.3.

- The voltammograms resulting from these single metal ion interactions with a graphite working electrode in an acid chloride matrix (0.1 M HCl) were recorded and analysed. The final concentration of a particular metal ion in solution approximated that found in a typical PML solution. Details regarding the dilution of synthetic single metal ion solutions were provided in Section 3.3.

- Once a qualitative understanding of the behaviour of a single metal ion at the graphite working electrode-solution interface was established, the complexity of the solutions analysed via CV was increased gradually. Voltammograms of different combinations of copper, palladium and platinum in a matrix of 0.1 M HCl were recorded and analysed. The final concentration and ratios of the different metal ions in solution approximated that found in a typical PML solution. Details regarding the combination of different synthetic single metal ion solutions were provided in Section 3.3.

- The potential scan ranges for specific CV experiments were varied to assist in the interpretation of voltammograms.

- Voltammograms recorded for experiments described in Chapter 3, (using a glassy carbon working electrode), were compared to voltammograms obtained whilst employing a graphite working electrode. This approach was used to assist with the interpretation of voltammograms obtained whilst employing the graphite particle electrode.

- Once a qualitative understanding of the behaviour of a combination of copper, palladium and platinum in a 0.1 M HCl matrix was established, actual PML solutions were analysed. Similarities in the

voltammograms obtained for synthetic and PML solutions were used to provide a qualitative explanation of the behaviour of the refinery effluent at the graphite electrode surface.

Validation

If the deposition of copper, palladium or platinum on a graphite working electrode was predicted via cyclic voltammetric methodologies, the predictions were validated. The following general procedure was used:

- The interpretation of a particular voltammogram was validated by holding the graphite working electrode at a potential where a specific metal ion was predicted to be reduced to its metallic form. Optical microscopy was utilised to confirm the presence of the particular metal on the electrode surface.
- Following metal deposition, the working electrode was held at potentials where the anodic dissolution (if predicted via CV) of the deposited metal was favourable. Optical microscopy was utilised to confirm the removal of the particular metal from the electrode surface.
- To reduce the time required to confirm the deposition or anodic dissolution of a particular metal, high overpotentials were applied to the working electrode. In addition, the solution was stirred to improve mass transport conditions. The concentration of the metal ions present in solution was also increased (to $g\ l^{-1}$ ranges) from the normal concentrations employed during CV experiments.

Exhaustive electrolysis

The purpose of the exhaustive electrolysis experiments was to determine what the maximum possible recovery of PGMs from a particular PML solution would be if a graphite working electrode was used as a cathode. No attempt was made to investigate the influence of different experimental parameters on the time taken to recover a particular metal. The optimisation of the recovery process would form part of the engineering

research project, where the parameters could be optimised using the flow regime and design of the proposed electrochemical reactor.

The following general procedure was used:

- The selected PML solution was mixed and filtered through a 0.45 μm cellulose nitrate membrane.
- A sample of ca. 15 ml PML solution was taken prior to the electrolysis experiment.
- A volume of 20 ml PML solution was added to the jacketed reaction vessel employed for the experiment. The temperature of the water bath connected to the reaction vessel was regulated between 24.9 °C and 25.1 °C for the duration of the experiment.
- The graphite working electrode and other required electrodes and equipment was connected.
- A cyclic voltammogram of the PML solution was recorded. Based on the information obtained from the voltammogram, a potential suitable for the deposition of PGMs was selected.
- The graphite working electrode was held at the selected potential for at least 14 hours. During this time a magnetic stirrer motor and stirrer bar was used to increase mass transport of the reactant to the working electrode. The nitrogen gas supply used to purge oxygen from the PML solution was also left open for the duration of the experiment.
- On completion of the metal deposition step, the working electrode was disconnected, and the PML solution was again filtered through a 0.45 μm cellulose nitrate membrane. A sample of ca. 15 ml of the filtered PML solution was taken.
- The PML solution samples taken prior to and after the electrolysis experiment were analysed for palladium and platinum content by means of Inductively Coupled Plasma Mass Spectrometry (ICP-MS),

whilst copper concentrations were determined by means of Inductively Coupled Plasma Optical Emission Spectroscopy (ICP-OES).

- The deposit present on the graphite working electrode was recovered and dissolved in aqua regia. The resultant solution was boiled down to ca. 1 ml, before it was made up to a volume of 10 ml with ultra pure water. This sample solution was analysed for copper, palladium and platinum content. In the case of palladium and platinum determinations ICP-MS was used, whilst ICP-OES was employed for the copper analyses.

To ensure that the results obtained from the exhaustive electrolysis experiments did in fact reflect a situation where the maximum theoretical amount of PGMs was removed from the PML solution, the following measures were adopted:

- The graphite working electrode had a large active surface area, ca. 6 mm diameter, compared to a total volume of 20 ml PML solution used. The construction of the graphite working electrode is described in Section 4.3.1.
- The solution was stirred to increase mass transport of the reactant to the working electrode.
- Reduction times of at least 14 hours were used.
- High overpotentials, compared to the predicted reduction potentials for the PGMs were applied to the working electrode.

Amminated complexes

The formation of amminated complexes, and the possible influence of these complexes on the recovery of PGMs from PML solutions were investigated. An excess of NH_3 ligands (in the form of NH_3 solution) was added to synthetic solutions containing copper, palladium and platinum in a 0.1 M HCl matrix. Enough NH_3 was added to increase the pH to ca.

9.5, where it was assumed that the ligand was present in excess. A qualitative interpretation of the interaction of different combinations of copper, palladium and platinum in a NH_3 matrix with a graphite working electrode was developed.

Following the analysis of synthetic solutions, PML solutions were treated with sodium hydroxide. Enough OH^- was added to increase the pH to ca. 9.5. The rationale behind the addition of sodium hydroxide was that the NH_4^+ ions present in the PML solution (refer to Table 1.1) would be deprotonated to form NH_3 ligands, which in turn may form amminated PGM complexes if it is favourable under the prevailing conditions.

Voltammograms of synthetic solutions containing a combination of copper, palladium and platinum (pH adjusted to ca. 9.5 with NH_3 solution) were compared to voltammograms of PML solutions (pH adjusted to ca. 9.5 with OH^- solution) in order to confirm the formation of amminated complexes.

Finally, exhaustive electrolysis experiments involving the pH-adjusted PML solution were carried out. The recoveries of PGMs from these solutions were compared to recoveries obtained without pH adjustments, to assess the impact of amminated species on the overall recovery process.

The following general procedure was adopted:

- Single component synthetic solutions of the major metal ions found in the PML namely copper, palladium and platinum were prepared. Details regarding the preparation of these solutions were provided in Section 3.3. The pH of the solutions was adjusted to values of ca. 9.5 with NH_3.

- The cyclic voltammograms resulting from the interaction of these pH-adjusted solutions with a graphite working electrode were recorded and analysed. The final concentration of a particular metal ion in solution approximated that found in a typical PML solution. Details regarding the dilution of synthetic single metal ion solutions were provided in Section 3.3.

- Once a qualitative understanding of the behaviour of a single metal ion at the graphite working electrode-solution interface was established, the complexity of the solutions analysed via CV was increased gradually. Voltammograms of different combinations of copper, palladium and platinum solutions (pH adjusted to ca. 9.5) were recorded and analysed. The final concentration and ratios of the different metal ions in solution approximated that found in a typical PML solution. Details regarding the combination of different synthetic single metal ion solutions were provided in Section 3.3.

- The potential scan ranges for specific CV experiments were varied to assist with the interpretation of voltammograms.

- Once a qualitative understanding of the behaviour of a combination of copper, palladium and platinum in a NH_3 matrix was established, actual PML solutions (pH adjusted to ca. 9.5) were analysed. Similarities in the voltammograms obtained for synthetic and PML solutions were used to provide a qualitative explanation of the behaviour of the refinery effluent at the graphite electrode surface.

- Exhaustive electrolysis experiments were carried out on PML solutions adjusted to pH values of ca. 9.5. A similar procedure to that described under the sub-heading “Exhaustive electrolysis” of this section (Section 4.2.2) was followed. The only difference was that an additional step involving the adjustment of the pH to values of ca. 9.5 was introduced. Samples of the PML were taken prior to the adjustment of pH, after the adjustment of pH, and after completion of the electrolysis experiment.

All samples were filtered through a 0.45 μm cellulose nitrate membrane prior to the sampling step. The dilution of the orginal PML solution due to the addition of sodium hydroxide was taken into consideration when the metal concentrations in the various samples were reported.

4.2.3 Data Presentation

The sign convention and units of expression defined in Chapter 2 (Section 2.1) also applies to the current chapter. Information related to data handling, the illustration and labelling voltammograms, and experimental conditions are identical to that provided in Chapter 3 (Section 3.2.3). The only difference is that a graphite working electrode with an active surface diameter of ca. 6 mm was used instead of glassy carbon or platinum disc electrodes.

Where reference is made to Cu^{+}, Cu^{2+} or Pd^{2+} the oxidation state of the metal ion is described as opposed to a particular species present in the test solution.

4.3 ELECTRODES, EQUIPMENT AND REAGENTS

Additional experimental information that was not provided in Chapter 2 and that is relevant to research work discussed in the subsequent sections of Chapter 4 is presented here.

4.3.1 Electrodes

A working electrode with an active surface consisting of isostatically pressed graphite particles was used for all experiments described in this chapter. The in-house construction of the electrode is described here.

Components

- Isostatically pressed graphite particles (Electrographite Carbon Co., grade ET-10, particle size range between 500 μm and 600 μm).

- Spectrographic carbon rod (Pelco International, grade 1, product no 60-32, 6.2 mm diameter).
- Epoxy Resin 1 (Struers, Epofix).
- Epoxy Resin 2 (Elite Chemical Industries, resin code NPEL 128, hardener code GEN 2000).
- Galvanised steel binding wire (Easi-Coil®, 1.25 mm diameter).
- Copper wire (strands recovered from normal electrical cord).
- Copper connector (University of the Witwatersrand, engineering workshop).
- Glass tube with total length of 12.5 mm, and a GL 14 thread end at the top of the tube. Outer diameter at bottom of tube 9 mm and inner diameter 7 mm. A B14 cone was fitted 70 mm from the bottom of the tube to allow fitment to the lid of the three-electrode electrochemical cell. (University of the Witwatersrand, chemistry department workshop).
- Screw cap to fit thread end at top of glass tube (Schott, GL14).

Preparation of epoxy resins

- Epoxy Resin 1: The resin and hardener were combined in a mass ratio of 10 parts resin to 1.2 parts hardener, and thoroughly mixed for approximately 3 minutes. Mixing was slow to prevent the formation of large volumes of air bubbles. After application to the required area, a curing time of 8 hours at room temperature was allowed. This was followed by a final curing step of 4 hours in a drying oven set to 60 °C.
- Epoxy Resin 2: The resin and hardener were combined in a mass ratio 10 parts resin to 4 parts hardener, and slowly mixed for approximately 3 minutes. The mixture was left to stand for 10 minutes to allow entrained air bubbles to reach the surface. After application to the required area, a curing time of 24 hours at room temperature was allowed. This was followed by a final curing step of 4 hours in a drying

oven set to 50 °C.

It should be noted that either of the two resins described above were used in the construction of the electrode. The different characteristics of the resins are discussed under the sub-heading “Electrode preparation” of this section (Section 4.3.1).

Construction

A piece of galvanised wire, with a length of ca. 2 cm and a diameter of 1.25 mm was inserted into one end of a spectrographic carbon rod. The spectrographic carbon rod in turn had a length of ca. 1 cm and a diameter of 6.2 mm. Insertion of the galvanised wire into the spectrographic carbon rod was facilitated by a small hole (ca. 6 mm deep and 1.2 mm in diameter) drilled into the middle of one of the rod ends. The wire was fitted tightly to ensure electrical contact between the wire and the spectrographic carbon. A drop of prepared epoxy resin was placed at the intersection of the spectrographic carbon rod surface with the galvanised wire to ensure that the wire remains in position.

The tip of the galvanised wire protruding from the spectrographic carbon rod was soldered onto a copper wire (length of ca. 9.5 cm), which in turn was soldered to a copper connector. The entire assembly was sealed into a glass tube by using a screw cap fitting over the connector (top of electrode), and epoxy resin to set the spectrographic carbon rod at the bottom of the glass tube. The spectrographic carbon rod end (opposite to the side attached to the galvanised wire) was allowed to extend 3 mm from the bottom of the glass tube.

Following the complete curing of the resin used to seal the spectrographic carbon rod into the glass tube, the end of the rod protruding from the glass tube was dipped into freshly prepared resin. The graphite particles were attached to the spectrographic rod surface containing the freshly prepared resin. After curing, the top layer of the graphite particles set on the

spectrographic carbon support was sanded off to expose a fresh, flat active surface.

When the electrode was in use, the copper connector served as the contact between the graphite particles and the potentiostat. The constructed electrode is illustrated in Figure 4.1.

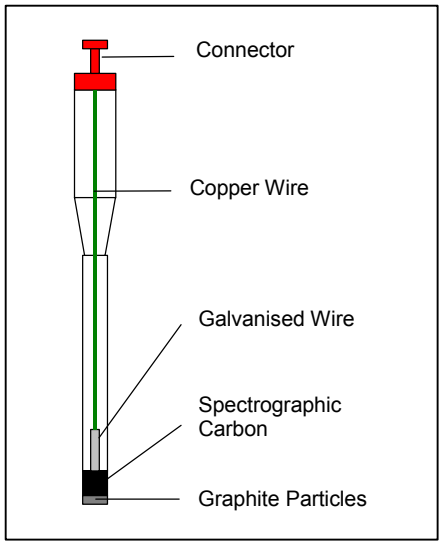

Figure 4.1 Illustration of in-house constructed working electrode with active surface consisting of isostatically pressed graphite particles, grade ET-10. (Note that the illustration was not drawn to scale).

Tools

The spectrographic carbon rod that was fitted to the electrode was cut to the required length by means of a small hacksaw. A mounted drill and a drill bit with a diameter of 1.2 mm were used to drill the hole into the spectrographic rod. Forceps, manufactured from PTFE, were used to assist with the placing of graphite particles on the spectrographic rod dipped in epoxy resin.

Working electrode preparation

Initially, Epoxy Resin 1 (Epofix) was used for the construction of the working electrodes. The disadvantage of using this specific product was that the 0.1 M HCl, used as background electrolyte in the majority of

experiments described in this chapter, slowly reacted with the resin. This necessitated the removal of the loose graphite particles from the spectrographic carbon support by means of a small file and fine sandpaper (grade P1200C) after a set of experiments. A new layer of graphite particles had to be adhered to the spectrographic carbon support, using fresh epoxy resin as described under the sub-heading “Construction” in Section 4.3.1.

Subsequently Epoxy Resin 2 (NPEL 128) was acquired. The advantage of using this particular product was associated with the fact that the resin did not show any visible signs of degradation over several sets of experiments. Between different sets of experiments, the electrode surface was refreshed by using fine sandpaper.

General characteristics

It should be noted that the characteristics of the constructed electrode differed from the normal commercially available working electrodes described in Chapters 2 and 3 in several ways.

The active surface of the constructed electrode consisted of a mixture of graphite and epoxy resin. Since the epoxy resins used in the construction process were not conductive, no reduction or oxidation processes occurred at surface sites covered by the resin. These sites were easily identified during experiments involving metal deposition. The area covered by epoxy resin was surrounded by metal deposited on the conducting graphite surface.

In some cases small holes were observed on the otherwise flat electrode surface. This occurred when a graphite particle held on the surface by epoxy resin came loose, leaving a hole where it originally was attached.

When a refreshed graphite electrode surface was observed by means of an optical microscope, shiny streaks were observed. This was a function

of light reflected from the carbon surface, and should not be confused with the presence of metal.

The refreshed active surface of a graphite working electrode is illustrated in Figure 4.2.

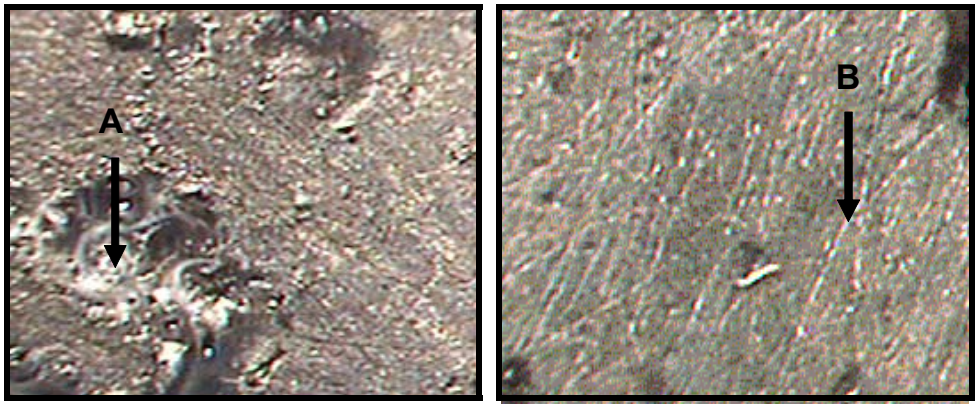

Figure 4.2 Images of freshly prepared active surfaces of a graphite working electrode prior to conducting experiments. Magnification: 13 X (stereo microscope).

A: Epoxy resin (non-conductive) present on the active electrode surface. Also note the hole in the surface where a graphite particle came loose.

B: Shiny streaks present on the electrode surface. This is a function of light reflected from the electrode surface when observed under the microscope, and should not be confused with the presence of metal.

Due to the difference in active surface areas of the constructed working electrode and the commercial working electrodes described in Chapters 2 and 3, the currents recorded whilst using the constructed electrode were significantly higher compared to the commercial electrodes.

From the method of construction it is apparent that the electrochemically active surface area of the constructed working electrode will always be different, depending on the ratio of epoxy resin to graphite on the particular surface, and the total area of the electrode that was exposed when it was refreshed by means of fine sandpaper.

Since the graphite working electrode was used to conduct qualitative CV experiments, metal deposition, or exhaustive electrolysis experiments, an accurate measure of active surface area was not critical. The variation of the active surface area between different sets of experiments did however make direct comparisons of the resultant voltammograms more difficult. In some cases the comparison between voltammograms recorded for experiments involving glassy carbon and graphite working electrodes was also complicated by the relative difference in the magnitude of recorded currents.

4.3.2 Equipment and Reagents

- Filtration apparatus capable of handling 0.45 μm membranes (Millipore).
- 0.45 μm cellulose nitrate membranes (Millipore).
- Ammonia solution, NH_3, 25 %, MM = 17.03 g mol^{-1}, Analytical Reagent (AR) grade; (Merck).
- Sodium hydroxide pellets, NaOH, MM = 40.00 g mol^{-1}, AR grade, (Saarchem).
- 10 M NaOH solution: The solution was prepared by dissolving 8 g NaOH pellets in 20 ml of ultra pure water.
- Nitric acid, HNO_3, 65 %, MM = 63.01 g mol^{-1}, AR grade (Saarchem).
- Aqua regia: Three parts of HCl (defined in Section 2.4.4) was mixed with one part HNO_3 to produce the required solution. Fresh batches of aqua regia were prepared for each set of experiments.

4.4 PROPERTIES OF GRAPHITE

Since isostatically pressed graphite particles were evaluated as a possible cathode material for the proposed electrochemical reactor, the properties

of the material will be described briefly.

The graphite used for the duration of the project (grade ET-10, Electrographite Carbon Co.) is artificial, and is classified as pyrolytic graphite. Normally pyrolytic graphite is produced by the decomposition of carbonaceous gasses such as methane at temperatures above 1200 °C. The product is collected by deposition on graphite or other suitable materials[42d].

In order to obtain a high degree of orientation along the c-axis, the graphite was subjected to a hot isostatic pressing step at 2800 °C. This form of graphite is characterised by low porosity and high corrosion resistance, fulfilling some of the requirements of a potential cathode material as discussed in Section 4.1.

The isostatically pressed graphite had a density of 1.75 g cm^{-3}, compared to typical densities of 1.5 g cm^{-3} for glassy carbon[41].

4.5 RESULTS AND DISCUSSION

The discussion of data presented in this chapter will in many cases involve a progression of the theory, methodologies and conclusions presented in Chapters 2 and 3. Where applicable, references to the material presented in earlier chapters will be provided. It will however be advisable to study Chapters 2 and 3 in detail, prior to the evaluation of material presented in this chapter.

4.5.1 Feasibility and Validation

Background electrolyte

A 0.1 M HCl background electrolyte was used for experiments involving synthetic solutions. In Section 3.5.1 it was noted that the useful potential range for studies of metal ions contained in this background electrolyte was determined by reactions involving hydrogen gas evolution (Equation

3.7) and the oxidation of chloride ions and water (Equations 3.8 and 3.9).

The interaction of a 0.1 M HCl background electrolyte with the graphite working electrode described in Section 4.3.1 was evaluated via CV, as illustrated in Figure 4.3.

It was noted that a significant reduction current due to the evolution of hydrogen gas developed at potentials more negative than -1.0 V, compared to potentials more negative than -0.30 V observed when a glassy carbon working electrode was used. The difference in the potentials at which significant reduction currents are observed is ascribed to the electrocatalytic properties associated with each of the electrode materials. Some of the factors influencing the electrocatalytic properties of electrode materials were highlighted in Section 3.4.

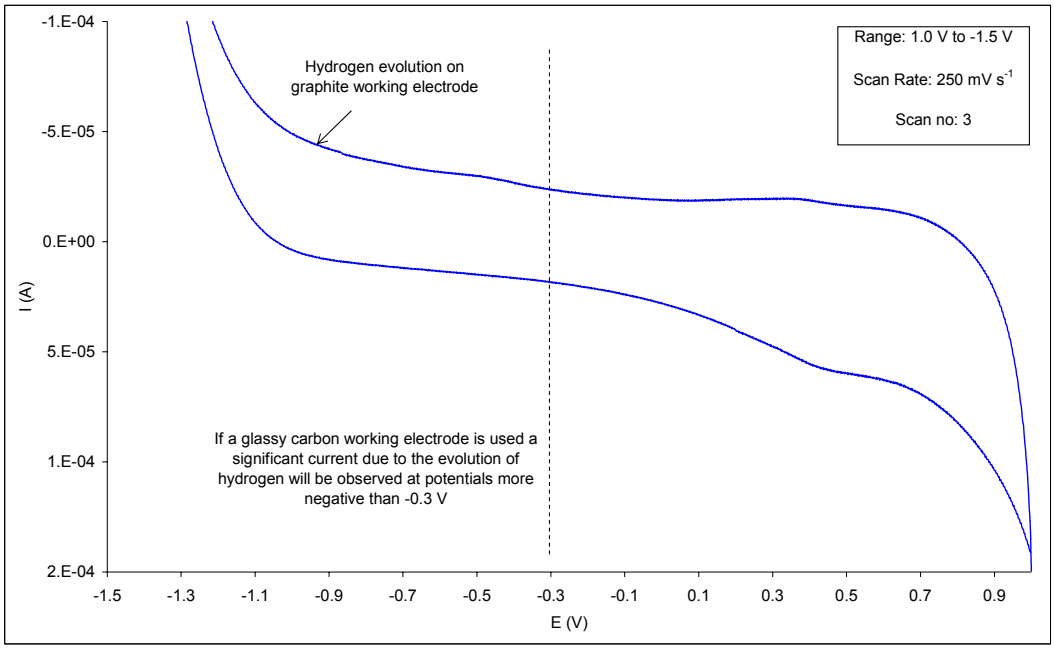

Figure 4.3 Cyclic voltammogram of a 0.1 M HCl background electrolyte solution, using a graphite working electrode.

The availability of a wider potential range when a graphite working electrode instead of a glassy carbon electrode is used in a 0.1 M HCl

matrix holds several advantages from an analytical and engineering point of view. From an analytical standpoint, the reduction or oxidation peaks associated with a particular reaction otherwise masked by the hydrogen generation current may be observed. If an electrochemical reactor is used, a higher overpotential for metal deposition could be applied without a significant loss in efficiency. The higher overpotential will in turn result in an increased rate of metal deposition.

Synthetic solutions

Cyclic voltammetric and metal deposition experiments involving the use of a graphite working electrode and synthetic solutions containing various combinations of copper, palladium and platinum in a 0.1 M HCl background electrolyte were carried out. These experiments formed part of the feasibility (CV) and validation (metal deposition) process employed to assess the viability of using isostatically pressed graphite particles as a cathode material for the proposed electrochemical reactor.

Reactions involving palladium (Figures 4.4 to 4.6). A comparison of the voltammograms obtained for the interaction of palladium ions with *(i)* a glassy carbon and *(ii)* a graphite working electrode is shown in Figure 4.4.

The interpretation of the voltammogram related to the glassy carbon electrode was discussed in Section 3.5.3 (Figure 3.6). It was concluded that the palladium ions were reduced to metal on the electrode surface. Anodic peaks associated with the oxidation of molecular hydrogen on deposited palladium metal centres, and the oxidation of palladium metal centres to ions were also identified.

The interpretation of the voltammmogram associated with the graphite working electrode was based on a comparison to the plot recorded for the glassy carbon working electrode. The cathodic current observed at C1 was ascribed to the formation of hydrogen gas on deposited palladium metal centres, whilst Peak A1 was associated with the anodic dissolution of palladium metal centres present on the graphite surface.

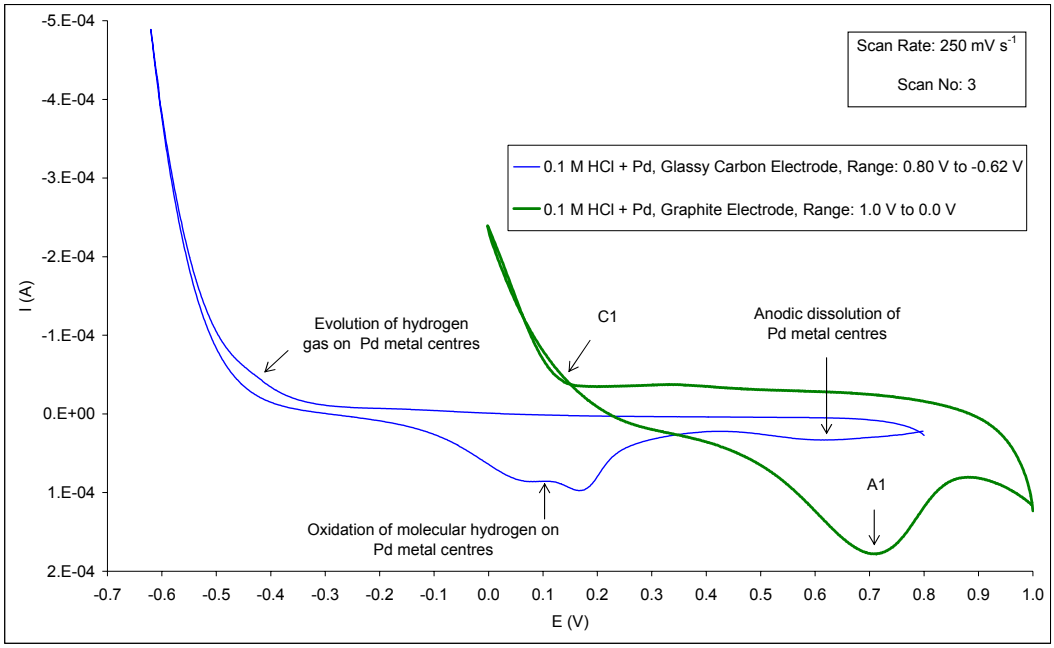

Figure 4.4 Comparison of cyclic voltammograms for a solution containing 196 mg l^{-1} palladium in a 0.1 M HCl background electrolyte when *(i)* a glassy carbon working electrode, and *(ii)* a graphite working electrode was used.

A comparison of the voltammograms revealed a very substantial shift in the relative potentials at which palladium was deposited. When a glassy carbon electrode was used, a significant current due to the evolution of hydrogen on deposited palladium metal centres was observed at potentials more negative than ca. -0.35 V , compared to potentials more negative than 0.15 V observed for the graphite working electrode. This implies that the overpotential required to deposit palladium metal centres on a graphite working electrode would be significantly smaller than that required for a glassy carbon electrode. The difference in the potential values observed for palladium deposition is ascribed to differences in the electrocatalytic properties of the various electrode surfaces.

Additional cyclic voltammetric experiments carried out with a graphite working electrode and a synthetic solution containing 196 mg l^{-1} palladium, as illustrated in Figure 4.5, revealed the presence of an additional oxidation peak (A2) when the scan range was extended to

potentials more negative than 0.0 V .

Peak A2 (Figure 4.5) was ascribed to the oxidation of molecular hydrogen present on active palladium metal centres, which in turn was deposited on the original graphite surface. A significant oxidation current was only observed when a sufficient amount of palladium metal centres were present to facilitate the reaction. In this case, the application of a higher overpotential (more negative than 0.0 V) resulted in the formation of a sufficient quantity of palladium metal centres.

Previous findings related to Figure 3.7 (Section 3.5.3), where the deposition of palladium on a glassy carbon electrode was investigated, also support the arguments used to interpret the voltammogram in Figure 4.5.

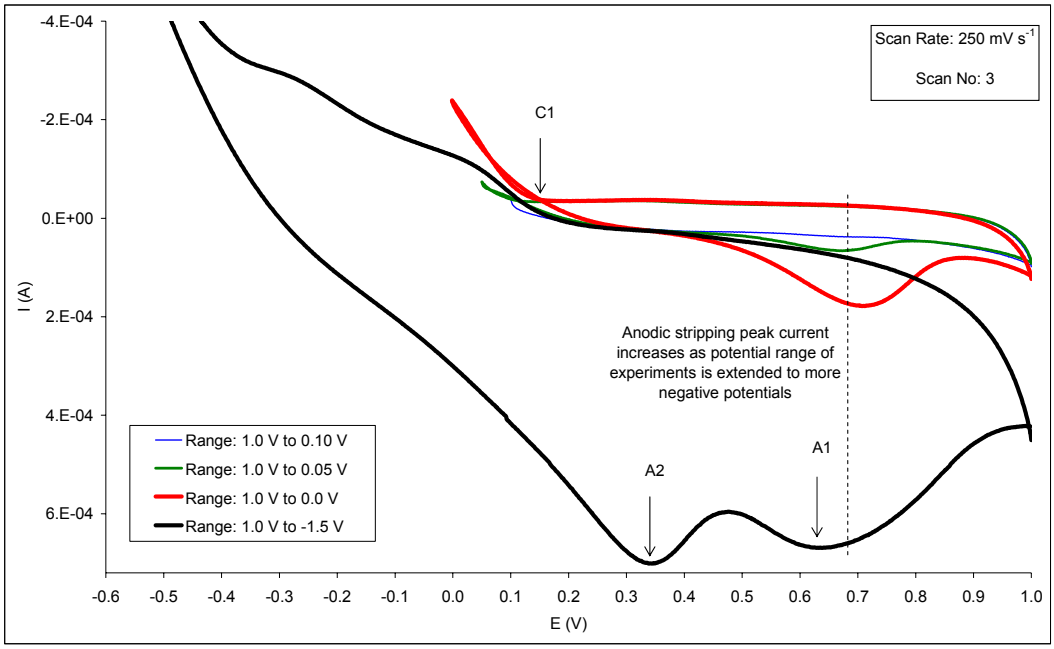

Figure 4.5 Cyclic voltammograms of a solution containing 196 mg l^{-1} palladium in a 0.1 M HCl background electrolyte, showing experiments where different potential ranges were utilised. A graphite working electrode was employed.

The electrochemical reduction of palladium ions present in a 0.1 M HCl matrix to form metal centres on the graphite working electrode surface,

and the subsequent anodic dissolution of the metal centres at favourable overpotentials was predicted via CV, as illustrated in Figures 4.4 and 4.5.

In order to validate these predictions metal deposition and anodic dissolution experiments as described under the sub-heading “Validation” of Section 4.2.2 were carried out. To deposit or anodically dissolve sufficient quantities of metals which can be observed via an optical microscope in a reasonable time frame, high overpotentials, high concentrations of the particular metal ion ($g\ l^{-1}$ range), and favourable mass transport conditions (stirring) were employed.

Deposition of palladium metal on the graphite working electrode was confirmed by applying a potential of -0.80 V to the electrode for 30 minutes, using a test solution containing 1 $g\ l^{-1}$ palladium in a 0.1 M HCl matrix. The anodic dissolution of part of the metal deposited on the graphite electrode surface was confirmed by applying a potential of 0.80 V for 38 minutes, whilst the electrode was contained in the same test solution used for the deposition experiment. Images of the graphite electrode surface after the deposition and anodic dissolution steps are shown in Figure 4.6.

Images of the graphite working electrode reveal the presence of palladium in the form of a fine black powder, and “flakes” of metal. The presence of the metal in a powder and “flake” form is thought to be a function of the potential applied to the working electrode during the deposition step. As higher overpotentials are applied to the electrode, the ratio of metal powder relative to sheet metal will increase.

Morphologies of deposits become important when the recovery of metals from a cathode is considered. Although anodic dissolution may be feasible, the mechanical recovery of metals from the cathode is also possible. If mechanical recovery of metals from the cathode material present in the proposed electrochemical reactor is considered to be a viable option, the deposits should be present in a powder form. Further

research related to factors influencing the formation of metal deposits in a fine powder form will be required if mechanical recovery is proposed.

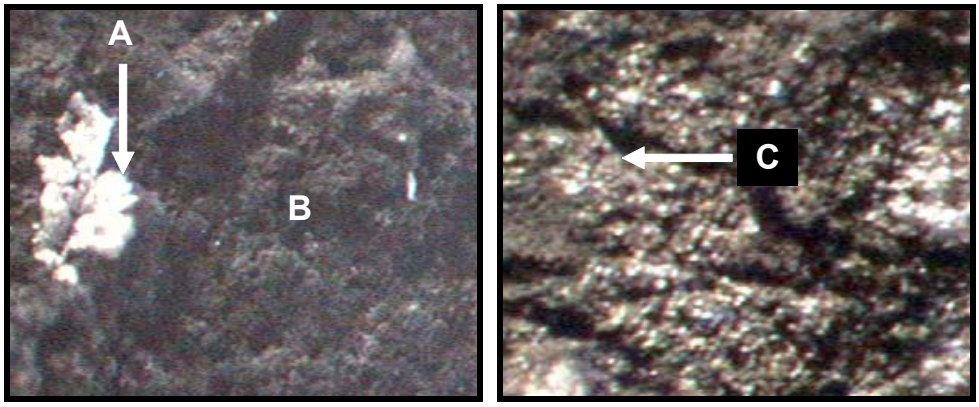

Figure 4.6 Images of graphite working electrode surface after metal deposition (left) and anodic dissolution (right) experiments. Magnification: 40 X (compound microscope).

A: "Flakes" of metal present on the electrode surface.

B: Palladium metal present in the form of a fine black powder.

C: Original graphite working electrode surface after anodic dissolution.

During the anodic dissolution experiment it was noted that the test solution turned into a dark murky colour, and that fine black particles were suspended in the solution. The image of the graphite electrode after the anodic dissolution experiment and the appearance of the test solution demonstrate that some of the palladium metal present on the electrode surface was removed.

The fact that palladium metal remained on the graphite surface after the anodic dissolution experiment may point to the fact that insufficient time was allowed for the dissolution process, or that the applied overpotential was too low. In Section 3.4.1 it was noted that a carbon electrode itself could undergo oxidation, depending on the applied potential. The oxidation of palladium metal to metal oxides, and the subsequent difficulties associated with the anodic dissolution of the metal oxides was also discussed in the literature review section of Chapter 1. The application of

high overpotentials to facilitate the anodic dissolution of palladium metal on a graphite working electrode should therefore receive careful consideration.

In Section 3.5.3, the drawn out shape of the anodic stripping peak for palladium present on a glassy carbon working electrode (illustrated in Figure 3.6) was ascribed to the possible influence of the background electrolyte. In Figure 4.4 it was noted that the anodic stripping peak for palladium present on a graphite working electrode had the same drawn out shape. The key to improving the kinetics of palladium removal from the graphite surface via anodic dissolution may therefore be associated with the characteristics of the background electrolyte.

As mentioned in Chapters 1 and 3, the focus of the research described in the present dissertation was on the quantitative removal of metal ions from refinery effluents via an electrochemical reactor. Limited time and resources inhibited further investigations related to the influence of solution matrices on anodic stripping efficiencies. If anodic stripping is considered to be a viable method of metal recovery from the cathode material contained in the proposed electrochemical reactor, further research will be required.

Reactions involving platinum (Figures 4.7 to 4.9). In Figure 4.7, the interaction of platinum ions (in 0.1 M HCl) with a glassy carbon and graphite working electrode is compared.

Peak C1 was associated with the formation of platinum metal centres on the graphite working electrode, after comparison to the voltammogram obtained whilst employing a glassy carbon electrode. Peak A1 was associated the oxidation of molecular hydrogen present on the deposited platinum metal centres.

It was also noted that the current on the forward sweep of the voltammogram recorded with the graphite working electrode was positive from ca. 0.55 V to ca. -0.25 V, implying an overall oxidative process. The

same phenomenon was observed for the voltammogram associated with the glassy carbon electrode.

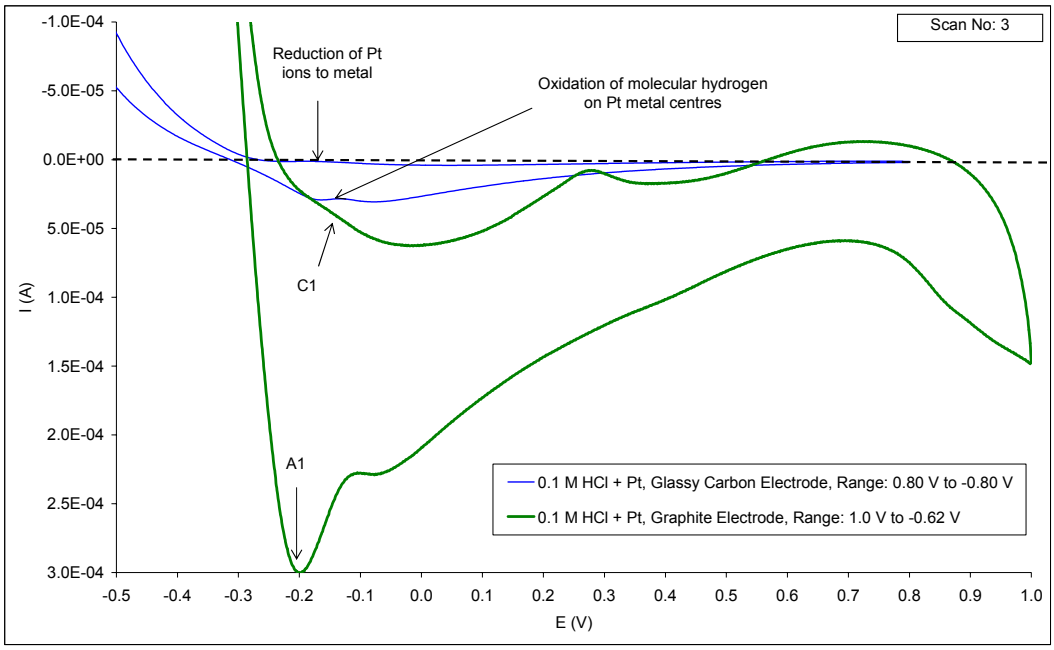

Figure 4.7 Comparison of cyclic voltammograms where *(i)* a glassy carbon working electrode was used with a solution containing 196 mg l^{-1} platinum in a 0.1 M HCl background electrolyte and *(ii)* a graphite working electrode was used with a solution containing 50 mg l^{-1} platinum in a 0.1 M HCl background electrolyte.

In Section 3.5.3 (Figure 3.9) it was postulated that a pseudo hydrogen electrode was formed, and that the oxidation of molecular hydrogen on platinum metal centres gave rise to the positive currents observed. It was also noted that this pseudo hydrogen electrode formed when sufficient numbers of finely divided platinum metal centres were present on the original glassy carbon surface.

This assumption seems to be supported by the voltammograms illustrated in Figure 4.8, where a graphite working electrode was employed. As the number of potential cycles is increased the currents on the forward sweep of the voltammogram continue to decrease, until an overall oxidation current is observed on the third potential sweep.

The assumption that the number of active metal centres on the surface of the working electrode surface increase with the number of potential scans also implies that metal is not anodically stripped under the experimental conditions applied during the experiment. Alternatively, the rate of metal removal may be significantly slower than the rate of deposition.

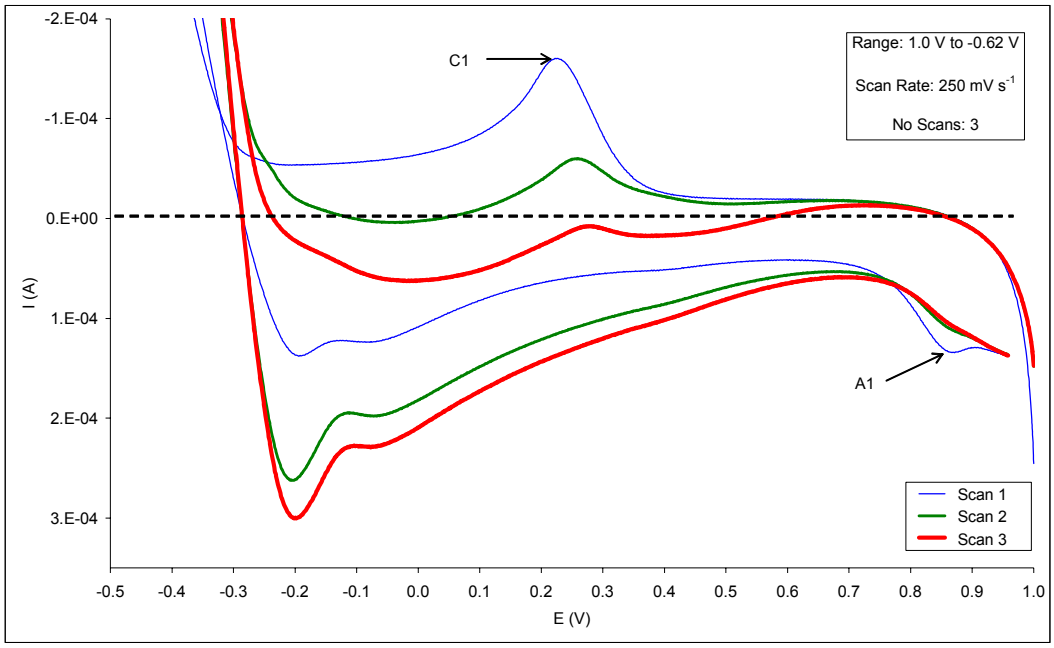

Figure 4.8 Cyclic voltammograms of a solution containing 50 mg l^{-1} platinum in a 0.1 M HCl background electrolyte, using a graphite working electrode.

The origin of Peaks C1 and A1 in Figure 4.8 could not be determined with certainty. Peak A1 may be ascribed to the oxidation of platinum metal centres present on the graphite electrode surface, possibly to PtO, as shown in Equation 3.13. The oxidation peak may also result from the anodic dissolution of platinum metal centres. Peak C1 may have resulted from the reduction of PtO formed as a result of the oxidation process described in Equation 3.13. It may also be possible that the overall reduction of platinum metal ions proceeded to metal via an intermediate platinum species, and that Peak C1 was indicative of the formation of the intermediate species.

From the discussions related to the interpretation of voltammograms

shown in Figures 4.7 and 4.8, it is apparent that many fundamental questions related to speciation, metal oxide formation, kinetics and the influence of the background electrolyte remains unanswered. These issues should be pursued in subsequent research projects.

In the context of the current research project, sufficient information regarding the interaction of platinum ions with a graphite working electrode was collected. It was concluded that *(i)* platinum ions are reduced to metal centres on the graphite electrode surface, and *(ii)* that the anodic dissolution of platinum metal centres present on the electrode surface in a 0.1 M HCl background electrolyte is kinetically slow compared to the deposition process, or *(iii)* does not take place at all, possibly due to the presence of oxide species.

These conclusions were tested via metal deposition and anodic dissolution experiments illustrated in Figure 4.9.

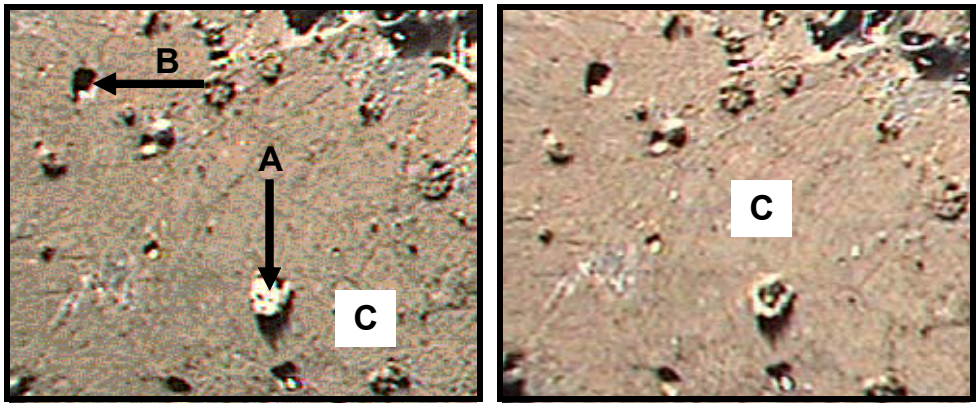

Figure 4.9 Images of graphite working electrode surface after metal deposition (left) and anodic dissolution (right) experiments. Magnification: 13 X (stereo microscope).

A: Loose graphite particle on electrode surface.

B: Hole left after graphite particle came loose.

C: Platinum deposit on working electrode surface.

For the metal deposition experiment, a potential of -0.62 V was applied to the working electrode for 15 minutes, whilst a potential of 0.95 V was

applied for 20 minutes during the anodic dissolution experiment. A solution containing 1.7 g l^{-1} platinum in a 0.1 M HCl background electrolyte was used.

From these images it was confirmed that platinum metal deposition did occur, and that the anodic dissolution of deposited metal did not occur at a significant rate in a 0.1 M HCl background electrolyte, even at applied potentials of 0.95 V .

Reactions involving copper (Figures 4.10 to 4.12). The electrochemical behaviour of copper ions contained in a 0.1 M HCl background electrolyte at both glassy carbon and graphite working electrode surfaces is shown in Figure 4.10.

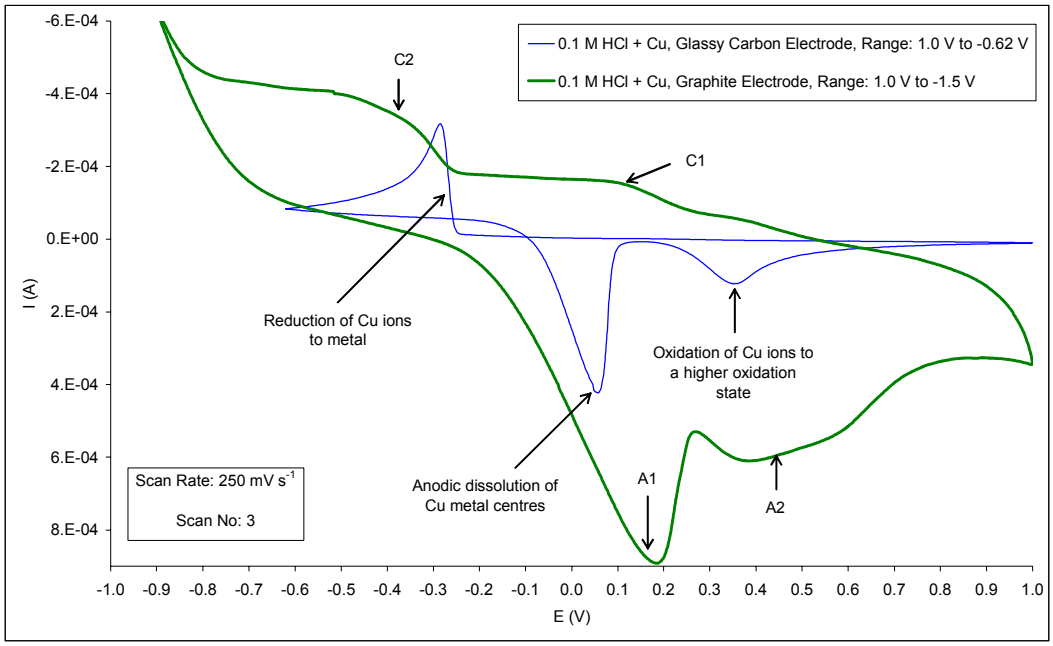

Figure 4.10 Comparison of cyclic voltammograms where *(i)* a glassy carbon working electrode was used with a solution containing 431 mg l^{-1} copper in a 0.1 M HCl background electrolyte and *(ii)* a graphite working electrode was used with a solution containing 174 mg l^{-1} copper in a 0.1 M HCl background electrolyte.

The interpretation of the voltammogram associated with the interaction of copper at a glassy carbon electrode surface was discussed via Figure 3.11

in Section 3.5.3.

By comparing the voltammogram obtained with the graphite working electrode to the voltammogram recorded with the glassy carbon working electrode, it was concluded that copper metal did deposit at the graphite electrode surface. This assumption was based on the fact that Peak A1 corresponded to the anodic stripping peak observed when copper metal was present on a glassy carbon surface. Further comparison to the voltammogram obtained for a glassy carbon electrode lead to the conclusion that Peak A2 was associated with the oxidation of copper ions, presumably from Cu^{+} to Cu^{2+}.

When the reduction peaks were compared a difference was noted. Two cathodic peaks (C1, C2) were observed when the graphite working electrode was used, compared to the single peak observed for the glassy carbon electrode experiment.

Additional cyclic voltammetric experiments involving the use of different potential scan ranges were carried out, as shown in Figure 4.11. From these experiments it was determined that Peak C2 was related to Peak A1. Since Peak A1 was identified as the anodic stripping peak for copper metal centres present on the original electrode surface, it was concluded that Peak C2 was indicative of the deposition of copper metal centres.

In Section 3.5.3 the slope of the reduction current leading to the peak associated with the deposition of copper metal on a glassy carbon surface (refer to Peak C1, Figure 3.11) was discussed. One of the reasons provided for the steep slope of the reduction current was the possible occurrence of a multi-electron transfer process. This implied that the characteristic shape of the reduction peak could be due to the overall reduction of Cu^{2+} to Cu^{0} via a multi-electron transfer step originally illustrated in Section 2.2.2.

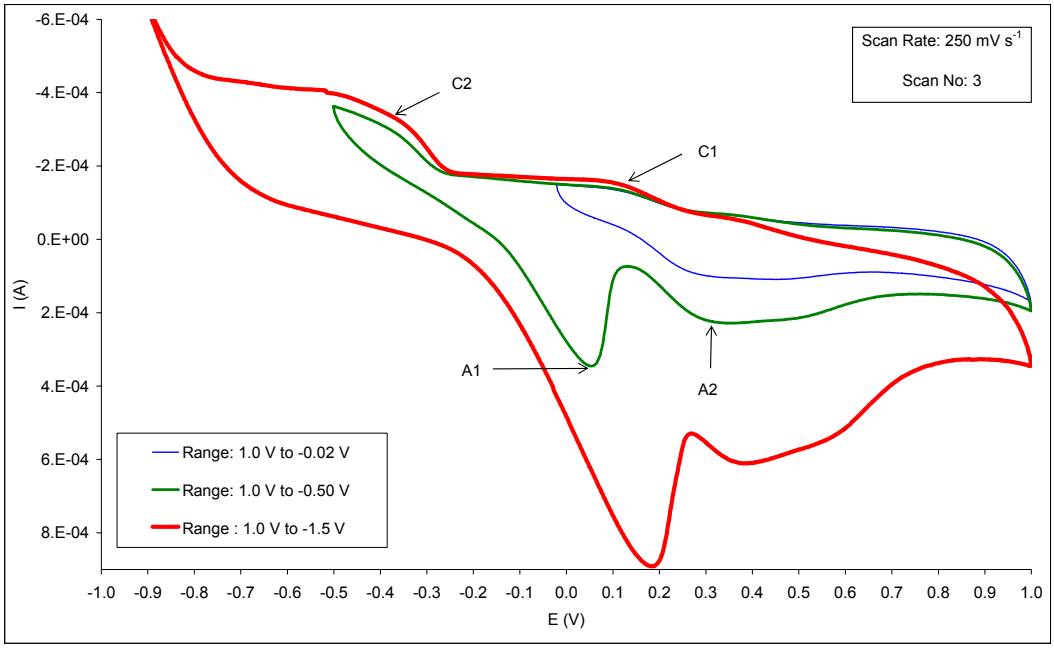

Figure 4.11 Cyclic voltammograms of a solution containing 174 mg l^{-1} copper in a 0.1 M HCl background electrolyte, using a graphite working electrode.

The slope of the current associated with the copper deposition peak on a graphite electrode surface (refer to Peak C2, Figures 4.10 and 4.11) resembles that of a normal one electron transfer process, such as the Fe^{3+}/Fe^{2+} couple illustrated in Figure 3.3. It is therefore possible that Peak C1 in Figures 4.10 and 4.11 is indicative of the reduction of Cu^{2+} to Cu^{+}, whilst Peak C2 is associated with the reduction of Cu^{+} to Cu^{0}.

From the analysis of voltammograms presented in Figures 4.10 and 4.11, it was concluded that *(i)* copper ions are reduced to metal centres on the graphite electrode surface, and *(ii)* that the anodic dissolution of copper metal centres present on the electrode surface in a 0.1 M HCl background electrolyte is occurring. These conclusions were tested via experiments illustrated in Figure 4.12.

During the metal deposition experiment, a potential of -1.25 V was applied to the working electrode for 25 minutes, whilst a potential of 0.57 V was employed for the same time period during the anodic dissolution

experiment. A solution containing 1 g l^{-1} copper in a 0.1 M HCl background electrolyte was used.

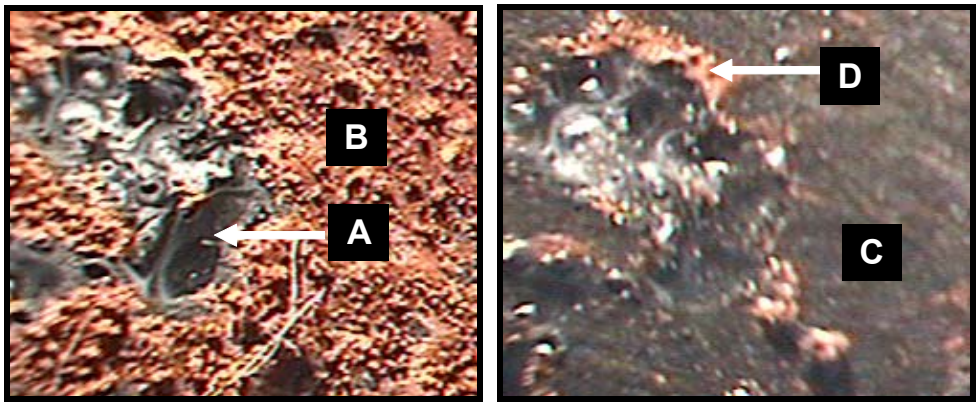

Figure 4.12 Images of graphite working electrode surface after metal deposition (left) and anodic dissolution (right) experiments. Magnification: 13 X (stereo microscope).

A: Epoxy resin (non-conductive) present on the active electrode surface.

B: Copper metal present on the working electrode surface.

C: Original graphite working electrode surface after anodic dissolution.

D: Copper metal remaining after anodic dissolution.

The images in Figure 4.12 confirmed that copper metal deposition did occur, and that the deposited metal was almost quantitatively removed under the prevailing experimental conditions.

Reactions involving copper and palladium (Figures 4.13 to 4.14). The interaction between a solution containing a combination of copper and palladium ions in a 0.1 M HCl background electrolyte and a graphite working electrode will be discussed via the voltammograms illustrated in Figures 4.13 and 4.14. References to studies involving the interaction of *(i)* copper and palladium, and *(ii)* copper, palladium and platinum with a glassy carbon working electrode as described in Section 3.5.3 (Figures 3.13 to 3.16, and Figures 3.20 and 3.21) will also be included in the discussion.

A comparison of the voltammograms recorded for the interaction of the graphite working electrode with test solutions containing *(i)* copper, *(ii)* palladium, and *(iii)* a combination of copper and palladium is shown in Figure 4.13. Initially it was observed that the voltammograms obtained for a solution containing palladium only and a solution containing copper and palladium were very similar, although the currents recorded for the latter solution were higher compared to that recorded for the palladium solution. This pointed to the possibility that copper and palladium ions took part in reactions with the graphite electrode.

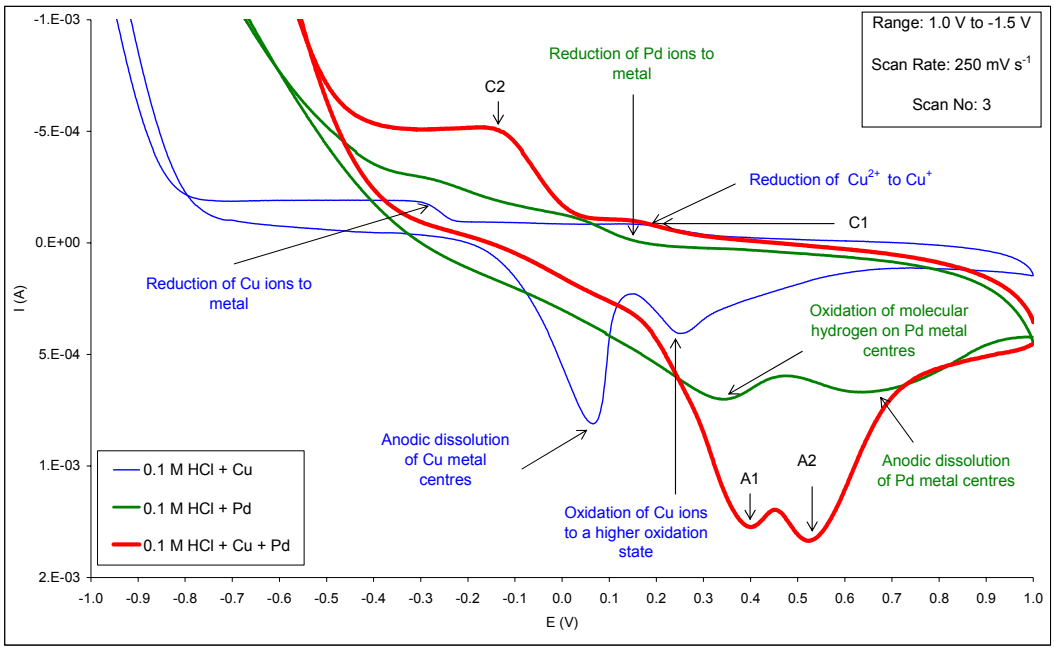

Figure 4.13 Cyclic voltammograms of solutions containing *(i)* 174 mg l^{-1} copper, *(ii)* 196 mg l^{-1} palladium, *(iii)* 170 mg l^{-1} copper and 189 mg l^{-1} palladium. The metal ions were contained in 0.1 M HCl background electrolyte, and a graphite working electrode was used in all cases.

The magnitude of the reduction current observed at Peak C2 (ca. -0.15 V) was four times the magnitude of the current observed at Peak C1 (ca. 0.20 V). This is indicative of a multi-electron transfer process, i.e. it is possible that the reduction of both copper and palladium contributed to the magnitude of Peak C2.

In Figure 4.5 the effect of potential scan ranges on the resulting voltammograms obtained for single component palladium solutions was investigated. Initially only one oxidation peak was noted, but as the potential range was extended to more negative values a second oxidation peak was observed. It was concluded that the initial oxidation peak was related to the anodic dissolution of palladium metal centres present on the graphite working electrode surface. The second oxidation peak observed at more negative potentials relative to the anodic dissolution peak was ascribed to the oxidation of molecular hydrogen present on the palladium metal centres.

When potential range experiments involving solutions containing both copper and palladium, as illustrated in Figure 4.14, were carried out two oxidation peaks (A1, A2) were noted at potentials similar to that observed for solutions containing palladium only. It was noted that the formation of these peaks corresponded to the applied potential range.

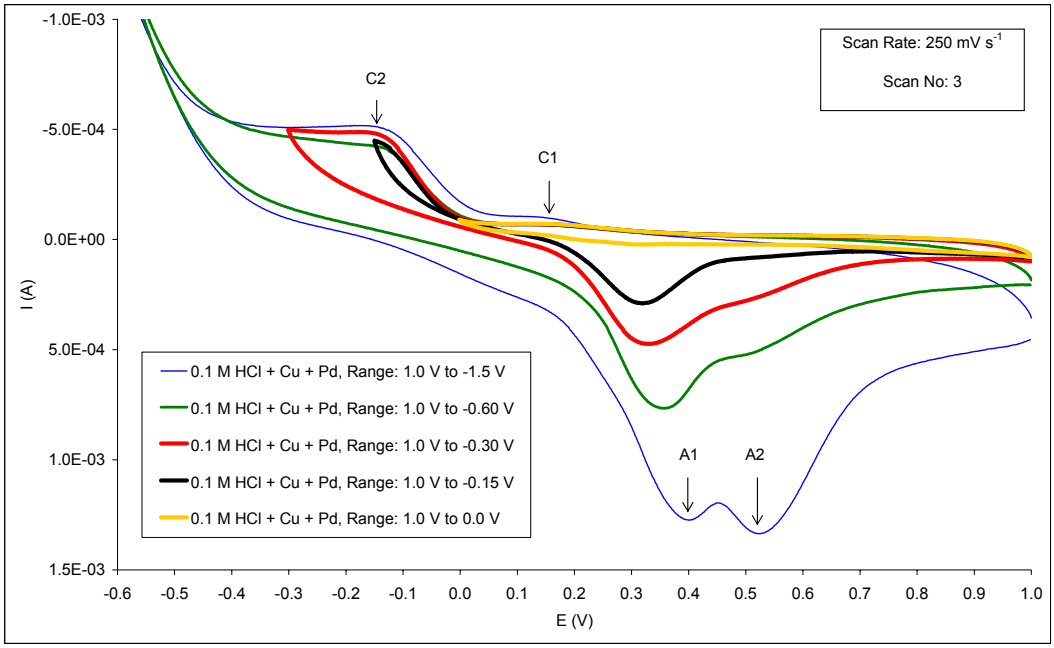

Figure 4.14 Cyclic voltammograms of a solution containing 174 mg l^{-1} copper and 189 mg l^{-1} palladium in a 0.1 M HCl background electrolyte, showing experiments where different potential ranges were utilised. A graphite working electrode was employed.

As in the case of the single component palladium solution, a second oxidation peak was only observed as the potential range was extended to more negative values.

The relative positions of the oxidation peaks observed for solutions containing both copper and palladium was however opposite to that observed for the single component palladium solution. In the case of the solution containing both copper and palladium ions, the second oxidation peak was now observed at more positive potentials relative to the first peak. This confirmed the earlier suggestion that copper and palladium ions contributed to the overall characteristics of the voltammogram obtained for solutions containing a combination of the two metal ions.

In Section 3.5.3 the interaction of a solution containing a combination of copper and palladium with a glassy carbon working electrode was investigated via the voltammograms shown in Figures 3.13 to 3.16. It was concluded that Peak C1 (Figures 3.13 to 3.16) was indicative of the deposition of copper metal centres, and that Peak C2 (Figures 3.13 to 3.16) was associated with the deposition of palladium metal centres.

The potential values for the formation of Peak C1 (Figures 3.13 to 3.16) was compared to the peak potential associated with the deposition of palladium from a single component solution on a glassy carbon surface (Figure 3.6). It was noted that Peak C1 (ca. -0.25 V) formed at potentials just negative to that observed for palladium deposition from a single component solution (ca. -0.20 V). It was also observed that the reduction peak associated with the deposition of copper from a solution containing both copper and palladium ions occurred at more positive potentials (ca. 0.10 V) relative to solutions containing only copper. These observations pointed to the possibility that the formation of palladium metal centres on the glassy carbon surface played a role in the subsequent deposition of copper when a combination of the respective metal ions was present.

A comparison of the interaction of solutions containing either palladium or a combination of copper and palladium with a graphite electrode, as

illustrated in Figure 4.13, supports this possibility. In this case the deposition of palladium from a solution containing palladium ions only was predicted at potentials of ca. 0.15 V, followed by reactions involving copper and palladium ions at potentials more negative potentials.

From discussions related to Figures 3.13 to 3.16, and Figures 3.20 and 3.21 it was concluded that copper metal was present as a surface deposit, and in alloys involving different combinations of palladium and platinum. It was concluded that Peak A1 in Figures 3.13 to 3.16 was indicative of the anodic dissolution of copper surface deposits, whilst Peak A3 was ascribed to the oxidation of copper contained in an alloy to Cu^{2+}.

By comparing the oxidation peaks in Figures 3.13 to 3.16, and Figures 3.20 and 3.21 to those recorded in Figure 4.14, it was concluded that Peak A1 of the latter figure indicated the anodic dissolution of copper metal from an alloy containing copper and palladium metal centres, whilst Peak A2 was indicative of the anodic dissolution of palladium from a combination of copper and palladium metals on the working electrode surface.

When the oxidation peaks of the voltammograms recorded for solutions containing both copper and palladium ions in Figures 3.13 to 3.16 (glassy carbon electrode) was compared to voltammograms recorded for similar solutions in Figures 4.13 and 4.14 (graphite electrode) a difference in the total number of significant peaks was noted. An extra peak, labelled A1 (ca. 0.0 V) was observed in the case where a glassy carbon electrode was employed. This indicated that the copper deposit on the graphite electrode was contained in an alloy, rather than a surface deposit.

Based on the discussions associated with Figures 4.13 and 4.14, and comparisons to Figures 3.13 to 3.16 and Figures 3.20 and 3.21 the following was concluded:

- Copper and palladium are reduced to their metallic forms on a graphite working electrode from solutions containing both of the metal ions.
- The characteristics of voltammograms observed for solutions

containing a combination of copper and palladium ions are similar when *(i)* a glassy carbon or *(ii)* a graphite working electrode is used. The initial deposition of palladium on the relevant electrode surface is thought to play a role in the subsequent deposition of copper.

- Peak C1 shown in Figures 4.13 and 4.14 is ascribed to the reduction of Cu^{2+} to Cu^{+}, whilst the presence of Peak C2 in the same illustrations is associated with the formation of copper and palladium metal centres. The fact that the magnitude of the reduction current at peak C2 is four times the magnitude of Peak C1 would indicate the overall reduction of Cu^{2+} and Pd^{2+} to their respective metallic states.

- Experiments involving the application of different potential scan ranges (Figure 4.14) indicated that Peaks A1 and A2 were associated with Peak C2. This pointed to the possibility of removing the deposited copper and palladium metal from the electrode surface via anodic dissolution. The voltammograms in Figure 4.14 also indicated that the ratio of palladium deposited in relation to copper increased as the potential scan ranges progressed to more negative potentials.

Reactions involving copper, palladium and platinum (Figure 4.15). A comparison of the interaction of *(i)* copper and palladium ions, and *(ii)* copper, palladium and platinum with a graphite working electrode is provided in Figure 4.15.

The voltammogram for the solution containing copper, palladium and platinum differ from the voltammogram recorded for copper and palladium in three ways. In the first instance, the slope of the reduction current associated with the catalytic generation of hydrogen gas is steeper for the solution containing three metal ions. This current also becomes significant at potentials of ca. -0.30 V, compared to potentials of ca. -0.55 V for voltammograms associated with solutions containing copper and palladium. The second difference relates to the presence of an oxidation peak at ca. -0.20 V (Peak A1) for the voltammogram associated with the

solution containing three metal ions. Thirdly, the magnitude of the oxidation currents recorded for Peaks A2 and A3 are lower when solutions containing copper, palladium and platinum are tested.

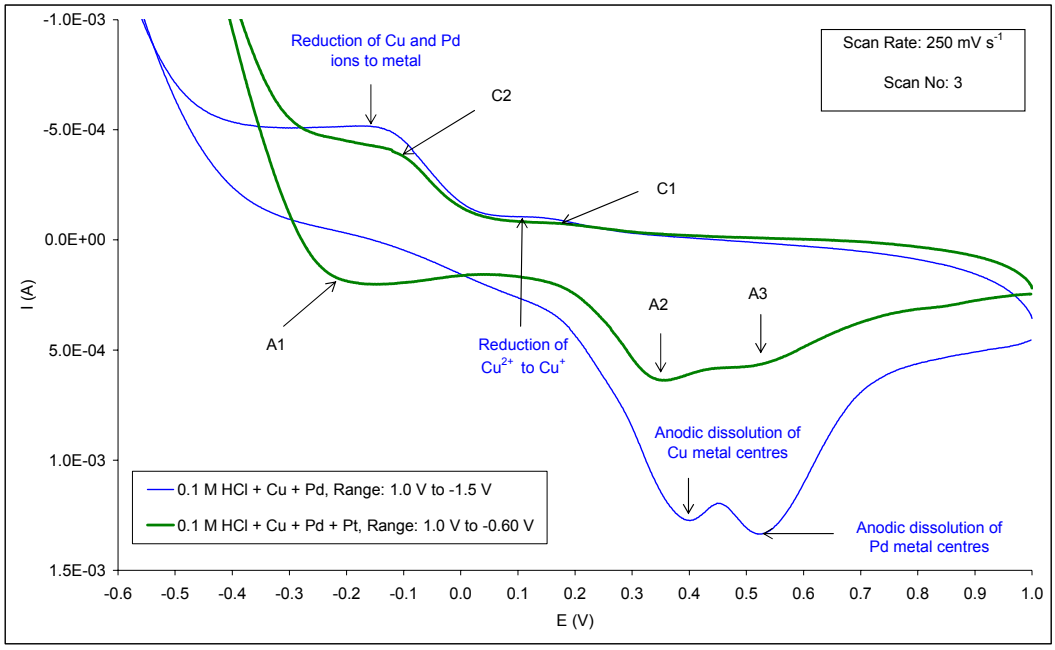

Figure 4.15 Cyclic voltammograms of solutions containing *(i)* 170 mg l^{-1} copper, 189 mg l^{-1} palladium, *(ii)* 170 mg l^{-1} copper, 189 mg l^{-1} palladium and 47 mg l^{-1} platinum. The metal ions were contained in 0.1 M HCl background electrolyte, and a graphite working electrode was used in all cases.

Differences related to the generation of the hydrogen evolution current are associated with changes in the overall electrocatalytic properties of the electrode surface. This implies that platinum metal centres must have formed where solutions containing copper, palladium and platinum were tested. The presence of Peak A1 is characteristic of the oxidation of molecular hydrogen on platinum metal centres (refer to discussions related to Figure 4.7) and confirms the deposition of platinum metal.

The decrease in the magnitude of the oxidation currents associated with Peaks A2 and A3 may be attributed to changes in the effective surface area of copper and palladium metal centres available for oxidation, since a

combination of copper, palladium and platinum metal centres were present on the electrode surface.

Based on the facts presented, the interaction of copper, palladium and platinum ions with a graphite electrode was interpreted as follows:

- As the potential applied to the graphite electrode progressed to more negative values, the reduction of Cu^{2+} to Cu^{+} was indicated by Peak C1.
- The formation of copper, palladium and platinum was associated with Peak C2.
- Peaks A2 and A3 are indicative of the anodic dissolution of copper and palladium from a combination of metals on the working electrode surface.

Palladium Mother Liquor (PML) solutions

Following experiments involving CV, a qualitative interpretation for the interaction of a synthetic solution containing a combination of copper, palladium and platinum (in 0.1 M HCl) with a graphite working electrode was established. The details were provided via discussions related to Figure 4.15.

In an attempt to predict the behaviour of actual PML solutions at a graphite working electrode surface, voltammograms for these refinery solutions were compared to voltammograms recorded for synthetic solutions containing different combinations of copper, palladium and platinum in a 0.1 M HCl matrix. An example of such a comparison is provided in Figure 4.16.

From the comparisons in Figure 4.16, it was apparent that there is a close correlation between the voltammograms observed for the synthetic and PML solutions. There is a closer correlation between the PML solution and the synthetic solution containing only copper and palladium, compared to

synthetic solutions containing a combination of copper, palladium and platinum. This was attributed to the fact that the particular PML solution used for the experiment only contained ca. 7 mg l^{-1} platinum.

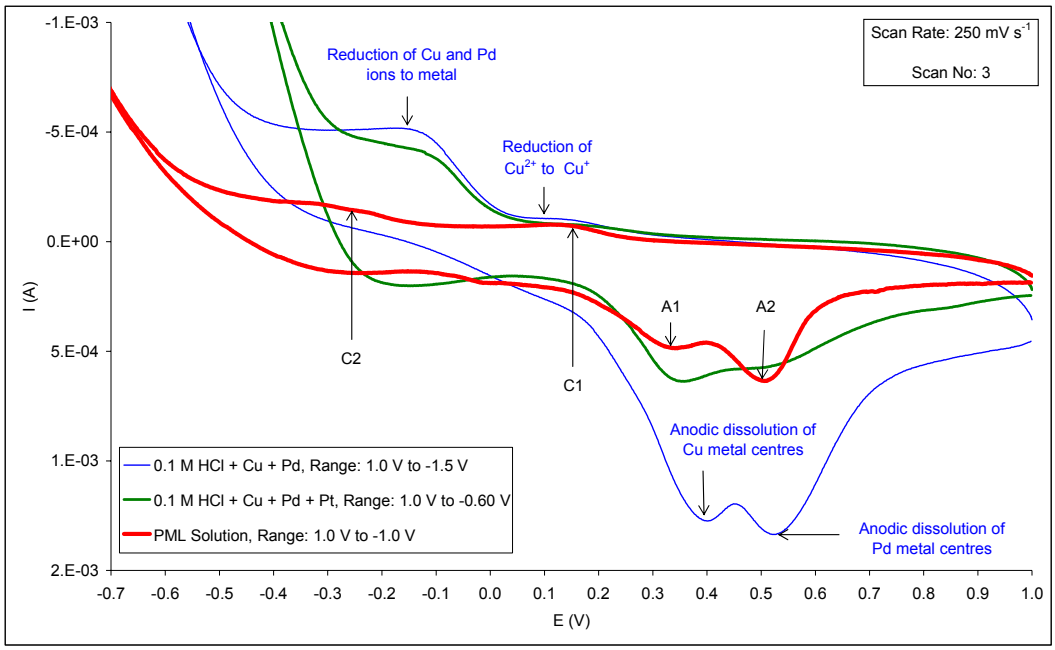

Figure 4.16 Cyclic voltammograms of synthetic solutions containing *(i)* 170 mg l^{-1} copper, 189 mg l^{-1} palladium, *(ii)* 170 mg l^{-1} copper, 189 mg l^{-1} palladium and 47 mg l^{-1} platinum, compared to a PML solution (refer to Table 4.1 for metal concentrations). The metal ions in the synthetic solution were contained in 0.1 M HCl background electrolyte. A graphite working electrode was used in all cases.

The major difference in the voltammograms observed for synthetic and refinery samples was related to the position of the PML solution peak labelled C2. This peak was observed at more negative potentials relative to the synthetic solutions. It was concluded that the shift of Peak C2 to more negative potentials was associated with the presence of stable metal -ligand complexes other than those found in the synthetic solutions. Higher overpotentials were required to reduce the palladium and platinum associated with these complexes to their metallic form on the graphite electrode surface.

Based on discussions involving Figure 4.16, and conclusions made under the sub-heading “Synthetic solutions” (Section 4.5.1), the following interpretation of voltammograms obtained for the interaction of a PML solution with a graphite working electrode was proposed:

- The reduction of Cu^{2+} to Cu^{+} was indicated by the presence of Peak C1.
- The deposition of copper, palladium and platinum was indicated by Peak C2.
- Peak A1 was ascribed to the anodic dissolution of copper from a metal alloy containing a combination of copper and palladium, or possibly copper, palladium and platinum. Peak A2 was associated with the anodic dissolution of palladium metal centres from the same alloy.

4.5.2 Exhaustive Electrolysis

In Section 4.5.1, the deposition of palladium and platinum from PML solutions via a graphite working electrode was predicted. The objective of the exhaustive electrolysis experiments described in this section was to determine the maximum possible recovery of PGMs from PML solutions when a graphite working electrode is used. A general procedure for the execution of exhaustive electrolysis experiments was provided Section 4.2.2.

The experiment described here was initiated by recording a voltammogram for the interaction of a typical PML solution with a graphite working electrode, as shown in Figure 4.17. Identification of the copper, palladium and platinum deposition peak was achieved by application of the methodologies applied in Section 4.5.1.

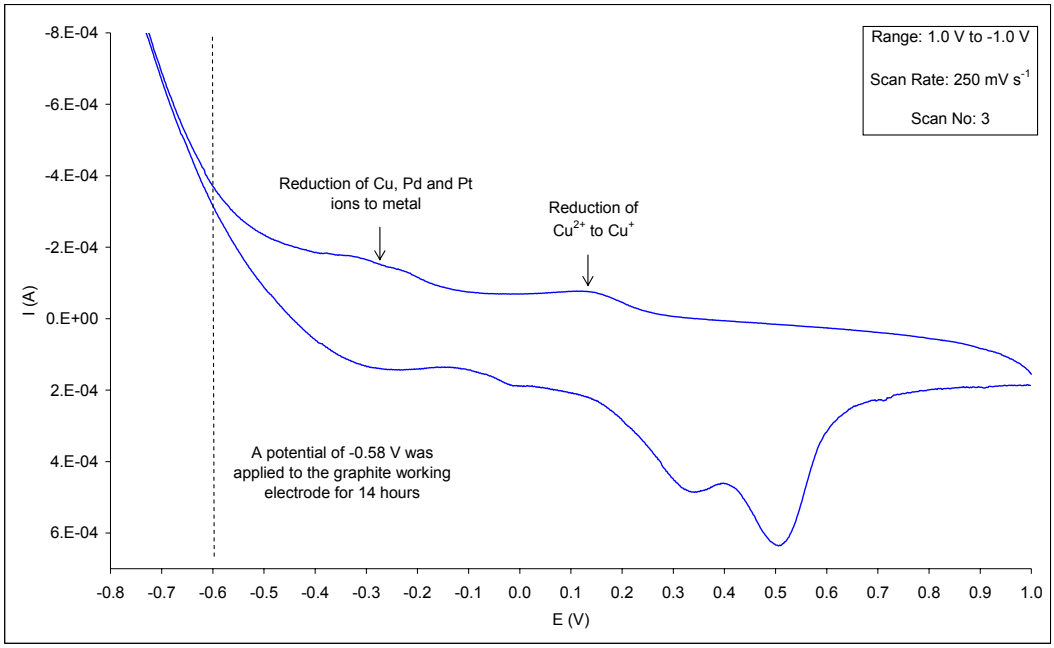

Figure 4.17 Cyclic voltammogram of a PML solution, using a graphite working electrode. (Refer to Table 4.1 for metal ion content).

Based on the information obtained from the voltammogram, it was decided to hold the potential of the graphite working electrode at -0.58 V. The rationale for selecting this particular reduction potential was based on achieving maximum recoveries (high overpotentials), whilst minimising the generation of excessive volumes of hydrogen gas. Excessive volumes of hydrogen gas were expected to reduce the efficiency of the electrolysis experiment due to coverage of the electrode by the generated gas. A total reduction time of 14 hours was used for the experiment to ensure that favourable conditions existed for the maximum possible removal of PGMs.

Prior to the exhaustive electrolysis experiment, the selected PML solution had a light green appearance. After applying a potential of -0.58 V to the graphite working electrode in contact with the PML solution for 14 hours, the appearance of the sample changed. Following the exhaustive electrolysis experiment, the solution was transparent. It was also noted that fine black particles were suspended in the PML solution.

A deposit consisting of a fine black powder interspersed with silver specs was noted on the active surface of the graphite working electrode. Gas bubbles, presumably hydrogen, were also adhered to the deposit found on the graphite electrode surface. A comparison of the copper, palladium and platinum content of the PML solution prior to and after the exhaustive electrolysis experiment is presented in Table 4.1. These samples were filtered prior to analysis, as described in Section 4.2.2.

Table 4.1 Comparison of copper, palladium and platinum content of a typical PML solution prior to and after exhaustive electrolysis.

Identification	**Cu** (mg l^{-1})	**Pd** (mg l^{-1})	**Pt** (mg l^{-1})
Prior to electrolysis	211	146	6.8
After electrolysis	0.3	0.2	$<$ 0.1

Note:

(a) Graphite working electrode held at -0.58 V for 14 hours.

(b) Copper concentrations determined via ICP-OES analyses, palladium and platinum concentrations determined by ICP-MS.

(c) pH of sample solution = 4.3.

The deposit present on the graphite working electrode surface, as well as the fine black particles suspended in the PML solution after completion of the exhaustive electrolysis experiment were recovered and combined. These solids were dissolved in aqua regia and submitted for ICP-OES and ICP-MS analyses, as described in Section 4.2.2. The purpose of these analyses was to confirm the deposition of copper, palladium and platinum on the graphite working electrode.

The mass of copper, palladium and platinum metal present in the 20 ml PML aliquot prior to the exhaustive electrolysis experiment was compared to the mass of corresponding metals found in the deposit collected after the experiment. Recoveries for copper, palladium and platinum were

calculated as 68 %, 65 % and 67 % respectively. The fact that some of the metal was not recovered was ascribed to losses observed during the collection of deposit from the porous graphite working electrode. Since low masses of deposit were handled (< 5 mg), even small losses would result in low recoveries. It should however be emphasised that the objective of dissolving the deposit was to confirm the presence of copper, palladium and platinum, as opposed to quantitative recovery. It was reasoned that analysis of the PML solution prior to and after electrolysis was a more reliable way of demonstrating quantitative metal recovery.

From the results presented in Table 4.1 it was concluded that palladium and platinum could be recovered quantitatively from a typical PML solution if a cathode material consisting of isostatically pressed graphite (grade ET-10, Electrographite Carbon Co.) was employed at suitable reduction potentials. The appropriate reduction potentials could in turn be predicted by interpreting the voltammograms recorded for PML solutions, as discussed in Section 4.5.1. Due to the similarity of the reduction potentials associated with the formation of copper, palladium and platinum metal centres (refer to Figure 4.17), copper was recovered with the PGMs. This resulted in a deposit containing copper, palladium and platinum.

Based on the conclusions presented in the previous paragraph, the isostatically pressed graphite particles were incorporated into the electrochemical reactor designed via the engineering project. This project was conducted in parallel with the fundamental research project described in this dissertation (discussed in Chapter 1, Sections 3.1 and 4.1).

As part of the engineering project, the removal of copper and palladium was monitored as a function of reactor operation time. The removal of copper and palladium from a PML solution (< 1 mg l^{-1}) was demonstrated under galvanostatic operating conditions[39].

It should be noted that the characteristics of the PML solution used for the exhaustive electrolysis experiment described here (Section 4.5.2) was assumed to be similar to that of typical solutions found at the refinery. Based on the metal content of the sample used for exhaustive electrolysis this appears to be true. It will however be wise to evaluate the effectiveness of the graphite particles using a large number of PML samples which reflect process variabilities found within the Precious Metals Refinery (PMR). These tests may involve the evaluation of metal recoveries for each of the PML solutions via the proposed electrochemical reactor. Where quantitative recoveries of PGMs cannot be achieved, further fundamental investigations may be conducted to identify the causes of incomplete recovery.

4.5.3 Amminated Complexes

In Section 4.1.1, the presence of amminated PGM complexes, and the possible influence of these complexes on the overall recovery of palladium and platinum from PML solutions was discussed. A general experimental procedure used to investigate the influence of these stable complexes was provided in Section 4.2.2. A graphite working electrode (refer to Section 4.3.1) was employed for all experiments.

Synthetic solutions containing various combinations of copper, palladium and platinum in a 0.1 M HCl matrix were spiked with NH_3 to increase the pH to ca. 9.5. The intention was to promote the formation of amminated metal complexes, and to study the interaction of these complexes with a graphite working electrode via CV.

PML solutions were spiked with sodium hydroxide to increase the pH to ca. 9.5. The rationale behind OH^- addition was that NH_4^+ ions present in the PML solution (refer to Table 1.1) would be deprotonated to form NH_3 ligands, which in turn may form amminated complexes if it is favourable under the prevailing conditions.

Voltammograms of synthetic and PML solutions adjusted to pH values of ca. 9.5 were then compared to investigate the possible formation of amminated PGM complexes in the refinery effluent.

Background electrolyte

A 0.1 M HCl background electrolyte was treated with NH_3 to increase the pH to 9.6. The voltammogram for the resulting pH 9.6 solution was compared to a voltammogram recorded for the solution prior to NH_3 addition, as illustrated in Figure 4.18.

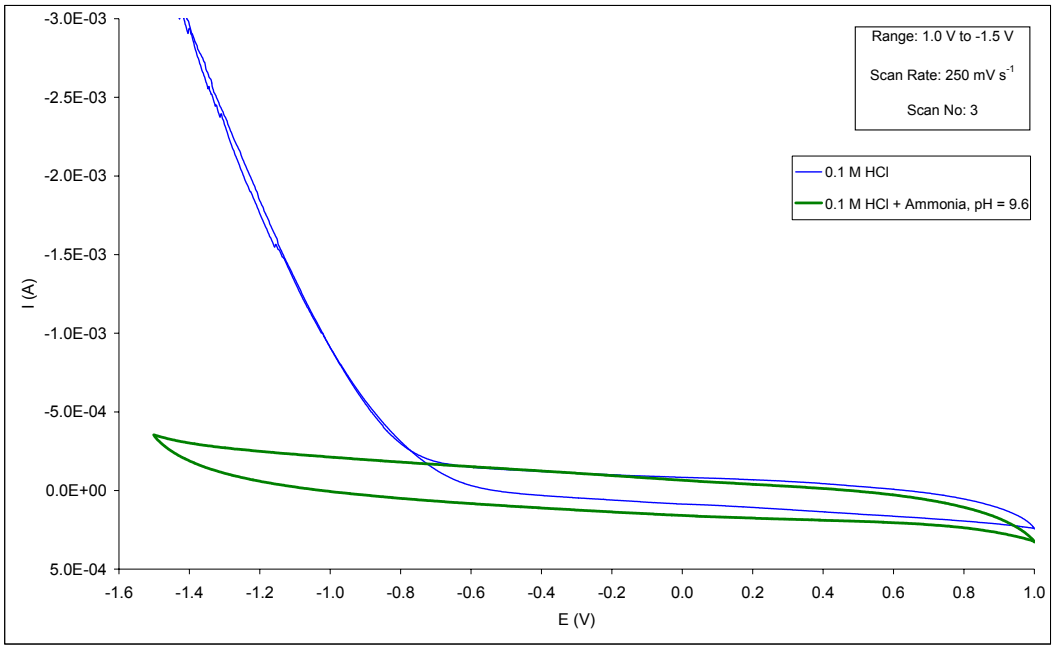

Figure 4.18 Comparison of cyclic voltammograms obtained for a 0.1 M HCl background electrolyte, and the same solution after NH_3 addition. A graphite working electrode was used.

In the case of the solution containing NH_3 it was found that the evolution of hydrogen occurred at more negative potentials relative to the original 0.1 M HCl background electrolyte. This was expected, due to the significant reduction of hydrogen ion concentration in the background electrolyte after NH_3 addition:

$$H^+ + NH_3 \leftrightarrow NH_4^+ \qquad (4.1)$$

Significant hydrogen evolution currents were only observed at potentials more negative than ca. -1.5 V when the solution containing NH_3 was analysed. A potential range between 1.0 V and -1.5 V was therefore available to observe the interaction between a graphite working electrode and metal ions contained in a NH_3 matrix.

Synthetic solutions

Reactions involving palladium (Figures 4.19 to 4.20). A comparison of voltammograms obtained for the interaction of a graphite working electrode with *(i)* a solution containing palladium ions in a 0.1 M HCl matrix, and *(ii)* the same solution after adjustment to a pH value of 9.7 with NH_3 is shown in Figure 4.19.

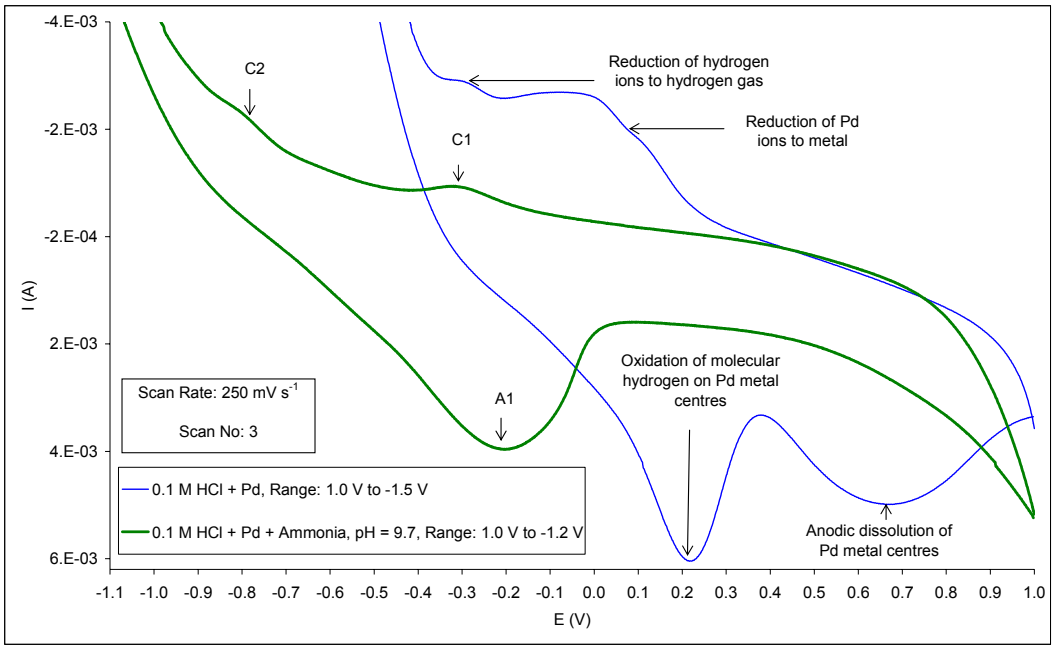

Figure 4.19 Comparison of cyclic voltammograms obtained for a solution containing 380 mg l^{-1} palladium in a 0.1 M HCl background electrolyte, and the same solution after NH_3 addition. A graphite working electrode was used.

In Figure 4.20, potential range experiments involving the solution containing palladium and NH_3 were carried out to confirm the association of Peak C2 with Peak A1.

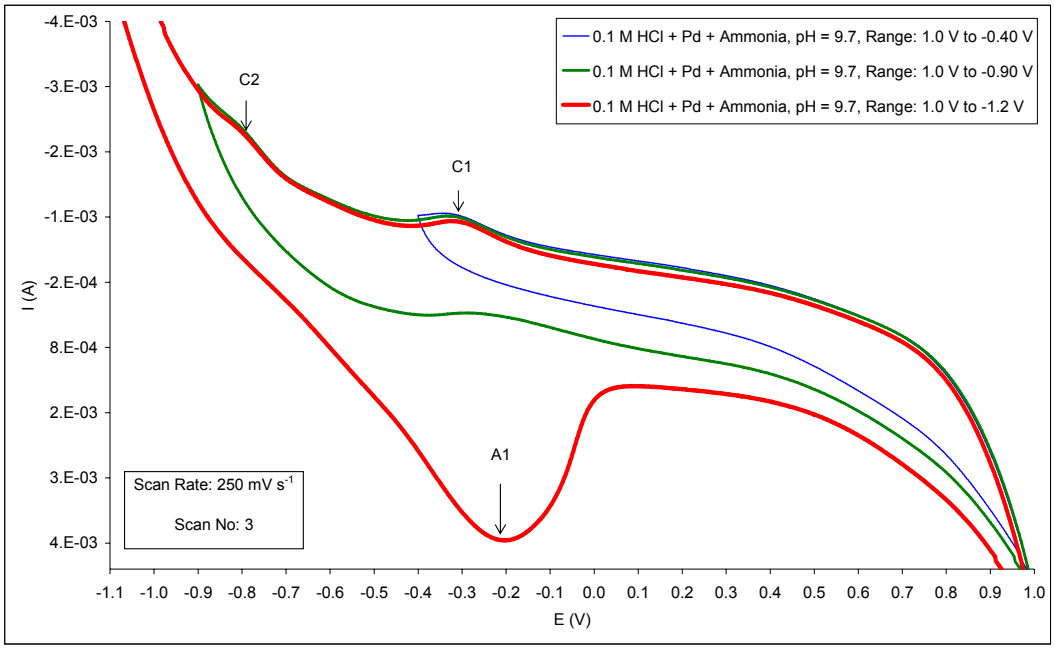

Figure 4.20 Cyclic voltammograms of a 380 mg l^{-1} palladium solution containing NH_3, showing experiments where different potential ranges were utilised. A graphite working electrode was employed.

An interpretation of the voltammogram associated with the 0.1 M HCl matrix was provided in Section 4.5.1 (Figures 4.4 and 4.5). It was concluded that palladium metal centres were deposited on the graphite electrode surface, and that the resultant palladium metal centres could be oxidised to palladium ions at suitable potentials.

When a voltammogram for the solution containing palladium in a NH_3 matrix was compared to a voltammogram associated with the deposition and anodic dissolution of palladium contained in a 0.1 M HCl matrix, as illustrated in Figure 4.19, two major differences were noted.

The first difference was related to the potentials at which Peaks C1 and C2 for the NH_3 solution were observed relative to reduction peaks identified

when a 0.1 M HCl solution was used. Peaks C1 and C2 occurred at more negative potentials compared to the corresponding peaks observed when a 0.1 M HCl matrix was used. This shift was ascribed to the presence of stable amminated palladium complexes, which necessitated the application of a higher overpotential to achieve the deposition of palladium metal centres on a graphite working electrode.

The second difference was associated with the fact that only one oxidation peak (A1) was observed when a NH_3 matrix was used, compared to the two oxidation peaks when a HCl matrix was used. Based on the comparative voltammograms in Figure 4.19, it was concluded that Peak C1 was associated with the formation of palladium metal centres on the graphite working electrode, whilst Peak C2 was ascribed to the reduction of hydrogen ions to hydrogen gas. Since Peak C2 was related to Peak A1 via potential range experiments shown in Figure 4.20, it was concluded that Peak A1 was indicative of the oxidation of molecular hydrogen on palladium metal centres.

The absence of a second oxidation peak for the voltammogram associated with the NH_3 matrix pointed to the fact that palladium metal centres were not removed anodically when a potential range of 1.0 V to -1.5 V and the background electrolyte for the particular experiment was used. This observation is also supported in literature, where it was reported that the anodic dissolution of palladium would be hindered in alkaline solutions due to the formation of a stable hydroxide layer on the metal[16].

It may however be possible that the anodic dissolution of palladium did occur at a slow rate under the given experimental conditions, and that the dissolution was not observed within the time domain of the particular CV scan.

Reactions involving platinum (Figure 4.21). In Figure 4.21, the behaviour of platinum ions contained in a 0.1 M HCl background electrolyte, and the behaviour of platinum ions in the same background electrolyte after pH

adjustment with NH_3 was compared via CV experiments utilising a graphite working electrode.

The interaction between platinum contained in a 0.1 M HCl background electrolyte and a graphite working electrode was originally discussed in Section 4.5.1 (Figure 4.8). It was concluded that platinum metal centres were deposited on the graphite working electrode, and that molecular hydrogen was oxidised on the platinum metal centres. No evidence was found for the anodic dissolution of platinum metal centres at an appreciable rate when experimental conditions associated with Figure 4.8 were employed.

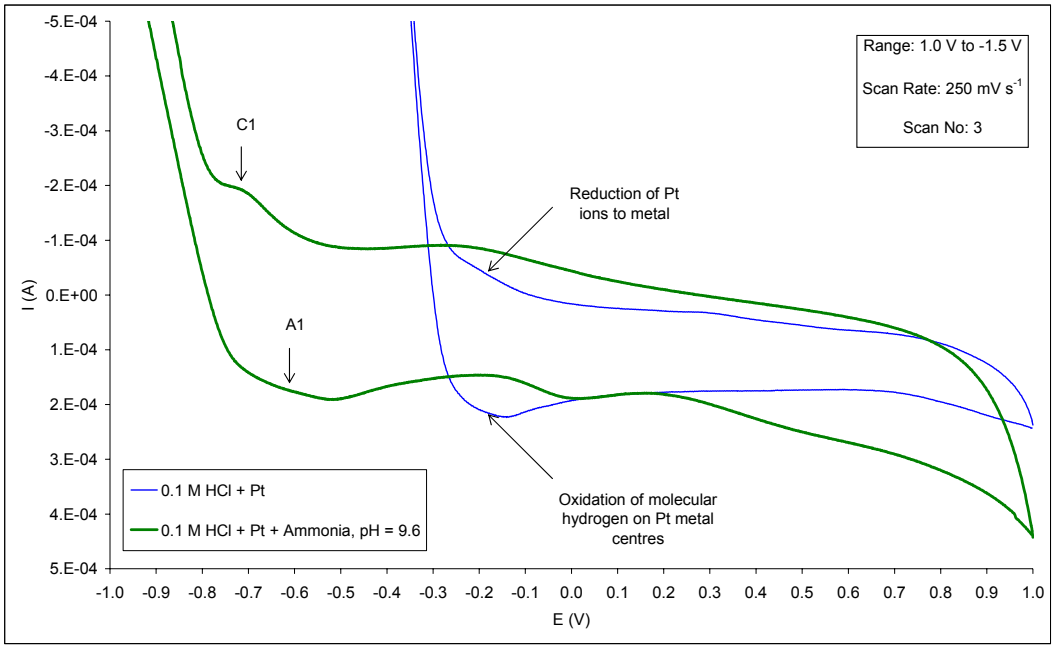

Figure 4.21 Comparison of cyclic voltammograms for a solution containing 50 mg l^{-1} platinum a 0.1 M HCl background electrolyte, and the same solution after NH_3 addition. A graphite working electrode was used.

When the voltammograms in Figure 4.21 were compared, it was noted that the plots associated with the NH_3 and HCl matrices exhibited similar characteristics. The only difference was associated with the potentials at which the reduction of platinum ions to its metallic form, and the subsequent oxidation of molecular hydrogen on platinum metal centres

were observed. For the HCl solutions the characteristic reduction and oxidation peaks were observed at ca. -0.25 V , whilst the corresponding peaks for the NH_3 solutions (C1, A1) were noted at potentials of ca. -0.75 V .

The shift of peak potentials to more negative values when a background electrolyte containing NH_3 was used could be ascribed to the presence of stable amminated platinum complexes. A higher overpotential was therefore required to deposit platinum from solutions containing these stable complexes.

Reactions involving combinations of copper, palladium and platinum (Figures 4.22 and 4.23). The interpretation of the voltammograms shown in Figures 4.22 and 4.23 was facilitated by comparison to *(i)* voltammograms obtained whilst employing a graphite working electrode and a 0.1 M HCl background, and *(ii)* voltammograms of single component solutions containing palladium or platinum ions in a NH_3 matrix as originally discussed via Figures 4.19 to 4.21.

A short discussion of the most important issues related to the voltammograms recorded whilst using a 0.1 M HCl background electrolyte is provided here to emphasise the relationship with the voltammograms in Figures 4.22 and 4.23, where solutions containing NH_3 were analysed.

In Section 4.5.1, the interaction of a graphite working electrode with palladium ions contained in a 0.1 M HCl background electrolyte was described with the aid of Figures 4.4 and 4.5. The reduction current ascribed to the evolution of hydrogen gas on palladium metal centres was observed at potentials more negative than ca. 0.15 V . In comparison, the hydrogen evolution current on deposited platinum metal centres was observed at potentials more negative than ca. -0.25 V when the same working electrode and background electrolyte was used. The deposition of platinum metal centres was discussed via Figures 4.7 and 4.8.

An outstanding feature of the interaction of a graphite working electrode with a combination of copper and palladium ions contained in a 0.1 M HCl background electrolyte (Section 4.5.1, Figures 4.13 and 4.14) was that the formation of palladium metal centres on the graphite working electrode initiated the deposition of copper. Platinum did not play a role in the deposition of copper, since it was deposited at more negative potentials relative to palladium. This was confirmed by the similarities of the voltammograms shown in Figure 4.15, where the deposition of platinum was observed at potentials more negative than -0.20 V .

When the interaction of a graphite working electrode with single component palladium and platinum solutions containing NH_3 was analysed via CV as illustrated in Figures 4.19 to 4.21, the reduction peak associated with palladium deposition was noted at ca. -0.30 V , compared to the platinum deposition peak at ca. -0.75 V . The fact that the deposition of palladium still occurred at more positive potentials relative to platinum pointed to the possibility that the mechanism for the interaction of copper, palladium and platinum in a HCl or NH_3 based background electrolyte with a graphite working electrode would be similar. This assumption was tested via the voltammograms shown in Figures 4.22 and 4.23.

In Figure 4.22 the interaction of a graphite working electrode with a solution containing a combination of copper and palladium ions was investigated by means of CV. The original 0.1 M HCl background electrolyte was spiked with NH_3 to a pH value of 9.7.

Based on comparisons to the voltammograms in Figures 4.13 and 4.14 (0.1 M HCl background electrolyte), Peak C1 in Figure 4.22 was ascribed to the overall reduction of copper and palladium ions to metal.

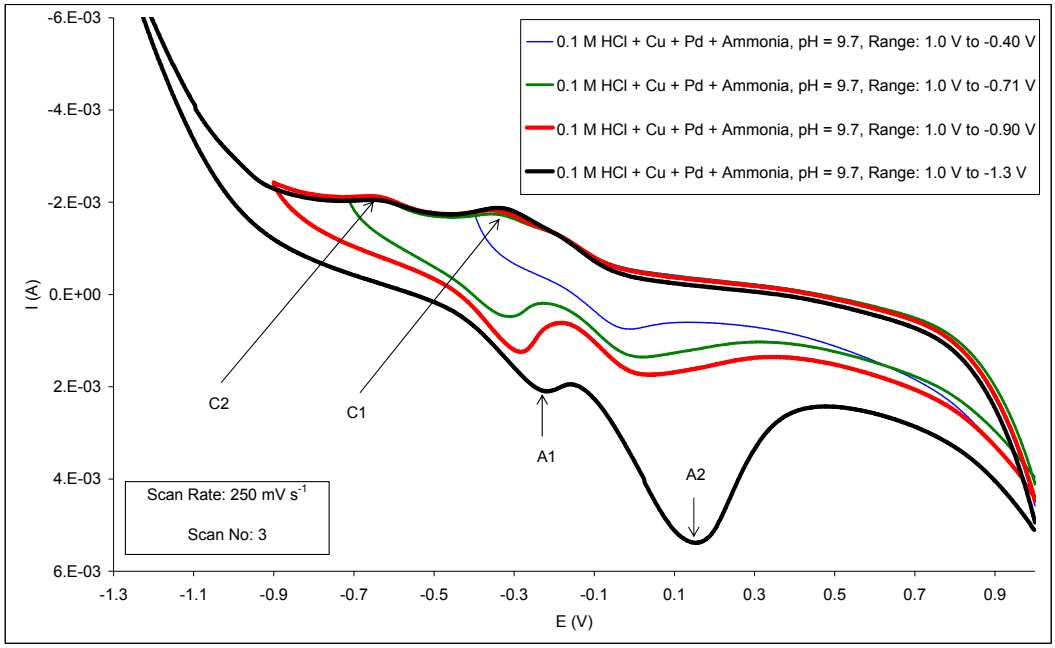

Figure 4.22 Cyclic voltammograms of a solution containing 350 mg l^{-1} copper and 380 mg l^{-1} palladium, showing experiments where different potential ranges were utilised. The original 0.1 M HCl background electrolyte was spiked with NH_3 prior to conducting the experiment. A graphite working electrode was employed.

When the formation of the oxidation peaks A1 and A2 of Figures 4.14 and 4.22 were analysed as a function of the potential scan range, an important difference was observed. As the potential scan range in Figure 4.14 was extended to more negative potentials, Peak A1 was noted. Upon further extension of the scan range, Peak A2 was observed at more positive potentials relative to Peak A1. When similar experiments were illustrated via Figure 4.22 (NH_3 solution), the opposite trend was noted. Peak A2 was observed initially, and upon extension of the scan range, Peak A1 was recorded at more negative potentials relative to Peak A2.

The difference in the order of oxidation peak formation observed in Figures 4.14 and 4.22 may be explained as follows:

- In Figure 4.14, Peak A1 was associated with the anodic dissolution of copper metal from a deposit containing copper and palladium metal,

whilst Peak A2 was identified as the stripping peak for palladium from the same deposit.

- When single component palladium solutions containing NH_3 were analysed, the absence of an anodic stripping peak was reported. In cases where the potential scan range for experiments involving this solution was extended to more negative overpotentials, a peak related to the oxidation of molecular hydrogen present on palladium metal centres was identified (refer to Figure 4.20, Peak A1).

- It was found that the relative positions of Peak A1 in Figures 4.20 and 4.22 corresponded (ca. -0.20 V). Peak A1 in Figure 4.22 was therefore ascribed to the oxidation of molecular hydrogen on palladium metal centres.

- Since the potential range experiments illustrated in Figure 4.22 indicated the association of Peaks C2 and A1, the cathodic peak was ascribed to the reduction of hydrogen ions on an electrode surface consisting of graphite, copper and palladium. Peak A2 was identified as the anodic stripping peak for copper.

The order in which Peaks A1 and A2 in Figure 4.22 appeared was therefore related to the fact that palladium metal was not anodically stripped from the electrode surface when solutions containing NH_3 were used. The oxidation peak associated with the anodic dissolution of copper metal centres (A2) was initially observed. As the potential scan range was extended to more negative values more palladium metal centres were formed on the working electrode surface. The presence of sufficient amounts of palladium metal centres facilitated the formation of Peak A1 due to the oxidation of molecular hydrogen. This mechanism was also illustrated in Figure 4.5, where a single component palladium solution (0.1 M HCl background electrolyte) was analysed.

In Figure 4.23 the interaction of a graphite working electrode with *(i)* platinum ions, *(ii)* a combination of copper and palladium ions and *(iii)* a

combination of copper, palladium and platinum ions are compared. In each case the metal ions were contained in a NH_3 matrix.

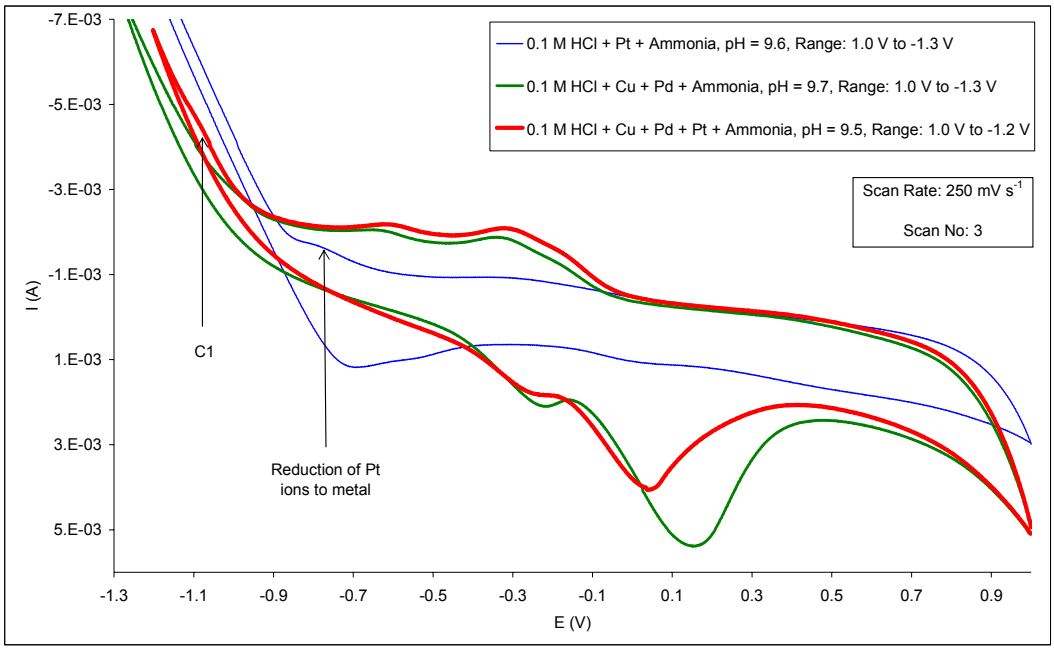

Figure 4.23 Cyclic voltammograms of solutions containing *(i)* 98 mg l^{-1} platinum, *(ii)* 350 mg l^{-1} copper, 380 mg l^{-1} palladium and *(iii)* 350 mg l^{-1} copper, 380 mg l^{-1} palladium, 98 mg l^{-1} platinum. The original 0.1 M HCl background electrolyte was spiked with NH_3 prior to conducting the experiments. A graphite working electrode was used in all cases.

When the voltammogram for the solutions containing copper, palladium and platinum was compared to the voltammogram for the solution containing a combination of copper and palladium, two major differences were noted. The first difference was associated with the presence of an additional reduction peak (C1) observed for the voltammogram where a combination of copper, palladium and platinum ions were present in solution. Secondly it was noted that the reduction current associated with the evolution of hydrogen observed for the same voltammogram had shifted to more a positive potential value relative to the voltammogram observed for the solution containing copper and palladium ions.

It was concluded that Peak C1 in Figure 4.23 indicated the deposition of

platinum metal on an electrode surface containing a combination of copper and palladium metal centres.

When the reduction peak associated with deposition of platinum from a single component solution was compared to Peak C1 (refer to Figure 4.23), it was noted that Peak C1 formed at more negative potentials. The relative positions of the peaks were ascribed to the electrocatalytic properties associated with the working electrode. These electrocatalytic properties vary in relation to the different types and combinations of metal centres found on a particular surface.

Palladium Mother Liquor (PML) solutions

Sodium hydroxide was added to PML solutions to increase the pH to ca. 9.5. As explained in Section 4.2.2 and the opening paragraph of the current section (Section 4.5.3), the rationale behind OH^- addition was that NH_4^+ ions present in the refinery effluent would be deprotonated to form NH_3 ligands, which in turn may form amminated complexes if it is favourable under the prevailing conditions.

In Figure 4.24, voltammograms recorded of a PML solution prior to and after OH^- addition is shown. In addition, a voltammogram obtained for a synthetic solution containing copper, palladium and platinum in a NH_3 matrix (identical to Figure 4.23) is illustrated.

When the voltammograms of the PML solutions before and after OH^- addition were compared, it was noted that the respective peak positions had shifted. Comparison of the PML solution after OH^- addition, and the synthetic NH_3 solution shown in Figure 4.24 revealed several similarities.

It was concluded that amminated metal-ligand complexes did form in the PML solution after OH^- addition, and that the complexes were similar to those contained in the synthetic solutions with a NH_3 matrix.

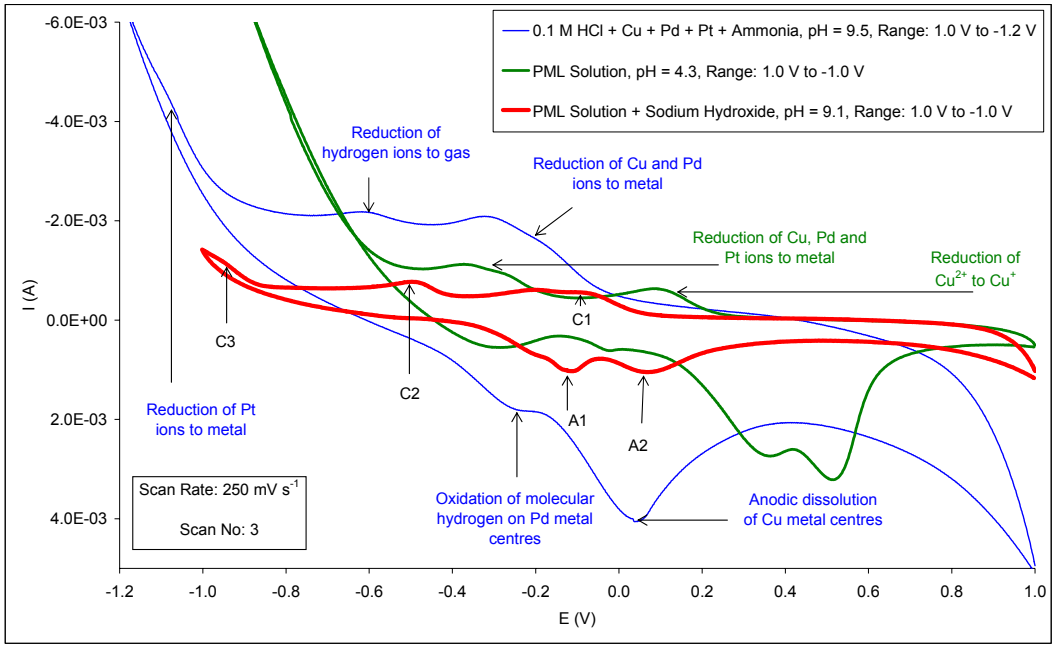

Figure 4.24 Comparison of cyclic voltammograms for *(i)* a synthetic solution containing 350 mg l^{-1} copper, 380 mg l^{-1} palladium, 98 mg l^{-1} platinum after NH_3 addition, *(ii)* a PML solution, and *(iii)* the same PML solution after OH^- addition. A graphite working electrode was used in all cases. (Refer to Table 4.2 for PML metal ion content).

Based on the comparison of the PML voltammogram after OH^- addition to the voltammogram of the synthetic solution with a NH_3 matrix (Figure 4.24), Peak C1 was ascribed to the deposition of copper and palladium metal centres. Peak C2 was associated with the reduction of hydrogen ions on an electrode surface consisting of graphite, copper and palladium, whilst Peak C3 was associated with the deposition of platinum.

Peak A1 was originally ascribed to the oxidation of molecular hydrogen on palladium metal centres. It was however noted that the magnitude of the current recorded for Peak A1 was similar to that of Peak A2. In contrast, it was observed that the ratio of corresponding peak currents for the synthetic solution (Figure 4.24) was 2:1, with the peak corresponding to A2 producing the highest current.

This lead to the conclusion that Peak A1 observed for the pH-adjusted PML solution may be a function of two reactions, namely the oxidation of molecular hydrogen on palladium metal centres, and the oxidation of copper metal (present on the electrode as a surface deposit) to Cu^{+}. Peak A2 was associated with the anodic dissolution of copper metal from a deposit containing copper and palladium metal.

It was concluded that palladium could not be anodically stripped from the working electrode surface when the pH of the PML solution was adjusted to ca. 9.5.

General comments

The data presented thus far in Section 4.5.3 has shown that the characteristics of the voltammograms obtained for various combinations of copper, palladium and platinum in a sample matrix containing NH_3 were in many respects similar to that observed for identical combinations of the metals in a HCl matrix. Reduction peaks for the various metal ions present in a NH_3 matrix did however all appear at more negative potentials relative to the peaks observed when solutions with HCl was used. The shift of the overall peak positions observed for solutions containing NH_3 was ascribed to the presence of amminated species, which were reduced at higher overpotentials due to the stability of the metal-ligand complexes.

Another difference in the characteristics of the voltammograms recorded for the two different matrices was the absence of an anodic stripping peak for palladium contained in NH_3 solutions. It may also be possible that the anodic dissolution of palladium occurred at a very slow rate compared to the time scale of the CV experiments conducted. The characteristics of the background electrolyte contributed to the fact that palladium was not dissolved anodically at a significant rate.

In order to confirm some of the observations made when the behaviour of combinations of copper, palladium and platinum were studied in NH_3 solutions, it would be necessary to perform validation tests similar to those carried out in Section 4.5.1. The occurrence or absence of the deposition and anodic dissolution of copper, palladium and platinum metal was confirmed by holding the working electrode at potentials predicted via CV. Due to the scope of the project (refer to Chapter 1) and limited resources it was not possible to validate the conclusions made when voltammograms associated with NH_3 solutions were analysed.

Generally the interpretation of voltammograms for multi-component solutions involving a NH_3 matrix proved to be difficult, and the assignment of electrochemical processes to particular peaks was less certain. A considerable research effort would be required to validate the interpretation of the associated voltammograms.

In the context of the research project, sufficient information was however available to indicate that the formation of amminated complexes involving copper, palladium and platinum would necessitate the application of higher overpotentials to initiate the deposition of the metals from solution.

Exhaustive electrolysis experiments

Experiments involving the PML solution after addition of OH^- were carried out. The recoveries of PGMs from these solutions were compared to recoveries obtained with normal PML solutions in order to quantify the impact of amminated species on the overall recovery process.

The exhaustive electrolysis experiment described here was initiated by adjusting the pH of the original PML solution (used for the experiment described in Section 4.5.2) from 4.3 to 9.1 with a 10 M NaOH solution. At pH values of ca. 8.5 the PML solution changed from a light green to a luminous blue colour. This indicated that new metal-ligand species formed.

Following the pH adjustment step, the PML solution was filtered to remove any solids that may have formed during the addition of OH^-.

The voltammograms of the PML solution prior to and after the adjustment of OH^- were illustrated in Figure 4.24. Peak C1 of the voltammogram recorded for the PML solution after pH adjustment was ascribed to the deposition of copper and palladium, whilst Peak C3 was associated with the deposition of platinum.

Based on the information obtained from the voltammogram, it was decided to hold the potential of the graphite working electrode at -1.0 V. The rationale for selecting this particular reduction potential was based on achieving maximum recoveries (high overpotentials), whilst minimising the generation of excessive volumes of hydrogen gas. Excessive volumes of hydrogen gas were expected to reduce the efficiency of the electrolysis experiment due to coverage of the electrode by the generated gas. A total reduction time of 17 hours was used for the experiment to ensure that favourable conditions existed for the maximum possible removal of PGMs.

After applying a potential of -1.0 V to the graphite working electrode in contact with the PML solution for 17 hours, the appearance of the sample was transparent. A deposit consisting of a fine black powder was noted on the active surface of the graphite working electrode. Gas bubbles, presumably hydrogen, were also adhered to the deposit found on the graphite electrode surface. These observations provided evidence that metal deposition did take place, and that hydrogen gas was evolved in the process.

The extent of metal deposition is illustrated in Table 4.2, where a comparison of the copper, palladium and platinum content of the PML solution *(i)* prior to OH^- addition, *(ii)* after OH^- addition and filtration and *(iii)* following exhaustive electrolysis is presented.

Table 4.2 Comparison of copper, palladium and platinum content of a typical PML solution prior to and after exhaustive electrolysis. The pH of the PML solution was adjusted from 4.3 to 9.1 with NaOH prior to exhaustive electrolysis.

Identification	**Cu** (mg l^{-1})	**Pd** (mg l^{-1})	**Pt** (mg l^{-1})
Prior to OH^- addition	210	144	6.8
After OH^- addition	85	144	6.8
After electrolysis	1.1	7.0	3.5

Note:

(a) Graphite working electrode held at -1.0 V for 17 hours.

(b) Copper concentrations determined by ICP-OES, palladium and platinum analysed by ICP-MS.

(c) All samples were filtered through a 0.45 μm cellulose nitrate membrane prior to ICP-OES and ICP-MS analyses.

(d) pH of the PML was adjusted with a 10 M NaOH solution.

From the results in Table 4.2 it was evident that a large fraction of copper was precipitated after OH^- addition. In the case of palladium and platinum no precipitation occurred when the pH of the PML solution was adjusted. This information may be useful where future studies related to the selective recovery of PGMs and copper from PML solutions is conducted.

When the results obtained for the exhaustive electrolysis experiment conducted on a PML solution as received from the refinery (refer to Table 4.1) were compared to the experiment involving a pH-adjusted PML solution, it was noted that the concentrations of copper, palladium and platinum remaining after electrolysis were higher for the latter experiment. The total PGM (palladium and platinum) concentration in the pH-adjusted PML solution after electrolysis was 10.5 mg l^{-1}. This would not meet the

requirement of PGM removal to concentrations < 10 mg l^{-1} with no single PGM present at concentrations of > 2 mg l^{-1}, as defined in the overall project objectives (refer to Chapter 1).

Due to the nature of the refining processes leading to the production of a typical PML, it is likely that the copper, palladium and platinum present in the solution would take the form of a mixture of chloro and ammine complexes. It may also be possible that the complexes contain both Cl^- and NH_3 ligands. The addition of OH^- to the PML solution created favourable conditions for the conversion of the remaining chloro complexes to amminated complexes. It should therefore be noted that the results shown in Table 4.2 reflect an extreme case to illustrate the maximum possible influence that amminated complexes may have on the overall removal of PGMs from the PML solution when a graphite working electrode is used.

Compared to the pH-adjusted PML solution, the total PGM concentration for the PML sample treated on an "as received" basis was < 1 mg l^{-1} after electrolysis. The fact that the copper, palladium and platinum concentrations in the pH-adjusted PML solutions were not reduced to < 1 mg l^{-1} may be explained in two possible ways:

- Due to the stability of the amminated complexes the potential applied to the working electrode (-1.0 V) and/or the reaction time (17 hours) were not sufficient to allow removal of the metals to concentrations of < 1 mg l^{-1}.
- It may be possible that metal-ligand complexes other than those identified via Peaks C1 and C3 in Figure 4.24 were present, and that the onset of the hydrogen evolution current at potentials more negative than -1.0 V masked the presence of additional reduction peaks. Since a potential of -1.0 V was applied to the graphite working electrode

during the exhaustive electrolysis experiment, species that would be reduced at more negative potentials were not removed.

From the discussions related to Table 4.2 it was shown that the quantitative removal of PGMs from PML solutions where ammine complex formation is favoured may not be possible under experimental conditions employed in this work. Further research related to the speciation of the PGMs under different experimental conditions is required to quantify the effect of stable amminated PGM complexes.

4.6 CONCLUSIONS

A summary of the objectives of the research associated with this chapter, and the experiments conducted to achieve these objectives are provided. This is followed by a discussion of the main conclusions, and proposed future research activities.

4.6.1 Summary of Research Activities

In this chapter the evaluation of isostatically pressed graphite particles (identified via the engineering project) as a possible cathode material for the proposed electrochemical reactor was described.

The main focus of the research was to use the methodologies discussed in Chapter 3 to evaluate the viability of using the graphite particles. If these qualitative investigations indicated that the use of graphite particles as a cathode was feasible, a quantitative evaluation of the level of PGM reduction in the PML solution followed. This was necessary to confirm if the use of the proposed cathode material would result in the removal of total PGMs present in the PML solution to concentrations < 10 mg l^{-1} with no single PGM present at concentrations of > 2 mg l^{-1}, as defined in the overall project objectives (refer to Chapter 1). In addition, the effect of NH_3 ligands on the overall recovery of PGMs from PML solutions was investigated.

To meet these research requirements, four different types of experiments were conducted. A three-electrode electrochemical cell with potentiostatic control, identical to the experimental set-up used in Chapter 2 was used to conduct the different experiments. For these experiments, a working electrode constructed from isostatically pressed graphite particles was used.

The first set of experiments involved investigations related to the feasibility of reducing palladium and platinum ions to their respective metallic states on a graphite working electrode, employing cyclic voltammetric methodologies. Detailed information was provided under the sub-heading "Feasibility studies" of Section 4.2.2.

For the second set of experiments the interpretation of particular voltammograms was validated by holding the graphite working electrode at potentials where a particular metal ion was predicted to be reduced to its metallic form. Optical microscopy was utilised to confirm the presence of the particular metal on the electrode surface. Detailed information was provided under the sub-heading "Validation" of Section 4.2.2.

When the deposition of PGMs was confirmed, the degree of metal ion removal was quantified via a third set of experiments involving exhaustive electrolysis. Detailed information was provided under the sub-heading "Exhaustive electrolysis" of Section 4.2.2.

The fourth set of experiments focussed on the effect of NH_3 ligands on the recovery of PGMs from PML solutions. Recoveries from a normal PML solution was compared to recoveries obtained when OH^- was added to the PML. The rationale behind the addition of sodium hydroxide was that the NH_4^+ ions present in the PML solution (refer to Table 1.1) would be deprotonated to produce NH_3 ligands, which in turn may form amminated PGM complexes. Detailed information was provided under the sub-

heading “Amminated complexes” of Section 4.2.2.

4.6.2 Feasibility and Validation

Studies involving CV predicted the deposition of copper, palladium and platinum on a graphite working electrode when the metal ions were present in single component solutions with a 0.1 M HCl background electrolyte. The anodic dissolution of these single metal deposits into a 0.1 M HCl background electrolyte was also predicted in the case of copper and palladium.

Confirmation of the deposition of copper, palladium and platinum from the single component solutions, as well as the anodic dissolution of copper and palladium was provided by holding the working electrode at favourable overpotentials predicted via the CV experiments, and studying the resulting electrode surface by optical microscopy.

In the case of synthetic solutions containing a combination of copper, palladium and platinum in a 0.1 M HCl background electrolyte, it was concluded that each of these metal ions deposited. The anodic dissolution of copper and palladium from a graphite working electrode surface containing a combination of copper, palladium and platinum metal centres in a 0.1 M HCl background electrolyte was also indicated.

The voltammograms recorded for actual PML solutions closely correlated with those observed for synthetic solutions containing a combination of copper, palladium and platinum in a 0.1 M HCl background electrolyte. It was therefore concluded that copper, palladium and platinum would be deposited from PML solutions when a cathode consisting of isostatically pressed graphite particles is used.

Detailed discussions related to these conclusions were presented in Section 4.5.1.

4.6.3 Exhaustive Electrolysis

Following confirmation that palladium and platinum contained in PML solutions could be reduced to their metallic forms on a cathode material consisting of isostatically pressed graphite particles, the degree of metal removal was quantified via exhaustive electrolysis experiments. The reduction potential applied to the graphite working electrode in contact with the PML solution was based on information obtained from relevant voltammograms.

The exhaustive electrolysis experiment associated with Table 4.1 indicated the quantitative removal of palladium and platinum from a PML solution. Due to the relative reduction potentials associated with the deposition of palladium, platinum and copper, the latter was co-deposited with the PGMs.

It should be noted that the characteristics of the PML solution used for the exhaustive electrolysis experiment described in this chapter was assumed to be similar to that of typical solutions found at the refinery. Based on the metal content of the sample this appears to be true. It would however be wise to evaluate the effectiveness of the graphite particles using a large number of PML samples which reflect process variabilities found within the PMR. These tests may involve the evaluation of metal recoveries for each of the PML solutions via the proposed electrochemical reactor. Where quantitative recoveries of PGMs cannot be achieved, further fundamental investigations may be conducted to identify the causes of incomplete recovery.

Detailed discussions related to these conclusions were presented in Section 4.5.2.

4.6.4 Amminated Complexes

Sodium hydroxide was added to the PML solution used for the experiment

associated with Table 4.1 to adjust the pH of the original solution from 4.3 to 9.1.

When the results obtained for the exhaustive electrolysis experiment conducted on a PML solution as received from the refinery (Table 4.1) were compared to the experiment involving a pH-adjusted PML solution (Table 4.2), it was noted that the concentrations of copper, palladium and platinum remaining after electrolysis were higher for the latter experiment.

The total PGM (palladium and platinum) concentration in the pH-adjusted PML solution after electrolysis was 10.5 mg l^{-1} whilst the total PGM concentration for the PML solution treated on an "as received" basis was < 1 mg l^{-1} after electrolysis.

The fact that the palladium and platinum concentrations in the pH-adjusted PML solutions were not reduced to < 1 mg l^{-1} may be explained in two possible ways:

- Due to the stability of the amminated complexes the potential applied to the working electrode (-1.0 V) and/or the reaction time (17 hours) were not sufficient to allow removal of the metals to concentrations of < 1 mg l^{-1}.
- It may be possible that metal-ligand complexes with thermodynamic reduction potentials more negative than -1.0 V were present. Since a reduction potential of -1.0 V was applied to the graphite working electrode, these complexes would not be reduced.

4.6.5 Future Research

In Chapter 3 the interaction of copper, palladium and platinum with a glassy carbon electrode surface was investigated. In Section 3.6.5 additional areas of research that would add to the fundamental understanding of processes occurring at the interface between a particular

cathode material and a typical refinery effluent were identified. It was noted that it may be more sensible to carry out the proposed research with the cathode material finally selected for the electrochemical reactor instead of a glassy carbon working electrode.

Since the feasibility of using isostatically pressed graphite particles in the proposed electrochemical reactor was demonstrated in this chapter, the areas of research identified in Section 3.6.5 also applies. These proposed areas of research will not be reproduced in this section. Additional areas of research not covered in Section 3.6.5 are listed below:

- It was noted that the metal deposits contained on the graphite working electrode surface after exhaustive electrolysis mainly consisted of a fine powder. This indicated that it may be possible to recover metals from the cathode by mechanical means. If the mechanical recovery of PGMs from the cathode is considered to be a viable option, additional research related to the factors influencing the morphology of deposits will be required.

- It will be useful to determine the possible degree of metal separation from a PML solution via the application of different reduction potentials. Knowledge of the composition of the resultant deposits will provide information related to the necessity of developing additional techniques to separate Base Metals from PGMs.

- In order to increase the fundamental understanding of processes occurring at the graphite working electrode surface, it will be necessary to investigate the factors influencing the formation of metal oxides on the electrode surface. The presence of metal oxides as opposed to metals may have an effect on the electrocatalytic properties of the electrode, and the possible anodic dissolution of the metal deposit.

- Investigations related to the possible influence of amminated PGM complexes on the recovery of PGMs from PML solutions highlighted the fact that knowledge of the speciation of the different metal-ligand

complexes is critical. Additional research regarding the speciation of copper, palladium and platinum will provide valuable fundamental information that could be used to design processes where metal separation or quantitative removal is important.

4.6.6 Final Comments

The feasibility of using isostatically pressed graphite particles as a cathode material for the quantitative removal of PGMs from a PML solution was demonstrated. As a result of the fundamental test work, the graphite particles were incorporated into the bench scale electrochemical reactor developed as part of the engineering research project. The quantitative removal of PGMs from a PML solution via this reactor was also demonstrated[39].

The project now reached a stage where it was necessary to focus research activities on the establishment of kinetic parameters. This would improve the fundamental understanding of the various redox reactions taking place at the electrode-solution interface by quantifying the rate at which these reactions are taking place. In addition, the experimental parameters may be incorporated into detailed engineering models that could be used to predict the performance of the proposed electrochemical reactor under different operating conditions.

5 KINETIC PARAMETERS

5.1 INTRODUCTION

The third phase of the fundamental research project involved the quantitative determination of kinetic parameters, and is described in this chapter.

To facilitate further discussions related to the determination and use of kinetic parameters, a short description of the relevant parameters that will be referred to in this chapter is provided.

5.1.1 Background

Symbols used in this chapter correspond to the description provided in the *List of Symbols*. In cases where the units of expression are different to those stated in the *List of Symbols*, the relevant units will be provided with the associated text.

The following parameters will be discussed:

- Rate constants for cathodic ($\vec{k}$) and anodic ($\overleftarrow{k}$) reactions.
- Standard rate constants (k_s).
- Partial cathodic ($\vec{j}$) and anodic ($\overleftarrow{j}$) current densities.
- Exchange current densities (j_o).
- Electron transfer coefficients for cathodic (α_C) and anodic reactions (α_A).
- Diffusion coefficients (D).
- Mass transfer coefficients (k_m).

Rate constants

The rate at which a chemical reaction occurs at an electrode surface is determined by the product of a rate constant and the concentration of the reactant at the electrode surface. The rate of reduction and oxidation is therefore expressed as follows:

$$Rate\ of\ reduction = \vec{k}\left(c_O\right)_{x=0} \tag{5.1}$$

$$Rate\ of\ oxidation = \overleftarrow{k}\left(c_R\right)_{x=0} \tag{5.2}$$

The rate of heterogeneous electron transfer will depend on the potential gradient existing at the electrode surface. This gradient, in turn, is dependent on the potential of the electrode. It is difficult to predict the variation of rate constants with potential from theory. An empirical relationship between rate constants and potential was however established, and can be expressed as follows[37e]:

$$\vec{k} = \vec{k}_o\, exp\frac{\left(-\alpha_C nFE\right)}{RT} \tag{5.3}$$

$$\overleftarrow{k} = \overleftarrow{k}_o\, exp\frac{\left(\alpha_A nFE\right)}{RT} \tag{5.4}$$

The constants $\vec{k}_o$ and $\overleftarrow{k}_o$ are defined as the rate constants for electron transfer when the potential is zero versus a defined reference, and has no fundamental significance due to their arbitrary nature.

Discussions related to the electron transfer coefficients (α), appearing in Equations 5.3 and 5.4 will be provided under the relevant sub-heading of this section.

The standard rate constant, k_s, is defined as the rate constant for both reduction and oxidation at the standard (E°) or formal ($E^{\circ'}$) potentials.

Exchange current densities

The observed current density (j) is the sum of the partial cathodic and anodic current densities:

$$j = \vec{j} + \overleftarrow{j} \tag{5.5}$$

At the equilibrium potential (E_e), the values for $\vec{j}$ and $\overleftarrow{j}$ are equal in magnitude but opposite in sign. The observed current density would therefore be zero. The magnitude of the partial current densities at equilibrium is known as the exchange current density:

$$j_o = -\vec{j} = \overleftarrow{j} \tag{5.6}$$

Exchange current density values provide a measure of electron transfer activity at the equilibrium potential. A high j_o value would result in the observation of current at low overpotentials, and is therefore an important indicator of the rate of reactions taking place at the surface of a particular electrode.

The exchange current density for a particular reduction-oxidation (redox) couple is related to the standard rate constant, k_s, and the bulk concentrations of the reactants:

$$j_o = nFk_s(c_O)^{\alpha_A}(c_R)^{\alpha_C} \tag{5.7}$$

Electron transfer coefficients

Electron transfer coefficients are related to the fraction of change in overpotential which leads to a change in the rate constant for electron transfer[37f]. This description becomes clear when Equations 5.3, 5.4 and 5.7 are studied. The sum of α_C and α_A is 1, and in many cases both of the coefficients have a value close to 0.5.

Diffusion coefficients

The supply of reactants and the removal of products from the electrode surface (mass transport) are necessary to ensure the continuation of electrochemical reactions. Diffusion is one mode of mass transport.

Diffusion is a physical process which involves the transport of species from more concentrated to less concentrated regions, until the concentration is equal in all regions. The rate of diffusion (flux) is described by Fick's first law:

$$Flux = -D\frac{dc(x)}{dx} \tag{5.8}$$

where $dc(x)/dx$ is the concentration gradient and D is the diffusion coefficient.

This expression is valid for linear diffusion to a planar electrode, i.e. the assumption is made that the electrode is flat and that the concentration varies in a perpendicular direction to the electrode surface.

Mass transfer coefficients

The mass transfer coefficient, k_m, may be considered as a rate constant for mass transport[37g]. This provides a basis for comparing the rates of electron transfer ($k_s c_R$ or $k_s c_O$) and mass transport ($k_m c_R$ or $k_m c_O$). Values for the mass transfer coefficient are related to the diffusion coefficient and the thickness of the diffusion layer (δ):

$$k_m = \frac{D}{\delta} \tag{5.9}$$

In Chapter 2 (Section 2.2.5, Equation 2.10) it was shown that δ could be determined via Rotating Disc Electrode (RDE) experiments. This equation

is shown again for ease of reference:

$$\delta = \frac{1.61\ \nu^{0.166} D^{0.33}}{\omega^{0.5}} \qquad (5.10)$$

where ν = kinematic viscosity ($m^2\ s^{-1}$).

5.1.2 Objectives

In the context of this chapter, the determination of kinetic parameters refers to experimental values obtained for j_o, α, k_s and k_m. These parameters would assist in the fundamental understanding of interactions between metal ions found in the Palladium Mother Liquor (PML) and the graphite cathode evaluated in Chapter 4 (refer to Section 4.3.1 for description) by quantifying the rate at which the interactions at the electrode surface occur. The parameters can also be used for engineering modelling purposes, where it is attempted to predict the performance of an electrochemical reactor (e.g. recovery) under specific operating conditions (e.g. applied current).

Ideally kinetic parameters for the interaction of the three major metal ions found in the Palladium Mother Liquor (PML) namely copper, palladium and platinum with the graphite particle cathode would be required. Kinetic parameters are however obtained for a particular redox couple. It is therefore important that (*i)* the different redox couples present in the system under investigation are known, and (*ii*) that no competing or side reactions occur with an associated redox couple during the experimental determination of the kinetic parameters.

The complexity of the interactions of a combination of copper, palladium and platinum with a graphite cathode (refer to Chapter 4) would make the accurate determination of the required parameters impossible. In addition, experimental procedures for the determination of kinetic parameters,

especially in cases where metal deposition occurred, still had to be established.

It was therefore decided to focus research activities on the determination of kinetic parameters for a single component synthetic solution containing one of the major metal ions found in the PML. The background matrix of this synthetic solution was prepared to approximate the matrix of an actual PML effluent.

This approach would allow the accurate determination of kinetic parameters for the redox couples associated with a particular metal ion. At the same time the applicability of different experimental procedures could be evaluated. Since the evaluation of experimental procedures was one of the research objectives, it was important to select a system that would not pose unnecessary complications when experiments are conducted. It was therefore decided to use copper instead of palladium or platinum, where the catalytic evolution of hydrogen on deposited metal centres would not play a significant role (refer to Chapters 3 and 4).

The objectives of the research activities associated with this chapter can be summarised as follows:

- Evaluate suitable experimental procedures for the determination of j_o, α, k_s and k_m.
- Use these procedures to report j_o, α, k_s and k_m values for redox couples associated with a synthetic solution containing copper ions in a background matrix approximating that of a PML solution. The electrode material will consist of the graphite particles employed in Chapter 4 (grade ET-10, particle size range between 500 μm and 600 μm, Electrographite Carbon Co.).
- Use the reported kinetic parameters to improve the fundamental understanding of processes occurring at the electrode-solution

interface. This data may also be used for engineering modelling purposes (refer to Section 5.1.2).

- Propose procedures that may be used to determine kinetic parameters for more complicated systems, e.g. palladium or platinum where hydrogen evolution occurs.

5.2 EXPERIMENTAL PROCEDURES

A short discussion of the experimental procedures used to determine the required kinetic parameters is provided in this section.

To determine kinetic parameters, plots of the current density (j) versus potential (E) of the particular redox couple under investigation are required. These $j-E$ plots may be recorded by means of potential step or slow potential sweep experiments under potentiostatic conditions, i.e. employing a three-electrode set-up.

In the case of potential step experiments the potential of the working electrode is changed rapidly (effectively instantaneously) from a value where no current passes (no chemical change occurs at the surface) to potential values where the electrode reaction of interest takes place. The current is recorded once steady state (stable current) is achieved. Current values are recorded at various potentials to construct a $j-E$ plot.

Slow potential sweep experiments are carried out at sweep rates typically between 1 and 10 mV s^{-1}. Instead of stepping the potential, a slow potential sweep is imposed on the working electrode, covering a predefined range. The current is recorded after each potential step to produce a $j-E$ plot.

From tests carried out in the course of this project, it was found that slow potential sweep experiments are preferable in cases where metal deposition reactions are studied. The reason is that more metal is

deposited on the electrode under study in the case of potential step experiments. This changes the characteristics of the electrode, which in turn makes it difficult to interpret or reproduce results. Slow potential sweep experiments were therefore employed when kinetic parameters were determined.

5.2.1 Reversible and Irreversible Electrode Reactions

Reversible and irreversible systems were discussed in Chapter 2 (Section 2.2.2). It was noted that reversible systems referred to electron transfer reactions that are fast enough to maintain the concentrations of oxidised and reduced forms in equilibrium with each other at the electrode surface when a given potential is applied. The proper equilibrium ratio for the oxidised and reduced forms is expressed by the Nernst equation, as shown in Equation 2.3.

Electrochemical irreversibility in turn, is caused by slow electron exchange of the redox species with the working electrode. In the case of irreversible systems, the Nernst equation is not obeyed.

A particular $j-E$ plot for a reaction may appear reversible or irreversible depending on the mass transport regime employed. If the rate of mass transport is substantially increased, a given surface reaction may be forced out of equilibrium.

Kinetic parameters cannot be obtained from a curve representing a reversible electrochemical process. Quantitative rate parameters can only be established under conditions where either electron transfer or mass transport is the sole rate determining step over a particular portion of a $j-E$ plot.

This implies that the k_m values for the particular reaction should be larger than the k_s values. In terms of k_m and k_s, larger values are defined as a

difference of at least one order of magnitude.

From an experimental point of view, increased mass transport conditions should be controlled and variable. In addition, the experimental conditions must be described by theoretical equations.

5.2.2 Active Surface Area of Working Electrode

The active surface area of the working electrode, i.e. the sites where electron transfer is taking place, should be used to calculate the current density values employed for $j-E$ plots. Due to the nature of the working electrode used for experiments described in this chapter (refer to Section 5.4.1), the active and geometric surface areas were different. This necessitated the experimental determination of the active surface area of the working electrode prior to recording $j-E$ plots.

Three different types of experiments may be used to determine the active surface area of a working electrode. These experiments involve the application of Cyclic Voltammetry (CV), Chronoamperometry, or the use of a RDE. A detailed discussion of these electroanalytical techniques was provided in Chapter 2 (Section 2.2). To calculate active surface areas via these experiments a redox couple with a known diffusion coefficient value, D, must be used.

Cyclic Voltammetry

The Randles – Sevčik equation may be used to determine the active surface area of a working electrode, if it is solved for the forward sweep of the first cycle of a reversible CV experiment conducted at 298 K. This equation was originally described in Chapter 2 (Section 2.2.2, Equation 2.4), and is shown again for ease of reference:

$$i_p = \left(2.69\times10^5\right) n^{3/2} A D^{1/2} \nu^{1/2} c \qquad (5.11)$$

where A = active surface area (cm^2); D = diffusion coefficient ($cm^2\ s^{-1}$); ν = potential scan rate ($V\ s^{-1}$); c = concentration of the reactive species in bulk solution ($mol\ cm^{-3}$).

Chronoamperometry

The active surface area of a working electrode may be determined by stepping the potential of the electrode to a value where the reduction or oxidation of the particular electroactive species used for the experiment is diffusion controlled. The Cottrell equation may then be used to calculate the active surface area.

This equation was originally described in Chapter 2 (Section 2.2.4, Equation 2.9), and is shown again for ease of reference:

$$i = \frac{nFD^{½}cA}{\pi^{½}t^{½}} \qquad (5.12)$$

where A = active electrode surface (cm^2); D = diffusion coefficient ($cm^2\ s^{-1}$); c = concentration of the reactive species in bulk solution ($mol\ cm^{-3}$).

If the recorded current (i) is plotted against the inverse of the square root of the recorded time ($1/\sqrt{t}$), the slope of the linear plot can be solved for A.

Rotating Disc Electrode experiments

Experiments involving a RDE may also be used to calculate the active surface area of an electrode. The fact that RDE experiments are used implies that the working electrode tip must be rotated during the experiment. Limiting current values (i_L) for the reduction or oxidation of the electroactive species used in the experiment is recorded at various rotation rates.

The Levich equation may then be used to calculate the active electrode surface area. This equation was originally described in Chapter 2 (Section 2.2.5, Equation 2.11), and is shown again for ease of reference:

$$i_L = 0.62\ nFD^{0.67} A \nu^{-0.166} c\omega^{0.5} \tag{5.13}$$

where c = concentration of species in bulk solution (mol m^{-3}); ν = kinematic viscosity (m^2 s^{-1}).

If values for i_L are plotted against the square root of the rate of rotation ($\sqrt{\omega}$) the slope of the linear plot can be used to determine the active surface area (A). When the Levich equation is used to determine the active surface area of a working electrode, the kinematic viscosity of the solution (ν) must be known in addition to the D value of the redox couple employed for the experiment.

5.2.3 Exchange Current Densities and Transfer Coefficients

In electron transfer controlled potential regions, the relationship between j and E is provided by the Butler Volmer equation:

$$j = j_o \left[exp \frac{(\alpha_A nF)}{RT} \eta - exp \frac{(-\alpha_C nF)}{RT} \eta \right] \tag{5.14}$$

A limiting form of the Butler Volmer equation may be used in cases where the overpotential (η) for a reduction or oxidation reaction is $>$ 52 mV. This is referred to as the Tafel approximation.

Tafel equations for the anodic and cathodic processes associated with a redox couple are shown in Equations 5.15 and 5.16 respectively:

$$log\ j = log\ j_o + \frac{(\alpha_A nF)}{2.3\ RT} \eta \tag{5.15}$$

$$log\ -j = log\ j_o - \frac{(\alpha_c nF)}{2.3\ RT} \eta \tag{5.16}$$

A Tafel plot for a particular redox couple may be obtained by recording $j-E$ values in the electron transfer controlled potential region, and plotting the resulting *log j* values as a function of η. It is important to note that absolute values of j should be used for the Tafel plot. A typical Tafel plot is illustrated in Figure 5.1.

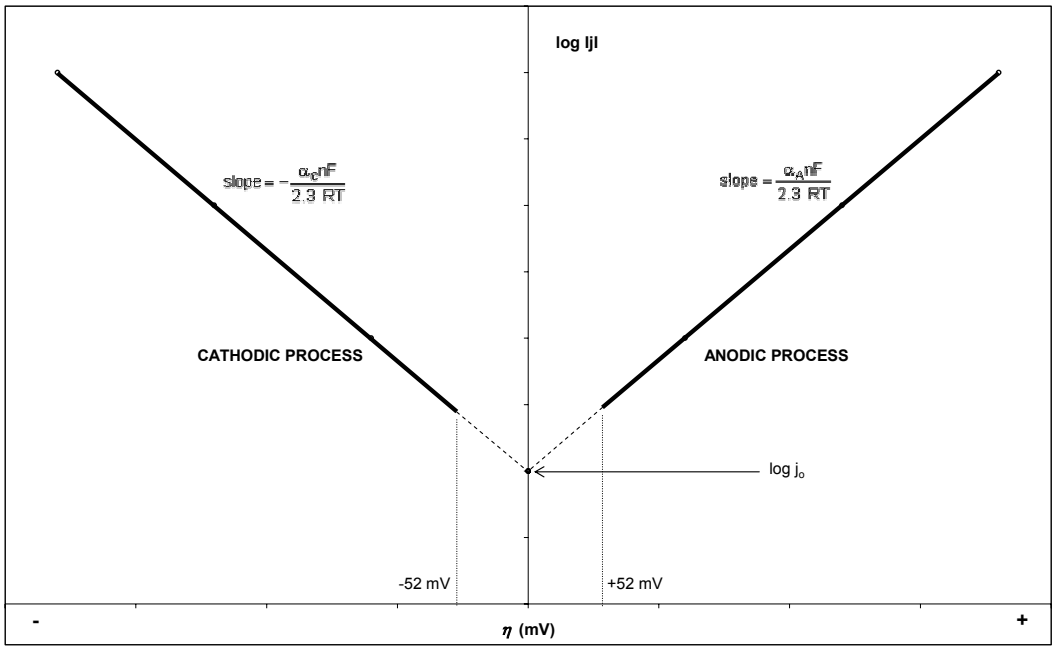

Figure 5.1 Example of a typical Tafel plot.

If the resultant linear plots for the anodic and cathodic processes are extrapolated to $\eta = 0$, a value for j_o can be calculated. The α values for the anodic and cathodic processes may be obtained from the slope of the linear plots if the number of electrons associated with the particular anodic or cathodic process is known.

Current densities at infinite rotation rates

In Section 5.2.1 it was mentioned that kinetic parameters cannot be obtained from a reversible curve, and that quantitative parameters can only be established under conditions where electron transfer is the sole rate determining step over a particular portion of a $j-E$ plot. It was also noted that the rate of mass transport can be increased to achieve these

conditions.

Mass transport conditions may be increased in a controlled fashion by means of RDE experiments (refer to Chapter 2, Section 2.2). The equipment used to conduct the experiments described in this chapter (see Chapter 2, Section 2.4.1) was capable of producing accurate rates of 1500, 2000, 2500 and 3000 rotations per minute (rpm). If a particular redox couple has a high k_s value, electron transfer may remain reversible even under conditions where a rate of 3000 rpm is employed. This implies that rate parameters cannot be determined unless a RDE system capable of substantially higher rotation rates is used.

Alternatively, procedures exist where data obtained at lower rotation rates (1500 to 3000 rpm for experiments described in this chapter) can be extrapolated to calculate the current density where the rate of rotation approximates infinity. Hence, mass transport limitations are removed, resulting in electron transfer controlled conditions.

The expression used to calculate current densities at infinite rotation rates via RDE experiments can be deduced from the Nernst diffusion layer model, and was explained by Pletcher[37h] as follows:

Step 1. The fluxes of oxidised and reduced species at the electrode surface must be equal.

$$k_m\left[c_O - (c_O)_{x=0}\right] = -k_m\left[c_R - (c_R)_{x=0}\right] \qquad (5.17)$$

where $k_m = \dfrac{D}{\delta}$

Step 2. The current density may be written in terms of the mass transport flux and the kinetics of electron transfer at the electrode surface.

$$j = -nFk_m\left[c_O - (c_O)_{x=0}\right] \qquad (5.18)$$

$$j = nF\left[\vec{k}(c_O)_{x=0} - \overleftarrow{k}(c_R)_{x=0}\right] \tag{5.19}$$

Step 3. Surface concentrations are eliminated by combining Equations 5.17 to 5.19.

$$\frac{1}{j} = \frac{1}{nF\,(\overleftarrow{k}c_R - \vec{k}c_O)} + \frac{\vec{k} + \overleftarrow{k}}{nFk_m(\overleftarrow{k}c_R - \vec{k}c_O)} \tag{5.20}$$

Step 4. Substitute k_m with D/δ, and δ with $-1.61\nu^{0.166}D^{0.33}/\omega^{0.5}$.

$$\frac{1}{j} = \frac{1}{nF\,(\overleftarrow{k}c_R - \vec{k}c_O)} + \frac{1.61\left(\vec{k} + \overleftarrow{k}\right)\nu^{0.166}}{nF\,(\overleftarrow{k}c_R - \vec{k}c_O)\,D^{0.67}}\frac{1}{\omega^{0.5}} \tag{5.21}$$

The forward and reverse electron transfer reactions only need to be considered if the potentials are within 60 mV of the equilibrium potential. Outside this range, the partial cathodic or anodic current potentials will dominate. If potentials $>$ 60 mV from the equilibrium are considered for an anodic reaction, Equation 5.21 can be simplified to the following expression:

$$\frac{1}{j} = \frac{1}{nF\overleftarrow{k}c_R} + \frac{1.61\nu^{0.166}}{nFc_RD^{0.67}}\frac{1}{\omega^{0.5}} \tag{5.22}$$

To determine current densities at infinite rotation rates via Equation 5.22, plots of $j-E$ relationships for a particular redox couple should be recorded at different experimental rotation rates via RDE experiments. At selected potentials of these $j-E$ plots, the inverse of the experimental current densities ($1/j$) are plotted against the inverse of the square root of the rotation rate ($1/\sqrt{\omega}$). According to Equation 5.22, a linear expression can be fitted to these points. The current density at an infinite rate of rotation for a given potential can then be calculated from the intercept of the linear plot.

The calculated current densities at infinite rotation rates may then be used to construct a Tafel plot as illustrated earlier in Figure 5.1. This will ensure that the j_o and α values obtained from the Tafel plot is calculated from data obtained under electron transfer controlled conditions.

Estimation of equilibrium potentials

Where current densities at infinite rotation rates are determined only for an anodic or cathodic process, values for j_o cannot be established via extrapolation of data points in a Tafel plot. In these cases a value for E_e is required. The E_e values reported in this chapter was estimated by using experimental data from slow potential sweep experiments recorded at an electrode rotation rate of 1500 rpm. A straight line (linear least squares) was fitted to experimental $log\ j$ data points recorded for anodic and cathodic currents, and the equilibrium potential was taken at the point where the two lines intersected.

5.2.4 Rate Constants

Rate constants may be calculated by solving Equation 5.22 for $\overleftarrow{k}$ where $1/\sqrt{\omega}$ is zero. Values for $\vec{k}$ may also be calculated via Equation 5.22 if the term c_R is replaced by c_O. The standard rate constant, k_s, is determined by plotting $log\,\overleftarrow{k}$ or $log\,\vec{k}$ as a function of potential. A value for k_s is obtained where the formal potential value (x-axis) intersects the $log\,\overleftarrow{k}$ or $log\,\vec{k}$ plot (y-axis).

Estimation of formal potentials

Formal potentials were estimated from voltammograms obtained via CV experiments, assuming that the redox couple under consideration was reversible. The relevant equation was originally described in Chapter 2 (Section 2.2.2, Equation 2.5) and is presented again for ease of reference:

$$E^{\circ'} = \frac{E_{pa} + E_{pc}}{2} \tag{5.23}$$

If reactions involve metal deposition, CV data cannot be used. In cases where the metal deposition reaction is reversible (high standard rate constant value), an expression for the determination of the formal potential may be established as follows:

Step 1. If the standard rate constant value is high, the electron transfer process at the surface will remain at equilibrium at all potentials and rotation rates, and the $j - E$ values can be derived from the Nernst equation.

$$E = E^{\circ'} + \frac{2.3\,RT}{nF} log\left[\frac{(c_O)_{x=0}}{(c_R)_{x=0}}\right] \tag{5.24}$$

Step 2. At any potential on the $j - E$ curve the current density for a cathodic reaction may be expressed as follows:

$$j = -nFk_m\left[c_O - (c_O)_{x=0}\right] \tag{5.25}$$

Step 3. Equation 5.25 may be re-arranged:

$$(c_O)_{x=0} = c_O + \frac{j}{nFk_m} \tag{5.26}$$

Step 4. The cathodic limiting current density (j_{LC}), is expressed by the following equation:

$$j_{LC} = -nFk_m c_O \tag{5.27}$$

Step 5. Equation 5.27 may be re-arranged:

$$c_O = -\frac{j_{LC}}{nFk_m} \tag{5.28}$$

Step 6. Substitute Equation 5.28 into Equation 5.25:

$$(c_O)_{x=0} = -\frac{j_{LC}}{nFk_m} + \frac{j}{nFk_m} \tag{5.29}$$

Step 7. Steps 2 to 6 are repeated for the anodic reaction to produce the following expression:

$$(c_R)_{x=0} = \frac{j_{LA}}{nFk_m} - \frac{j}{nFk_m} \tag{5.30}$$

Step 8. By substituting Equations 5.29 and 5.30 into Equation 5.24, and re-arranging the resultant expression the following relationship is obtained:

$$E = E^{\circ'} + \frac{2.3\,RT}{nF} log\left[\frac{j - j_{LC}}{j_{LA} - j}\right] \tag{5.31}$$

Step 9. In cases where metal ions are reduced to their metallic form, Equation 5.31 may be simplified to produce the following expression:

$$E_e = E^{\circ'} + \frac{2.3\,RT}{nF} log\frac{(j_L - j)}{j} \tag{5.32}$$

From Equation 5.32 it is evident that the formal potential is obtained where the magnitude of the current density is exactly half the limiting current density value. The amount of electrons involved in the reduction reaction may also be determined from the slope of the linear plot obtained from Equation 5.32.

5.2.5 Mass transfer coefficients

The mass transfer coefficient, k_m, can be estimated from RDE theory for different rates of rotation if values for the diffusion coefficient for the particular reaction and the kinematic viscosity (ν) of the solution is known:

$$k_m = \frac{D^{0.67}\omega^{0.5}}{1.61\nu^{0.166}} \tag{5.33}$$

The diffusion coefficients can be determined experimentally via the Levich equation (refer to Equation 5.13). Kinematic viscosities may be obtained experimentally or estimated from literature. In the case of solutions containing a mixture of components, a molar weighted average value can be used, based on the literature values of the individual components.

Values for k_m at different rates of rotation can also be determined by application of RDE experimental data:

$$k_m = \frac{i_L}{nFAc} \tag{5.34}$$

where c = concentration of a particular species in bulk solution (mol m^{-3}).

5.3 EXPERIMENTAL DESIGN AND DATA PRESENTATION

In Section 5.1.2 it was noted that experiments involving the determination of j_o, α, k_s and k_m would be conducted on a synthetic solution containing copper ions in a background matrix approximating that of a PML solution. The preparation of this solution, and the concentrations of its constituent ions will be described in Section 5.4.2. A blank solution containing the same background matrix as the copper synthetic solution was used to establish net currents used in the calculation of kinetic parameters. The copper solution will be referred to as the Cu solution for the remainder of the chapter.

To assist in the interpretation of experimental data obtained from the Cu solution, and to confirm the methodology employed to calculate the kinetic parameters, it was decided to subject a reference material to the same experimental and data handling procedures used for the Cu solution. The reduction of $Fe(CN)_6^{3-}$ to $Fe(CN)_6^{4-}$ was employed as the reference. A blank solution containing the same background matrix as the $Fe(CN)_6^{3-}$ synthetic solution was used to establish net currents used in the

calculation of kinetic parameters for the reference. The procedure for the preparation of the reference solution and its associated blank, and the concentrations of ions contained in these solutions will be provided in Section 5.4.2. The reference will be referred to as the $Fe(CN)_6^{3-}$ solution for the remainder of the chapter.

5.3.1 Working Electrode

In Section 5.1.2 it was noted that the graphite particles employed in Chapter 4 would be used as the electrode material. Since RDE experiments were employed, it was necessary to use an electrode tip that could be rotated. A rotating tip containing the graphite particles required for experimental work associated with this chapter was not available commercially and therefore had to be constructed in-house. The construction of the electrode tip is described in Section 5.4.1.

Due to the nature of the electrode construction it was possible that the active surface area of the electrode could change between different sets of experiments. This fact will be clarified further in Section 5.4.1. The active surface area was determined prior to conducting a new set of experiments.

5.3.2 Experimental

Kinetic parameters were determined by employing the following general procedure:

- A qualitative interpretation of the interaction between ions contained in a particular solution and the graphite working electrode was obtained via CV and slow potential sweep experiments. This data was used to identify the relevant redox couples.
- The active surface area of the graphite working electrode was calculated via experiments described in Section 5.2.2.
- Slow potential sweep experiments were conducted to obtain $j-E$ plots for each of the identified redox couples at rotation rates of 1500,

2000, 2500 and 3000 rpm. The relevant potential range was based on observations made during CV experiments.

- The data obtained via the $j-E$ plots was used to calculate current densities and rate constants at infinite rotation rates via Equation 5.22. These calculated current density and rate constant values were used to determine j_o, α and k_s estimates for the identified redox couples as described in Sections 5.2.3 and 5.2.4.
- Experimental data obtained from $j-E$ plots described under the third bullet point of this section (Section 5.3.2) was used to calculate k_m values for the identified redox couples as described in Section 5.2.5.

In all cases the current densities of the appropriate blanks were subtracted from the current densities for the $Fe(CN)_6^{3-}$ and Cu solutions prior to the calculation of kinetic parameters.

5.3.3 Data Presentation

The sign convention and units of expression defined in Chapter 2 (Section 2.1) also applies to the current chapter.

All potential values were measured relative to a silver-silver chloride ($Ag/AgCl$) reference electrode containing a 3 M KCl solution. Experimental data was obtained at a temperature of 25 °C ± 0.1 °C.

The active electrode surface was determined experimentally prior to conducting experiments used to calculate kinetic parameters, and is provided in the text with the relevant data. Data related to the measurement of current was background corrected prior to the calculation of active electrode surface areas or kinetic parameters.

CV or slow potential sweep experiments always proceeded to more negative potentials relative to the starting potential.

Where voltammograms were illustrated, peaks that are labelled with the letter “C” denote cathodic peak potentials (E_{pc}) recorded during a particular experiment, whilst peaks labelled with the letter “A” refer to anodic peak potentials (E_{pa}). Where more than one data set was presented in a particular illustration, differentiation was achieved via line colour and thickness.

If a straight line was fitted to experimental data points the linear least squares method via Microsoft Excel (2002) was used. The linear expressions displayed in the charts carry more significant figures than that specified by the significant figure convention. The additional digits served as guard digits since the values in the linear expression were used in an intermediate calculation step. This approach prevented rounding errors in the final numerical result.

Where reference is made to Cu^{+} or Cu^{2+}, the oxidation state of the copper ions is described, as opposed to a particular copper species present in solution.

It should be noted that the sign convention and data presentation formats described here also applies to the illustrations presented in *Appendix B*.

5.4 ELECTRODES, EQUIPMENT AND REAGENTS

A three-electrode electrochemical cell with potentiostatic control, identical to the experimental set-up described in Chapter 2 was used to conduct the experiments described in this chapter. For these experiments a rotating graphite working electrode was employed, instead of the glassy carbon or platinum disc electrodes listed in Chapter 2.

Information provided in Section 2.4 (equipment, electrodes, reagents) and Section 2.5 (experimental procedure) also applies to experiments described in this chapter. The only difference is that a 3 M KCl solution

was used in the salt bridge instead of 0.1 M HCl.

Additional experimental information that was not provided in Chapter 2, and is relevant to the experimental work associated with the current chapter is provided here.

5.4.1 Electrodes

A rotating working electrode tip with an active surface consisting of isostatically pressed graphite particles was used for all experiments described in this chapter. The in-house construction of the electrode will subsequently be described.

Components

- Isostatically pressed graphite particles (grade ET-10, particle size range between 500 μm and 600 μm, Electrographite Carbon Co.).
- PTFE rod (9 mm diameter).
- Epoxy Resin (Elite Chemical Industries, resin code NPEL 128, hardener code GEN 2000). The preparation of the resin was described in Chapter 4, Section 4.3.1.
- Glassy carbon tip working electrode with disc diameter of 2 mm for 663 VA Stand (Metrohm, order no. 6.1204.110).

Construction

The electrode had to be rotated, which meant that it had to connect to a rotating driving shaft which, in turn, was connected to a potentiostat. It was therefore decided to modify a commercial glassy carbon RDE tip (Metrohm), which already had all the necessary electrical and mechanical components.

A PTFE sleeve (ca. 2 cm long) with one of the ends still closed was manufactured from a rod and fitted over the existing glassy carbon tip

electrode. A hole was drilled in the bottom of the sleeve (adjacent to the glassy carbon disc). The hole was aligned with the glassy carbon disc, and had the same approximate diameter (ca. 2 mm) as the glassy carbon disc. The depth of the hole drilled into the closed end of the sleeve was also in the region of 2 mm. The glassy electrode carbon tip with the fitted PTFE sleeve was turned on a lathe to ensure that assembly was centered when rotated by the driving axle of the experimental assembly.

A mixture of graphite particles and an acid resistant epoxy resin was pressed into the hole of the PTFE sleeve. After curing, the top layer of resin and graphite was sanded off to expose a fresh, flat active surface. The active graphite surface and the adjacent PTFE surface were then polished on a polishing wheel by means of diamond paste to produce a smooth flat surface. The equipment, consumables, and procedure employed to prepare a working electrode surface with diamond paste were originally described in Chapter 2 (Sections 2.4.3 and 2.5.2).

A diagram of the modified glassy carbon electrode is presented in Figure 5.2, whilst an image of the polished active graphite surface of the modified electrode is shown in Figure 5.3.

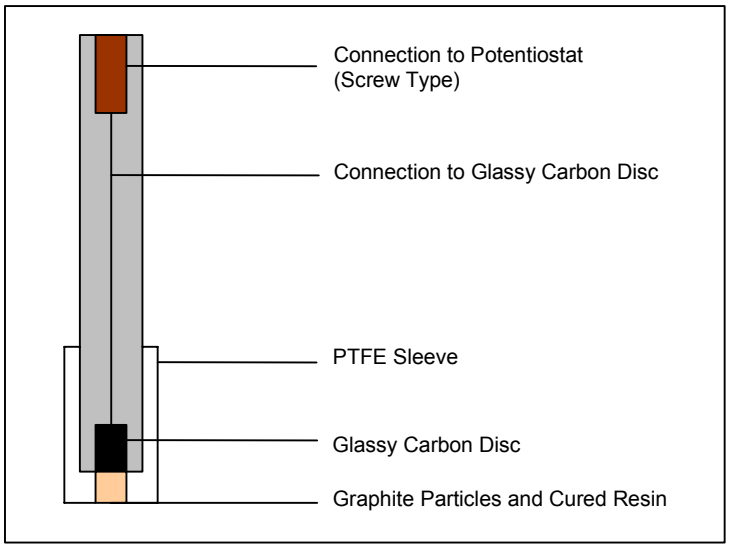

Figure 5.2 Illustration of in-house constructed rotating working electrode with active surface consisting of isostatically pressed graphite particles, grade ET-10, sourced from the Electrographite Carbon Co.
(Note that the illustration was not drawn to scale).

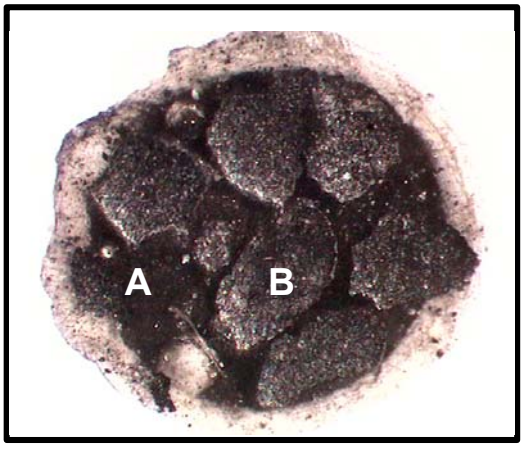

Figure 5.3 Image of freshly prepared active surface of a rotating graphite working electrode prior to conducting experiments. Magnification: 45 X (stereo microscope).

A: Epoxy resin (non-conductive) used to adhere graphite particles to electrode assembly.

B: Graphite particle.

The image in Figure 5.3 illustrates why the active surface area of the electrode should be used instead of the geometric surface area. The

presence of non-conducting epoxy resin on the surface of the electrode is clearly visible and electron transfer will only take place on exposed graphite surfaces. In addition, it was impossible to predict if the exposed graphite surfaces at the electrode-solution interface was in electrical contact with the glassy carbon disc via other graphite particles contained in the PTFE sleeve. The active surface area also had to be established every time the electrode surface was polished, due to the fact that the surface area of the exposed graphite particles could change during the polishing process.

5.4.2 Reagents and Solutions

A description of the reagents and solutions used for experiments discussed in this chapter is provided in this section.

Reagents

- Potassium chloride, KCl, MM $= 74.55\ g\ mol^{-1}$, Analytical Reagent (AR) grade; (Saarchem). This reagent was originally described in Chapter 2, Section 2.4.4 and is presented again for ease of reference.
- Potassium ferricyanide, $K_3[Fe(CN)_6]$, MM $= 329.25\ g\ mol^{-1}$, Guaranteed Reagent (GR) grade; (Merck).
- Copper (II) chloride, $CuCl_2.2H_2O$, MM $= 170.48\ g\ mol^{-1}$, AR grade, (Saarchem).
- Sodium chloride, $NaCl$, MM $= 58.44\ g\ mol^{-1}$, Chemically Pure (CP) grade; (Associated Chemical Enterprises).
- Ammonium acetate, CH_3COONH_4, MM $= 77.09\ g\ mol^{-1}$, AR grade, (Saarchem).
- Glacial acetic acid, CH_3COOH, MM $= 60.05\ g\ mol^{-1}$, CP grade, (Associated Chemical Enterprises).

- Hydrochloric acid, HCl, 32 %, MM = 36.46 g mol^{-1}, AR grade, (NT Laboratory Supplies). This reagent was originally described in Chapter 2, Section 2.4.4 and is presented again for ease of reference.

Solutions

- 0.1 M HCl solution: The solution was prepared by diluting a volume of concentrated AR grade acid by a factor of ten, using ultra pure water. The preparation of this solution was originally described in Chapter 2, Section 2.4.4 and is presented again for ease of reference.

- $Fe(CN)_6^{3-}$ solution: A 0.1 M KCl solution was prepared by dissolving 0.75 g of the salt in 100 ml ultra pure water. The pH of this solution was adjusted to 3 by the drop wise addition of 0.1 M HCl. This 0.1 M KCl solution (pH 3) acted as the background solution. A mass of 6.6 mg $K_3[Fe(CN)_6]$ was added to 20 ml portions of the background solution to produce a 0.001 M $Fe(CN)_6^{3-}$ solution.

- Cu solution: A mass of 5.84 g $NaCl$ and 7.71 g CH_3COONH_4 was weighed out. A volume of ca. 10 ml ultra pure water was added to the mixture of crystals. This was followed by the addition of 5.72 ml CH_3COOH by means of a hand held autopipette. Following the dissolution of the $NaCl$ and CH_3COONH_4 crystals contained in the mixture of water and CH_3COOH, the solution was diluted to a volume of 100 ml with ultra pure water. The resulting mixture contained 1 M $NaCl$, 1 M CH_3COONH_4, 1 M CH_3COOH and was buffered at a pH of 4.3. This solution was used as the background. A mass of 10.2 mg $CuCl_2.2H_2O$ was added to 20 ml portions of the background solution to produce a 0.003 M or 191 mg l^{-1} Cu solution.

5.5 RESULTS AND DISCUSSION

In Section 5.3.2 the general procedure employed for the determination of

kinetic parameters reported in this chapter was described. The first step involved the identification of redox couples associated with the interaction of the test solution with a graphite working electrode (refer to Section 5.4.1 for details regarding construction and electrode characteristics). In Section 5.1.2 the rationale of using copper ions in a background solution approximating that of a typical PML solution was provided. The experiments used for the identification of the relevant redox couples associated with this Cu solution (refer to Section 5.4.2 for description of solution components) will subsequently be described.

5.5.1 Identification of Redox Couples

The interaction of the Cu solution with the graphite working electrode was investigated via conventional CV experiments, as illustrated in Figure 5.4. In addition, slow potential sweep experiments were employed to record $j-E$ plots for the forward and reverse scans. The graphite working electrode tip used for these experiments was rotated at different rates, as shown in Figure 5.5.

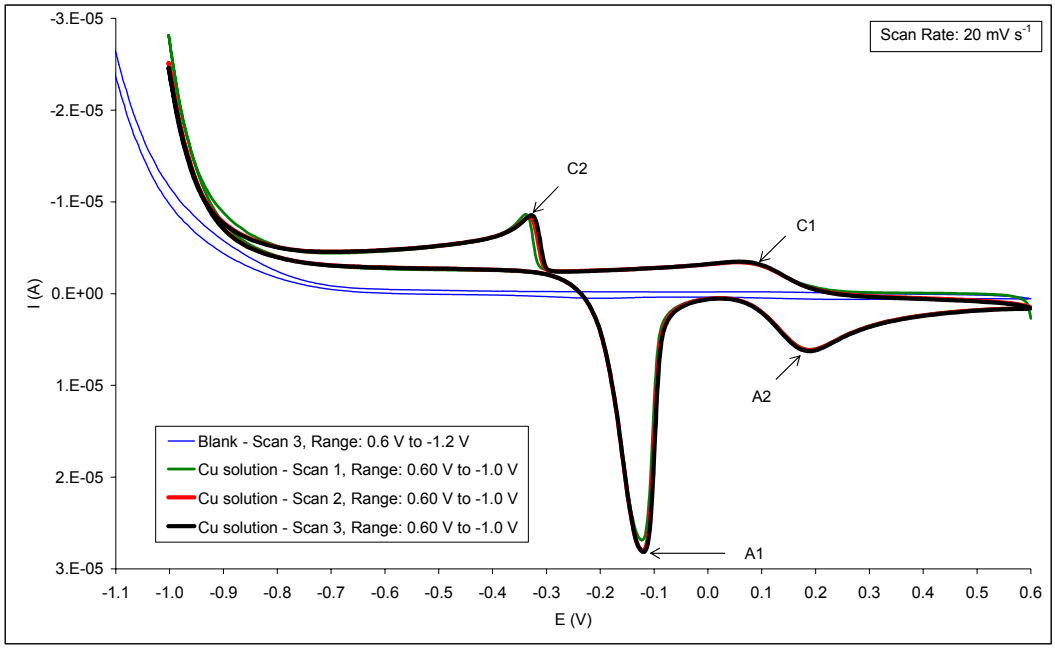

Figure 5.4 Cyclic voltammograms of a Cu solution and its associated background solution, using a graphite working electrode.

The characteristics of the voltammogram in Figure 5.4 is similar to voltammograms obtained for synthetic solutions containing copper ions in a 0.1 M HCl matrix (refer to Chapter 4, Figures 4.10 and 4.11). The peaks in Figure 5.4 were identified by comparison to the voltammogram illustrated in Figure 4.11. Peak C1 in Figure 5.4 was ascribed to the reduction of Cu^{2+} to Cu^{+}, whilst Peak C2 was associated with the reduction of Cu^{+} to Cu^{0}. In the case of the anodic peaks, A1 was identified as the stripping peak involving the oxidation of copper metal to Cu^{+}, whilst A2 was ascribed to the oxidation of Cu^{+} to Cu^{2+}.

When the magnitudes of Peaks C1 and C2 were compared, it was noted that the current at C2 was almost 2.5 times larger than the current recorded at C1. This contradicts the earlier interpretation of the voltammogram where it was concluded that Cu^{2+} was reduced to metal via two distinct one-electron reduction steps occurring at Peaks C1 and C2. If this was true, the magnitude of the reduction current at C2 should have been double that of C1, implying an equal current contribution to each of the processes indicated by Peaks C1 and C2.

In Figure 5.4, the current observed after the formation of Peak C1 (forward scan, ca. 0.08 V to -0.30 V) did not decay as expected during a normal CV scan. When the same potential range was analysed in Figure 5.5, a slow increase in the reduction current was noted. This indicated that a slow reduction process occurred subsequent to the reduction of Cu^{2+} to Cu^{+}. Initially it was concluded that the current could be ascribed to the slow reduction of Cu^{+} to Cu^{0}. The formation of copper metal centres would however only be feasible (thermodynamically) at more negative potentials relative to the point where the reverse scan forming the nucleation loop crosses the forward scan[37i] (ca. -0.20 V). If the above supposition holds, another reduction reaction had to occur.

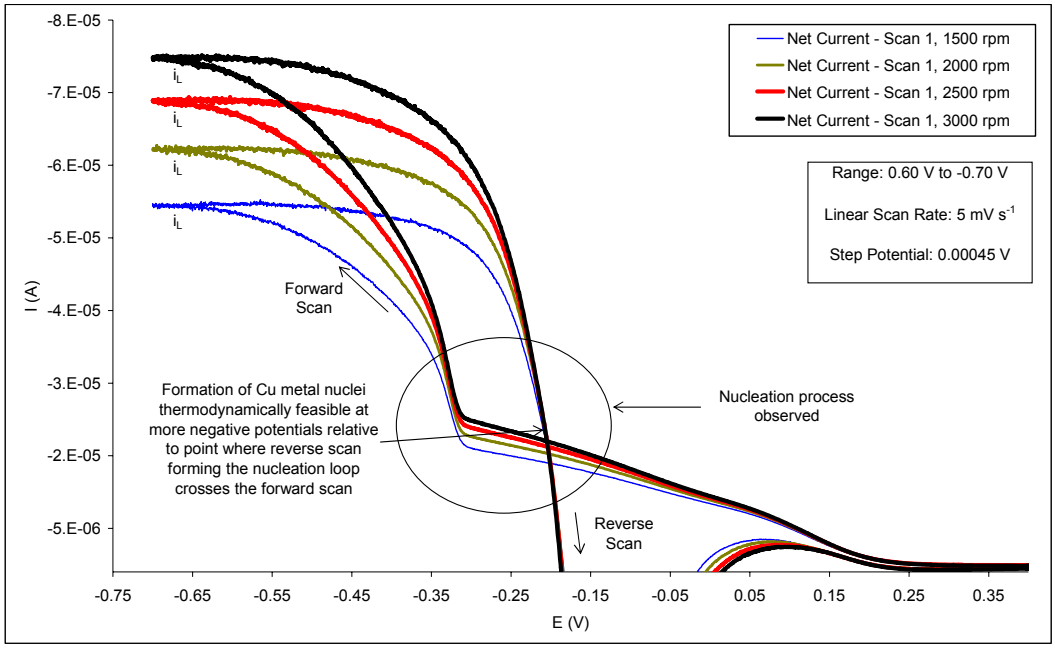

Figure 5.5 Slow potential sweep experiments for a Cu solution, using a rotating graphite working electrode.

The fact that background corrected (net) currents were used in Figure 5.5 pointed to the fact that the slow reduction reaction did not involve the direct interaction of any of the background components with the working electrode (i.e. NaCl, CH_3COONH_4, CH_3COOH) or reactions related to the graphite electrode surface itself. The exact nature of this slow reduction reaction could not be established.

It may be possible that the reduction of Cu^{2+} to Cu^{+} was inhibited as soon as the slow reduction reaction commenced at ca. 0.08 V. This could explain the fact that the reduction current at Peak C2 in Figure 5.4 was 2.5 times larger than the reduction current at Peak C1. Further evidence of an inhibitive effect was obtained from the $j-E$ plots in Figure 5.5. According to the Levich Equation (refer to Equation 5.13) i_L is proportional to $\sqrt{\omega}$. The magnitude of the limiting current at 3000 rpm should therefore be 1.4 times (33 %) higher than the limiting current at 1500 rpm. This was true when the limiting current densities in Figure 5.5 were compared at -0.70

V . When the currents at -0.30 V were compared, the value at 3000 rpm was only 1.2 times (18 %) higher than the current at 1500 rpm.

In Section 5.2.4 it was noted that Equation 5.32 could be used to determine the amount of electrons involved in a metal deposition reaction, provided that the reaction is reversible. This expression was used to establish if the deposition of copper metal from the Cu solution proceeded via a one-electron transfer reaction (Cu^{+} to Cu^{0}) as originally predicted via Figure 5.4. The data presented in Figure 5.5 was employed to plot values of E versus $log\left[(j_L - j)/j\right]$ covering the potential range where copper deposition occurred. This plot is illustrated in Figure 5.6.

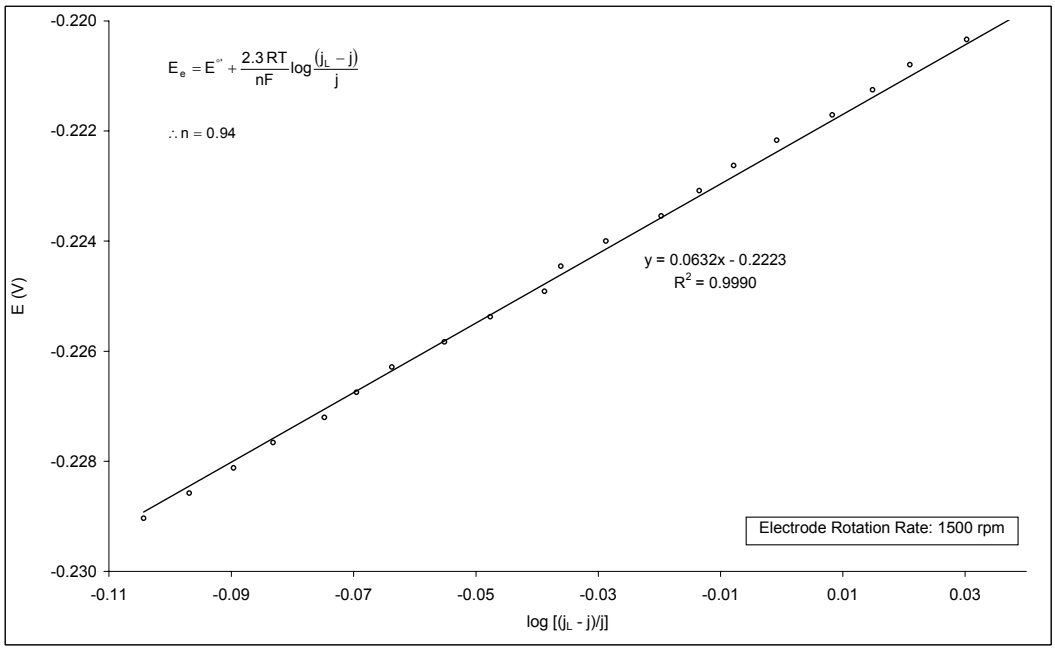

Figure 5.6 Data plot illustrating the calculation of the number of electrons transferred during the reaction involving copper metal deposition on a graphite working electrode. A Cu solution was employed, and data was recorded on completion of the metal nucleation process.

The following facts regarding the data used for the plot should be kept in mind (refer to Figure 5.5):

- Current values were converted to current densities by using an active

electrode surface area of 2.39 mm^2. Experiments involving the determination of the active surface area of the graphite electrode will be described in Section 5.5.2.

- Current density values of the reverse scan (i.e. electrode surface on completion of nucleation process) were used. Electron transfer for this scan was assumed to be reversible, based on the steep $j-E$ plot observed. The current density values for the forward scan could not be used due to complications associated with the nucleation process (note the catalytic process at ca. -0.30 V involving the reduction of copper ions on copper metal centres).

By solving the slope of the linear expression in Figure 5.6 for n, a value of 0.94 was obtained. This indicated that the deposition of copper on a graphite electrode, on completion of the nucleation process, would involve a one electron transfer reaction.

From the information obtained via Figures 5.4 to 5.6, it was decided to calculate kinetic parameters for the following redox couples:

- The reduction of Cu^{2+} to Cu^{+} on a graphite electrode surface. This will be referred to as the Cu^{2+}/Cu^{+} (C) redox couple for the remainder of the chapter.

- The reduction of Cu^{+} to Cu^{0} on a graphite electrode surface after completion of the nucleation process. This will be referred to as the Cu^{+}/Cu^{0} (C+Cu) redox couple for the remainder of the chapter.

In Section 5.3 it was noted that a reference material would be analysed with the test solutions to assist with the interpretation of experimental data and to confirm the methodology employed to calculate the kinetic parameters. The reduction of $Fe(CN)_6^{3-}$ to $Fe(CN)_6^{4-}$ on a graphite electrode surface was investigated, using the same methodologies

employed for the Cu solution. This will be referred to as the $Fe(CN)_6^{3-}/Fe(CN)_6^{4-}$ redox couple.

5.5.2 Active Surface Area of the Working Electrode

The experimental determination of the active electrode surface area of a working electrode by application of the Randles – Sevčik, Cottrell and Levich equations was discussed in Section 5.2.2. To calculate active surface areas via these experiments a redox couple with a known diffusion coefficient value (D) must be used. If the Levich equation is used, the kinematic viscosity of the solution (ν) should also be known.

The $Fe(CN)_6^{3-}$ solution described in Section 5.4.2 was used for the experimental determination of the active surface area of the graphite working electrode via the $Fe(CN)_6^{3-}/Fe(CN)_6^{4-}$ redox couple. For this solution, a D value of 6.3 $\times$ 10^{-10} m^2 s^{-1} was used[36c]. Where the Levich equation was used a value of 9.97 $\times$ 10^{-7} m^2 s^{-1} was assumed for ν [46a]. It should be noted that accurate values for ν is unnecessary when the Levich equation is applied, as a small error would have little effect on the final value calculated for the active surface area of the electrode.

Application of the Randles – Sevčik equation

The equation is only valid if the reaction on the particular electrode surface meets the criteria for reversibility (refer to Chapter 2, Section 2.2.2). Test work indicated that the reduction of $Fe(CN)_6^{3-}$ to $Fe(CN)_6^{4-}$ was not fully reversible on the graphite particle electrode, and the method was therefore not utilised to calculate the active surface area of the electrode.

Application of the Cottrell equation

The $Fe(CN)_6^{3-}$ solution was analysed via Chronoamperometric experiments. The results are presented graphically in Figures 5.7 and 5.8.

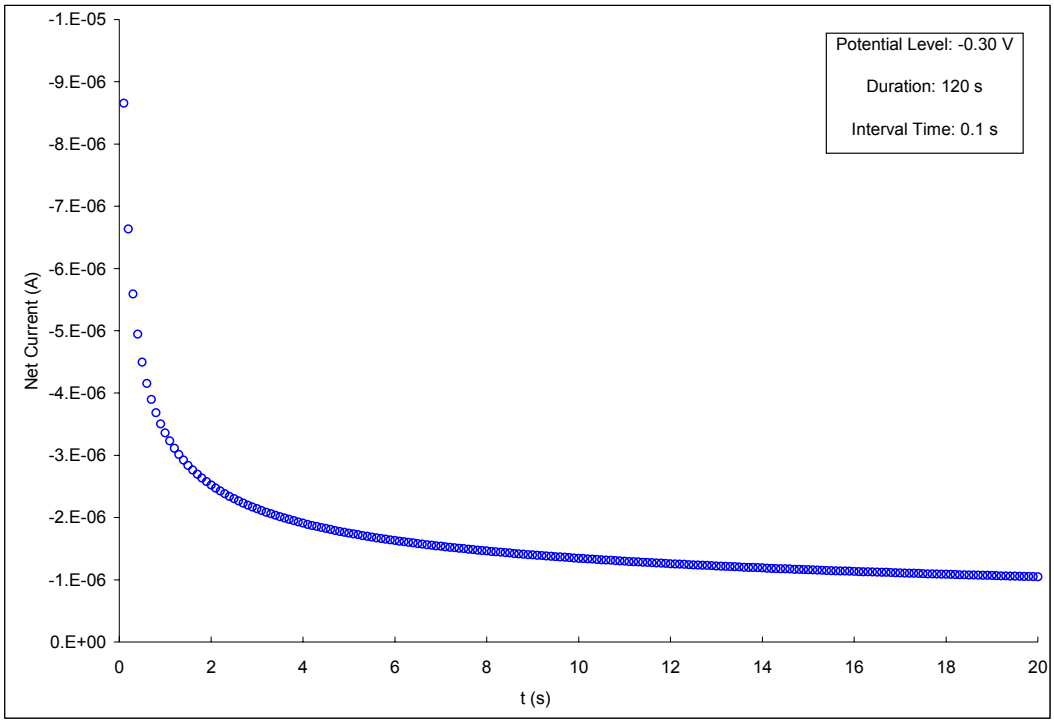

Figure 5.7 Chronoamperometric experiment involving a $Fe(CN)_6^{3-}$ solution used to establish the active surface area of a graphite working electrode.

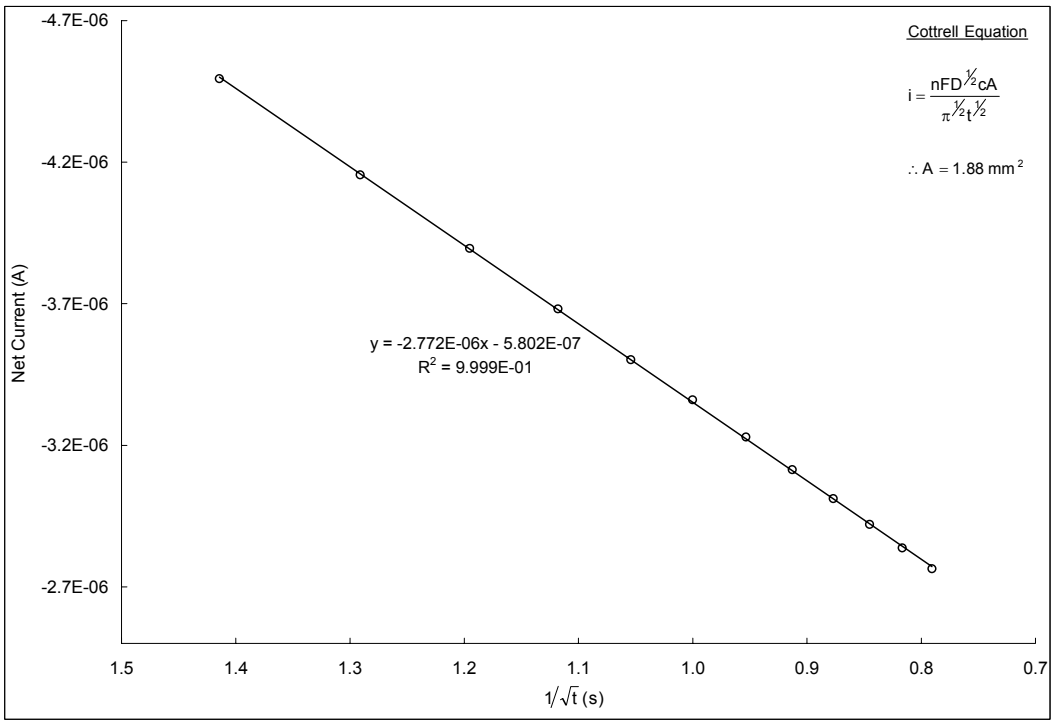

Figure 5.8 Plot used to calculate the active surface area of a graphite working electrode via the Cottrell equation. Data obtained from Figure 5.7.

By solving the slope of the linear expression shown in Figure 5.8 for A, the active surface area of the working electrode was calculated to be 1.88 mm^2. A concentration value of 1.078 mol m^{-3} was used.

Application of the Levich equation

On completion of the Chronoamperometric experiments, the same $Fe(CN)_6^{3-}$ solution was subjected to RDE experiments in order to calculate the active surface area of the working electrode via the Levich equation. Data obtained from this experiment is presented graphically in Figures 5.9 and 5.10.

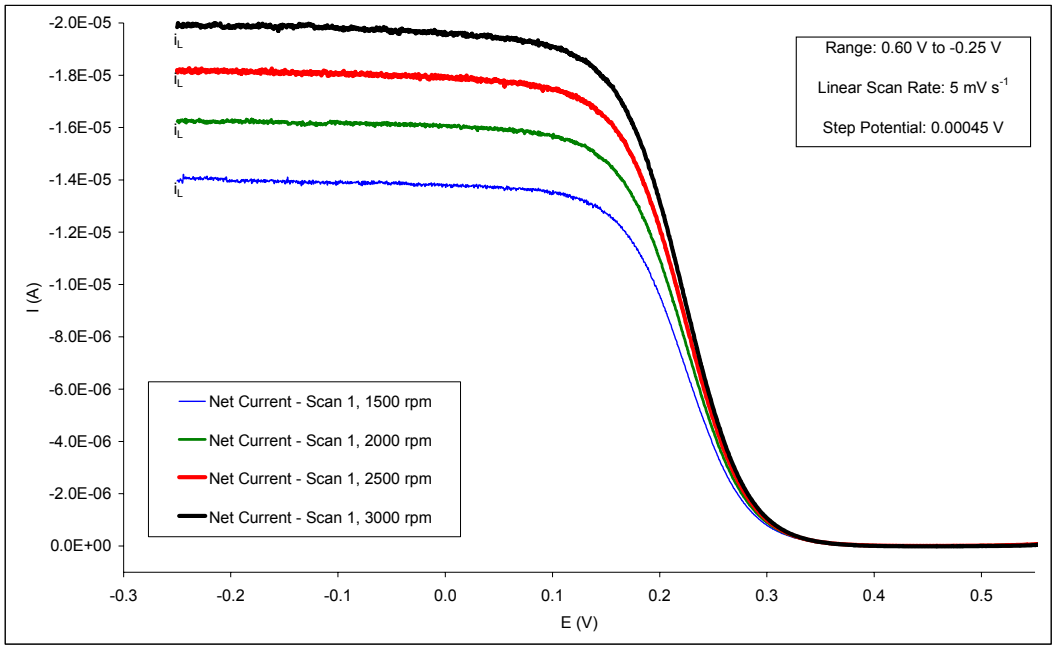

Figure 5.9 Slow potential sweep experiment involving a $Fe(CN)_6^{3-}$ solution used to establish the active surface area of a graphite working electrode.

By solving the slope of the linear expression shown in Figure 5.10 for A, the active surface area of the electrode was calculated to be 2.39 mm^2. Although the coefficient of determination (R^2) for the linear expression in Figure 5.10 indicate a good fit for the data points it would be ideal to employ more data points over a wider range of rotation rates.

Unfortunately the equipment available for these experiments (refer to Chapter 2, Section 2.4.1) did not allow the use of rotation rates other than 1500, 2000, 2500 and 3000 rpm.

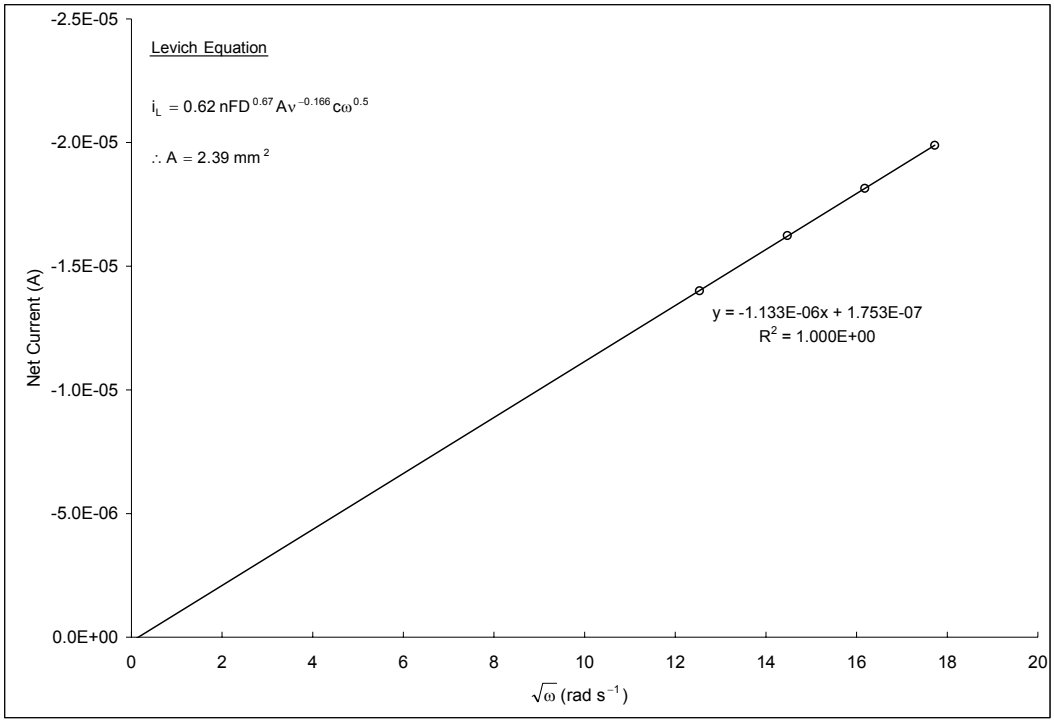

Figure 5.10 Plot used to calculate the active surface area of a graphite working electrode via the Levich equation. Data obtained from Figure 5.9.

General discussion

The surface area calculations by means of the Cottrell and Levich equations were reproducible. When the active surface areas obtained via Figures 5.7 to 5.10 were compared to additional experiments conducted on two different days, combined averages of 1.90 mm^2 (standard deviation 0.02 mm^2, n = 3) and 2.43 mm^2 (standard deviation 0.10 mm^2, n = 3) were obtained via application of the Cottrell and Levich equations respectively. The comparative active surface area calculations are illustrated in Figures B1 and B2 of *Appendix B*.

The electrode was polished with diamond paste prior to conducting experiments on each of the respective days. This indicated that the

polishing step did not have a major impact on the active surface of the working electrode.

From the averaged active surface area values, it is evident that a significant difference exists between surface area values calculated via the Cottrell and Levich equations. When the geometric surface area of the working electrode was estimated via the software associated with a stereo microscope (refer to Chapter 2, Section 2.4.3 for a description of the microscope and software), a value of 2.07 mm^2 was obtained.

The lower active surface area value obtained by means of the Cottrell equation (compared to the geometric surface area) is to be expected, as the surface of the electrode contained both graphite particles and non-conducting epoxy resin. The higher calculated surface area obtained by application of the Levich equation can be ascribed to the porosity of the graphite surface, and the eccentricity of the RDE resulting in non-laminar flow. This value does not reflect the true surface area which can be obtained under ideal conditions, i.e. a non-porous surface rotated under laminar flow conditions.

Since the kinetic parameters reported in this chapter were calculated from $j-E$ plots involving a RDE, it was decided to use the surface area obtained from the Levich calculation, where similar RDE experiments were employed. This approach corrected deviations from ideal conditions introduced as a result of the electrode material (porosity) and experimental equipment (eccentricity) employed.

5.5.3 Exchange Current Densities and Transfer Coefficients

Exchange current densities and electron transfer coefficients were determined for the $Fe(CN)_6^{3-}/Fe(CN)_6^{4-}$ redox couple associated with the $Fe(CN)_6^{3-}$ solution as well as the Cu^{2+}/Cu^{+} (C) and Cu^{+}/Cu^{0} (C+Cu) redox couples associated with the Cu solution. Prior to these experiments,

the active electrode surface area was calculated to be 2.39 mm^2 (refer to Figures 5.9 and 5.10) via application of the Levich equation.

Values for j_o and α were obtained by calculating current densities at infinite rotation rates for each of the redox couples. The resulting current densities were used to construct Tafel plots from which α values were derived. Estimated equilibrium potentials (refer to Section 5.2.3) were utilised to establish j_o values from the Tafel plot.

The determination of current densities at infinite rotation rates for the reduction of $Fe(CN)_6^{3-}$ between potentials of 0.30 V and 0.22 V is shown in Figure 5.11. The Tafel plot incorporating the calculated current densities is presented in Figure 5.12. In Figure 5.13, the estimation of the equilibrium potential for the $Fe(CN)_6^{3-}/Fe(CN)_6^{4-}$ redox couple is illustrated.

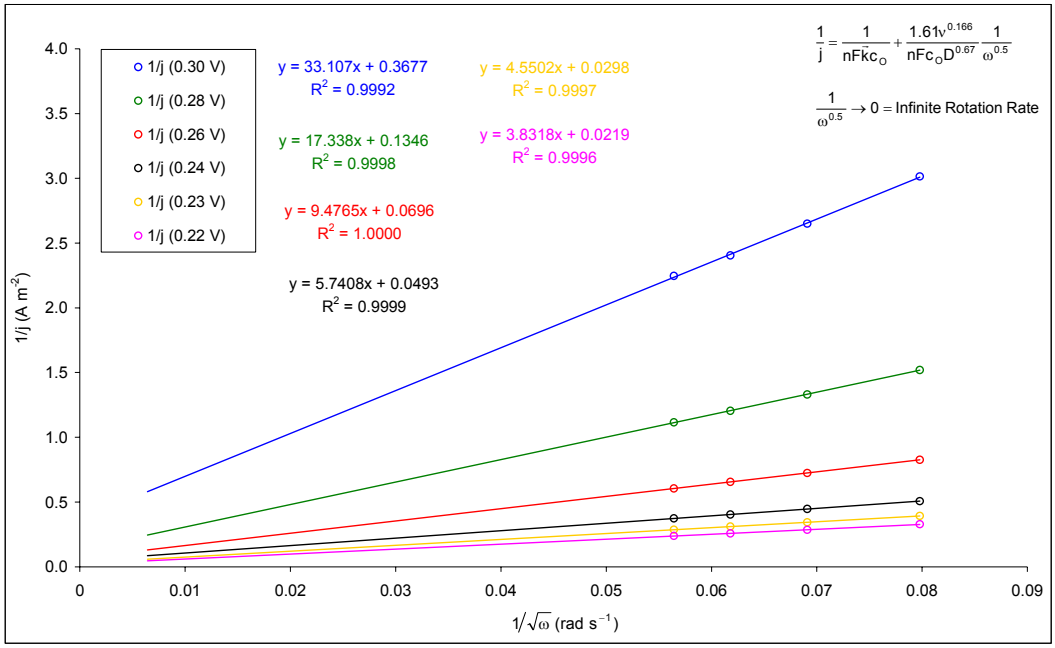

Figure 5.11 Plots used to calculate current densities at infinite rotation rates for the $Fe(CN)_6^{3-}/Fe(CN)_6^{4-}$ redox couple, using a graphite working electrode.

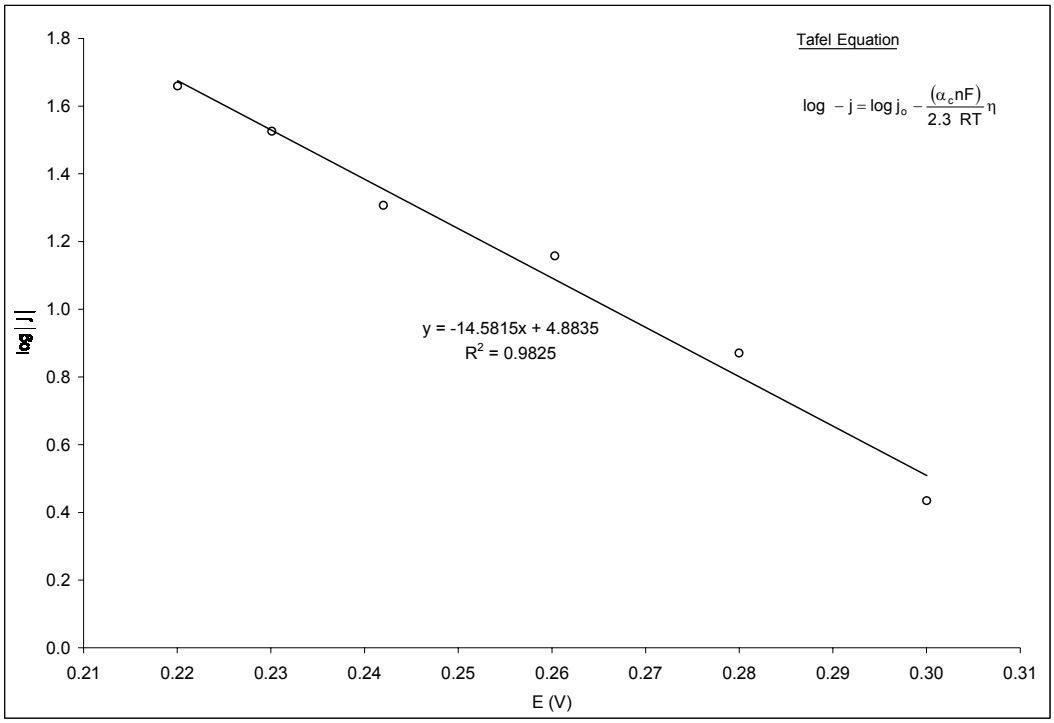

Figure 5.12 Plot used to calculate the exchange current density and electron transfer coefficient values for the $Fe(CN)_6^{3-}/Fe(CN)_6^{4-}$ redox couple, using a graphite working electrode.

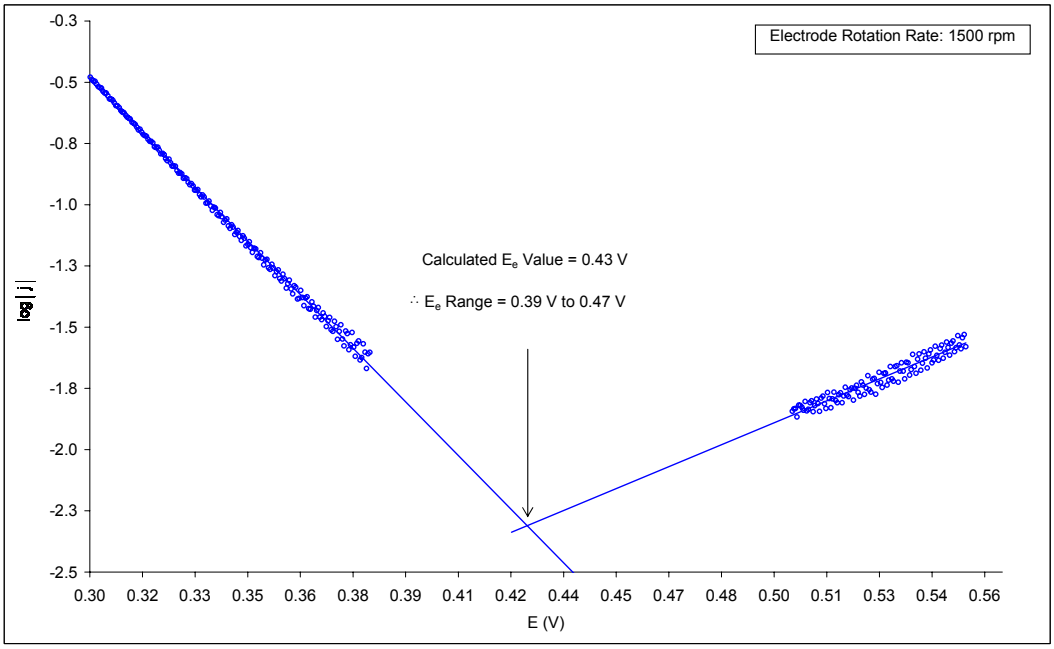

Figure 5.13 Estimation of the equilibrium potential for the $Fe(CN)_6^{3-}/Fe(CN)_6^{4-}$ redox couple, using a graphite working electrode.

Due to possible errors associated with the estimation of E_e values a range in which the actual value would likely appear was used instead of a discrete value. The range was established by using the calculated E_e value $\pm$ 10 %. As a consequence, j_o values were also reported as a range, rather than discrete values.

The same approach was followed for the determination of j_o and α values associated with the Cu^{2+}/Cu^{+} (C) and Cu^{+}/Cu^{0} (C+Cu) redox couples. Graphs illustrating the establishment of current densities at infinite rotation rates and Tafel plots and are illustrated in Figures 5.14 to 5.17. Plots used to estimate equilibrium potentials for the Cu^{2+}/Cu^{+} (C) and Cu^{+}/Cu^{0} (C+Cu) redox couples are illustrated in Figures B3 and B4 of *Appendix B*.

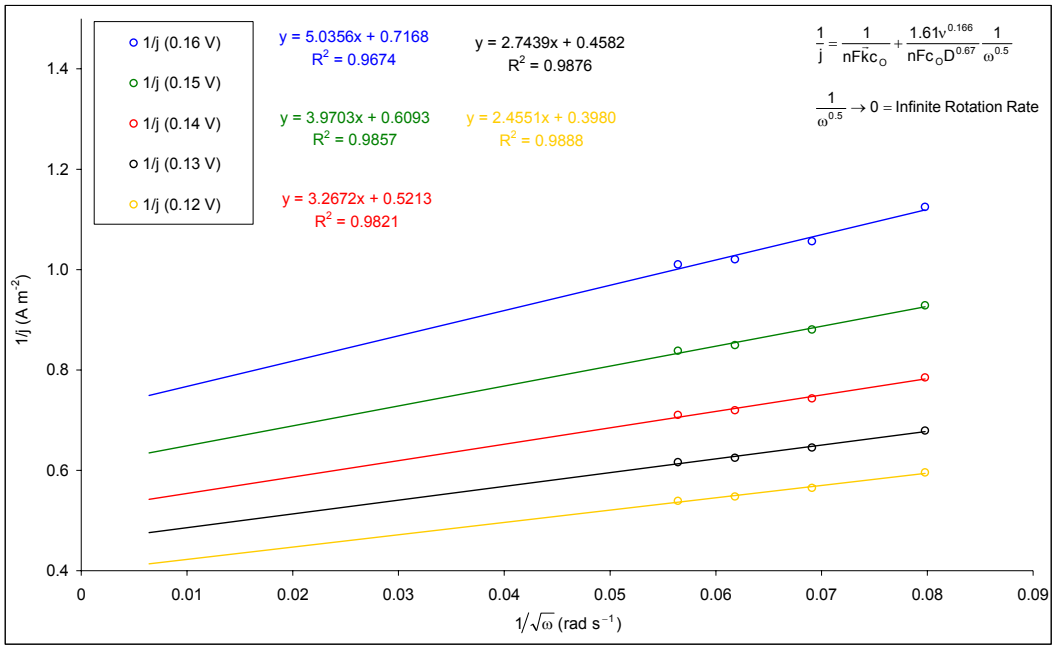

Figure 5.14 Plots used to calculate current densities at infinite rotation rates for the Cu^{2+}/Cu^{+} (C) redox couple, using a graphite working electrode.

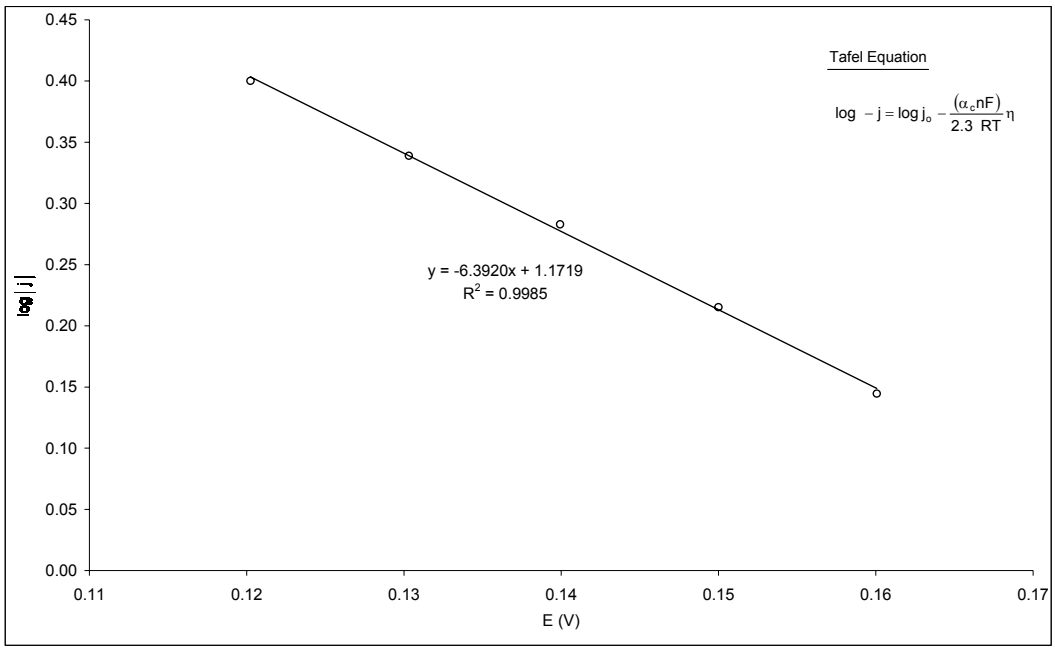

Figure 5.15 Plot used to calculate the exchange current density and electron transfer coefficient values for the Cu^{2+}/Cu^{+} (C) redox couple, using a graphite working electrode.

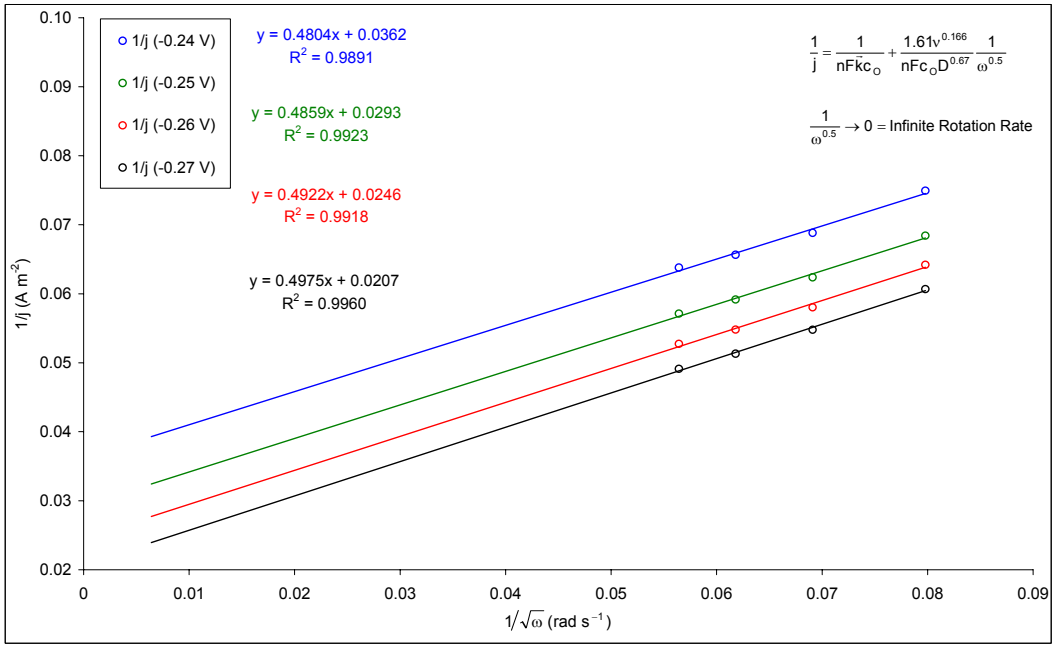

Figure 5.16 Plots used to calculate current densities at infinite rotation rates for the Cu^{+}/Cu^{0} (C+Cu) redox couple, using a graphite working electrode.

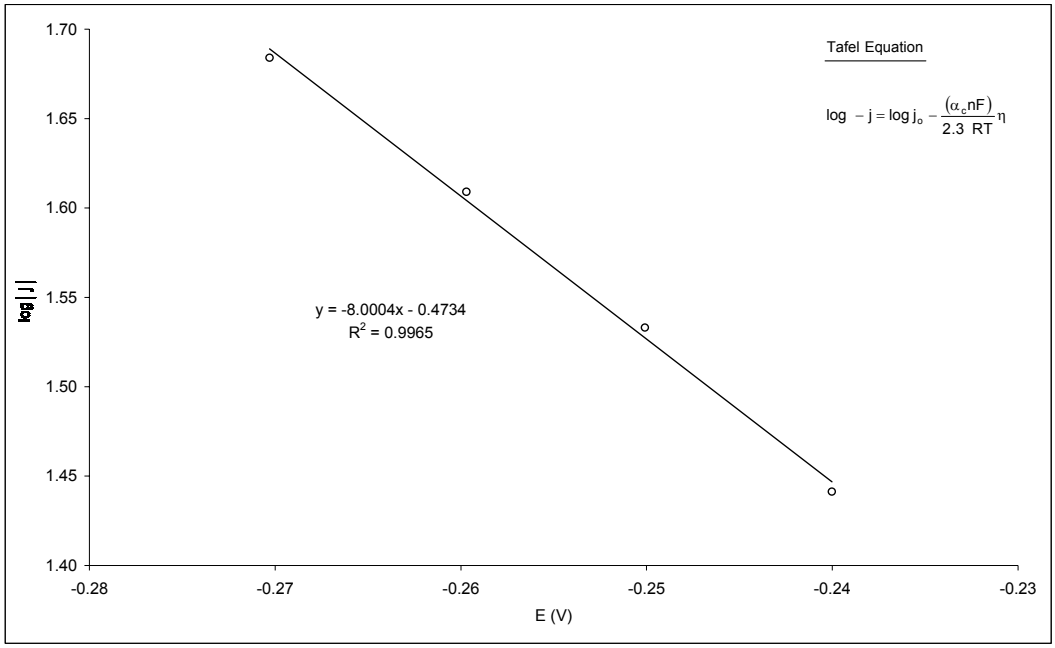

Figure 5.17 Plot used to calculate the exchange current density and electron transfer coefficient values for the Cu^{+}/Cu^{0} (C+Cu) redox couple, using a graphite working electrode.

When the plots in Figures 5.14 to 5.17 were studied, a number of trends became apparent. In the case of the current density plots (Figures 5.14 and 5.16), it was noted that the data points did not follow an exact linear trend. This was confirmed by the fact that data points for rotation rates of 1500 and 3000 rpm were normally observed above the linear least squares trend line, whilst data points for 2000 and 2500 rpm were observed below the trend line. The curvature of these plots became less pronounced as a particular experiment proceeded to more negative potentials.

A study of the linear least square lines fitted to the Tafel plots illustrated in Figures 5.15 and 5.17 also indicated that a straight line was fitted to data points with a slight natural curvature.

The trends described for the plots involving the Cu solution were not observed when the $Fe(CN)_6^{3-}/Fe(CN)_6^{4-}$ redox couple was investigated.

This indicated the possible presence of competing side reactions where components of the Cu solution interact with the graphite working electrode surface. At this stage no quantitative explanation for the trends associated with the Cu solution plots can be provided.

It should be noted that the data for Figures 5.11 to 5.17 and Figures B3 and B4 (*Appendix B*) were obtained from the slow potential sweep $j-E$ plots originally illustrated in Figures 5.5 and 5.9.

A summary of the j_o and α values calculated for the various redox couples associated with the $Fe(CN)_6^{3-}$ and Cu solutions is presented in Table 5.1.

Table 5.1 Exchange current densities and electron transfer coefficients calculated for redox couples associated with $Fe(CN)_6^{3-}$ and Cu solutions.

Redox Couple	Parameter	Value
$Fe(CN)_6^{3-}/Fe(CN)_6^{4-}$	α	0.86
	j_o (A m^{-2})	1.1×10^{-2} - 1.6×10^{-1}
Cu^{2+}/Cu^{+} (C)	α	0.38
	j_o (A m^{-2})	2.7×10^{-2} - 8.6×10^{-2}
Cu^{+}/Cu^{0} (C+Cu)	α	0.47
	j_o (A m^{-2})	7.7×10^{0} - 1.6×10^{1}

From the data in Table 5.1 it is apparent that the j_o value for the Cu^{+}/Cu^{0} (C+Cu) redox couple is orders of magnitude greater than the value for the Cu^{2+}/Cu^{+} (C) redox couple. Therefore, at a given overpotential, the

reduction of Cu^{+} to Cu^{0} will be orders of magnitude faster than the reduction of Cu^{2+} to Cu^{+}.

5.5.4 Rate Constants

Rate constants were determined by using the current densities at infinite rotation rates previously calculated in Section 5.5.3. This was achieved by solving Equation 5.22 for $\vec{k}$ where $1/\omega^{0.5}$ is zero as described in Section 5.2.4. The standard rate constant, k_s, was determined by plotting $log\,\vec{k}$ as a function of potential. A value for k_s was obtained where the formal potential value (x-axis) intersected the $log\,\vec{k}$ plot (y-axis).

Standard rate constants for the $Fe(CN)_6^{3-}/Fe(CN)_6^{4-}$ and Cu^{2+}/Cu^{+} (C) redox couples were established. Current densities at infinite rotation rates determined via Figures 5.11 and 5.14 were used, whilst the required formal potential values were estimated from voltammograms obtained via CV experiments. The estimation of formal potentials was originally described in Section 5.2.4.

The $log\,\vec{k}$ plots for the $Fe(CN)_6^{3-}/Fe(CN)_6^{4-}$ and Cu^{2+}/Cu^{+} (C) redox couples are illustrated in Figures 5.18 and 5.19 respectively. Formal potential values for the $Fe(CN)_6^{3-}/Fe(CN)_6^{4-}$ and Cu^{2+}/Cu^{+} (C) redox couples were estimated from the voltammograms illustrated in Figures B5 (*Appendix B*) and 5.4 respectively.

Due to the fact that the redox couples under investigation were not fully reversible, exact $E^{\circ'}$ values could not be determined. For this reason, a potential range was used instead of a discrete value. The cathodic (E_{pc}) and anodic (E_{pa}) peak potentials recorded for a particular CV experiment was used to establish the potential range.

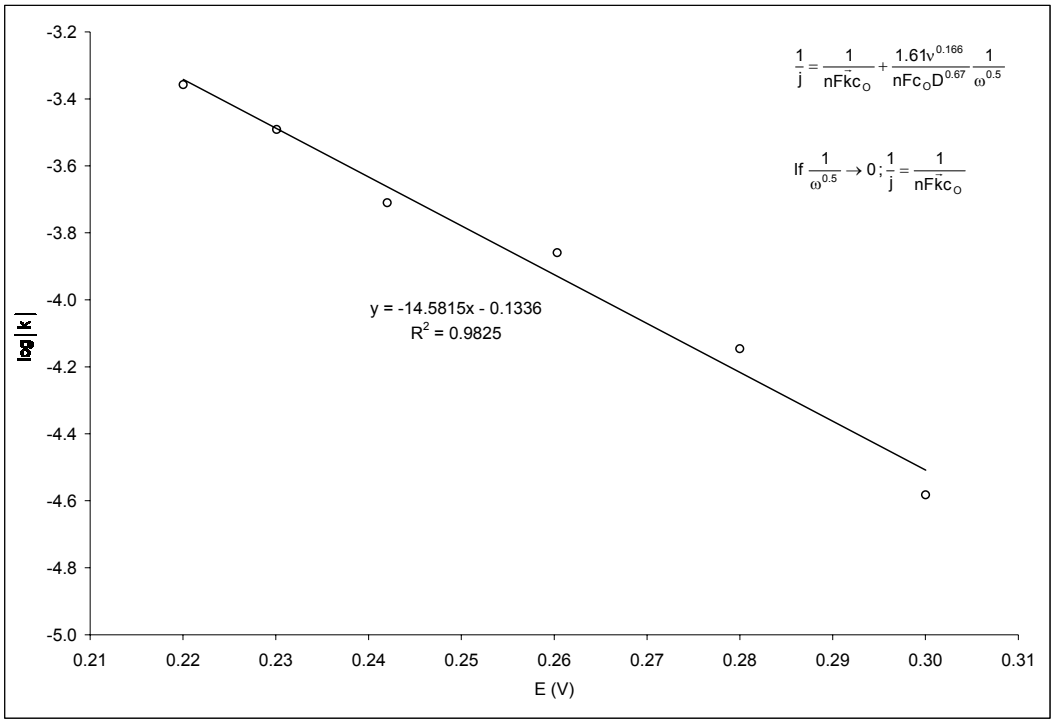

Figure 5.18 Plot used to calculate the standard rate constant for the $Fe(CN)_6^{3-}/Fe(CN)_6^{4-}$ redox couple, using a graphite working electrode.

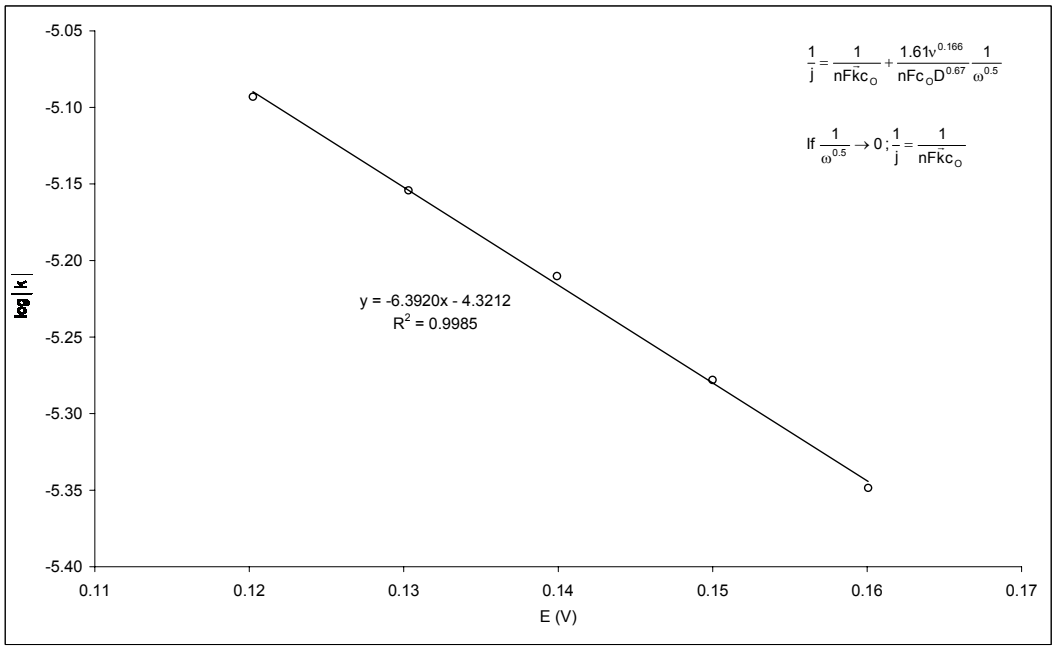

Figure 5.19 Plot used to calculate the standard rate constant for the Cu^{2+}/Cu^{+} (C) redox couple, using a graphite working electrode.

A summary of the k_s values calculated for the redox couples associated with the $Fe(CN)_6^{3-}$ and Cu solutions is presented in Table 5.2. Since the formal potential was reported as a range, k_s values were also reported as a range, rather than discrete values.

Table 5.2 Standard rate constants calculated for redox couples associated with $Fe(CN)_6^{3-}$ and Cu solutions.

Redox Couple	Parameter	Value
$Fe(CN)_6^{3-}/Fe(CN)_6^{4-}$	$E^{\circ'}$ (V)	0.19 - 0.27
	k_s $(m\ s^{-1})$	1.2×10^{-4} - 1.2×10^{-3}
Cu^{2+}/Cu^{+} (C)	$E^{\circ'}$ (V)	0.09 - 0.19
	k_s $(m\ s^{-1})$	2.9×10^{-6} - 1.3×10^{-5}

Values for the Cu^{+}/Cu^{0} (C+Cu) redox couple could not be determined since the concentration of Cu^{+} in the bulk solution (c_R term in Equation 5.22) was not known. To establish the standard rate constant for the Cu^{+}/Cu^{0} (C+Cu) redox couple, it would be necessary to use a Cu solution with a known amount of Cu^{+} instead of the Cu^{2+} ions used in the current solution (refer to Section 5.4.2 for Cu solution components).

In a theoretical exercise it was assumed that the concentration of Cu^{+} was equal to the concentration of Cu^{2+} in the bulk solution. When a $E^{\circ'}$ value of -0.25 V was used, a k_s value of 1.1×10^{-3} m s^{-1} was calculated for the Cu^{+}/Cu^{0} (C+Cu) redox couple.

5.5.5 Mass Transfer Coefficients

In Section 5.2.5 the calculation of k_m values for different rates of rotation was described. It was noted that these values could be estimated from RDE theory (Equation 5.33) or the use of experimental RDE data (Equation 5.34). The calculation of k_m values for the redox couples associated with the $Fe(CN)_6^{3-}$ and Cu solutions by the application of Equations 5.33 and 5.34 will be discussed in this section.

For the application of Equation 5.33, values for D and ν are required. The Levich equation (Equation 5.13) was used to determine D values, using an active surface area of 2.39 mm^2 for the working electrode (refer to Figures 5.9 and 5.10). In the case of the $Fe(CN)_6^{3-}$ solution a value of 9.97 $\times$ 10^{-7} m^2 s^{-1} was used for ν [46a], whilst a value of 1.17 $\times$ 10^{-6} m^2 s^{-1} was used for the Cu solution. The Cu solution value was calculated by using a molar weighted average, based on the literature values of the individual components[46b].

The calculation of the D values for the $Fe(CN)_6^{3-}/Fe(CN)_6^{4-}$ and Cu^+/Cu^0 (C+Cu) redox couples is illustrated in Figure 5.20. In the case of the Cu^+/Cu^0 (C+Cu) redox couple a value of 8.0 $\times$ 10^{-10} m^2 s^{-1} was calculated, whilst a value of 6.3 $\times$ 10^{-10} m^2 s^{-1} was obtained for the $Fe(CN)_6^{3-}/Fe(CN)_6^{4-}$ redox couple. It should be noted that the raw data for the calculation of the k_m values was obtained from $j-E$ plots originally illustrated in Figures 5.5 and 5.9.

In Section 5.5.2 the active surface area of the graphite working electrode was established via a $Fe(CN)_6^{3-}$ solution and application of the Levich equation. A literature value[36c] of 6.3 $\times$ 10^{-10} m^2 s^{-1} was used for D. The fact that the literature value is again obtained from experimental data confirms the general methodology and data handling procedures used.

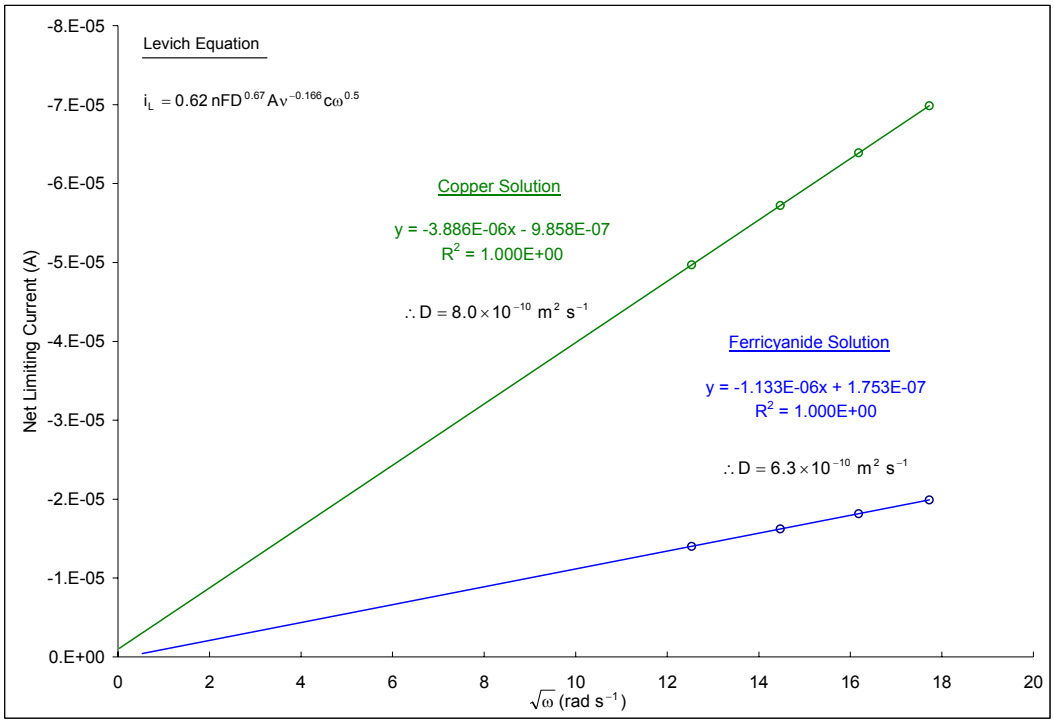

Figure 5.20 Plots used to calculate the diffusion coefficients for the $Fe(CN)_6^{3-}/Fe(CN)_6^{4-}$ and Cu^+/Cu^0 (C+Cu) redox couples, using a graphite working electrode.

A value for *D* could not be established for the Cu^{2+}/Cu^+ (C) redox couple. When the slow potential sweep experiment for a Cu solution was discussed in Section 5.5.1 via Figure 5.5, a gradual increase in the current on the forward sweep of the scan was observed subsequent to the reduction of Cu^{2+} to Cu^+. Evidence pointing to the suppression of the current following the reduction of Cu^{2+} to Cu^+ was also found. These factors contributed to the fact that accurate limiting current values could not be established.

When attempts were made to plot i_L values for the Cu^{2+}/Cu^+ (C) redox couple as a function of $\sqrt{\omega}$, linear plots were obtained. These plots did however not pass through the origin like the linear expressions obtained for the $Fe(CN)_6^{3-}/Fe(CN)_6^{4-}$ and Cu^+/Cu^0 (C+Cu) redox couples. The Levich equation could therefore not be used to determine a *D* value for

the Cu^{2+}/Cu^{+} (C) redox couple, as the assumption that the process is under mass transport control could not be confirmed.

The calculated D values for the $Fe(CN)_6^{3-}/Fe(CN)_6^{4-}$ and Cu^{+}/Cu^{0} (C+Cu) redox couples and literature values for ν were substituted into Equation 5.33 to establish k_m values at rotation rates of 1500, 2000, 2500 and 3000 rpm.

Limiting current values from Figures 5.5 and 5.9 were also substituted into Equation 5.34 to establish k_m values at rotation rates of 1500, 2000, 2500 and 3000 rpm for the $Fe(CN)_6^{3-}/Fe(CN)_6^{4-}$ and Cu^{+}/Cu^{0} (C+Cu) redox couples. A comparison of k_m values obtained via Equations 5.33 and 5.34 is provided in Tables 5.3 and 5.4.

Table 5.3 Mass transfer coefficients calculated from RDE theory for redox couples associated with $Fe(CN)_6^{3-}$ and Cu solutions.

Equation	Redox Couple	Rotation Rate (rpm)	k_m ($m\ s^{-1}$)
$k_m = \frac{D^{0.67}\omega^{0.5}}{1.61\nu^{0.166}}$	$Fe(CN)_6^{3-}/Fe(CN)_6^{4-}$	1500	5.3×10^{-5}
		2000	6.1×10^{-5}
		2500	6.8×10^{-5}
		3000	7.5×10^{-5}
	Cu^{+}/Cu^{0} (C+Cu)	1500	6.1×10^{-5}
		2000	7.0×10^{-5}
		2500	7.8×10^{-5}
		3000	8.6×10^{-5}

Table 5.4 Mass transfer coefficients calculated from RDE experimental data for redox couples associated with $Fe(CN)_6^{3-}$ and Cu solutions.

Equation	Redox Couple	Rotation Rate (rpm)	k_m ($m\ s^{-1}$)
$k_m = \frac{i_L}{nFAc}$	$Fe(CN)_6^{3-}/Fe(CN)_6^{4-}$	1500	5.6×10^{-5}
		2000	6.5×10^{-5}
		2500	7.3×10^{-5}
		3000	8.0×10^{-5}
	Cu^{+}/Cu^{0} (C+Cu)	1500	6.7×10^{-5}
		2000	7.7×10^{-5}
		2500	8.6×10^{-5}
		3000	9.4×10^{-5}

A good correlation was observed between k_m values (i.e. same order of magnitude) reported for the different redox couples calculated via Equations 5.33 and 5.34. It was however noted that k_m values obtained via Equation 5.34 always produced higher values compared to calculations via Equation 5.33. At this stage, no apparent explanation for this systematic difference can be provided.

5.5.6 General

When the active surface area of the graphite working electrode was determined via application of RDE experiments and the Levich equation (Section 5.5.2, Figure 5.10) it was noted that ideally, more data points should have been used over a wider range of rotation rates. This was not possible since the equipment available for the experiments (refer to

Chapter 2, Section 2.4.1) did not allow the use of rotation rates other than 1500, 2000, 2500 and 3000 rpm.

It should be kept in mind that the same limitation existed when current densities at infinite rotation rates and diffusion coefficients were established via RDE experiments. Inaccuracies in these determinations would inevitably lead to inaccuracies in the calculation of j_o, α, k_s and k_m values.

In Section 5.2.1 it was noted that quantitative rate parameters could only be established in conditions where either electron transfer or mass transport is the sole rate determining step over a particular portion of a $j-E$ plot. This implied that the k_m values for the particular reaction should be larger than the k_s values by at least one order of magnitude. When the k_s and k_m results reported in Tables 5.2 to 5.4 were compared it was evident that the k_m values were either smaller or similar to the comparative k_s values. This validated the decision to use current densities at infinite rotation rates for the calculation of kinetic parameters.

5.6 CONCLUSIONS

A summary of the objectives of the research associated with this chapter, and the experiments conducted to achieve these objectives is provided. This is followed by a discussion of the main conclusions, and proposed future research activities.

5.6.1 Summary of Research Activities

The third phase of the fundamental research project described in this dissertation involved the quantitative determination of kinetic parameters. In the context of this chapter, the determination of kinetic parameters refers to experimental values obtained for j_o, α, k_s and k_m. These parameters would assist in the fundamental understanding of interactions

between metal ions found in the PML and the graphite cathode evaluated in Chapter 4 by quantifying the rate at which the interactions at the electrode surface occurs. The parameters can also be used for engineering modelling purposes, where it is attempted to predict the performance of an electrochemical reactor under specific operating conditions.

The rationale for using the Cu solution (refer to Section 5.4.2 for composition) in experiments described in this chapter was discussed in Section 5.1.2. In addition to the Cu solution, it was decided to use a $Fe(CN)_6^{3-}$ solution (refer to Section 5.4.2 for composition) as a reference. The purpose of the reference was to validate experimental procedures and data handling procedures used for the Cu solution.

Experimental design

The various experimental procedures that could be used to determine j_o, α, k_s and k_m values were described in Section 5.2. An important conclusion was that when metal deposition reactions are studied, slow potential sweep experiments should be utilised instead of potential step experiments. The reason is that more metal is deposited on the electrode surface under investigation in the case of potential step experiments. This changes the characteristics of the electrode, which in turn makes it difficult to interpret or reproduce results.

In Section 5.1.2 it was noted that the graphite particles employed in Chapter 4 would be used as the electrode material. Since RDE experiments were employed, it was necessary to use an electrode tip that could be rotated. A rotating tip containing the graphite particles required for experimental work associated with this chapter was not available commercially and therefore had to be constructed in-house. The construction of the electrode tip was described in Section 5.4.1.

Due to the nature of the electrode construction it was possible that the active surface area of the electrode could change between different sets of experiments. The active surface area was therefore calculated prior to conducting a new set of experiments.

A detailed procedure for the experimental determination of the required kinetic parameters was provided in Section 5.3.2. In essence this involved *(i)* the identification of the redox couples associated with the Cu solution, *(ii)* the determination of the active surface area of the working electrode, *(iii)* the use of slow potential sweep experiments to obtain $j-E$ plots under various mass transport conditions (RDE rotation rates), and *(iv)* the calculation of rate parameters from the experimental $j-E$ plots.

5.6.2 Identification of Redox Couples

The identification of redox couples associated with the interaction of a Cu solution and a graphite working electrode surface was discussed in Section 5.5.1.

Two redox couples were identified, namely the reduction of Cu^{2+} to Cu^{+} and the reduction of Cu^{+} to Cu^{0}. In the case of metal deposition (i.e. Cu^{+} to Cu^{0}) it was concluded that $j-E$ plots on completion of the nucleation process should be used for the calculation of kinetic parameters. This was necessary due to the catalytic reduction of copper ions on copper metal centres during the nucleation process.

5.6.3 Active Surface Area of Working Electrode

The experimental determination of the active electrode surface area of a working electrode by application of the Randles - Sevčik, Cottrell and Levich equations was described in Section 5.2.2. A $Fe(CN)_6^{3-}$ solution (refer to Section 5.4.2) was used as a reference.

Since the kinetic parameters reported in this chapter were calculated from

$j-E$ plots involving a RDE, it was decided to use the surface area obtained from the Levich calculation, where similar RDE experiments were employed. It was concluded that this approach corrected deviations from ideal conditions introduced as a result of the electrode material (porosity) and experimental equipment (eccentricity) employed.

5.6.4 Kinetic Parameters

Exchange current densities, electron transfer coefficients and standard rate constants for the redox couples associated with the $Fe(CN)_6^{3-}$ and Cu solutions were reported in Tables 5.1 and 5.2. From the exchange current densities it is evident that the rate of copper deposition (Cu^{+} to Cu^{0}) would be orders of magnitude greater than the reduction of Cu^{2+} to Cu^{+} at a given overpotential. This was ascribed to the fact that copper metal nuclei would catalyse the reduction of Cu^{+} to Cu^{0}.

The kinetic parameters reported in Tables 5.1 and 5.2 were derived from calculated current densities at infinite rotation rates, as described in Sections 5.2.3 and 5.5.3. When the k_s and k_m results reported in Tables 5.2 to 5.4 were compared it was evident that the k_m values were either smaller or similar than the comparative k_s values. This validated the decision to use current densities at infinite rotation rates, since quantitative rate parameters can only be established in conditions where k_m values for the particular reaction is larger than the corresponding k_s values by at least one order of magnitude (refer to Section 5.2.1).

5.6.5 General

The determination of kinetic parameters via the application of various methodologies as described in Sections 5.2 and 5.5 was demonstrated.

Due to the inaccuracies associated with the estimation of equilibrium and formal potentials, j_o and k_s values could only be reported as a range,

rather than discrete values (refer to Sections 5.5.3 and 5.5.4). The reported ranges would therefore provide an estimate of the order of magnitude of j_o and k_s, rather than an accurate value.

In addition, several unexplained experimental anomalies were observed, which could have an impact on the accuracy of the reported kinetic parameters:

- In Section 5.5.1 the interaction of a Cu solution with a rotating graphite working electrode was investigated via slow potential sweep experiments, as illustrated in Figure 5.5. It was observed that the reduction current on the forward sweep slowly increased over the potential range 0.08 V to -0.30 V. The exact nature of this slow reduction process could not be established.

  Due to the slow increase in reduction current at potentials more negative than 0.08 V accurate limiting currents could not be established for the reduction of Cu^{2+} to Cu^{+}. As a consequence, k_m values could not be reported for this redox couple.

- In Section 5.5.3 current densities at infinite rotation rates and exchange current densities for the redox couples associated with the Cu solution was established via Figures 5.14 to 5.17. A study of the linear least squares lines indicated that a linear expression was fitted to data points with a slight natural curvature.

  The trends described for the plots involving the Cu solution was not observed when the $Fe(CN)_6^{3-}/Fe(CN)_6^{4-}$ redox couple was investigated. This indicated the possible presence of competing side reactions. No quantitative explanation for the trends associated with the Cu solution plots could be provided.

- In Section 5.5.5 mass transfer coefficients for redox couples associated with $Fe(CN)_6^{3-}$ and Cu solutions were calculated via expressions

derived from RDE theory and RDE experimental data, as illustrated in Tables 5.3 and 5.4. The values reported via the two different approaches were of the same order of magnitude, although a systematic difference between the data sets was observed. This trend was evident for both the $Fe(CN)_6^{3-}$ and Cu solutions, and was ascribed to a systematic error in the experimental or data handling procedures.

From the discussion related to the observed experimental anomalies, it is evident that mechanistic information pertaining to the interaction of a particular redox couple with a working electrode surface (e.g. formation of reaction intermediates, adsorption) is imperative if accurate kinetic parameters are required.

If kinetic parameters associated with the deposition of palladium or platinum need to be determined, the complexity of the various experiments will increase due to the catalytic generation of hydrogen gas on the deposited metal centres. In the case of palladium or platinum deposition, deconvolution techniques will be required to produce $j-E$ plots that reflect the reduction of a particular PGM complex in the absence of hydrogen ion reduction currents.

5.6.6 Future Research

Although the objectives listed in Section 5.1.2 were achieved, several areas of research which could improve the accuracy of the quantitative data produced via the methodologies described in this chapter were identified:

- Investigate the cause of experimental anomalies described in Section 5.6.5. One aspect of these investigations would probably involve fundamental research related to reaction mechanisms. The advantage of investigating reaction mechanisms associated with the Cu solution is that the methodologies could be applied to more complex systems, e.g. the deposition of palladium or platinum. Knowledge of reaction

mechanisms will play an important role in the identification of redox couples associated with a particular test solution and electrode material, and the interpretation of experimental data obtained for a particular redox couple.

- Investigate the use of deconvolution techniques to make the establishment of kinetic parameters associated with palladium and platinum deposition feasible.

- In Section 5.5.4 it was noted that standard rate constants for the reduction of Cu^{+} to Cu^{0} could not be determined since the concentration of Cu^{+} in the bulk solution (c_R term in Equation 5.22) was not known. It is proposed that the standard rate constant be established via a Cu solution with a known concentration of Cu^{+} ions. Care should be taken to ensure the Cu^{+} ions are not oxidised to Cu^{2+} when these experiments are attempted.

- In Section 5.5.6 it was noted that equipment used to conduct RDE experiments did not allow the use of rotation rates other than 1500, 2000, 2500 and 3000 rpm. This could introduce inaccuracies in the determination of *(i)* active working electrode surface areas, *(ii)* current densities at infinite rotation rates and *(iii)* diffusion coefficients. Errors associated with these determinations would inevitably lead to inaccuracies in the calculation of j_o, α, k_s and k_m values. It would be informative to repeat the experiments described in Chapter 5 with RDE equipment that can achieve a wider range of rotation rates.

- The rotating working electrode tip containing the graphite particles required for experimental work was not available commercially and therefore had to be constructed in-house. Due to the nature of the electrode construction (refer to Section 5.4.1) it was necessary to determine the active electrode surface area prior to each set of experiments. In order to improve the accuracy and reproducibility of experimental current density values, future electrode tips should be

prepared by a commercial manufacturer. This may be achieved by supplying the manufacturer with graphite rods (ET-10, Electrographite Carbon Co.) which could be inserted into electrode blanks.

6 CONCLUSIONS

In this chapter it will be shown how the objectives of the project, originally stated in Chapter 1, were achieved via the research activities described in the dissertation.

Detailed conclusions related to the research conducted with each phase of the project were provided in Chapters 3 to 5. The discussions in this chapter are intended to provide an overview of the most important conclusions rather than the provision of detailed information already provided in the relevant chapters.

To facilitate this discussion, a summary of the aims and objectives of the project will be provided, followed by a discussion of the main conclusions arrived at during different phases of the research project.

6.1 AIMS AND OBJECTIVES

The general aim of the project was to investigate the feasibility of recovering Platinum Group Metals (PGMs) from refinery effluents via an electrochemical process rather than conventional chemical reduction techniques. There are several advantages associated with the use of electrochemical recovery methods. These include aspects related to health and safety, the environment, process efficiencies, reduced chemical loads and the small size of an electrochemical reactor in comparison to traditional chemical reduction plants.

It was decided to investigate the possibility of depositing low concentrations of PGMs on a cathode material contained in an electrochemical reactor, using a selected refinery effluent. The Palladium Mother Liquor (PML) generated at Anglo Platinum's Precious Metals Refinery (PMR) was selected for this purpose. This stream was selected

because *(i)* previous test work indicated that palladium complexes in the effluent were amenable to electrochemical reduction, *(ii)* the recovery of palladium from the solution would have financial benefits, and *(iii)* the PML could be used to assess the influence of amminated PGM complexes on recovery.

The recovery of PGMs (palladium and platinum) from PML solutions would be deemed successful if their concentrations could be reduced to levels equal to or better than that achieved via the current chemical reduction process. Current process specifications require a total PGM concentration in effluent streams of < 10 mg l^{-1}, with no single PGM present at concentrations > 2 mg l^{-1}.

To develop a practical electrochemical reactor capable of recovering PGMs from a PML solution, inputs from the chemistry and chemical engineering disciplines were required. As a consequence, two research projects were initiated. One project focussed on fundamental issues related to the interaction of metal ions with a particular electrode material, whilst the other focussed on engineering aspects associated with the design of an electrochemical reactor. The fundamental research project was described in this dissertation.

Fundamental research activities concentrated on the provision of critical information required to operate an electrochemical reactor. This information was in turn used to assist in the development of a bench scale electrochemical reactor via the engineering project[39].

6.1.1 Fundamental Research Objectives

Based on the aims of the project and limited availability of fundamental information in the literature, specific objectives were defined for the fundamental research project. These objectives were originally described in Chapter 1 (Section 1.5) and are restated here. To facilitate future

references in this chapter, each of the objectives were numbered.

Objective 1

Establish methodologies that can be used to develop a qualitative understanding of the interactions occurring at an electrode-solution interface. The interaction between metal ions found in a typical PML solution and a selected cathode material will be investigated. Special attention will be given to reactions involving the deposition of metals on a particular cathode, as well as factors that will catalyse or inhibit certain reduction-oxidation (redox) reactions. Although issues related to the possible anodic dissolution of metals deposited on a cathode will receive some attention, the emphasis will be placed on the recovery of PGMs, as stated in the aims of the investigation.

Objective 2

Use the established methodologies to assess the feasibility of recovering palladium and platinum from the PML using a particular cathode material in the proposed electrochemical reactor.

Objective 3

If qualitative investigations indicated that the use of a particular cathode material was feasible, quantify the level of PGM reduction in the PML solution. This will confirm if the use of the proposed cathode material would result in the removal of the total PGMs present in the PML solution to concentrations < 10 mg l^{-1}, with no single PGM present at concentrations > 2 mg l^{-1}, as described in Section 1.2.1.

Objective 4

Quantify the possible influence of amminated PGM complexes on the overall recovery of PGMs from a typical PML solution.

Objective 5

Establish methodologies that may be used to determine kinetic parameters associated with a particular redox couple. These parameters include exchange current densities, electron transfer coefficients, standard rate constants and mass transfer coefficients.

Objective 6

Use the established methodologies to determine kinetic parameters for selected redox couples. This data will quantify the rate at which the reactions take place at the electrode-solution interface, and can also be used for future engineering modelling purposes.

6.2 CHAPTER 3 (PHASE 1)

Phase 1 of the fundamental research project involved the development of a qualitative understanding of the interactions of the different metal ions contained in the PML with a particular cathode material. To achieve this, Cyclic Voltammetry (CV) was used. The interpretation of voltammograms obtained from CV experiments conducted in multi-component solutions such as the PML can be difficult, especially when metal deposition reactions occur.

In Chapter 3 the objective of the research activities was to develop the necessary methodologies to interpret voltammograms obtained when multi-component solutions were analysed, and metal deposition occurred.

The interaction of the various metal ions contained in a typical PML solution with a glassy carbon working electrode was investigated via CV. Single component synthetic solutions containing metal ions normally found in a PML solution were prepared and analysed. The resultant voltammograms were studied in order to understand the interaction of the single metal ion with a glassy carbon electrode. Following the successful investigation of single component solutions, the complexity of the synthetic solutions was increased to contain different combinations of metal ions.

To assist in the interpretation of voltammograms, techniques associated with *(i)* the variation of experimental potential scan ranges, *(ii)* the use of a Fe^{3+} witness ion, and *(iii)* the use of a platinum disc electrode were employed.

Finally voltammograms for synthetic solutions were compared to voltammograms of a typical PML solution. These comparisons led to a qualitative interpretation of the interaction between the metal ions contained in a PML solution and a glassy carbon working electrode.

It was concluded that voltammograms of typical PML solutions containing a combination of many different metal ions, and other cations and anions (refer to Table 1.1) could be interpreted by comparison to voltammograms of synthetic solutions containing only copper, palladium and platinum ions in a 0.1 M HCl matrix. The deposition of a combination of copper, palladium and platinum metal centres from PML solutions (via a glassy carbon working electrode) was predicted.

The research activities associated with Chapter 3 resulted in the achievement of Objective 1 as defined in Section 6.1.1.

6.3 CHAPTER 4 (PHASE 2)

Phase 2 of the fundamental research project involved the application of methodologies developed in Phase 1 to assess the feasibility of using particular cathode materials in the proposed electrochemical reactor.

6.3.1 Feasibility and Validation

The objective of the research activities described in Chapter 4 was to assess the feasibility of using isostatically pressed graphite particles (grade ET-10) as a cathode material in the electrochemical reactor developed via the engineering project.

Synthetic solutions containing combinations of copper, palladium and

platinum in a 0.1 M HCl matrix were analysed via CV, using a working electrode constructed of isostatically pressed graphite particles (referred to as a graphite working electrode in the rest of the chapter). The resulting voltammograms were compared to those obtained when PML solutions were analysed under identical conditions. Voltammograms were interpreted by application of methodologies developed in Chapter 3.

If the deposition of copper, palladium or platinum from single component synthetic solutions were predicted via CV analyses, the predictions were validated. The graphite working electrode was held at potentials where the deposition of a particular metal would be favourable, as predicted from CV experiments. Following the metal deposition experiment, the presence of the metal on the graphite working electrode was confirmed by observing the active surface under an optical microscope.

From the metal deposition experiments and the interpretation of voltammograms, it was concluded that palladium and platinum could be deposited on the graphite working electrode from PML solutions. Due to the similarities of the potentials at which metal deposition was favourable, copper co-deposited with palladium and platinum.

6.3.2 Exhaustive Electrolysis

With the feasibility of palladium and platinum deposition confirmed, the extent of PGM removal from PML solutions was established. This was achieved by conducting exhaustive electrolysis experiments with PML solutions and a graphite working electrode. It was demonstrated that the concentrations of palladium and platinum in the PML solution could be reduced to < 1 mg l^{-1}. Copper was co-deposited with the PGMs, and the concentration of copper remaining after exhaustive electrolysis was < 1 mg l^{-1}.

6.3.3 Amminated Complexes

The influence of amminated PGM complexes on the overall recovery of palladium and platinum from PML solutions was investigated via CV and exhaustive electrolysis experiments. The formation of amminated complexes in synthetic solutions was achieved by addition of NH_3 solution to adjust the pH values of the solutions to ca. 9.5. In the case of PML solutions NaOH was added to adjust the pH of the solutions to ca. 9.5. The rationale was that the NH_4^+ ions present in the PML (refer to Table 1.1) would deprotonate on addition of OH^- ions to form NH_3 ligands. These ligands would in turn form complexes with PGM ions present in the PML.

The interaction between PML solutions containing amminated PGM complexes and a graphite working electrode was established by CV experiments and interpretation of the resulting voltammograms. It was concluded that copper, palladium and platinum deposited. The deposition of the metals all occurred at more negative potentials relative to PML solutions that were not treated with NaOH. This was ascribed to the stability of the amminated metal-ligand complexes.

Exhaustive electrolysis experiments were conducted to establish the extent of PGM removal. It was found that the concentrations of palladium and platinum remaining in the PML were reduced to 7.0 mg l^{-1} and 3.5 mg l^{-1} respectively. The concentration of copper in solution was reduced to 1.1 mg l^{-1}. It should however be noted that a large fraction of copper was precipitated from the PML after addition of NaOH. The copper concentration prior to NaOH addition was 210 mg l^{-1}, compared to a concentration of 85 mg l^{-1} after NaOH addition.

The fact that the specification of total PGM concentrations below 10 mg l^{-1}

with no single PGM present at concentrations greater than 2 mg l^{-1} was not achieved after exhaustive electrolysis experiments may be explained by the presence of additional PGM complexes in the pH-adjusted PML solutions. It is possible that the onset of the hydrogen reduction current masked the presence of additional reduction peaks associated the deposition of PGMs. Since the working electrode was held at a potential more positive to that required for the evolution of significant quantities of hydrogen gas, the PGMs associated with these additional complexes would not be reduced.

Alternatively the kinetics of metal deposition from amminated complexes present in the PML solution was slow in comparison to the time scale of the exhaustive electrolysis experiments

It should be noted that the experiments related to amminated complexes were designed to illustrate the maximum possible influence on the recovery of PGMs.

6.3.4 General

The research activities associated with Chapter 4 resulted in the achievement of Objectives 2 to 4 as defined in Section 6.1.1.

6.4 CHARACTERISTICS OF VOLTAMMOGRAMS

Throughout Chapters 3 and 4 it was noted that the presence of palladium and platinum metal centres on a working electrode surface initiated the deposition of other metals originally present as ions in the test solution.

In Chapter 3, where a glassy carbon working electrode was employed for the majority of experiments, it was found that the presence of palladium metal centres on the electrode surface facilitated the deposition of copper from solutions containing a mixture of copper and palladium ions. When test solutions containing a combination of copper, palladium and platinum

ions were analysed, the presence of platinum metal centres initiated the deposition of copper and palladium.

If a graphite working electrode (isostatically pressed particles, grade ET-10) was employed as described in Chapter 4, it was noted that the presence of palladium on the electrode surface also facilitated the deposition of copper. When a mixture of copper, palladium and platinum was analysed, it was found that the presence of palladium metal centres also played a role in the deposition of a combination of copper and platinum.

The fact that particular metal centres played a role in the deposition of other metal ions present in the test solution was attributed to the electrocatalytic properties of the deposited metal centres.

It was concluded that the potential at which particular metal centres deposited on a working electrode surface determined the subsequent interactions of other metal ions present in the test solution. These interactions in turn led to the characteristics of voltammograms recorded for CV experiments. This conclusion was confirmed by a comparison of voltammograms recorded via glassy carbon and graphite working electrodes.

When the interaction between a single component synthetic solution containing palladium ions and a glassy carbon working electrode was investigated via CV, the reduction peak associated with the deposition of palladium metal was observed at ca. -0.23 V (refer to Figure 3.6). Similar experiments involving a single component platinum solution indicated the presence of the reduction peak ascribed to the deposition of platinum at ca. -0.18 V (refer to Figure 3.9).

If a graphite working electrode was used instead of a glassy carbon electrode, a reduction current ascribed to the evolution of hydrogen on

palladium metal centres (deposited from a synthetic single component solution) was observed at potentials more negative than ca. 0.15 V, as shown via Figure 4.4. The reduction current indicating the evolution of hydrogen gas on platinum metal centres deposited from a single component synthetic solution was observed at potentials more negative than ca. -0.25 V (refer to Figure 4.7).

In the case of the graphite working electrode, palladium metal centres were deposited as CV experiments proceeded to more negative potentials. Since the deposition of palladium occurred at significantly more positive potentials relative to platinum, the characteristics of the voltammograms recorded for test solutions containing a combination of palladium, platinum and copper ions were a function of the interaction of the metal ions in solution with palladium metal centres.

When a glassy carbon working electrode was used, the reduction peaks for the deposition of palladium and platinum from single component solutions were observed at potentials of ca. -0.23 V and ca. -0.18 V respectively. In this case the deposition of copper and palladium from multi-component solutions essentially occurred on platinum metal centres.

6.5 CHAPTER 5 (PHASE 3)

The third phase of the fundamental research project involved the quantitative determination of kinetic parameters. In the context of this dissertation, the determination of kinetic parameters refers to experimental values obtained for exchange current densities (j_o), electron transfer coefficients (α), standard rate constants (k_s) and mass transfer coefficients (k_m).

Values for these parameters would contribute to the fundamental understanding of interactions between metal ions found in the PML and the graphite cathode evaluated in Chapter 4, by quantifying the rate at

which the interactions at the electrode surface occurs. The parameters can also be used for engineering modelling purposes, where the performance of an electrochemical reactor under specific operating conditions is predicted.

The objective of the research activities associated with Chapter 5 was to evaluate experimental procedures that could be used to determine kinetic parameters for selected redox couples. It was decided to focus research activities on the determination of kinetic parameters for a single component synthetic solution containing one of the major metal ions found in the PML. The background electrolyte of this synthetic solution was prepared to approximate the matrix of an actual PML effluent.

This approach allowed the accurate determination of kinetic parameters for the redox couples associated with a particular metal ion. At the same time the applicability of different experimental procedures was evaluated.

Since the evaluation of experimental procedures was one of the research objectives, it was important to select a system that would not pose unnecessary complications when experiments are conducted. It was decided to use copper in a background electrolyte approximating that found in a PML solution (referred to as the Cu solution) instead of palladium or platinum, where the catalytic evolution of hydrogen on deposited PGM centres would play a significant role.

In addition to the Cu solution, a $Fe(CN)_6^{3-}$ solution was used as a reference. The purpose of using the $Fe(CN)_6^{3-}/Fe(CN)_6^{4-}$ redox couple as a reference was to validate experimental procedures and data handling procedures employed for the Cu solution.

6.5.1 Identification of Redox Couples

For the Cu solution, two redox couples were identified. CV experiments were used to identify the redox couples. The first redox couple involved the reduction of Cu^{2+} to Cu^{+} on a graphite electrode surface, whilst the second redox couple was ascribed to the reduction of Cu^{+} to Cu^{0} on a graphite electrode surface after completion of the nucleation process.

6.5.2 Experimental

To determine kinetic parameters, plots of the current density (j) versus potential (E) of the particular redox couple under investigation are required. These $j-E$ plots may be recorded by means of potential step or slow potential sweep experiments under potentiostatic conditions, i.e. a three-electrode set-up is employed. It was concluded that slow potential sweep experiments were preferable in cases where metal deposition reactions occurred. The reason was that more metal deposited on the electrode under study in the case of potential step experiments. This changed the characteristics of the electrode, which in turn made it difficult to interpret or reproduce results. Slow potential sweep experiments were therefore employed when kinetic parameters were determined.

6.5.3 Active Surface Area

The graphite working electrode used for the calculation of kinetic parameters was not available commercially, and had to be constructed in-house. Due to the nature of construction, the electrochemically active surface area of the electrode had to be determined experimentally.

It was concluded that the application of the Levich equation to slow potential sweep experimental data recorded with a Rotating Disc Electrode (RDE) would be the most appropriate technique to determine the electrochemically active surface area of the graphite working electrode. The conclusion was based on the fact that kinetic parameters reported in this chapter were also calculated from $j-E$ plots involving a RDE. This

compensated for deviations from ideal conditions introduced as a result of the electrode material (porosity) and experimental equipment (eccentricity).

6.5.4 Determination of Kinetic Parameters

Quantitative rate parameters can only be established in conditions where either electron transfer or mass transport is the sole rate determining step over a particular portion of a $j-E$ plot. The rate of mass transport for a particular experiment could be increased to achieve these conditions. Mass transport conditions may be increased in a controlled fashion by means of RDE experiments. The equipment used to conduct the experiments described in Chapter 5 was capable of producing accurate rates of 1500, 2000, 2500 and 3000 rotations per minute (rpm). If a particular redox couple has a high k_s value, electron transfer may remain reversible even under conditions where a rate of 3000 rpm is employed. This implied that rate parameters could not be determined unless a RDE system capable of substantially higher rotation rates was used.

Alternatively, procedures exist where data obtained at lower rotation rates (1500 to 3000 rpm for experiments described in this chapter) can be extrapolated to calculate the current density where the rate of rotation approximates infinity. Hence, mass transport limitations are removed, resulting in electron transfer controlled conditions. This approach was employed in Chapter 5.

Values for j_o and α were calculated by constructing Tafel plots from calculated current densities at infinite rotation rates. Since current densities were calculated for cathodic processes only, the equilibrium potential (E_e) had to be established before j_o and α could be determined. Due to the inaccuracies associated with the determination of E_e values, j_o and α were reported in ranges rather than discrete values.

A similar approach was followed for the determination of k_s values. In this case rate constant values for a cathodic reaction ($\vec{k}$) was calculated from current densities at infinite rotation rates. The $\vec{k}$ data was plotted as a function of potential. A k_s value was obtained at the formal potential ($E^{\circ'}$). Due to the inaccuracies associated with the determination of $E^{\circ'}$ values, k_s was reported in ranges rather than discrete values.

Values for k_m were determined by application of RDE theory and the experimental determination of diffusion coefficient values, or the direct application of RDE experimental data.

6.5.5 General

The research activities associated with Chapter 5 resulted in the achievement of Objectives 5 and 6, defined in Section 6.1.1.

6.6 FUTURE RESEARCH

In Chapter 1 (Section 1.3), it was noted that the feasibility of PGM recovery via an electrochemical reactor had to be demonstrated within a reasonably short period. The fundamental research project therefore concentrated on the provision of information that was critical to the development of the electrochemical reactor.

The areas of research covered in the fundamental research project were defined by issues related to the design of a practical electrochemical reactor. Due to the focus of the fundamental research project it was not possible to investigate the many complex fundamental issues in detail. The intention was to provide critical information required for the design of an electrochemical reactor, whilst identifying areas where additional fundamental research would be required.

In Chapters 3 to 5 additional areas of research associated with a particular phase of the project were identified and listed. A summary of the most

important issues will be provided in this section.

6.6.1 Metal Deposits

It would be necessary to determine the composition of metal deposits obtained under particular operating conditions. This will provide an indication of the degree of metal separation and product purity.

The morphology of the metal deposit is also important. If a powder deposit is obtained, it may be possible to recover the metals from the cathode by mechanical means. If the recovery of products from the cathode by mechanical means is deemed to be a viable option, further investigations related to the factors controlling the morphology of metal deposits will be required.

6.6.2 Recovery of PGMs from Cathode

The quantitative removal of palladium and platinum from a PML solution was demonstrated via the research activities described in this dissertation. To make the use of an electrochemical reactor in a refinery practical, the deposited PGMs would have to be recovered from the cathode.

Research related to metal recovery processes (e.g. anodic dissolution) and the mechanisms controlling these processes need to be conducted.

6.6.3 Hydrogen Evolution

From an electroanalytical point of view, the evolution of hydrogen becomes problematic when quantitative experiments (e.g. the determination of kinetic parameters) are carried out. It would be necessary to investigate the application of deconvolution techniques to overcome the interference of hydrogen reduction currents.

The generation of hydrogen gas via an electrochemical reactor is also problematic from a safety and efficiency point of view. Further research associated with the inhibition of hydrogen evolution may assist in

controlling the problem.

6.6.4 Speciation

A detailed fundamental understanding of the interaction of PGM complexes with a particular cathode material would require knowledge of the different metal-ligand species present in solution.

Further studies associated with the application of different speciation methodologies would be required.

6.6.5 Reaction Mechanisms

In addition to knowing which PGM complexes are present in solutions treated via the electrochemical reactor, it is important to understand the mechanisms which lead to the deposition of metals on a particular cathode material. This includes aspects related to the formation of intermediates, adsorption processes, and the influence of sample matrices.

If the anodic dissolution of metal deposits from the cathode of an electrochemical reactor is feasible, further research related to the mechanisms controlling these processes would also be required. An important aspect would be the influence of metal oxides on dissolution efficiencies.

A study of reaction mechanisms may involve the application of analytical techniques such as spectroelectrochemistry, and the use of a Rotating Ring Disc Electrode (RRDE).

6.7 FINAL COMMENTS

The objectives of the project were achieved via the research activities described in this dissertation. In addition, the methodologies developed as a result of the research project may be used to investigate the possible electrochemical recovery of PGMs from other refinery effluents.

7 APPENDICES

Appendix A — Voltammograms of single component synthetic solutions of antimony, bismuth, gold, lead, rhodium, ruthenium and tellurium deposited within the potential range applicable to a 0.1 M HCl matrix and a glassy carbon working electrode.

Figure A1 to Figure A7

Appendix B — Data plots used to calculate kinetic parameters for redox couples associated with the $Fe(CN)_6^{3-}$ and Cu solutions as described in Chapter 5.

Figure B1 to Figure B5

APPENDIX A

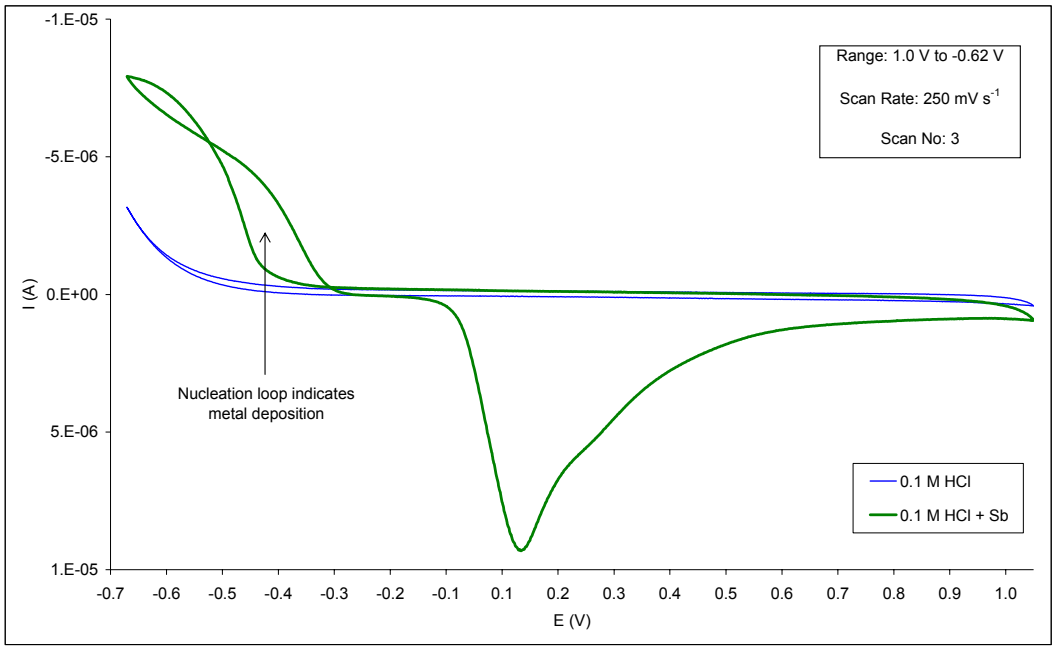

Figure A1 Cyclic voltammograms of a 0.1 M HCl background electrolyte, and the background electrolyte containing 48 mg l^{-1} antimony, using a glassy carbon working electrode.

APPENDIX A

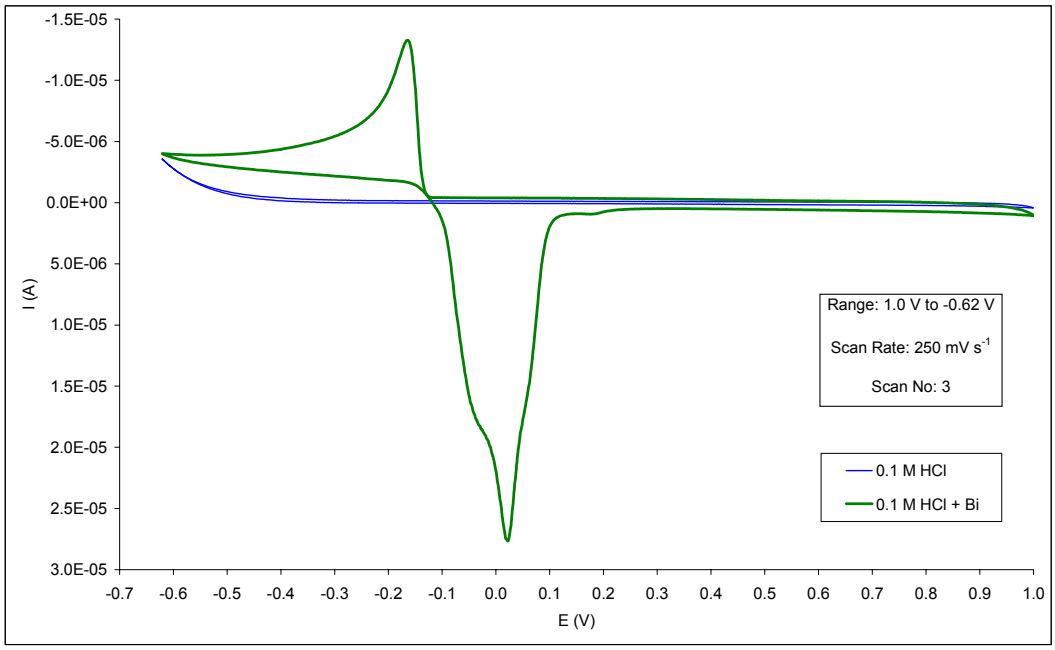

Figure A2 Cyclic voltammograms of a 0.1 M HCl background electrolyte, and the background electrolyte containing 48 mg l^{-1} bismuth, using a glassy carbon working electrode.

APPENDIX A

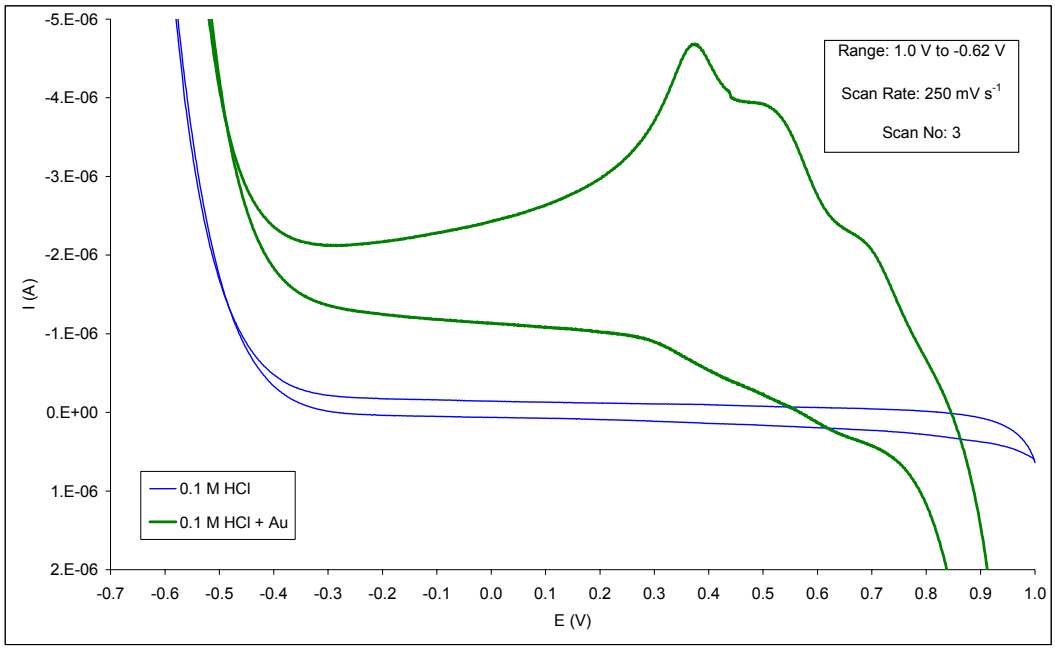

Figure A3 Cyclic voltammograms of a 0.1 M HCl background electrolyte, and the background electrolyte containing 50 mg l^{-1} gold, using a glassy carbon working electrode.

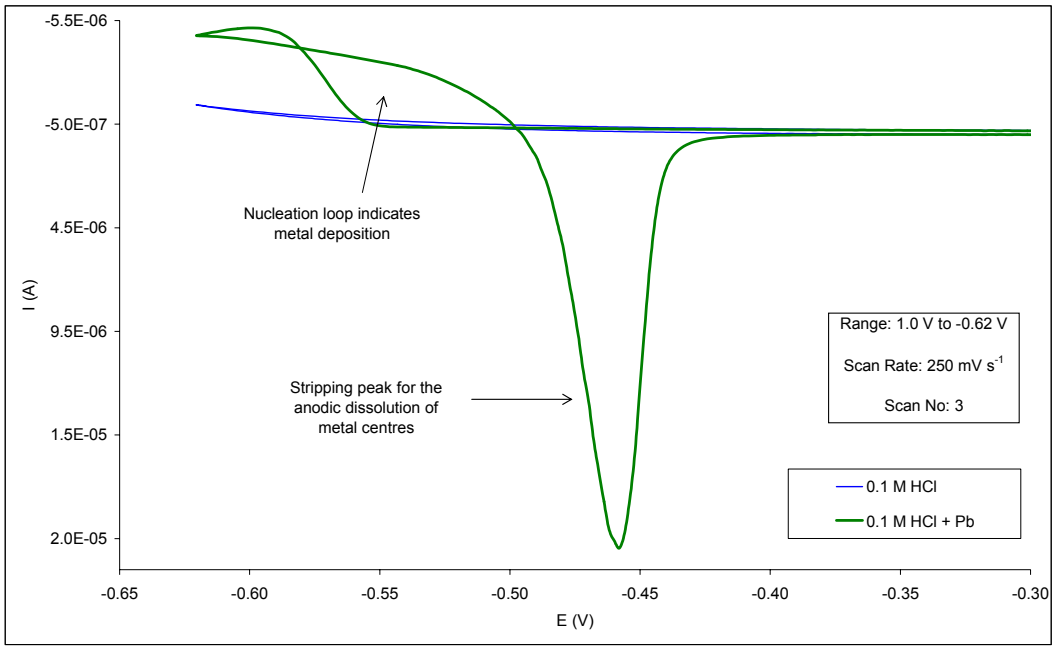

Figure A4 Cyclic voltammograms of a 0.1 M HCl background electrolyte, and the background electrolyte containing 48 mg l^{-1} lead, using a glassy carbon working electrode.

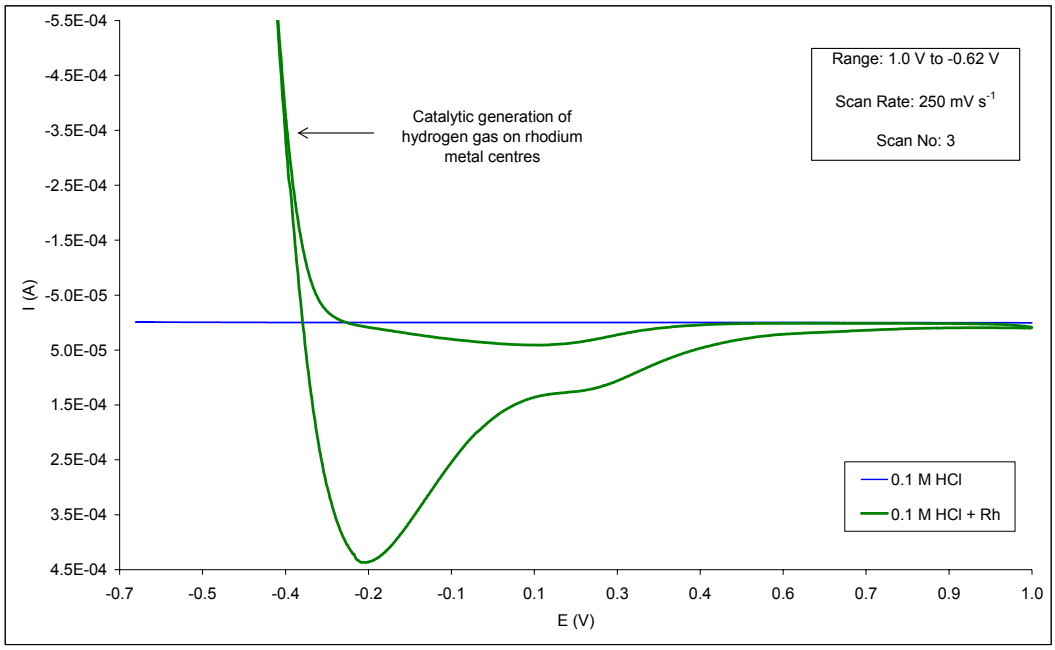

Figure A5 Cyclic voltammograms of a 0.1 M HCl background electrolyte, and the background electrolyte containing 48 mg l^{-1} rhodium, using a glassy carbon working electrode.

APPENDIX A

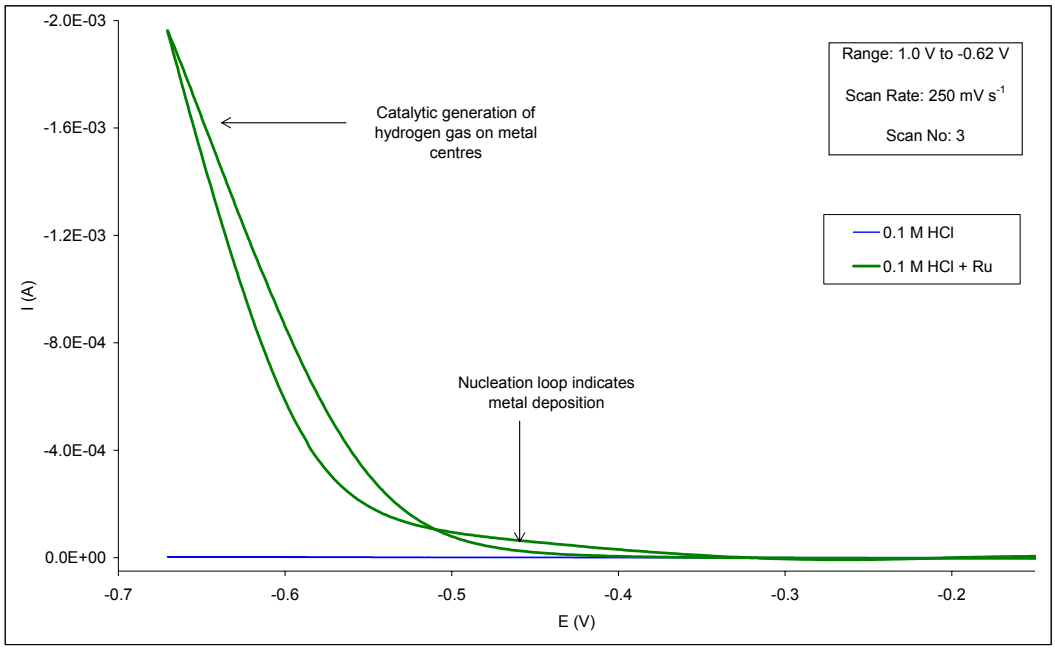

Figure A6 Cyclic voltammograms of a 0.1 M HCl background electrolyte, and the background electrolyte containing 48 mg l^{-1} ruthenium, using a glassy carbon working electrode.

APPENDIX A

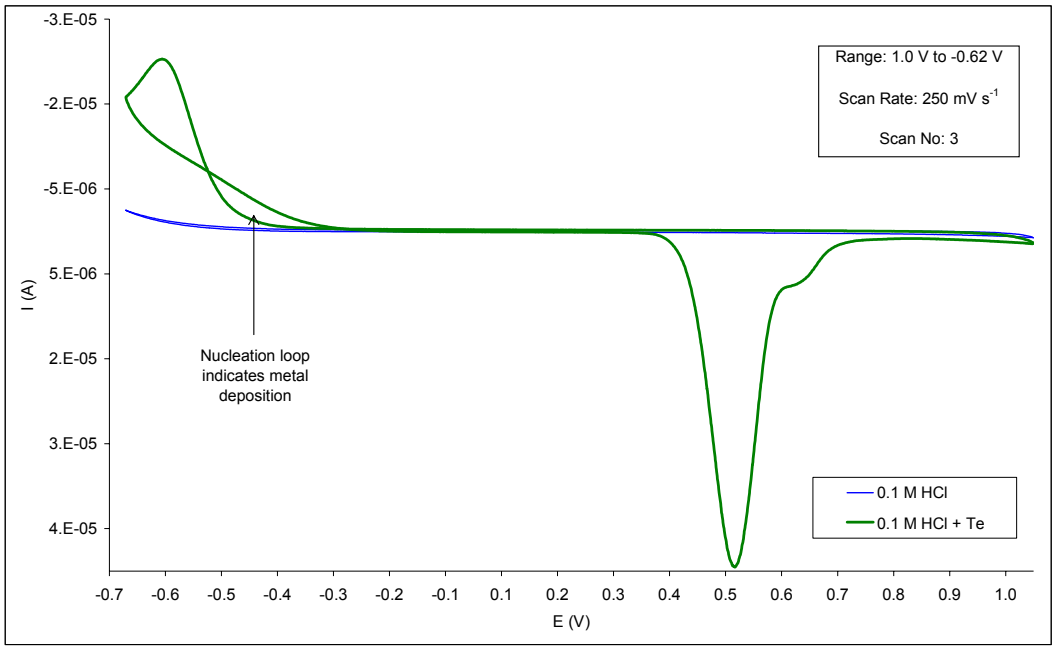

Figure A7 Cyclic voltammograms of a 0.1 M HCl background electrolyte, and the background electrolyte containing 48 mg l^{-1} tellurium, using a glassy carbon working electrode.

APPENDIX B

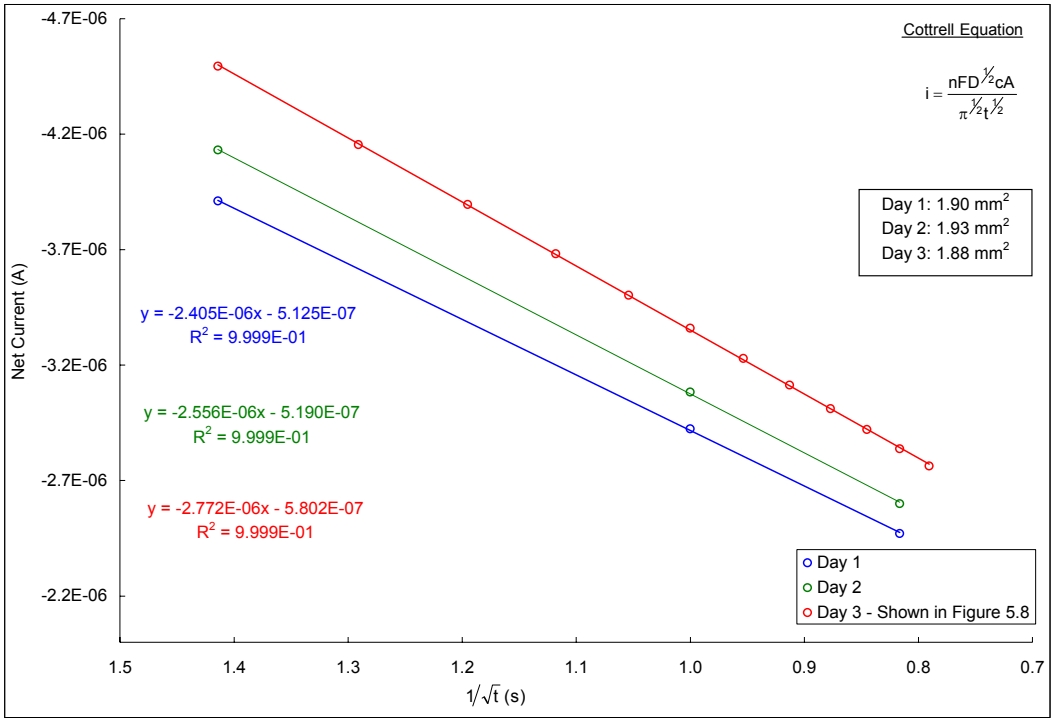

Figure B1 Plots used to calculate the active surface area of a graphite working electrode via the Cottrell equation. Data obtained from experiments conducted on $Fe(CN)_6^{3-}$ solutions on three different days.

Note: Interval times of 0.5 s were used for chronoamperometric experiments conducted on Days 1 and 2, as opposed to interval times of 0.1 s employed on Day 3.

APPENDIX B

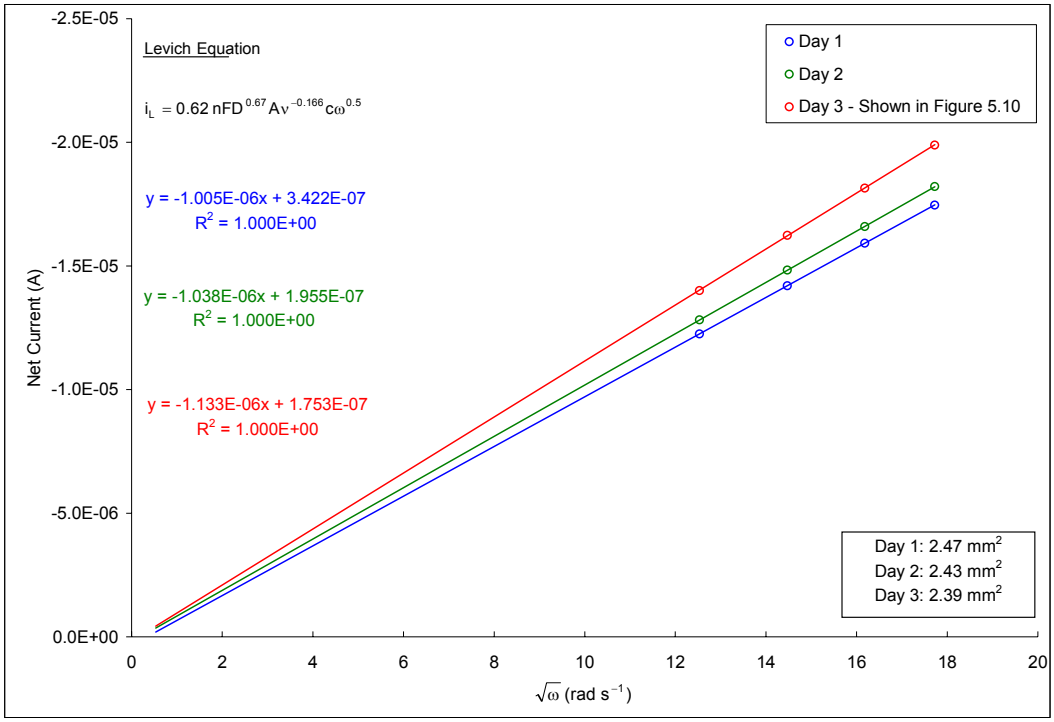

Figure B2 Plots used to calculate the active surface area of a graphite working electrode via the Levich equation. Data obtained from experiments conducted on $Fe(CN)_6^{3-}$ solutions on three different days.

APPENDIX B

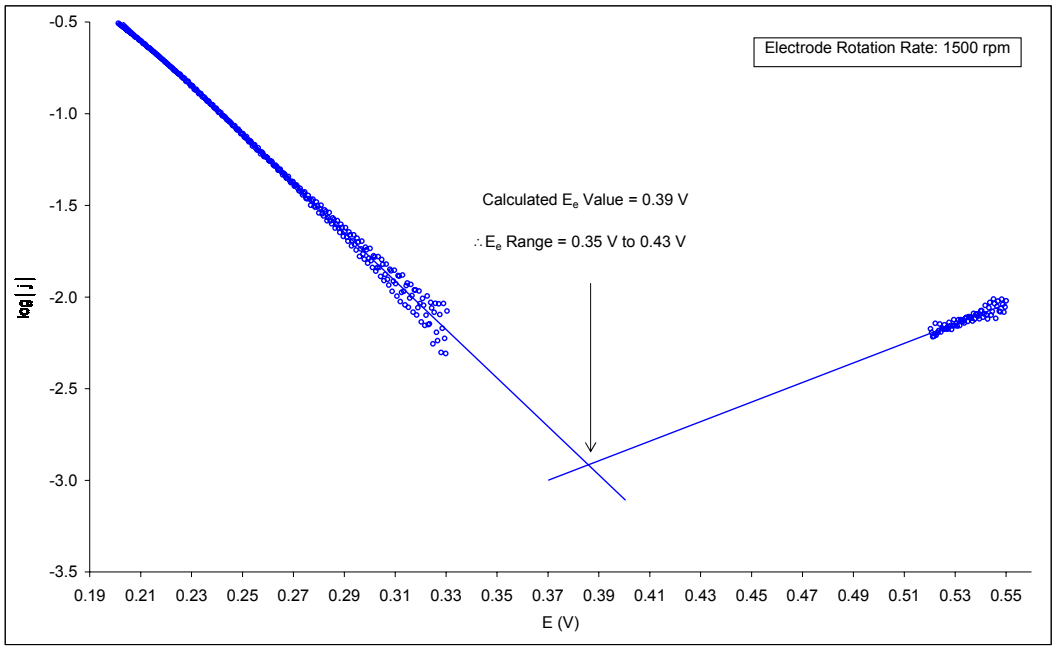

Figure B3 Estimation of the equilibrium potential for the Cu^{2+}/Cu^{+} (C) redox couple, using a Cu solution and a graphite working electrode.

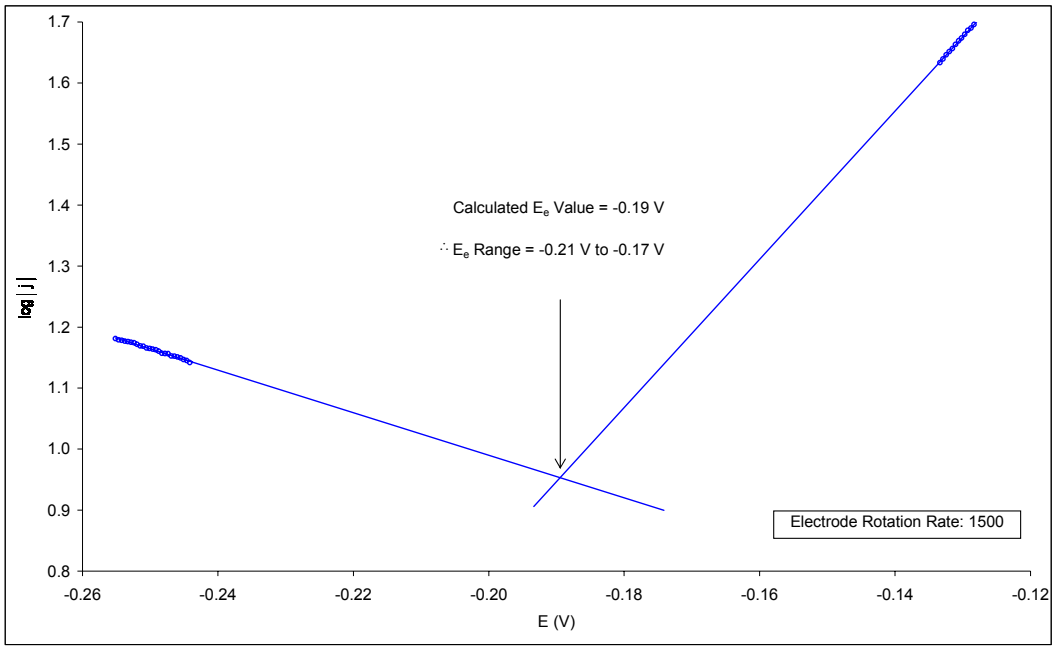

Figure B4 Estimation of the equilibrium potential for the Cu^{+}/Cu^{0} (C+Cu) redox couple, using a Cu solution and a graphite working electrode.

APPENDIX B

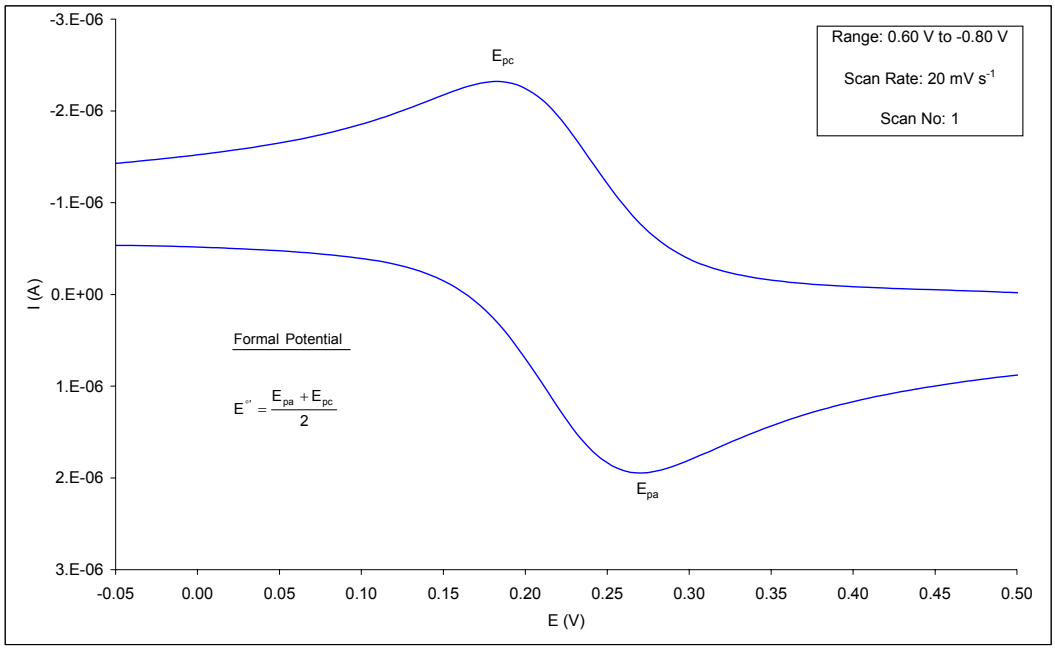

Figure B5 Estimation of formal potential for the $Fe(CN)_6^{3-}/Fe(CN)_6^{4-}$ redox couple associated with a $Fe(CN)_6^{3-}$ solution, using a graphite working electrode.

8 REFERENCES

1 . Gimeno, A., Hernández Creus, A., Carro, P., González, S., Salvarezza, R.C., and Arvia, A.J. Electrochemical formation of palladium islands on HOPG: Kinetics, morphology, and growth mechanisms, *J. Phys. Chem. B*, vol. 106, no. 16, 2002, pp. 4232-4244.

2 . Zubimendi, J.L., Vázques, L., Ocón, P., Vara, J.M., Triaca, W.E., Salvarezza, R.C., and Arvia, A.J. Early stages of platinum electrodeposition on highly oriented pyrolytic graphite: Scanning tunnelling microscopy imaging and reaction pathway, *J. Phys. Chem.*, vol. 97, no. 19, 1993, pp. 5095-5102.

3. Li, F., Zhang, B., Dong, S., and Wang, E. A novel method of electrodepositing highly dispersed nano palladium particles on glassy carbon electrode, *Electrochim. Acta*, vol. 42, no. 16, 1997, pp. 2563-2568.

4 . Georgolios, N., Jannakoudakis, D., and Karabinas, P. Pt electrodeposition on PAN-based carbon fibres, *J. Electroanal. Chem.*, vol. 264, 1989, pp. 235-245.

5 . Naohara, H., Ye, S., and Uosaki, K. Electrochemical layer-by-layer growth of palladium on Au(111) electrode surface: Evidence of important role of adsorbed Pd complex, *J. Phys. Chem. B*, vol. 102, no. 22, 1998, pp. 4366-4373.

6 . Le Penven, R., Levason, W., and Pletcher, D. Studies of the electrodeposition of palladium from baths based on $\left[Pd(NH_3)_2X_2\right]$ salts, *J. Appl. Electrochem.*, vol. 20, 1990, pp. 399-404.

7 . Le Penven, R., Levason, W., and Pletcher, D. Studies of platinum electroplating baths Part I: The chemistry of a platinum tetrammine baths, *J. Appl. Electrochem.*, vol. 22, 1992, pp. 415-420.

8 . Gregory, A.J., Levason, W., Noftle, R.E., Le Penven, R., and Pletcher, D. Studies of platinum electroplating baths Part III: The electrochemistry of $Pt(NH_3)_{4-x}(H_2O)_x^{2+}$ and $PtCl_{4-x}(H_2O)_x^{(2-x)-}$, *J. Electroanal. Chem.*, vol. 399, 1995, pp. 105-113.

9 . Kim, K.S., Gossmann, A.F., and Winograd, N. X-Ray photoelectron spectroscopic studies of palladium oxides and the palladium-oxygen electrode, *Anal. Chem.*, vol. 46, no. 2, Feb. 1974, pp. 197-200.

10 . Hoare, J.P. *J. Electrochem. Soc.*, vol. 111, 1964, p. 610, (quoted from Ref. 9).

11 . Gossner, K., and Mizerna, E. The anodic behaviour of Pd electrodes in 1 M H_2SO_4, *J. Electroanal. Chem.*, vol. 125, 1981, pp. 347-358.

12 . Bolzán, A.E., Martins, M.E., and Arvia, A.J. The complex processes involved at Pd electrodes in 1 M H_2SO_4 in the potential range of electroadsorption-electrodesorption reactions, *J. Electroanal. Chem.,* vol. 157, 1983, pp. 339-358.

13 . Bolzán, A.E., Martins, M.E., and Arvia, A.J. The electrodissolution of base palladium in relation to the oxygen electroadsorption and electrodesorption in sulphuric acid solution, *J. Electroanal. Chem.,* vol. 172, 1984, pp. 221-233.

14 . Burke, L.D., and Casey, J.K. An examination of the electrochemical

behaviour of palladium electrodes in acid, *J. Electrochem. Soc.,* vol. 140, no. 5, May 1993, pp. 1284-1291.

15 . Burke, L.D., and Casey, J.K. An examination of the electrochemical behaviour of palladium in base, *J. Electrochem. Soc.,* vol. 140, no. 5, May 1993, pp. 1292-1298.

16 . Bolzán, A.E. Phenomenological aspects related to the electrochemical behaviour of smooth palladium electrodes in alkaline solutions, *J. Electroanal. Chem.,* vol. 380, 1995, pp. 127-138.

17 . Burke, L.D., and Roche, M.B.C. An electrochemical investigation of monolayer and multilayer oxide films on palladium in aqueous media, *J. Electroanal. Chem.,* vol. 186, 1985, pp. 139-154.

18 . Chierchie, T., and Mayer, C. Structural changes of surface oxide layers on palladium, *J. Electroanal. Chem.,* vol. 135, 1982, pp. 211-220.

19 . Hawkins, F.A., and Nicol, M.J. *An Electrochemical Investigation of the Dissolution and Passivation of Platinum in Acid Solutions*, Randburg, South Africa: National Institute for Metallurgy, Apr. 1976, pp. 1-37. (Report No. 1800).

20 . Folquer, M.E., Zerbino, J.O., Tacconi, N.R., and Arvia, A.J. Kinetics of aging of the oxygen monolayer on platinum under a complex potentiodynamic pertubation program, *J. Electrochem. Soc.,* vol. 126, no. 4, Apr. 1979, pp. 592-598.

21 . Ragotzky, V.S., and Tarasevich, M.R. Oxygen adsorption on platinum and platinum metals Part I: Investigation of the adsorption mechanism by the potentiodynamic method, *J. Electroanal. Chem.,*

vol. 101, 1979, pp. 1-17.

22 . Rand, D.A.J., and Woods, R. A study of the dissolution of platinum, palladium, rhodium and gold electrodes in 1 M sulphuric acid by cyclic voltammetry, *J. Electroanal. Chem.,* vol. 35, 1972, pp. 209-218.

23 . Styrkas, A.D., and Styrkas, D. Electrochemical dissolution of metals of the platinum group by alternating current, *J. Appl. Electrochem.*, vol. 25, 1995, pp. 490-494.

24 . Lubert, K.-H., Guttmann, M., and Beyer, L. Voltammetric study of the immobilization of palladium at the surface of carbon paste electrodes, *Electroanal.*, vol. 8, no. 4, 1996, pp. 320-325.

25 . Lubert, K.-H., Guttmann, M., and Beyer, L. Electrode reactions and accumulation of hydrogen at carbon paste electrodes in the presence of tetrachloropalladate, *J. Electroanal. Chem.,* vol. 462, 1999, pp. 174-180.

26 . Lubert, K.-H., Guttmann, M., and Beyer, L. Formation of palladium complex at carbon paste surface in chloride solution as studied by cyclic voltammetry, *Collect. Czech. Chem. Comm.*, vol. 66, 2001, pp. 1457-1472.

27 . Dunsch, L., Inzelt, G., Horanyi, G., and Lubert, K.-H. Electrochemical studies of polymeric carbons. II. Surface layer formation on glassy carbon electrodes in chloride solutions as studied by radiotracer techniques, *Isotopenpraxis*, vol. 26, no. 7, 1990, pp. 343-346.

28 . Al-Akl, A., and Attard, G.A. Anion effects in the UPD of copper on Pd/Pt(111) bimetallic electrodes, *J. Phys. Chem. B*, vol. 101, no. 23,

1997, pp. 4597-4606.

29 . Tsventarnyi, E.G., and Kravtsov, V.I. Kinetics and mechanism pertaining to electroreduction of ammonia complexes of palladium (II) at the palladium electrode, *Russian J. Electrochem.*, vol. 35, no. 5, 1999, pp. 545-551.

30 . Hubbard, A.T., and Anson, F.C. Study of the electrochemistry of chloride and bromide complexes of platinum (II) and (IV) by thin layer electrochemistry, *Anal. Chem.*, vol. 38, no. 13, Dec. 1966, pp. 1887-1893.

31 . Nachtigall, D., Artelt, S., and Wünsch, G. Speciation of platinum-chloro complexes and their hydrolysis products by ion chromatography. Determination of platinum oxidation states, *J. Chromatogr. A*, vol. 775, 1997, pp. 197-210.

32. Thompson, S.D., Jordan, L.R., Shukla, A.K., and Forsyth, M. Platinum electrodeposition from $H_3Pt(SO_3)_2OH$ solutions, *J. Electroanal. Chem.,* vol. 515, 2001, pp. 61-70.

33. Skoog, D.A., Holler, F.J., and Nieman, T.A. *Principles of Instrumental Analysis*, 5th ed., Harcourt Brace College Publishers, 1998, (a) p. 639, (b) p. 58, (c) p. 640, (d) p. 591.

34. Mabbot, G.A. An introduction to cyclic voltammetry, *J. Chem. Ed.*, vol. 60, no. 9, Sep. 1983, (a) pp. 697-698, (b) p. 701.

35. Kissinger, P.T., and Heineman, W.R. Cyclic voltammetry, *J. Chem. Ed.*, vol. 60, no. 9, Sep. 1983, pp. 702-704.

36 . Gosser Jr., D.K. *Cyclic Voltammetry: Simulation and Analysis of Reaction Mechanisms*, New York: VCH Publishers, 1993, (a) p. 75,

(b) p. 29, (c) p. 34.

37 . Pletcher, D. *A First Course in Electrode Processes*, Hants: Alesford Press, 1991, (a) p. 171, (b) p. 173, (c) pp. 32-75, (d) p. 114, (e) p. 11, (f) p. 13, (g) p. 27, (h) p. 143, (i) p. 260.

38. Lee, A.F. *Modern Applications of Polarography and Voltammetry to Inorganic Analysis*, Randburg, South Africa: Council for Mineral Technology, Jul. 1983, p. 1. (Report No. M95).

39 . Ferreira, B.K. *Electrochemical Reactor for PGM Recovery*, MSc Dissertation, University of the Witwatersrand, Johannesburg, 2004.

40 . Kissinger, P.T., and Heineman, W.R. eds. *Laboratory Techniques in Electroanalytical Chemistry,* New York: Marcel Dekker, 1984, pp. 308-310.

41 . Tarasevich, M.R., and Khrushcheva, E.I. Electrocatalytic properties of carbon materials, In: Conway, B.E., Bockris, J.O.M., and White, R.E. eds. *Modern Aspects of Electrochemistry*, New York: Plenum, 1989, vol. 19, pp. 295-350.

42 . Kinoshita, K. *Carbon: Electrochemical and Physicochemical Properties*, New York: Wiley, 1988, (a) pp. 337-352, (b) p.372, (c) p. 356, (d) p. 11.

43 . van Aswegen, A., and Cukrowski, I. *The Electrochemistry of Metal Ions in Industrial Streams*, Johannesburg, South Africa: Anglo Platinum Research Centre, Sep. 2002, pp. 67-89.

44 . Mayne, P.J. Reduction of Iridium in Solution, *Polyhedron*, vol. 3, no. 8, 1984, pp. 1013-1015.

45 . MacGregor, J.J. *Electrochemical destruction of stable complexes*, Matthey Rustenburg Refiners, patent no. US4201636, 1980, p. 1.

46 . Weast, R. C. ed. *CRC Handbook of Chemistry and Physics*, 59th ed., CRC Press Inc., 1978, (a) p. D-289, (b) pp. D-267, D-298, D-299.